

NORTHWESTERN UNIVERSITY

New Discoveries in *N*-Heterocyclic Carbene-Catalyzed Homoenolate and
Hydroacylation Reactions

A DISSERTATION

SUBMITTED TO THE GRADUATE SCHOOL IN PARTIAL FULFILLMENT
OF THE REQUIREMENTS

for the degree

DOCTOR OF PHILOSOPHY

Field of Chemistry

By

Audrey Chan

EVANSTON ILLINOIS

June 2008

© Copyright by Audrey Chan 2008

All Rights Reserved

ABSTRACT

New Discoveries in *N*-Heterocyclic Carbene-Catalyzed Generation of Homoenolates And Hydroacylation Reactions

Audrey Chan

N-Heterocyclic carbene catalysis has recently emerged as an important field in organic chemistry. Two new strategies have been developed to advance the use of *N*-heterocyclic carbenes (NHCs) as Lewis-base organic catalysts. The first approach utilizes NHCs to catalyze the generation of homoenolates and the conjugated Breslow intermediate is added to different electrophiles to provide various organic compounds. The second method employs NHCs to catalyze the hydroacylation of activated ketones by using an aldehyde as a hydride equivalent and an acylating agent.

The ability to generate unconventional nucleophiles, such as homoenolates, under catalytic conditions can facilitate the construction of organic molecules via nontraditional bond formations. NHCs derived from benzimidazolium salts are effective nucleophilic catalysts for generating homoenolate species *in situ* from α,β -unsaturated aldehydes. These homoenolate nucleophiles undergo protonation and the resulting activated carbonyl unit is trapped with an alcohol nucleophile, thereby promoting an efficient conversion of a α,β -unsaturated aldehyde into a saturated ester.

The NHC-generated homoenolates can also successfully undergo a formal [3+3] cycloaddition reaction with azomethine imines to give tetrahydro-5*H*-pyrazolo[1,2-*a*]pyridazine-1,8-dione. The reaction is highly diastereoselective (>20:1 dr) and favors the formation of the all *syn* stereoisomer. Additionally, the direct amination of the NHC-generated homoenolates can be achieved when employing 1-acyl-2-aryldiazenes to produce substituted pyrazolidinones through a formal [3+2] cycloaddition reaction. The pyrazolidinones can undergo reductive N-N bond cleavage to give β -amino acid derivatives.

N-Heterocyclic carbenes derived from triazolium salts are effective catalysts for the hydroacylation of activated ketones. The addition of a nucleophilic carbene species to an aromatic aldehyde generates a reducing equivalent that adds to an activated ketone. The subsequent alcohol product undergoes an acylation event with the resulting acyl heteroazolium intermediate formed *in situ* between the NHC and the aldehyde. The process demonstrates that NHCs can catalyze a multi-component process by transforming an aldehyde into a mild hydride source as well as an acylating agent. This concept can be extended to the desymmetrization of *meso*-diols by utilizing a chiral NHC and an aldehyde in the presence of MnO₂ as the oxidant.

Thesis Advisor: Professor Karl A. Scheidt

Acknowledgements

I had an exceptional experience during my graduate career at Northwestern University. First, I would like to express my deep and sincere gratitude to my research advisor, Professor Karl A. Scheidt. His wisdom, enthusiasm and commitment to the highest standards have facilitated my progression as a scientist. He is an outstanding advisor who has challenged me to accomplish far beyond what I thought I was capable of and for this, I am forever grateful.

The members of my dissertation committee, Professor Richard Silverman and Professor SonBinh Nguyen, have generously given their time and expertise to advise and guide me during my studies here at Northwestern University. I thank them for their contribution and their good-natured support.

I would also like to extend many thanks to my colleagues and friends. First I would like to thank the previous Scheidt group members. Dr. Anita Mattson was an outstanding coworker and an excellent friend. To my past bay-mates, Dr. Chris Galliford and Dr. Bill Morris, thank you for keeping me constantly entertained in lab. Dr. Margaret Biddle has been a great friend and coworker who will be missed. I also enjoyed working with Dr. Ashwin Bharadwaj, Dr. Michael Myers, Dave Ballweg, Dr. Rob Lettan, Dr. Manabu Wadamoto, and Dr. Alex Mathies. Next, I would like to thank the current members of the group beginning with Dan Custar who has been a fantastic office-mate and friend. Both Dustin Raup and Antoinette Nibbs have been great friends and I wish them the best of luck. Eric Phillips has been a valued NHC team member and I wish him the best of luck leading the NHC team. My office-mates, Dr. Yasufumi Kawanaka, Becky Farmer and Roxanne Atienza are all talented individuals with whom I've enjoyed working with. A special thanks to Troy Reynolds for solving my crystal structures and Brooks

Maki for computer assistance. Dr. Tom Zabawa, John Roberts, Erika Crane and Amanda Baize have also been great coworkers and I enjoyed interacting with them.

I wish to thank my parents for their unconditional love and support throughout this process. The sacrifices they have made for my siblings and I to achieve our goals will never be forgotten. To my siblings, I wish to thank you for your words of encouragement throughout the years. To my soon-to-be in-laws, thank you for the support and the fun trips we have shared together.

I am immensely grateful to my fiancé, Richard Kelley, to have experienced this journey with me. Your encouragement and support is unmatched and I am looking forward to spending the rest of my life with you.

Lastly, I also want to thank Dow Chemical Company for financial support through a graduate fellowship.

List of Abbreviations

18-c-6	18-crown-6
Ar	aryl
Ac	acetyl
Bp	boiling point
BINAP	2,2'-bis(diphenylphosphino)-1,1'-binaphthyl
BINOL	1,1'-bi(2-naphthol)
Boc	tert-butyloxycarbonyl
Bu	butyl
chiralphos	(2S,3S)-Bis(diphenylphosphino)-butane
dba	dibenzylidene acetone
DBN	1,5-diazabicyclo[4.3.0]non-5-ene
DBU	1,8-diazabicyclo[5.4.0]undec-7-ene
DEAD	diethylazodicarboxylate
DIPEA	diisopropylethylamine
DMAP	4-(dimethylamino)pyridine
DMSO	dimethylsulfoxide
dr	diastereomeric ratio
ee	enantiomeric excess
equiv	equivalents
ESI	electrospray ionization mass spectrometry
GC	gas chromatography
HPLC	high pressure liquid chromatography

IBX	2-iodoxybenzoic acid
IMES	2,4,6-trimethylphenylimidazole
IPA	isopropanol
IR	infrared
KHMDS	potassium hexamethyldisilazane
KOtBu	potassium <i>tert</i> -butoxide
LRMS	low resolution mass spectroscopy
LUMO	lowest unoccupied molecular orbital
MALDI-TOF	matrix assisted laser desorption ionization time-of-flight
Me	methyl
Mp	melting point
Ms	mesylate
NHC	<i>N</i> -heterocyclic carbene
NMR	nuclear magnetic resonance
NOE	nuclear Overhauser effect
NR	no reaction
ORTEP	Oak Ridge thermal ellipsoid plot
Ph	phenyl
PhH	toluene
PCC	pyridinium chlorochromate
R _f	response factor
Rt	room temperature
<i>s</i> factor	selectivity factor

TADDOL	(-)-trans- α,α' -(dimethyl-1,3-dioxolane-4,5-diyl)bis-(diphenylmethanol)
TBS	<i>tert</i> -butyldimethylsilyl
TBDPS	<i>tert</i> -butyldiphenylsilyl
TES	triethylsilyl
Tf	triflate
THF	tetrahydrofuran
TLC	thin layer chromatography
TMAF	tetramethylammonium fluoride
TMS	trimethylsilyl
<i>p</i> -TsOH	<i>para</i> -toluenesulfonic acid
UV	ultraviolet

Dedication

This work is dedicated to *Dad, Mom, My Siblings and My One and Only*

Table of Contents

List of Tables	16
List of Schemes	17
List of Figures	20
Chapter 1	23
1.1 Introduction: Nature's Inspiration towards NHC Catalysis	23
1.2 N-Heterocyclic Carbenes as Umpolung Catalysts	24
1.2.1 NHC-Catalyzed Benzoin Condensation	27
1.2.2 NHC-Catalyzed Stetter Reaction	31
1.3 Extended Umpolung Reactivity	34
1.3.1 Extended Umpolung Reactivity with Ring-Opening or Elimination Functionalities	35
1.3.2 Conjugated Umpolung Reactivity	38
1.4 N-Heterocyclic Carbene Catalyzed Generation of Homoenolates	42
1.4.1 Development of NHC-Catalyzed Generation of Homoenolates	42
1.4.2 Examination of Nucleophiles in Homoenolate Protonation Reaction	44
1.4.3 Examination of Aldehyde Scope for Homoenolate Protonation Reaction	46
1.4.4 Examination of Phenol Structure for Homoenolate Protonation Reaction	48
1.4.5 Examination of Kinetic Resolution of Secondary Alcohols	49
1.4.6 Asymmetric Homoenolate Protonation	51
1.5 Attempts to Expand the Homoenolate Reaction with New Acceptors	53
1.5.1 Examination of New Electrophiles and Dipolarophiles for NHC-Catalyzed Homoenolate Reactions	53

1.5.2 Intramolecular Homoenolate Reactions.....	12
1.5.3 Attempts to Develop New Homoenolate Precursors	57
1.6 A Formal [3+3] Cycloaddition Reaction between NHC-Generated Homoenolates and Azomethine Imines	61
1.6.1 Optimization of Homoenolate Additions to Azomethine Imines	65
1.6.2 Reaction Scope of Homoenolate Additions to Azomethine Imines	66
1.6.3 Investigation of Proposed Mechanistic Pathway	72
1.6.4 Explanation for High Diastereoselectivity for the Formal [3+3] Cycloaddition reaction.....	75
1.6.5 Utility of Pyridazinone Products.....	77
1.6.6 Asymmetric NHC-Catalyzed Homoenolate Addition to Azomethine Imines.....	78
1.7 Amination of Homoenolates Catalyzed by N-Heterocyclic Carbenes	79
1.7.1 Preparation of Diazene Substrates	80
1.7.2 Optimization of the NHC-Catalyzed Amination of Homoenolates	81
1.7.3 Examination of Proposed Reaction Pathway and Reductive Side Product Formation	83
1.7.4 Reaction Scope of NHC-Catalyzed Amination of Homoenolates	89
1.7.5 Asymmetric Synthesis of Pyrazolidinones via NHC-Catalyzed Amination of Homoenolates	93
1.7.6 Conversion of Pyrazolidinones to β -Amino Acid Derivatives	94
1.8 Summary	95
1.9 Experimental Section	96
1.9.1 Preparations of α,β -Unsaturated Aldehydes.....	98

	13
1.9.2 Experimental for NHC-Catalyzed Protonation of Homoenolates	99
1.9.2.1 General Procedure for NHC-Catalyzed Protonation of Homoenolates	99
1.9.2.2 Characterization of Saturated Esters	100
1.9.3 Kinetic Resolution of Secondary Alcohol Data.....	103
1.9.4..... NHC-Catalyzed Formal [3+3] Cycloaddition Reaction between Homoenolates and Azomethine Imines	104
1.9.5 General Procedure for NHC-Catalyzed Protonation of Homoenolates	105
1.9.6 Amination of Homoenolates Catalyzed by N-Heterocyclic Carbenes	112
1.9.6.1 General Procedure for the Amination of Homoenolates Catalyzed by NHC	112
1.9.6.2 Characterization of Pyrazolidinones	113
1.9.7 Enantioselective Amination of Enals with 1-Acyl-2-Aryldiazenes.....	119
1.9.8 Procedure for the Synthesis of β -Amino Acid Derivatives	122
1.9.9 Selected NMR Spectra.....	124
Chapter 2.....	145
2.1 Introduction.....	145
2.1.1 Metal-Catalyzed Hydroacylation of Aldehydes across Olefins.....	145
2.1.2 The Tishchenko Reaction	148
2.1.3 NHC-Promoted Redox Reactions with an Aldehyde.....	149
2.2 N-Heterocyclic Carbene-Catalyzed Hydroacylation of Activated Ketones	153
2.2.1 Proposed Catalytic Pathway for NHC-Catalyzed Hydroacylation Process.....	155
2.2.2 Optimization of NHC-Catalyzed Hydroacylation of Activated Ketones	155
2.2.3 Substrate Scope of the Hydroacylation Reaction.....	157

	14
2.2.4 Mechanistic Studies for Hydroacylation Reaction	162
2.2.5 NHC-Catalyzed Asymmetric Hydroacylation Reactions	164
2.3 Intramolecular Hydroacylation Processes.....	165
2.4 Attempted NHC-Catalyzed Hydroacylation Reactions	168
2.5 NHC-Catalyzed Desymmetrization of Meso-Diols	170
2.6 Summary	175
2.7 Experimental.....	177
2.7.1 Preparations of α -Ketoesters	177
2.7.2 NHC-Catalyzed Hydroacylation of Activated Ketones.....	178
2.7.2.1 General Procedure for Triazolium-Catalyzed Reaction with Protic Solvent.....	178
2.7.2.2 2-Hydroxyacetate Characterization	178
2.7.2.3 General Procedure for Triazolium-Catalyzed Reaction with Aprotic Solvent	180
2.7.2.4 Alkyl Benzoate Characterizations.....	181
2.7.2.5 General Procedure for the Crossover Experiment	185
2.7.2.6 General Procedure for NHC-catalyzed Intramolecular Hydroacylation Reaction	186
2.7.3 NHC-Catalyzed Desymmetrization of Meso-Diols	187
2.7.3.1 General Procedure for NHC-Catalyzed Desymmetrization of Meso-Diols	187
2.7.3.2 Determination of Enantiomeric Excess	188
2.7.4 Selected NMR Spectra.....	191
Chapter 3	202

	15
3.1 Introduction.....	202
3.2 Synthesis of Benzimidazolium Salts.....	203
3.2.1 Synthesis of 1, 3-DimethylBenzimidazolium Iodide.....	203
3.2.2 Synthesis of N,N'-Bis (S)- α -methylbenzyl-benzimidazolium salts and 1-(S)- α -methylbenzyl-2-phenyl-3-n-butyl-benzimidazolium chloride.....	204
3.2.3 Synthesis of 1,3-Diphenylbenzimidazolium iodide and 1-Mesityl-3-Methylbenzimidazolium Iodide Salts	206
3.3 Synthesis of Triazolium Salts	209
3.3.1 Synthesis of Triazolium Salts Derived from Amino Alcohols	209
3.3.2 Synthesis of Triazolium Salts Derived from Lactams or Amides	216
3.4 Synthesis of Chiral Imidazolium Salts.....	219
3.5 Summary	220
3.6 Experimental.....	221
3.6.1 Synthesis of Benzimidazolium Salts III-8, III-9, III-14, III-17	222
3.6.1.1 Synthesis of N1-Mesityl-N3-Methylbenzimidazolium Iodide Salt (III-25)	222
3.6.2 Synthesis of Chiral Triazolium Salts Derived from Amino Alcohols	225
3.6.2.1 Synthesis of N ² -Mesityl-(5 <i>R</i> , 6 <i>S</i>)-6,8-dihydro-5,6-diphenyl-5H-[1,2,4]triazole-[3,4- <i>c</i>][1,4] oxazine tetrafluoroborate (III-48):.....	229
3.6.3 Synthesis of Triazolium Salts Derived from Lactams and Amides	231
3.6.4 Selected NMR Spectra.....	234
References.....	251
Appendix 1.....	264
Appendix 2.....	271

Appendix 3.....	16 277
-----------------	-----------

List of Tables

Table 1-1. Examination of catalyst structure and alcohol source	43
Table 1-2. Examination of alcohols as nucleophiles on homoenolate reaction	45
Table 1-3. Examination of α,β -unsaturated aldehydes as homoenolate precursors	47
Table 1-4. Impact of phenol structure on homoenolate protonation reaction.....	49
Table 1-5. Examination of new acceptors for homoenolate reactions.....	55
Table 1-6. Catalyst survey for intramolecular homoenolate reaction with I-87	58
Table 1-7. Catalyst survey for intramolecular homoenolate reaction with I-92	61
Table 1-8. Optimization of homoenolate addition to azomethine imine I-114.....	72
Table 1-9. Examination of the reaction scope of homoenolate addition to azomethine imine....	73
Table 1-10. Optimization with sulfonyl-substituted diazenes	86
Table 1-11. Optimization with acylaryldiazenes as homoenolate acceptor.....	88
Table 1-12. Reaction Scope of NHC-catalyzed amination of homoenolates	93
Table 1-13. Summarized data for kinetic resolution study	104
Table 2-1. Inuoe's NHC-catalyzed redox reactions with aldehydes.....	151
Table 2-2. Survey of NHCs for hydroacylation reaction.....	156
Table 2-3. Survey of solvent for hydroacylation process	157
Table 2-4. Examination of the aldehyde scope.....	158
Table 2-5. Examination of the keto ester scope.....	160
Table 2-6. Substrate scope of NHC-catalyzed synthesis of benzofuranones.....	167
Table 2-7. Attempted NHC-catalyzed hydroacylation reactions with new electrophiles.....	170
Table 2-8. NHC-catalyzed desymmetrization of <i>cis</i> -1,2-cyclohexane diol.....	173

	17
Table 2-9. Desymmetrization of <i>cis</i> -1,2-cyclohexane diol.....	175
Table 3-1. Conditions for selective palladium-catalyzed amination	208
Table 3-2. Synthesis of chiral triazolium salts from amino alcohols.....	211
Table 3-3. Synthesis of chiral triazolium salts with modified conditions.....	213
Table 3-4. Synthesis of triazolium salts derived from <i>N</i> -methyl acetamide.....	218

List of Schemes

Scheme 1-1. Early carbenes observed by Arduengo and Enders.....	26
Scheme 1-2. The proposed catalytic cycle of the benzoin condensation.....	28
Scheme 1-3. Chiral benzoin condensation.....	29
Scheme 1-4. Acylsilanes as acyl anion precursors	29
Scheme 1-5. Intramolecular crossed-benzoin reaction	30
Scheme 1-6. Achiral and chiral intramolecular crossed-benzoin reaction	30
Scheme 1-7. Asymmetric synthesis of 4-chromanones I-19	31
Scheme 1-8. The Stetter reaction	31
Scheme 1-9. Achiral and chiral NHC-catalyzed intramolecular reactions	32
Scheme 1-10. Enantio- and diastereoselective intramolecular Stetter reactions	33
Scheme 1-11. One-pot sequential amination-Stetter reaction.....	33
Scheme 1-12. Sila-Stetter and biomimetic Stetter	34
Scheme 1-13. Extended <i>umpolung</i> reactivity catalyzed by NHC.....	35
Scheme 1-14. Extended <i>umpolung</i> reactions with ring-opening functionality.....	36
Scheme 1-15. Extended <i>umpolung</i> reactions with α -elimination functionality	37
Scheme 1-16. NHC-catalyzed generation of homoenolate and proposed catalytic cycle	39

	18
Scheme 1-17. Conjugated <i>umpolung</i> reactivity in cross-condensation reactions.....	40
Scheme 1-18. Protonation of NHC-generated homoenolates	41
Scheme 1-19. Cycloaddition reactions with NHC-generated homoenolates	42
Scheme 1-20. An interesting and insightful result.....	44
Scheme 1-21. NHC-catalyzed kinetic resolution of secondary alcohols	50
Scheme 1-22. Asymmetric protonation with chiral NHCs	51
Scheme 1-23. Asymmetric protonation with chiral proton source	53
Scheme 1-24. General dipolar reactivity pattern for NHC-generated homoenolates	54
Scheme 1-25. Synthesis of homoenolate intramolecular substrate 1-87	57
Scheme 1-26. Second generation of enals for intramolecular homoenolate reactions	59
Scheme 1-27. Reason to develop new homoenolate precursors	63
Scheme 1-28. Preparation and exploration of α -keto acid and α -keto carboxylate as homoenolate precursors	64
Scheme 1-29. Preparation of a α,β -unsaturated acyl silane	65
Scheme 1-30. NHC catalyzed homoenolate addition to azomethine imines	66
Scheme 1-31. Early examination of formal [3+3] cycloaddition reactions between homoenolates and azomethine imine I-103a.....	67
Scheme 1-32. Observation of formal [3+2] cycloaddition product	68
Scheme 1-33. Azomethine imine scope with C ₄ - and C ₅ -position varied	74
Scheme 1-34. Proposed catalytic pathway of homoenolate addition to azomethine imine.....	75
Scheme 1-35. Synthesis of homoenolate intermediate precursor	76
Scheme 1-36. Examination of I-122a and 122b in homoenolate addition reactions	77
Scheme 1-37. Selective ring-opening of pyridazinone with nucleophiles.....	79

	19
Scheme 1-38. Enantioselective synthesis of pyridazinones.....	80
Scheme 1-39. Synthesis of azobenzene and (arenediazosulfonyl)-benzene.....	82
Scheme 1-40. Synthesis of acyl-substituted diazenes.....	83
Scheme 1-41. Examination of DEAD as homoenolate acceptor	84
Scheme 1-42. Optimization with 1,2-diphenyl diazene as homoenolate acceptor	85
Scheme 1-43. Examination of Diazenes I-135a and I-136a as homoenolate acceptors	86
Scheme 1-44. Proposed catalytic pathway for NHC-catalyzed amination of homoenolates	90
Scheme 1-45. Attempt to turn reactivity towards homoenolate formation.....	91
Scheme 1-46. Investigation of asymmetric amination of homoenolates	95
Scheme 1-47. Synthesis of β -amino amides from pyrazolidinone	96
Scheme 2-1. First reported hydroacylation process by Sakai and coworkers.....	146
Scheme 2-2. Proposed catalytic pathway for transition metal-promoted hydroacylation	146
Scheme 2-3. Chelation-assisted intermolecular hydroacylation process.....	148
Scheme 2-4. The Tishchenko reaction.....	149
Scheme 2-5. Mixed Tishchenko reaction.....	149
Scheme 2-6. Divergent reactivity of tetrahedral intermediate II-7	150
Scheme 2-7. NHC-catalyzed reduction of nitrobenzenes with aldehydes.....	152
Scheme 2-8. NHC-catalyzed oxidation of aldehydes to esters	152
Scheme 2-9. Aldehydes and alcohol scope of Miyashita's oxidation reactions	153
Scheme 2-10. NHC-catalyzed hydroacylation of ketones	154
Scheme 2-11. Proposed catalytic pathway for NHC-catalyzed hydroacylation reaction	155
Scheme 2-12. Cross-over experiment	162
Scheme 2-13. Benzoin as hydride donor to hydroacylate ketones	163

	20
Scheme 2-14. NHC-catalyzed asymmetric hydroacylation	165
Scheme 2-15. NHC-catalyzed intramolecular hydroacylation to give benzofuranones	166
Scheme 2-16. NHC-catalyzed intramolecular hydroacylation to give indanones	167
Scheme 2-17. NHC-catalyzed intramolecular hydroacylation to give γ -lactones	168
Scheme 2-18. NHC-catalyzed tandem oxidation of alcohols to esters	171
Scheme 2-19. Meso-diols examined for NHC-catalyzed desymmetrization	172
Scheme 3-1. Synthesis of 1, 3-dimethylbenzimidazolium iodide.....	203
Scheme 3-2. Synthesis of (<i>S</i>)- α -methylbenzyl substituted benzimidazolium salts	205
Scheme 3-3. Synthesis of 1-((<i>S</i>)-1-phenylethyl)-3-butylbenzimidazolium iodide	206
Scheme 3-4. Synthesis of 1,3-diaryl-phenylenediamines	207
Scheme 3-5. Synthesis of 1-mesityl-3-methylbenzimidazolium iodide	208
Scheme 3-6. Synthesis of chiral amino alcohols	210
Scheme 3-7. Synthesis of triazolium salt III-49.....	214
Scheme 3-8. Attempts to synthesize chiral triazolium salts derived from amino acids	215
Scheme 3-9. Synthesis of triazolium salt derived from pyrrolidin-2-one.....	217
Scheme 3-10. Synthesis of chiral imidazolium salt	219

List of Figures

Figure 1-1. Acyl anion generation by the polarity reversal of carbonyl compounds	24
Figure 1-2. Types of <i>N</i> -heterocyclic carbene and “push-pull” synergistic effects	25
Figure 1-3. Examination of amines as nucleophiles in homoenolate reactions	46
Figure 1-4. Reason for observed decreased reactivity for α -substituted aldehydes	48
Figure 1-5. Chiral benzimidazolium salts surveyed for kinetic resolution studies.....	50

	21
Figure 1-6. Intramolecular substrates with heteroatom backbone	59
Figure 1-7. Homoenolate precursors other than α,β -unsaturated aldehyde	62
Figure 1-8. ^1H NMR experiments confirmed the irreversible addition of the NHC to the azomethine imine	69
Figure 1-9. New benzimidazolium salts with larger substituents	70
Figure 1-10. Examination of new azomethine imines with substitution at C_5	71
Figure 1-11. Azomethine ketimine and 1,2-diazetidinium ylide	74
Figure 1-12. Proposed model for homoenolate addition to azomethine imine	78
Figure 1-13. Homoenolate amination strategy	81
Figure 1-14. New triazolium salts to improve the homoenolate amination reaction	92
Figure 2-1 Hydroacylation across a π -bond	145
Figure 2-2. Unsuccessful hydroacylation substrates	161
Figure 2-3. Mass spectrometry spectrum for crossover experiment	163
Figure 2-4. Chart summarizing the base-catalyzed acyl transfer data	174
Figure 3-1. Amino alcohols used in the synthesis of triazolium salts	209

Chapter 1

N-Heterocyclic Carbene-Catalyzed Generation of Homoenolates

Portions of this chapter appear in the following publications:

- Chan, A.; Scheidt, K. A. "New Advances in *N*-Heterocyclic Carbene Catalysis," *Nature* **2008**, submitted.
- Maki, B. E.; Chan, A.; Scheidt, K. A. "Protonation of Homoenolate Equivalents Generated by *N*-Heterocyclic Carbenes," *Synthesis* **2008**, 8, 1306-1315.
- Chan, A.; Scheidt, K. A. "Direct Amination of Homoenolates Catalyzed by *N*-heterocyclic Carbenes," *J. Am. Chem. Soc.* **2008**, 130, 2740-2741.
- Chan, A.; Scheidt, K. A. "Highly Stereoselective Formal [3+3] Cycloaddition of Enals and Azomethine Imines Catalyzed by *N*-Heterocyclic Carbenes," *J. Am. Chem. Soc.* **2007**, 129, 5334-5335.
- Chan, A.; Scheidt, K. A. "Conversion of α,β -Unsaturated Aldehydes into Saturated Esters: An *Umpolung* Reaction Catalyzed by Nucleophilic Carbenes," *Org. Lett.* **2005**, 7(5), 905-908.

Chapter 1

1.1 Introduction: Nature's Inspiration towards NHC Catalysis

Scientists continue to look at Nature for inspiration to develop powerful and enabling reactions capable of generating complex molecules for use in medicine, materials research and biology. An elegant and key biological transformation utilizes the cofactor thiamine, a coenzyme of vitamin B₁, to transform α -keto acids into acetyl CoA, a major building block for polyketide synthesis (Figure 1-1). In this process, a normally electron deficient molecule (e.g. pyruvic acid) is converted into an intermediate that possesses electron density on the carbon atom that was initially part of the carbonyl system. These carbonyl or acyl anions are unusual since they have “reversed polarity” when compared to the initial keto acids. In 1954, Mizuhara and coworkers proposed that the active catalytic species of thiamine-dependent enzymatic reactions is a highly unusual divalent carbon-containing species called an *N*-heterocyclic carbene (NHC).¹ An alternative description of the active thiamine cofactor employs the term “zwitterion” which can be viewed as a resonance form of the carbene description. Either way, this unique cofactor accomplishes fascinating Lewis base-catalyzed transformation by utilizing the C₂ lone pair of electrons. Several decades later, Schneider and coworkers determined the X-ray structure of a transketolase enzyme isolated from the budding yeast *Saccharomyces cerevisiae*² which reveals that the thiamine cofactor is located in a narrow channel at the center of the enzyme body. The elaborate chemical surroundings at the active catalytic center of the enzyme allows for the production of acetyl CoA via a carbonyl anion intermediate to proceed with high selectivity.

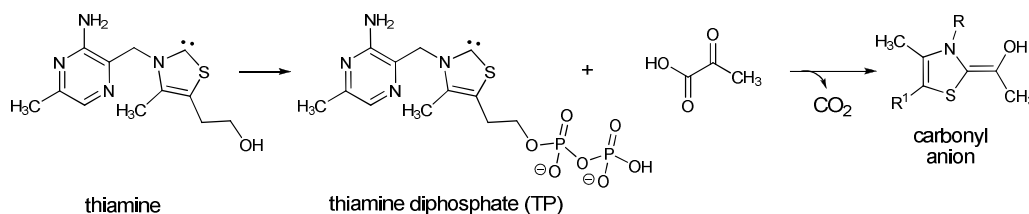


Figure 1-1. Acyl anion generation by the polarity reversal of carbonyl compounds

Inspired by this unusual biochemical process, investigators have sought to mimic the enzymatic system by developing synthetic catalysts that resemble the active catalytic species of the cofactor thiamine diphosphate. Researchers have studied and exploited the unique properties of NHCs to discover highly useful modes of reactivity. Chemists have shown that NHCs are important carbon-based ligands for metals in the field of organometallic chemistry. Researchers in the 20th century discovered that NHCs are excellent Lewis base catalysts. Chemists have shown that thiamine-related NHCs are useful catalysts for a limited set of *umpolung* (polarity-reversal) processes such as the benzoin condensation and Stetter reaction. However, only recently have researchers greatly expanded the scope of the NHC-catalyzed polarity reversal concept to include homoenolate reactivity and extended its utility to catalyze a number of different reactions.

1.2 *N-Heterocyclic Carbenes as Umpolung Catalysts*

Though researchers have demonstrated that nucleophilic carbenes can catalyze a wide range of transformations, much effort has been devoted to understanding the inherent stability and reactivity of carbenes derived from various heteroazolium salts. There are three main classes of NHC precursors that include thiazoliums, imidazoliums and triazoliums (Figure 1-2). While the NHCs resulting from these three classes of heterocycles are closely related, it is

important to note their stability and reactivity differ significantly. These differences in reactivity enable certain carbenes to be better suited for one type of reaction versus another. The acidity of the azolium salts at the C₂ position is one factor that differs considerably between the three classes of NHCs. Thiazolium salts are most acidic with a pK_a (in DMSO) estimated to be 16³ while imidazolium salts are more basic with a pK_a (in DMSO) ranging from 20-24.⁴⁻⁶ Data regarding the pK_a of triazolium salts have not yet been determined.

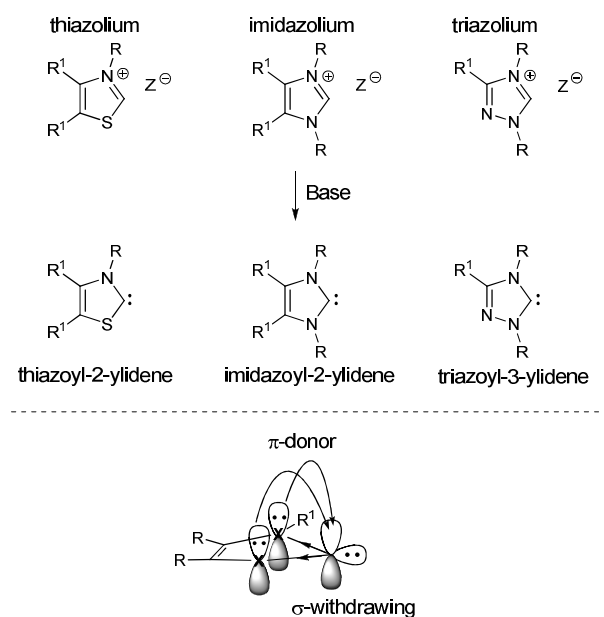
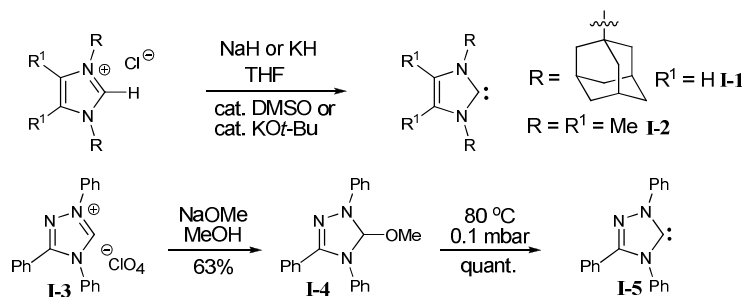


Figure 1-2. Types of *N*-heterocyclic carbene and “push-pull” synergistic effects

In the early 1960's, Wanzlick reported that the stability of a carbene is dramatically enhanced in the presence of amino substituents and attempted to prepare a carbene center at the 2-position of the imidazole ring.^{7, 8} However, only the dimeric electron-rich olefin was isolated. Later in 1970, Wanzlick and coworkers demonstrated that potassium *tert*-butoxide can deprotonate imidazolium salts to afford the imidazol-2-ylidene, which can be trapped with

phenyl isothiocyanate and mercury salts, but he never reported the isolation of the free carbene (Scheme 1-1).⁹⁻¹¹ Following these results, in 1991, Arduengo and coworkers isolated a stable crystalline *N*-heterocyclic carbene from the deprotonation of 1,3-di-1-adamantylimidazolium chloride (**I-1**) with sodium or potassium hydride in the presence of a catalytic amount of either potassium *tert*-butoxide or dimethyl sulfoxide (Scheme 1-1).¹² The structure of **I-1** was unequivocally established by single-crystal X-ray analysis and was determined to be thermally stable.

Scheme 1-1. Early carbenes observed by Arduengo and Enders



The nature of the stabilization is due to the steric and electronic effects of the substituents on the molecule. The two adamantyl substituents of **I-1** should hinder reaction of the carbene center with external reagents as well as prevent self-dimerization (Scheme 1-1). In 1992 Arduengo et al. expanded the carbene library by successfully isolating carbene **I-2** from 1,3,4,5-tetramethyl-imidazolium chloride via treatment with sodium hydride and catalytic amounts of potassium *tert*-butoxide in tetrahydrofuran.¹³ The successful isolation of carbenes with less bulky substituents demonstrates that electronic factors may have greater impact on the stability

of the carbene than steric effects. The electronic factors operate in both the π and σ framework resulting in a “push-pull” synergistic effect to stabilize the generated carbene (Figure 1-2). The π -donation into the carbene from the out of the plane π -orbital of the heteroatoms adjacent to the C₂ position provides stabilization to the typical electrophilic reactivity of carbenes. In the σ -framework, additional stability is provided by the σ -electron-withdrawing effects of the electronegative heteroatoms to moderate the nucleophilic reactivity of the carbene. The combination of these two effects serves to increase the singlet-triplet gap and stabilize the singlet carbene over the more reactive triplet state.¹⁴

The electronic properties of NHCs also contribute to their unique reactivity. Lewis bases are normally considered as electron-pair donors. However, the singlet carbenes of NHCs are distinct Lewis bases that have both σ -basicity and π -acidity characteristics. The combination of these characteristics allows the NHCs to react as powerful nucleophiles which, opens up the possibility for the development of a distinct class of catalytic processes.

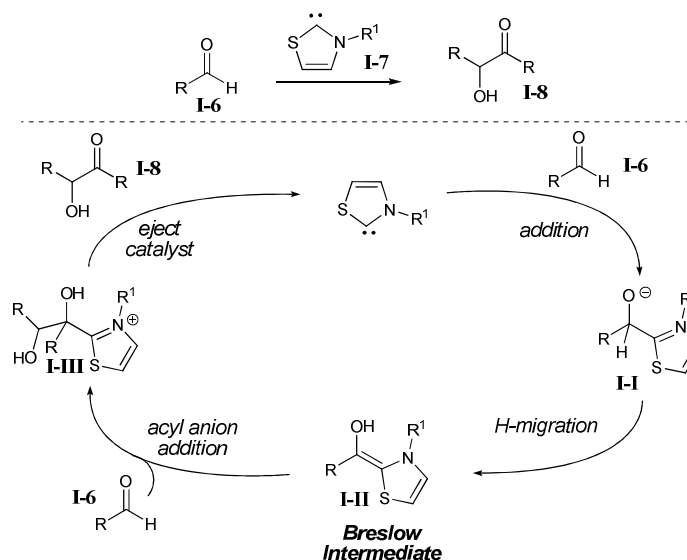
Inspired by Arduengo's success, Enders and coworkers reported the first synthesis of the crystalline triazole-derived carbene **I-5**.¹⁵ The carbene was obtained from triazolium salt **I-3** by addition of sodium methoxide to give the adduct **I-4** followed by thermal decomposition (Scheme 1-1). Carbene **I-5** was the first carbene to be commercially available.

1.2.1 NHC-Catalyzed Benzoin Condensation

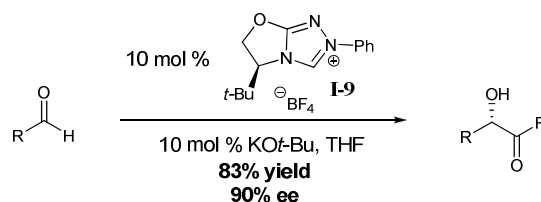
The earliest application of these unique Lewis bases was the development of the benzoin reaction. This *Umpolung* process utilizes a thiamine-related NHC as nucleophilic catalysts. This area has been well reviewed and the origins of most recent NHC advances are intrinsically related to these early studies. In 1943, Ugai and coworkers reported that thiazolium salts can

catalyze the self-condensation of benzaldehyde to produce benzoin.¹⁶ Later, Breslow proposed the mechanism in 1958, in which the active catalytic species is a nucleophilic carbene derived from a thiazolium salt **I-7** (Scheme 1-2) that adds to an aldehyde **I-6** to generate the carbanion known as the Breslow intermediate (**I-II**).¹⁷ Upon formation of the acyl anion, it adds to a second equivalent of aldehyde to result in α -hydroxyketones (**I-8**) as products.

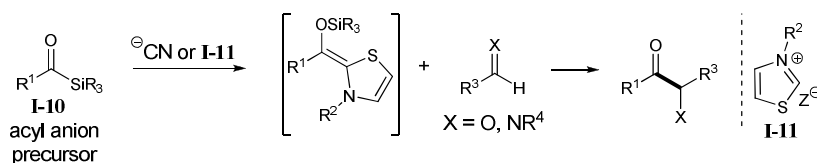
Scheme 1-2. The proposed catalytic cycle of the benzoin condensation



Since the disclosure of the mechanism, much work has been done to render the newly formed stereogenic center enantioselective with the development of chiral thiazolium and triazolium salts. In 2002, Enders and coworkers accomplished the first high yielding and highly enantioselective intermolecular benzoin condensation (Scheme 1-3).¹⁸

Scheme 1-3. Chiral benzoin condensation

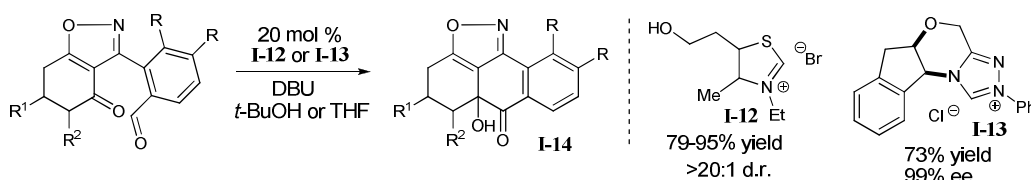
The next logical extension of the benzoin reaction is the cross coupling of different aldehydes with other aldehydes and ketones, which has the drawback of forming multiple products. Researchers have been able to produce chemoselective reactions by using two different aldehydes and selectively generating a more stable Breslow intermediate with aromatic aldehydes rather than aliphatic aldehydes.^{19, 20} Additionally, Johnson and coworkers^{21, 22} and Scheidt and coworkers²³ used acylsilanes **I-10** as superior acyl anion precursors, which avoid the usual problem of self-condensation (Scheme 1-4). An asymmetric variant of the cross-benzoin between an aldehyde and an imine was demonstrated by Miller and coworkers to give 87% ee of the α -amidoketone products.²⁴ You and coworkers have recently shown that aromatic aldehydes can also be coupled to unactivated imines to form α -aminoketones under thermodynamic control.²⁵

Scheme 1-4. Acylsilanes as acyl anion precursors

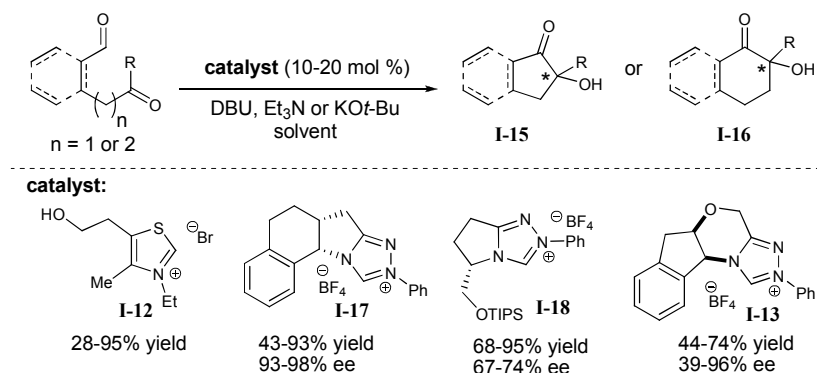
In contrast to intermolecular variants, intramolecular benzoin condensations have received little attention until recently. The first advance in this area was made in 2003 when

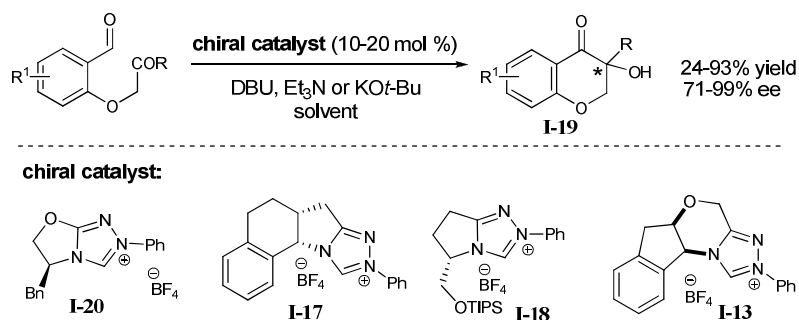
Suzuki and coworkers revealed preanthraquinones **I-14** can be prepared via an intramolecular benzoin reaction between an aldehyde and ketone (Scheme 1-5).²⁶ A subsequent report in 2006 by the Suzuki group showed that the process can be rendered enantioselective by use of a chiral carbene **I-13** (Scheme 1-5).²⁷ Enders and coworkers and Suzuki and coworkers have both independently demonstrated that various five- and six-membered cyclic acyloins (**I-15** or **I-16**) can be obtained as the racemate or the enantiopure form by employing an achiral (**I-12**) or chiral azolium salt (**I-13**, **I-17**, **I-18**) as the precatalyst (Scheme 1-6).²⁷⁻³⁰ Both groups have also reported that carbenes derived from chiral triazolium salts (**I-13**, **I-17**, **I-18**, **I-20**) can catalyze the asymmetric synthesis of 3-hydroxy-4-chromanones **I-19** (Scheme 1-7).^{31, 32}

Scheme 1-5. Intramolecular crossed-benzoin reaction

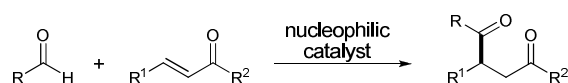


Scheme 1-6. Achiral and chiral intramolecular crossed-benzoin reaction



Scheme 1-7. Asymmetric synthesis of 4-chromanones **I-19****1.2.2 NHC-Catalyzed Stetter Reaction**

In the early 1970's, Stetter and coworkers demonstrated thiazolium catalysis can be employed to accomplish the addition of acyl anions to 1,4-conjugate acceptors (Scheme 1-8).³³ This transformation has proven to be a highly useful carbon-carbon bond forming strategy that has attracted the attention of researchers interested in producing 1,4-dicarbonyl species.^{34, 35} The reactive intermediate is proposed to be the same as the benzoin condensation, the Breslow intermediate, with the nucleophilic addition at the β -position of a conjugate acceptor rather than addition to the carbonyl carbon.

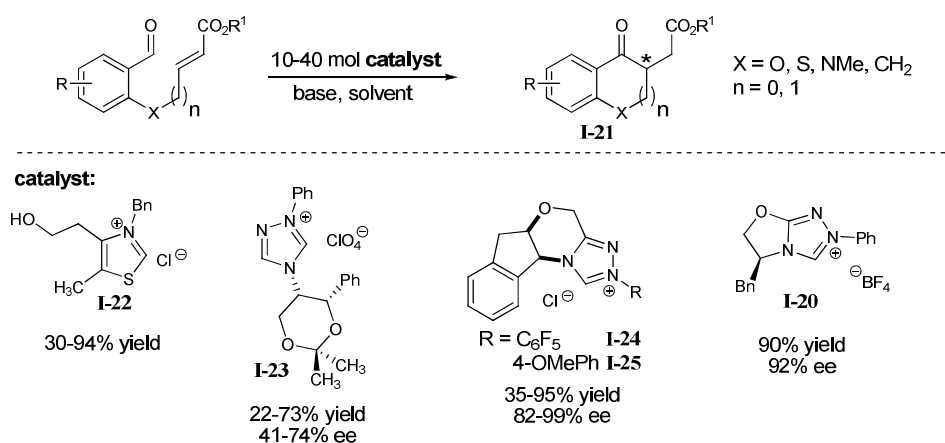
Scheme 1-8. The Stetter reaction

While the asymmetric intermolecular Stetter reaction has been proven difficult to achieve, significant advances have been made in the development of highly enantioselective intramolecular Stetter reactions. Early work reported by Ciganek demonstrated the ability to accomplish an NHC-catalyzed intramolecular Stetter using catalyst **I-22** to synthesize achiral

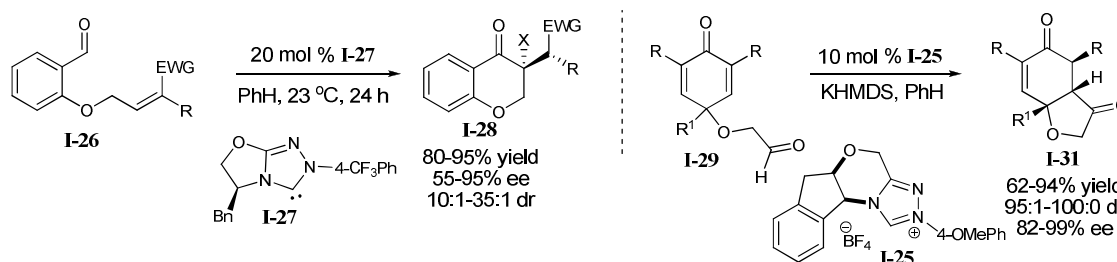
benzofuran and benzopyran derivatives in moderate to excellent yields (Scheme 1-9).³⁶

Investigators including Enders and coworkers, Rovis and coworkers and Harmada and coworkers have reported that enantiopure heterocycles such as **I-21** (X = O, S or CH₂) can be synthesized with chiral triazolium salts (**I-20**, **I-23** to **I-25**) as the carbene precursor to give up to 99% ee.³⁷⁻⁴² This method was also extended to substrates with aliphatic backbones to give the five- and six-membered rings in excellent yields and selectivities.

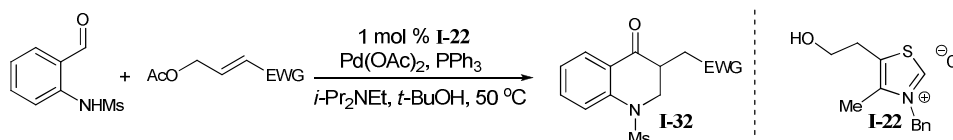
Scheme 1-9. Achiral and chiral NHC-catalyzed intramolecular reactions

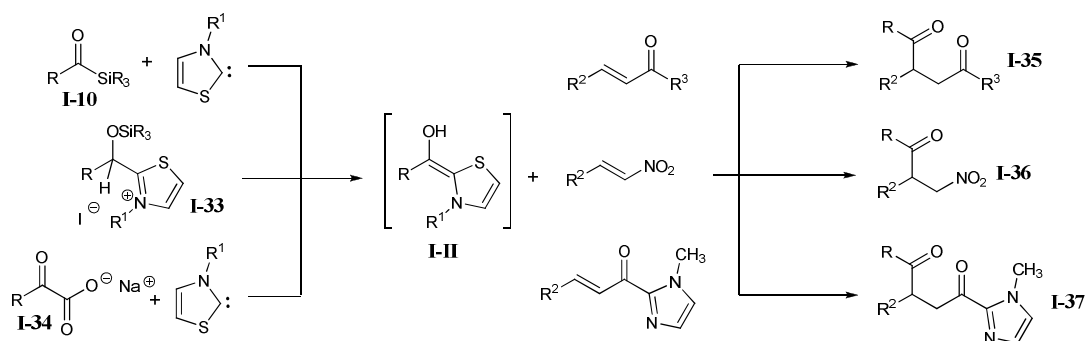


Recent advances in expanding the Stetter reaction include establishing reaction conditions for an enantio- and diastereoselective variants utilizing α,β -disubstituted acceptors, **I-26** (Scheme 1-10). The major challenge was to secure a diastereoselective proton transfer onto the hypothetical enolate intermediate. Rovis and coworkers overcame this challenge with the free carbene **I-27** to afford chromanones **I-28** with up to 95% ee and diastereomeric ratios of up to 35:1.⁴³ In 2006, Liu and Rovis utilized the concept of desymmetrization for the enantio- and diastereoselective synthesis of hydrobenzofuranones **I-31** in an intramolecular Stetter reaction.⁴⁴

Scheme 1-10. Enantio- and diastereoselective intramolecular Stetter reactions

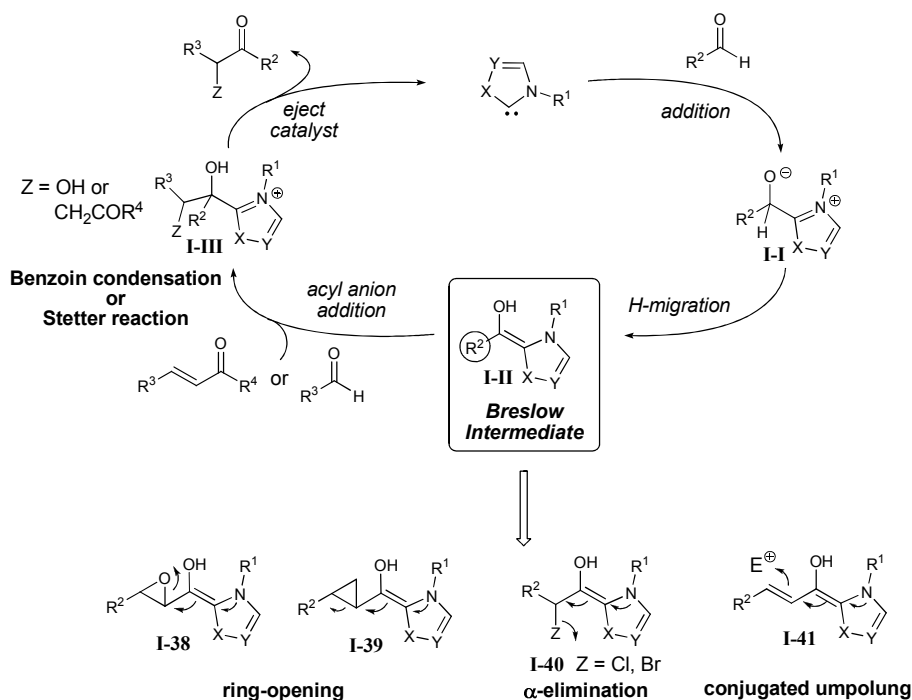
In 2006, Hamada and coworkers developed a one-pot sequential multicyclic process to give racemic dihydroquinolinones **I-32** via a Pd-catalyzed allylic amination-thiazolium salt-catalyzed Stetter reaction cascade (Scheme 1-11).⁴⁵ As in the benzoin case, acylsilanes (**I-10**) could be used as acyl anion precursors and applied to the Stetter reaction. Scheidt and coworkers utilized this strategy with a thiazolium-catalyzed reaction of the acylsilanes and the conjugate acceptor to give the corresponding 1,4-dicarbonyl compounds (**I-35**) in good yields (Scheme 1-12).^{46, 47} In a further contribution, Scheidt and coworkers could perform a nucleophilic acylation of nitroalkenes for the preparation of β -nitroketones **I-36**.⁴⁸ The acyl anion equivalents were generated in situ from the corresponding thiazolium-carbinol **I-33**, which prevents the rapid base-induced decomposition of the nitroalkene. The Scheidt laboratory also demonstrated that the Stetter reaction could be done in a biomimetic fashion in which after addition of a thiazolium catalyst to the keto substrate **I-34**, the Breslow intermediate **I-II** could be generated upon decarboxylation.⁴⁹

Scheme 1-11. One-pot sequential amination-Stetter reaction

Scheme 1-12. Sila-Stetter and biomimetic Stetter

1.3 Extended Umpolung Reactivity

During the 20th century much focus has been on the benzoin condensation and Stetter reactions. From the proposed catalytic cycle for both the benzoin condensation and Stetter reaction, formation of the Breslow intermediate is evident upon addition of the nucleophilic carbene to the aldehyde followed by a formal proton migration (Scheme 1-13). Recently, researchers have sought to expand the NHC-catalyzed *umpolung* reactions to include ring-opening, α -elimination and conjugated *umpolung* reactivities. Starting from the Breslow intermediate **I-II**, the *umpolung* reactivity can be extended by using further functionalized donor substrates (**I-38 to I-40**), such as epoxides, formylcyclopropanes or α -haloaldehydes that can allow subsequent formation of activated carbonyl species to react with various nucleophiles. The addition of an NHC to an α,β -unsaturated aldehyde generates a conjugated *umpolung* system (**I-41**), where the β -position to the carbonyl functionality no longer behaves as a Michael acceptor but instead as a nucleophile, also known as a homoenolate.

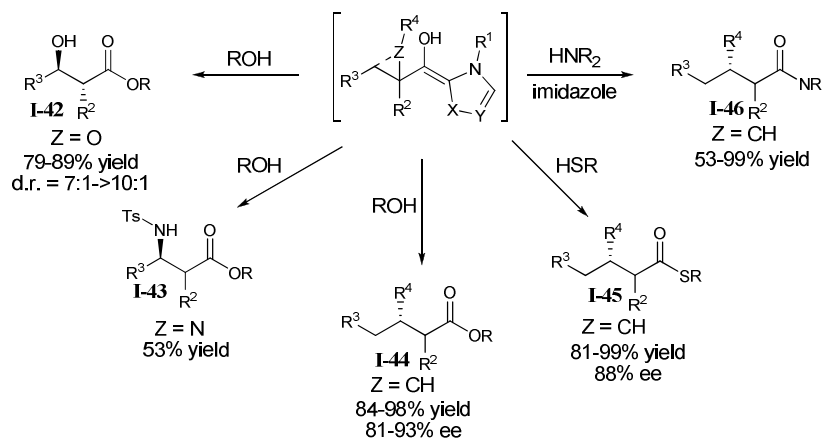
Scheme 1-13. Extended *umpolung* reactivity catalyzed by NHC

1.3.1 Extended Umpolung Reactivity with Ring-Opening or Elimination Functionalities

Studies into the extended *umpolung* reactivity began with a catalytic, diastereoselective method that generates β -hydroxyesters (**I-42**) from epoxyaldehydes using a thiazolium salt as precatalyst (Scheme 1-14).⁵⁰ An internal redox reaction occurs in which upon formation of the Breslow intermediate, the epoxide ring opens to give the active carboxylate after tautomerization. Nucleophilic attack by an alcohol produces the ester product in good yields favoring the formation of the *anti*- β -hydroxyesters. Later, Sohn and Bode demonstrated that the same concept can be extended to formylcyclopropanes in which a triazolium salt can be employed as the precatalyst to cleave the C-C bond and ring-open the formylcyclopropane to give the activated carboxylates.⁵¹ Alcohols and thiols can be added to give the ester (**I-44**) and thioester (**I-45**) products and regenerate catalyst. In a later disclosure, Bode and coworkers

reported the NHC-catalyzed amidations of formylcyclopropanes by using an imidazole as the promoter to produce **I-46**.⁵²

Scheme 1-14. Extended *umpolung* reactions with ring-opening functionality

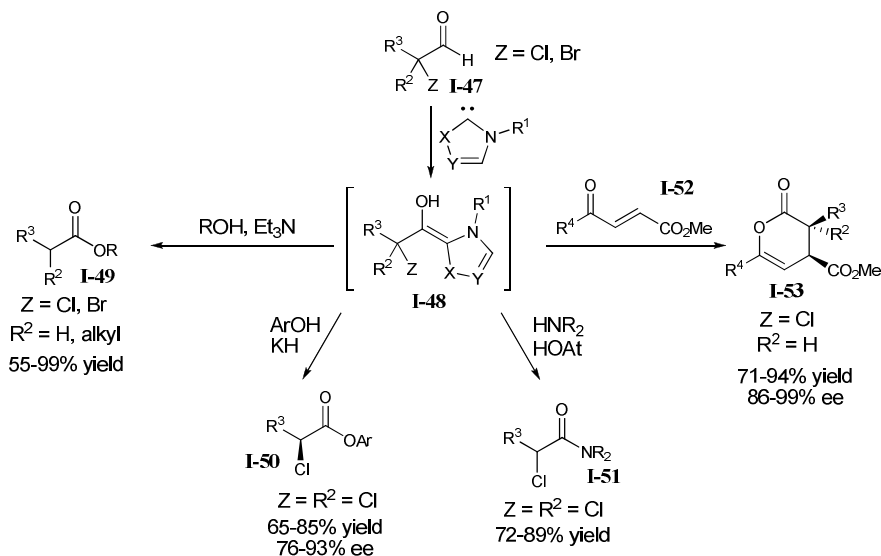


In 2004, Rovis and coworkers demonstrated that nucleophilic carbenes derived from triazolium and thiazolium salts are effective catalysts for the conversion of α -haloaldehydes (**I-47**) into acylating agents.⁵³ Based on their proposed catalytic cycle, the addition of the carbene to the α -haloaldehyde followed by proton migration to the alkoxide should provide the Breslow intermediate (**I-48**). The α -halogen can then be eliminated to access the enol intermediate. Upon tautomerization, an active acyl species is generated and is trapped by primary and secondary alcohols, phenols as well as anilines (Scheme 1-15) to form the corresponding esters (**I-49**) and amides. In 2005, Rovis and coworkers disclosed a communication that describes the enantioselective protonation of chiral enolates in the synthesis α -chloroesters by using a chiral triazolium salt as the precatalyst.⁵⁴ The chiral enolate is formed by expelling the halogen as HCl, which undergoes selective protonation to generate the activated acyl intermediate. Trapping the

activated carbonyl with an alcohol nucleophile provides the enantiopure α -haloester (**I-50**).

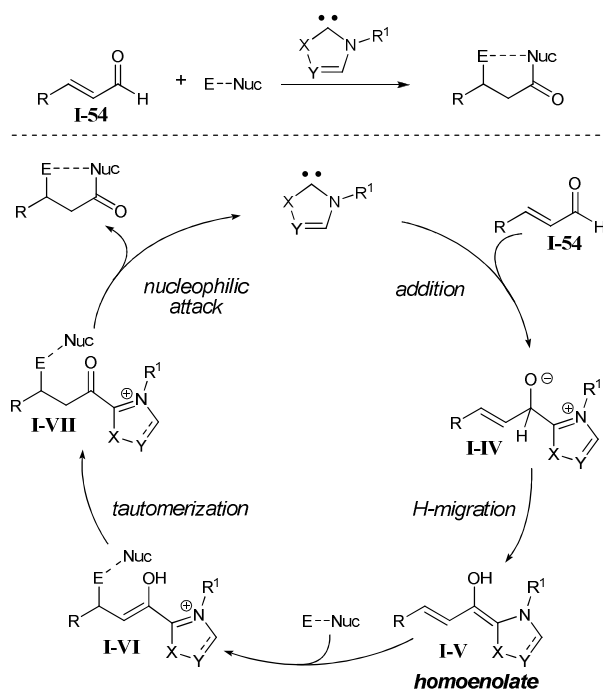
More recently, Rovis and coworkers reported that NHCs derived from a triazolium salt can catalyze the α -redox reaction to give amides (**I-51**) upon addition of a catalytic amount of HOAt and stoichiometric amount of amines as the nucleophiles.⁵⁵ The research group of Bode disclosed an extension of the α -haloaldehydes by showing that NHCs can catalyze a hetero-Diels-Alder reaction with impressively low catalyst loading of 0.5 mol %.⁵⁶ In this case, a reactive enolate dienophile is derived from the racemic α -chloroaldehyde, and it reacts with 4-oxo-enoates (**I-52**) as the hetero-diene to give dihydropyran-2-ones **I-53** in excellent enantioselectivity.

Scheme 1-15. Extended *umpolung* reactions with α -elimination functionality



1.3.2 Conjugated Umpolung Reactivity

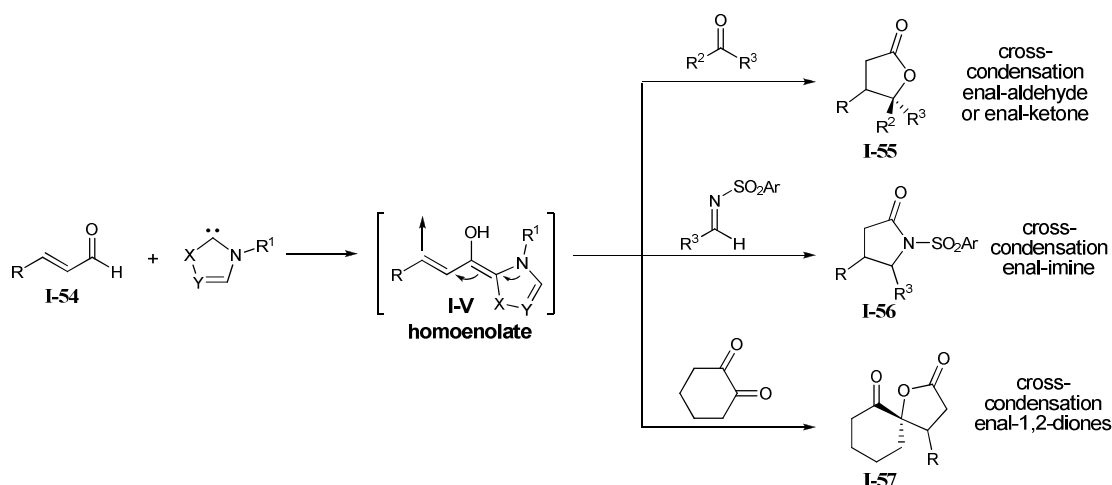
A related strategy to the NHC-catalyzed formation of an acyl anion is to access the vinylogous carbonyl anion. Researchers have recently realized that under appropriate organocatalytic conditions, an α,β -unsaturated aldehyde (**I-54**) could be converted into unique homoenolate nucleophiles with subsequent electrophilic characteristics at the carbonyl carbon (Scheme 1-16). Inspired by the proposed catalytic cycle of the NHC-catalyzed benzoin reaction, we hypothesized that the extension of carbonyl anion reactivity to a β -position could be achieved by use of an alkene in the form of α,β -unsaturation. The addition of a nucleophilic carbene catalyst to the carbonyl compound should generate a tetrahedral intermediate **I-IV**, and subsequent hydrogen migration would generate the reactive dienamine **I-V**. The unique nucleophilic character of the carbonyl carbon is then extended to the β -position and, in the presence of an electrophile, should produce enol **I-VI**. After tautomerization of **I-VI** to activated ester **I-VII**, the attack of a suitable nucleophile, either tethered to the electrophile or separate, completes the catalytic cycle.

Scheme 1-16. NHC-catalyzed generation of homoenolate and proposed catalytic cycle

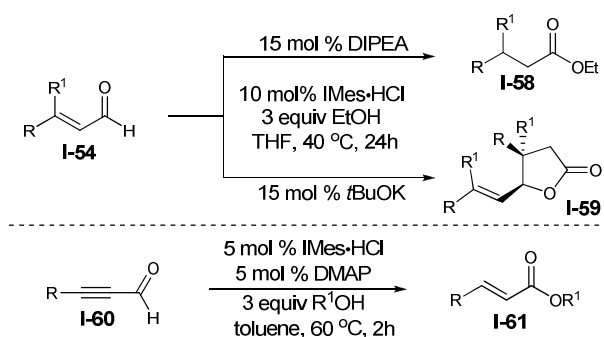
Concurrent with the studies from the Scheidt group, both Glorius and coworkers⁵⁷ and Bode and coworkers⁵⁸ have independently developed a direct annulation of enals **I-54** and aldehydes catalyzed by the sterically demanding imidazoliums salt, IMes·HCl, to form stereoselective γ -butyrolactones (**I-55**) via a homoenolate intermediate (Scheme 1-17). Glorius and coworkers were also able to perform the cross-condensation of enals with ketones to give highly substituted γ -butyrolactones. Under remarkably mild conditions, the homoenolate intermediate **I-V** is generated in situ and coupled with an aldehyde to result in an alkoxide intermediate. Intramolecular attack of the catalyst-bound carbonyl carbon by the alkoxide regenerates the catalyst and yields the desired γ -butyrolactone in moderate to good yields, favoring the formation of the *cis*-diastereomers. Subsequent work by He and Bode shows that the condensation of homoenolate to electron-rich *N*-sulfonyl imines provides γ -lactams (**I-56**) in

good yields and moderate diastereomeric ratios.⁵⁹ Work by Nair demonstrated that 1,2-dicarbonyl compounds, 1,2-cyclohexane dione and isatin, are efficient electrophiles to undergo annulation with enals to provide spiro γ -butyrolactones (**I-57**) via a homoenolate intermediate.⁶⁰

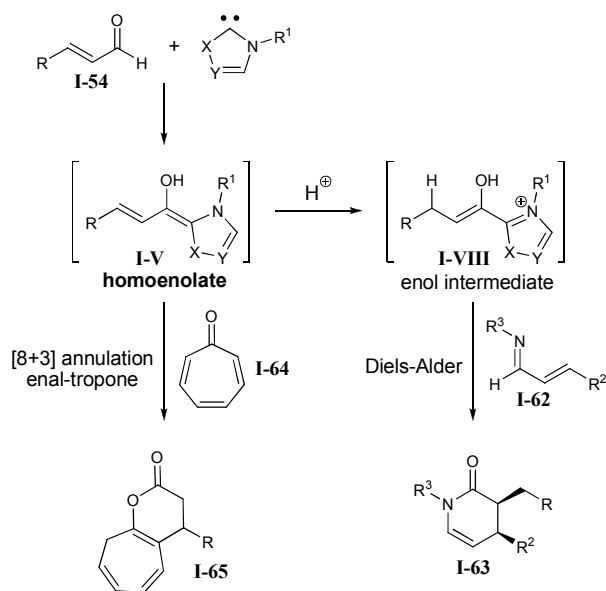
Scheme 1-17. Conjugated *umpolung* reactivity in cross-condensation reactions



After our report that NHC-generated homoenolates can be protonated, Sohn and Bode observed that the base used in the reaction determines the fate of the generated homoenolates (Scheme 1-18).⁶¹ Strong bases such as KO t -Bu promote the carbon-carbon bond formation to give γ -lactones **I-59**, as observed in enal-aldehyde cross condensations, while weaker bases such as diisopropylethylamine (DIPEA) allow protonation of the nucleophilic homoenolate and the formation of the activated carbonyl unit that is trapped by alcohols to give esters (**I-58**). A further extension of the reaction was shown by Zeitler in the stereoselective preparation of (*E*)-configured α,β -unsaturated esters (**I-61**) starting with propargylic-derived aldehydes **I-60**.⁶²

Scheme 1-18. Protonation of NHC-generated homoenolates

Besides cross-condensation and protonation reactions, NHC-mediated homoenolates can also undergo cycloaddition reactions (Scheme 1-19). In 2006, Bode and coworkers revealed the first enantioselective azadiene Diels-Alder reaction catalyzed by NHC.⁶³ The dienophile of the reaction is generated in situ in which the generated homoenolate **I-V** is protonated and the subsequent highly reactive enol **I-VIII** undergoes a $\text{LUMO}_{\text{diene}}$ -controlled cyclization with *N*-sulfonyl α,β -unsaturated imines (**I-62**) to give the dihydropyridinone (**I-63**) product in excellent enantio- and *cis*-diastereoselectivity. It was observed by Nair and coworkers that IMes-catalyzed generated homoenolates can react with tropones **I-64** via an unexpected [8+3] annulation pathway to give bicyclic δ -lactones **I-65**.⁶⁴

Scheme 1-19. Cycloaddition reactions with NHC-generated homoenolates

1.4 *N*-Heterocyclic Carbene Catalyzed Generation of Homoenolates

1.4.1 Development of NHC-Catalyzed Generation of Homoenolates

Shortly after Bode⁵⁰ and Rovis⁵³ reported that NHCs catalyze the formation of extended *umpolung* reactivity from epoxyaldehydes and α -haloaldehydes, we began to investigate whether *N*-heterocyclic carbenes can add to α,β -unsaturated aldehydes to catalyze the generation of conjugated *umpolung* reactivity known as homoenolates. Homoenolates are important nucleophiles that are essentially the *umpolung* equivalent of conjugate addition reactions. Although this uncommon reactivity pattern has significant utility in organic synthesis, establishing the requisite nucleophilic character at the β -position of a carbonyl compound is challenging.

We began our investigations of this intriguing strategy by employing the simplest electrophile, a proton (Table 1-1). The use of the optimal alcohol would presumably serve a

double purpose as an electrophilic source and then subsequent nucleophile. To probe this possibility, cinnamaldehyde (**I-54a**) and various alcohols were heated in toluene in the presence of catalytic quantities of ammonium salts **I-67** to **I-69** and DBU. Initially, our approach used a single reagent as the potential proton donor and subsequent nucleophile required for catalyst turnover. With 5.0 equivalents of ethanol and ammonium salt **I-67**, we were pleased to isolate the desired ester in 30% yield (entry 1), but clearly the system required improvement. More acidic alcohols were examined with the hope that the increased acidity will improve the protonation process, but as the alcohol increased in acidity, the amount of desired product also decreased (entries 2-4). Presumably, the more acidic alcohols also have a decrease in nucleophilicity to form the ester product and regenerate the catalyst.

Table 1-1. Examination of catalyst structure and alcohol source

entry	ROH	pKa (H ₂ O)	catalyst (mol%)	additive	yield (%)
1	EtOH	16	I-67 (30 mol%)	—	30 (I-66a)
2	CF ₃ CH ₂ OH	12	I-67 (30 mol%)	—	17 (I-66b)
3	PhOH	10	I-67 (30 mol%)	—	42 (I-66c)
4	4-NO ₂ -Ph	7	I-67 (30 mol%)	—	0 (I-66d)
5	BnOH	15	I-67 (30 mol%)	PhOH	58 (I-66e)
6	BnOH	15	I-68 (10 mol%)	PhOH	47 (I-66e)
7	BnOH	15	I-69 (20 mol%)	PhOH	82 (I-66e)
8	BnOH	15	I-69 (5 mol%)	PhOH	83 (I-66e)

catalyst:

I-67

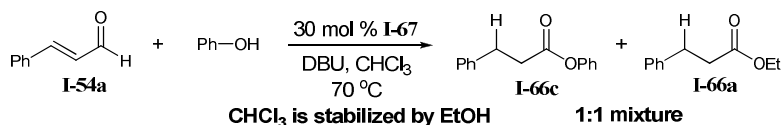
I-68

I-69

Fortuitously, while using phenol as the alcohol in chloroform subjected to Al₂O₃ filtration, but not distillation, a substantial amount of ethyl ester was observed (Scheme 1-20).

Our initial hypothesis for this result was that the putative activated acylation agent (Scheme 1-16, **I-VII**) was being trapped by the ethanol typically added to stabilize chloroform. Armed with this knowledge that the electrophile and nucleophile can be decoupled in this manner, we discovered that the use of 2.0 equivalents of phenol as the proton source and 5.0 equivalents of a second alcohol as the nucleophile affords improved yields for the reaction. A survey of catalysts **I-67** to **I-69** showed that imidazolium salt **I-69** resulted in the best yields with using only 5 mol % catalyst loading (Table 1, entry 8).

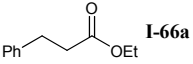
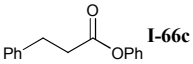
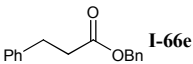
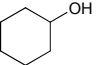
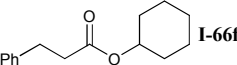
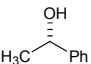
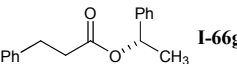
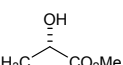
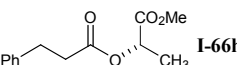
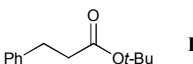
Scheme 1-20. An interesting and insightful result



1.4.2 Examination of Nucleophiles in Homoenolate Protonation Reaction

Encouraged by these results, we proceeded to examine the ability of other alcohols to act as nucleophiles in the presence of a Brønsted acid such as phenol (Table 1-2). Primary and secondary alcohols afford good to high yields of the corresponding esters when using cinnamaldehyde **I-54a**. Not surprisingly, the use of sterically demanding *tert*-butyl alcohol only afforded the phenyl ester in a 56% yield. The generation of the phenyl ester is the default product observed when the potential nucleophile does not undergo addition. Usually with less hindered alcohols, this competition is not problematic. When chiral secondary alcohols are employed, their stereochemical integrity is not diminished (entries 5-6).

Table 1-2. Examination of alcohols as nucleophiles on homoenolate reaction

$ \begin{array}{c} \text{O} \\ \parallel \\ \text{Ph}-\text{CH}=\text{CH}-\text{CHO} \\ \text{I-54a} \end{array} + \text{R-OH} \xrightarrow[\text{DBU, toluene}]{\begin{array}{c} 5 \text{ mol\% I-69} \\ 2 \text{ equiv PhOH} \end{array}} \begin{array}{c} \text{H} \quad \text{O} \\ \quad \parallel \\ \text{Ph}-\text{CH}-\text{CH}-\text{C}-\text{OR} \\ \text{I-66} \end{array} $				
entry	ROH	time (h)	product	yield (%)
1	EtOH	4	 I-66a	72
2	PhOH	6	 I-66c	56
3	BnOH	2	 I-66e	82
4		6	 I-66f	57
5		6	 I-66g	77
6		6	 I-66h	61
7	<i>t</i> -BuOH	6	 I-66i	NR

We next turned our attention to examine amines as nucleophiles (Figure 1-3). The use of typical nitrogen-based nucleophiles in this general transformation such as anilines, sulfonamides, amides, carbamates, morpholinones and maleimides, did not afford desired products. The result from this intense reaction screening underscores the crucial balance of acids and bases present in the process. The amines **I-70a-h** were screened in both, the presence and absence of PhOH. Under the reaction conditions when 2.0 equivalents of PhOH were employed, only phenyl ester **I-66c** was recovered as product. However when no phenol additive was used, the reactions did not proceed at all with amine substrates **I-70a-g**. Surprisingly, during the examination of many of these potential nucleophiles, we did identify that β -amino alkylidene malonate **I-70h** affords modest yields of the corresponding bis-ester amide product (**I-71h**). In the absence of phenol,

51% of the amide was isolated, but with 2.0 equivalents of phenol, only 35% of the amide product was observed along with a small amount of the phenyl ester product **I-66c**.

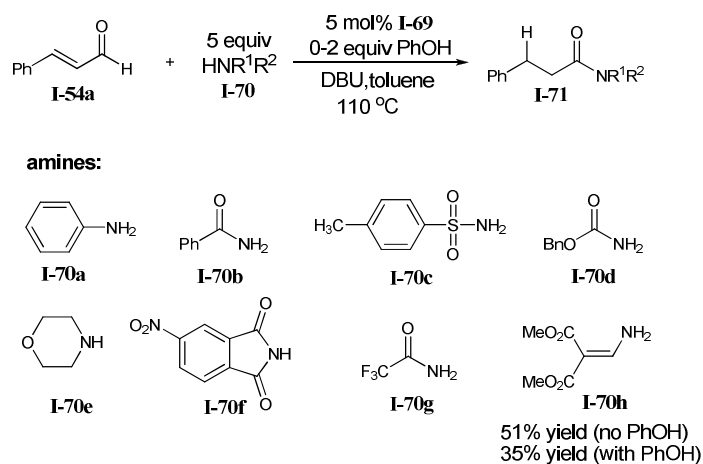


Figure 1-3. Examination of amines as nucleophiles in homoenolate reactions

1.4.3 Examination of Aldehyde Scope for Homo enolate Protonation Reaction

The overall homo enolate protonation reaction can successfully accommodate various α,β -unsaturated aldehyde (Table 1-3). Electron-rich and electron-deficient cinnamaldehydes are competent substrates for the reaction (entries 2 and 3). The use of branched β -alkyl substituents affords fully saturated esters in good yields (entry 4). Interestingly, the extended dienyl system of sorbaldehyde is disrupted in the reaction to afford the γ,δ -unsaturated ester in moderate yields (entry 5).

Table 1-3. Examination of α,β -unsaturated aldehydes as homoenolate precursors

entry	R	R ¹	R ²	yield (%)	product
1	Ph	H	H	82	I-66e
2	4-MeO-Ph	H	H	76	I-66j
3	4-Cl-Ph	H	H	71	I-66k
4	<i>n</i> -propyl	H	H	90	I-66l
5	H ₃ C(CH=CH)	H	H	70	I-66m
6	Ph	H	CH ₃	82	I-66n
7	Ph	Ph	H	82	I-66o
8	4-Cl-Ph	Ph	H	86	I-66p
9	CH ₃	CH ₃	H	NR	—

Disubstitution at the β -position of unsaturated aldehydes leads to divergent reactivity depending on the substituents. For example, aldehydes with at least one β -aryl substituent are competent substrates (Table 1-3, entries 6-8), but surprisingly, β,β -dialkyl compounds afford no product (entry 9).

The reaction time for most of the aldehyde substrates are between 2-6 hours; however, α -methylcinnamaldehyde required 48 hours for complete consumption of the aldehyde (Table 1-3, entry 6). We postulate that the allylic strain inherent to the key homoenolate intermediate inhibits protonation at the β -position by impeding the formation of a fully conjugated system (Figure 1-4). When a more sterically hindered heteroazolium salt, such as IMes·HCl, is employed as the carbene precursor with α -methylcinnamaldehyde, no product is observed because the formation of a conjugated system is completely prevented by the allylic strain. However, precatalyst **I-69** has less sterically demanding methyl substituents that allow equilibration to the conjugated system under thermal conditions to provide the desired product.

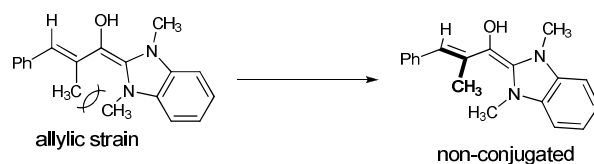


Figure 1-4. Reason for observed decreased reactivity for α -substituted aldehydes

1.4.4 Examination of Phenol Structure for Homoenolate Protonation Reaction

Although phenols have the optimal acidity for this *umpolung* process, 20-30% of the phenyl ester product can be observed when employing secondary alcohol nucleophiles such as cyclohexanol. This competition between phenol and hindered secondary alcohols, as the nucleophile, prompted us to examine more proton donors with similar levels of acidity to phenol (Table 1-4). By additional substitution at the 2- and 6-positions of the phenol ring, the generation of phenyl ester **I-66c** can be minimized in the reaction. By increasing the size of the substituents from 2,6-dimethylphenol (entry 2) to 2,6-di-*tert*-butyl-4-methylphenol (entry 3), the level of phenyl ester can be completely suppressed.

Table 1-4. Impact of phenol structure on homoenolate protonation reaction

entry	ArOH	yield (%) of I-66f	yield (%) of I-66c
1		57	26
2		58	20
3		65	0

1.4.5 Examination of Kinetic Resolution of Secondary Alcohols

We hypothesized that the use of a chiral imidazolium salt would generate chiral activated esters capable of enantiodiscrimination. This transformation would be synthetically useful in the organocatalytic kinetic resolution of secondary alcohols while also lending credence to the participation of **I-VII** (Scheme 1-16) as a viable intermediate along the catalytic cycle. To probe this possibility, several chiral benzimidazolium salts were made according to methods disclosed by Diver and coworkers (Figure 1-5).^{65, 66} We chose to only test chiral benzimidazolium salts because these salts proved to be the best class of carbene precursors for the protonation of homoenolate intermediates. The difference in counterions for benzimidazolium salts **I-72a-c** did not have any impact on the reaction as all three catalysts provided similar results with catalyst **I-72a** giving the highest *s* factor value. The asymmetric benzimidazolium salts **I-73** resulted in low conversion to the desired product.

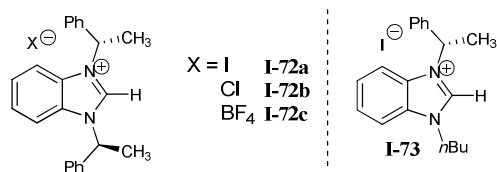
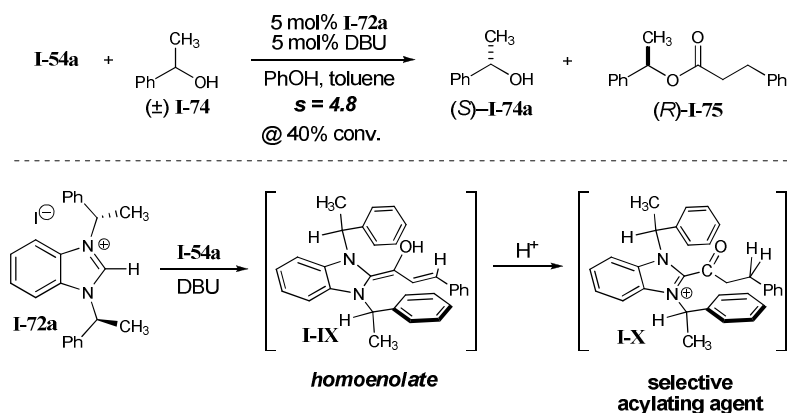


Figure 1-5. Chiral benzimidazolium salts surveyed for kinetic resolution studies

Gratifyingly, when chiral imidazolium salt **I-72a** was employed as the catalyst in the reaction with 5.0 equivalents of racemic 1-phenylethanol (**I-74**), 2.0 equivalents of phenol, cinnamaldehyde (**I-54a**), and DBU, the average *s* factor for this transformation at 40% conversion, is 4.8 (Scheme 1-21). Presumably, a chiral intermediate present in the catalytic cycle of this reaction, such as **I-X**, has sufficient facial selectivity to undergo preferential reaction with the (*R*)-stereoisomer of 1-phenylethanol to produce the (*R*)-enantiomer of the ester product **I-75** and not react with the (*S*)-stereoisomer of the 1-phenylethanol (**I-74a**).

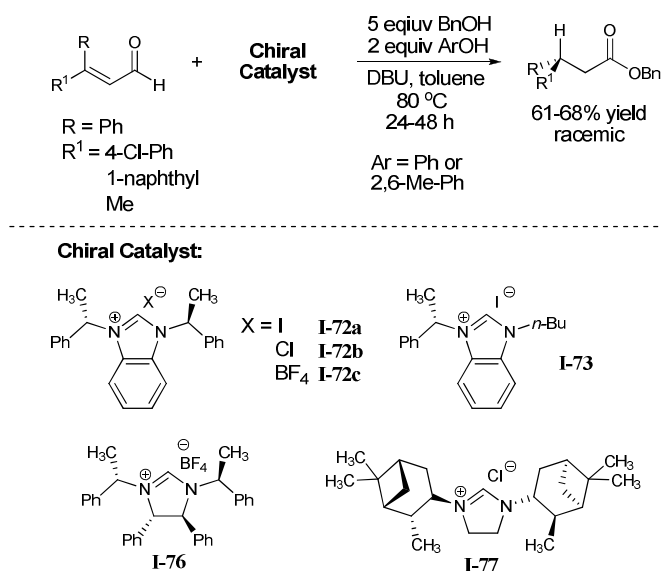
Scheme 1-21. NHC-catalyzed kinetic resolution of secondary alcohols



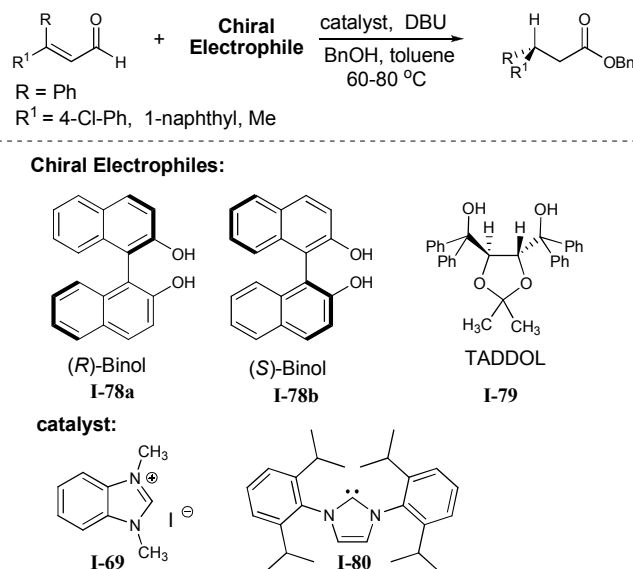
1.4.6 Asymmetric Homoenolate Protonation

In addition to using the chiral benzimidazolium salts **I-72a-c** and **I-73** to kinetically resolve 1-phenylethanol, we also attempted to use the chiral precatalysts to asymmetrically protonate the homoenolate intermediate when starting with β,β -disubstituted enals (Scheme 1-22). Three different β,β -disubstituted enals were synthesized from commercially available starting materials and were tested with six imidazolium salts in the presence of a proton source and benzyl alcohol. We found that catalysts **I-72a-c** and **I-73** produced the desired products in moderate yields but as a racemic mixture. We postulate that the chirality on the azolium salt does not extend to the β -position of the enal to provide any selectivity. Catalysts **I-76** and **I-77** resulted in no product formation. From the data we conclude that it is important to use unsaturated imidazolium salts instead of a saturated imidazolium salt as the precatalyst to promote the protonation of the homoenolate intermediate.

Scheme 1-22. Asymmetric protonation with chiral NHCs



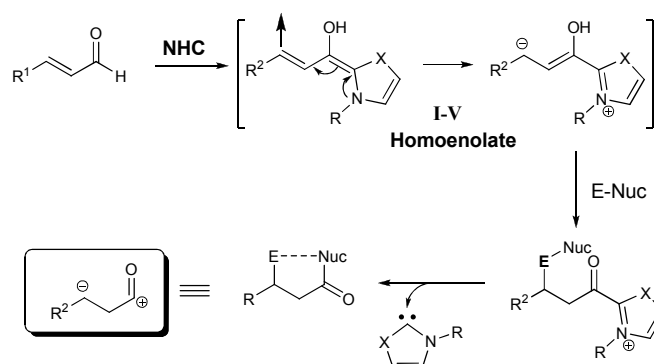
In addition to trying to protonate the β -position enantioselectively, with chiral imidazolium salts, we also used a chiral proton source to achieve this goal (Scheme 1-23). We postulated that a chiral proton source, such as enantioenriched BINOL **I-78** or TADDOL **I-79**, can provide selective protonation of the homoenolate intermediate. We first tested with the *R* and *S* enantiomers of BINOL and catalyst **I-69** with DBU as base and anticipated that the chiral aryl alcohol will be acidic enough to protonate. The reaction was allowed to proceed for several days, and we observed mainly starting material and a small amount of product. When TADDOL was employed, the same result as BINOL was observed. One factor that we considered was that neither the BINOL nor the TADDOL were responsible for the small amount of protonation but instead it may be the benzyl alcohol or the conjugate acid of the base, DBU, promoting the protonation. To probe these possibilities, a control was performed with catalyst **I-69**, DBU, β,β -disubstituted enal (Ph, 4-Cl-Ph), and BnOH in toluene, and it was observed that a small amount of product was indeed produced. Additionally, to test the possibility that the conjugate acid of the base was performing the protonation, we also tested the free-carbene, catalyst **I-80**. With the free-carbene as catalyst, no base is necessary, and if the free-carbene catalyzes the reaction, then the conjugate acid of the base is not the proton source of the reaction. We observed no reaction when catalyst **I-80** was used in the reaction, which suggests that the conjugate acid may contribute to the protonation step.

Scheme 1-23. Asymmetric protonation with chiral proton source

1.5 Attempts to Expand the Homoenolate Reaction with New Acceptors

1.5.1 Examination of New Electrophiles and Dipolarophiles for NHC-Catalyzed Homoenolate Reactions

To expand the utility of the NHC-catalyzed homoenolate reactions, we examined a variety of different electrophiles or dipolarophiles as acceptors to the homoenolate intermediate. We envisioned that these nucleophilic organocatalytic transformations have immense potential, since the homoenolate intermediate (**I-V**) can be viewed as a unique dipole with nucleophilicity initially at the β -carbon and subsequent electrophilicity at the original carbonyl carbon (Scheme 1-24). This reactivity pattern can be used with a variety of electrophilic species as secondary electrophiles to undergo different reaction manifolds. One example is cycloaddition processes in which imines, ketones, activated alkenes and alkynes could cyclize with the homoenolates to give γ -lactams, γ -lactones, cyclopentanones, and cyclopentenones, respectively.

Scheme 1-24. General dipolar reactivity pattern for NHC-generated homoenolates

We first investigated whether imines are competent substrates to cyclize with the homoenolate intermediates to give γ -lactams (Table 1-5, entries 1-5). We tested several different types of imines that have various substituents on the nitrogen including aryl, alkyl, phosphoryl, and sulfonyl. Aryl and alkyl substituted imines resulted in hydrolysis of the imines to benzaldehyde and the corresponding amines. The more electrophilic phosphoryl and sulfonyl imines resulted in no product formation. The reason for this observation is that the NHC adds to the imines irreversibly, resulting in consumption of the catalyst.

Different alkylidene malonates were examined next with the anticipation that they would cyclize with the NHC-generated homoenolates to give substituted cyclopentanone products (entries 6-10). However, after surveying several different catalysts (**I-68**, **I-69**, and **I-81**) with variously substituted alkylidene malonates, no products were observed.

In addition to imines and alkylidene malonates, we also examined conjugate acceptors (Table 1-5, entries 11-13). Catalysts **I-69** or **I-82** resulted in no reaction with these electrophiles. However, a small amount of the γ -lactone of the enal is observed when using catalyst **I-81** in the reaction. The γ -lactone is formed via a homoenolate addition to the carbonyl of a second equivalent of the enal. This is a common occurrence when the acceptor is not as electrophilic as

the α,β -unsaturated aldehyde, resulting in homoenolate addition to the enal instead of the acceptor. An activated alkyne such as DMAD, was also examined with NHC-generated homoenolates (entry 14) to potentially give cyclopentenones, but the reaction did not proceed at all.

Table 1-5. Examination of new acceptors for homoenolate reactions

$\text{R}-\text{CH}=\text{CH}-\text{CHO} + \text{E-Nuc} \xrightarrow[\text{THF or toluene}]{10-20 \text{ mol \% catalyst, DBU}} \text{R}-\text{CH}(\text{E})-\text{CH}(\text{Nuc})-\text{CHO}$			
<div style="display: flex; justify-content: space-around; align-items: center;"> <div style="text-align: center;"> I-68 </div> <div style="text-align: center;"> I-69 </div> <div style="text-align: center;"> I-81 </div> <div style="text-align: center;"> I-80 </div> <div style="text-align: center;"> I-82 </div> </div>			
entry	E-Nuc	catalyst	expected product
1	R ¹	I-69, I-81, I-80	
2	Ph	I-69, I-81	
3	CH ₂ Ph	I-69	
4	P(O)(OEt) ₂	I-69	
5	P(O)Ph ₂	I-69, I-81	
6	SO ₂ Ph	I-69	
7	Ph	I-69, I-81	
8	4-NO ₂ -Ph	I-68, I-69, I-81	
9	4-OMe-Ph	I-68, I-69, I-81	
10	NH ₂	I-68, I-69, I-81	
11	EtO ₂ C	I-69, I-81, I-82	
12	Ph	I-69	
13	Ph	I-69	
14	MeO ₂ C	I-69, I-81	
15	Ph	I-69, I-81, I-80	
16	PhO-Si(CH ₃) ₂ -t-Bu	I-69, I-81, I-80	
17	O	I-80	

Besides cycloaddition processes with homoenolates, we also explored another reaction manifold in which the secondary electrophile and nucleophile can be decoupled from the same

reacting species to add to the unique dipolar reactivity pattern of the homoenolate intermediates. Such reacting partners that were tested include sulfides and silyl-protected nucleophiles (Table 1-5, entries 15-17). When testing diphenylsulfide, we thought that upon addition of the homoenolate to the sulfide, an aryl thiol would be produced that could attack the acyl azolium intermediate to give the thioester product and regenerate the catalyst. Unfortunately, this reaction did not proceed. As with the silyl-protected phenol and morpholine, it was envisioned that the silyl group would react similarly as an alcohol, the silyl group would be attacked by the homoenolate, and the resulting phenoxide and morpholine would serve as the nucleophile to form the phenyl ester and morpholine amide products and regenerate the catalyst. Again, both silyl protected substrates gave no desired product.

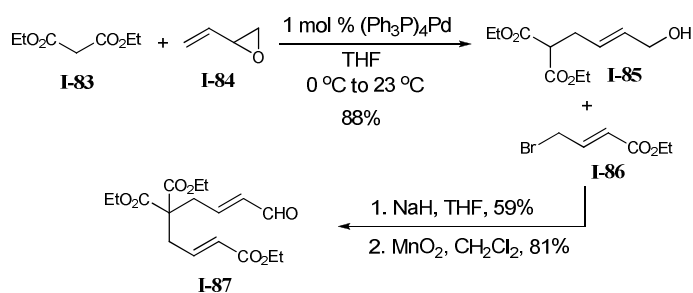
After examining a variety of secondary electrophiles as homoenolate acceptors, it was clear that the challenge with NHC catalysis is the presence of two distinct electrophiles during a reaction, the α,β -unsaturated aldehyde and the homoenolate acceptor. A productive reaction requires a unique balance of the electronics of the two electrophiles used in the reaction. This process must allow for selective interaction between the carbene and the α,β -unsaturated aldehyde. Irreversible addition of the carbene catalyst to the secondary electrophile (e.g. the homoenolate acceptor) would result in no reaction. On the other hand, if the secondary electrophile is not as electrophilic as the enal, then the generated homoenolate can add to a second equivalent of the α,β -unsaturated aldehyde instead of the secondary electrophile, resulting in the formation of γ -lactones instead of desired product.

1.5.2 Intramolecular Homoenolate Reactions

We have demonstrated that homoenolate equivalents could be generated via NHC-catalysis and undergo an internal redox reaction in the presence of alcohols. However, intermolecular addition of the homoenolates to a variety of different acceptors proved to be difficult thus far, because a unique balance of electronics between the two electrophiles is necessary for the reaction to occur. Next, we decided to explore homoenolate additions in an intramolecular fashion to afford highly complex bicyclic carbocycles.

The first substrate that was synthesized for an intramolecular homoenolate reaction was substrate **I-87** (Scheme 1-25). The substrate is readily available after three simple manipulations starting from commercially available butadiene monoxide (**I-83**) and diethyl malonate (**I-84**). The intermediate **I-85** can be made in good yield via a palladium catalyzed alkylation of diethyl malonate with butadiene monoxide. A second alkylation with bromocrotonate (**I-86**), followed by oxidation of the resulting allylic alcohol with MnO_2 produces substrate **I-87**.

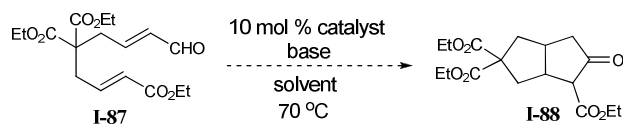
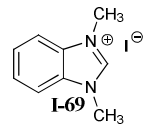
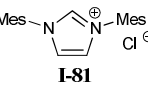
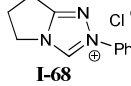
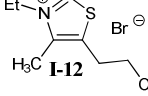
Scheme 1-25. Synthesis of homoenolate intramolecular substrate **I-87**



With access to substrate **I-87**, we began to test whether an intramolecular homoenolate cycloaddition reaction can be effected to provide the bicyclic compound **I-88** (Table 1-6). Four different heteroazolium salts were examined as catalyst with either DBU or KHMDS as base and

10:1 THF/*t*-BuOH or benzene as solvent. Catalyst **I-69** and **I-81** would afford 10-20% yield of a new compound (entries 1-5). Although we were unable to identify the structure of the new compound, we were fairly certain that it was not the desired carbocycle product **I-88**. Catalysts **I-68** and **I-12** did not catalyze the reaction at all; only starting enal **I-87** remained as determined by ^1H NMR spectroscopy (entries 6-7).

Table 1-6. Catalyst survey for intramolecular homoenolate reaction with **I-87**

 <p style="text-align: center;"> <chem>CCOC(=O)C(=O)C=CC=CC=O</chem> $\xrightarrow[70\text{ }^\circ\text{C}]{10\text{ mol \% catalyst, base, solvent}}$ <chem>CCOC(=O)C1CCC2C(=O)C(=O)CC12</chem> </p> <p style="text-align: center;">I-87 I-88</p>			
entry	catalyst	base	solvent
1	 <p style="text-align: center;">I-69</p>	DBU	10:1 THF/ <i>t</i> -BuOH
2		KHMDS	benzene
3			10:1 THF/ <i>t</i> -BuOH
4	 <p style="text-align: center;">I-81</p>	DBU	10:1 THF/ <i>t</i> -BuOH
5		KHMDS	10:1 THF/ <i>t</i> -BuOH
6	 <p style="text-align: center;">I-68</p>	DBU	10:1 THF/ <i>t</i> -BuOH
7	 <p style="text-align: center;">I-12</p>	DBU	10:1 THF/ <i>t</i> -BuOH

Concurrent with the above intramolecular experiments, we also proposed to synthesize compounds **I-89** and **I-90** and carry out the NHC-catalyzed intramolecular cyclization, which can produce bicyclic heterocycles **I-91** (Figure 1-6). Attempts to synthesize both enals via alkylation methods were unsuccessful.

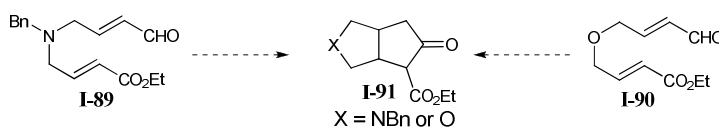
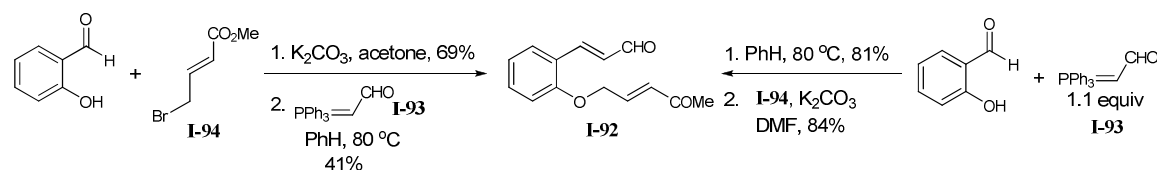


Figure 1-6. Intramolecular substrates with heteroatom backbone

The aspiration to discover an intramolecular homoenolate reaction was not completely discouraged by the initial unsuccessful attempts. We next focused our attention towards the synthesis of substrate **I-92** (Scheme 1-26). The first attempt involved *O*-alkylation of salicylaldehyde followed by a Wittig reaction to give the enal. This route was initially taken because it was postulated that the presence of the phenol functionality may become problematic for the Wittig reaction. Since the yields via the initial route were moderate, reversing the two steps actually improved the overall yield of the reaction. Using only 1.1 equivalents of the Wittig reagent (**I-93**), the enal was obtained in good yields, and after minor optimization of the alkylation step, substrate **I-92** was obtained in an improved overall 68% yield.

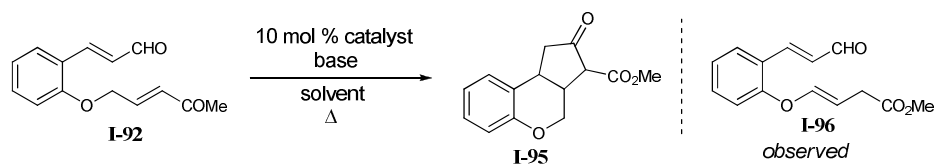
Scheme 1-26. Second generation of enals for intramolecular homoenolate reactions

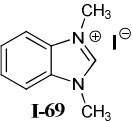
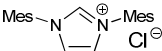
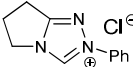
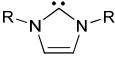
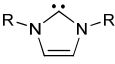


With substrate **I-92** in hand, we first screened for the optimal catalyst that would promote the intramolecular homoenolate cyclization reaction (Table 1-7). Catalysts **I-69**, **I-81** and **I-68** were tested along with different bases and solvents (entries 1-15). It was observed that the reaction did not produce the desired product **I-95** but instead a small quantity of the isomerized

starting material **I-96**. After a quick investigation in the literature, we found that this observation is not surprising, since Sunitha and Balasubramanian⁶⁷ have reported that methyl γ -aryloxycrotonates can easily isomerize to the β,γ -unsaturated derivative of methyl γ -aryloxycrotonates under thermal conditions and in the presence of a mild base, such as K_2CO_3 . Even though we observed mostly isomerized side product, we were able to isolate 7% of the desired product under the reaction conditions specified in entry 2.

After realizing that the use of base causes the isomerization of the starting material, carbenes were directly employed in the reaction instead of the typical *in situ* generation of the carbene under basic conditions (entries 16-17). Unfortunately, carbene **I-80** resulted in no formation of either the desired product or the isomerized side product. Carbene **I-97** only produced the isomerized side product.

Table 1-7. Catalyst survey for intramolecular homoenolate reaction with **I-92**

entry	catalyst	base	solvent
1	 I-69	DBU	PhH
2		KHMDS	THF
3			PhH
4		KHMDS, 18-c-6	THF
5		KOtBu	THF
6		KOtBu, 18-c-6	THF
7		KH	THF
8		KH, 18-c-6	THF
9		Et ₃ N	THF
<hr/>			
10	 I-81	DBU	THF/tBuOH
11		KHMDS	THF
12		Et ₃ N	THF
<hr/>			
13	 I-68	DBU	THF/tBuOH
14		KHMDS	THF
15		Et ₃ N	THF
<hr/>			
16	 I-80	R = 2,6-diisopropyl phenyl	THF
<hr/>			
17	 I-97	R = adamantyl	THF

1.5.3 Attempts to Develop New Homoenolate Precursors

Nature's precursor to an acyl anion is an α -keto acid in which in the presence of thiamine diphosphate converts pyruvic acid to acetyl-CoA via a carbonyl anion intermediate. Inspired by this enzymatic transformation, we envisioned that α -keto carboxylates (**I-98**) and α -keto acids (**I-99**) could be competent homoenolate precursors where the generated acyl anion would be extended to the β -carbon (Figure 1-7). Additionally, our group has reported that acylsilanes are competent carbonyl anion precursors when using thiazolium-derived carbenes as catalyst. Therefore, efforts were made towards the synthesis of **I-100** as a homoenolate precursor.

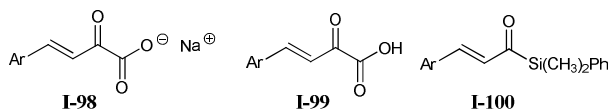
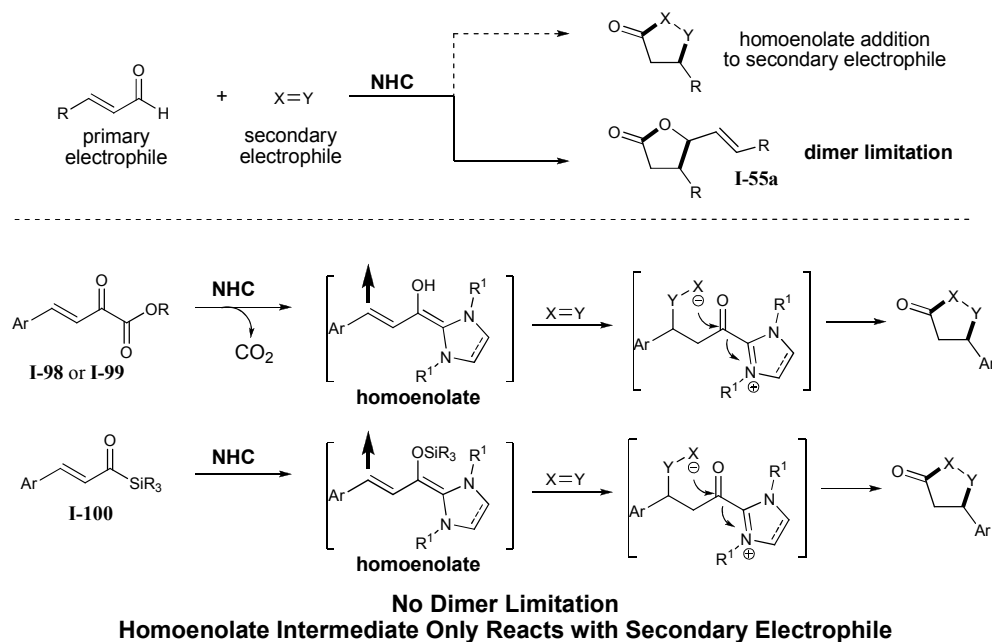


Figure 1-7. Homoenolate precursors other than α,β -unsaturated aldehyde

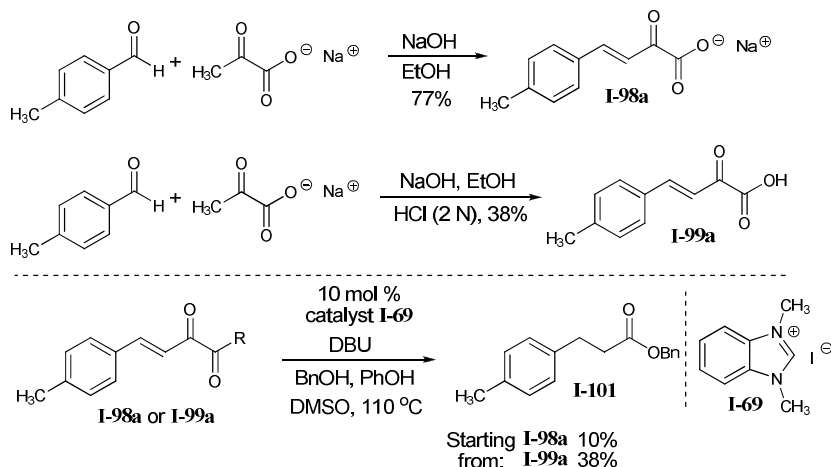
An important reason to develop new homoenolate precursors is to eliminate the use of an α,β -unsaturated aldehyde as the homoenolate precursor (Scheme 1-27). Employing an aldehyde as the nucleophilic precursor can be complicated by the intrinsic high reactivity of the aldehyde because the homoenolate intermediate can undergo addition to the starting aldehyde, thereby affording self-condensation products (**I-55**). Utilizing a homoenolate precursor that does not possess the aldehyde removes the reactive moiety from the reaction completely. In general, this strategy allows for a broad inclusion of many classes of electrophiles, and the homoenolate generated *in situ* would not compete between addition to the desired substrate and addition to the aldehyde precursor.

Scheme 1-27. Reason to develop new homoenolate precursors

To begin our investigations we first required efficient methods to access the α -keto acids, α -keto carboxylates and acyl silanes. The α -keto acids and α -keto carboxylates were prepared according to previously published procedures by Saba and co-workers⁶⁸ (Scheme 1-28). In these approaches, the carboxylates (**I-98**) were easily obtained via an aldol condensation between the aldehyde and the sodium pyruvate salt. Additional treatment of the α -keto carboxylate with 2 N HCl produces the α -keto acid (**I-99**). Although we were successful in synthesizing the α -keto carboxylate and acid, the use of either one as the homoenolate precursor proved to be difficult due to their extreme insoluble nature. The α -keto carboxylate **I-98a** and α -keto acid **I-99a** were insoluble in most solvents except in DMSO, which required heating to 110 °C to go into solution. The reactivity of the carboxylate and acid as the homoenolate precursor were explored with the homoenolate protonation conditions previously developed except toluene was replaced by DMSO as the solvent. The yields for the α -keto carboxylate and the α -keto acid as the

umpolung precursors to produce the benzyl ester were 10% and 38%, respectively. The low yields may be due to the change in solvents. Although it was disappointing, we continued to test the α -keto acid as the homoenolate precursor with different imines and alkylidene malonates, but, unfortunately, no desired products were observed for any of the reactions.

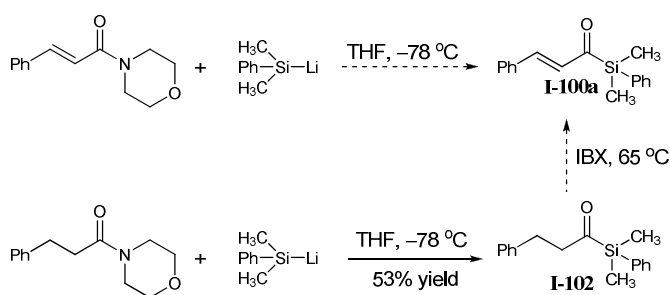
Scheme 1-28. Preparation and exploration of α -keto acid and α -keto carboxylate as homoenolate precursors



We next turned our attention to the synthesis of α,β -unsaturated acyl silanes (**I-100**). We initially thought that we could apply the method for the synthesis of alkyl silanes developed in our laboratory⁶⁹ towards the synthesis of our desired acyl silanes. The addition of dimethylphenyl silyl lithium to an α,β -unsaturated morpholine amide in THF at -78 °C should provide the corresponding acyl silane **I-100a** (Scheme 1-29). Unfortunately, these conditions resulted in no reaction. However, under the same conditions using hydrocinnamyl morpholine amide, we attained a 53% yield of the alkyl acyl silane **I-102**, and we proceeded to oxidize it to the desired α,β -unsaturated acyl silane by a method developed in the Nicolaou laboratory.⁷⁰

When the alkyl acyl silane was heated to 65 °C in the presence of IBX, the substrate decomposed to unidentifiable compounds. Although there are published methods⁷¹⁻⁷³ to access the unsaturated acyl silane, we decided that the number of steps required to generate these potential substrates was prohibitive.

Scheme 1-29. Preparation of a α,β -unsaturated acyl silane

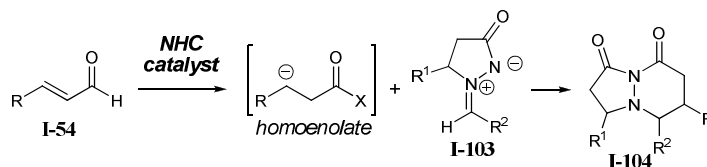


1.6 A Formal [3+3] Cycloaddition Reaction between NHC-Generated Homoenolates and Azomethine Imines

The successful conversion of α,β -unsaturated aldehydes to saturated esters via protonation of homoenolates, from the previous study, confirmed that NHCs can promote the generation of homoenolates and subsequently add to electrophiles. Although the experiments following this initial report were met with limited success, we continued to focus our efforts to discover novel reactions with NHC-generated homoenolates. We next turned our attention towards developing a formal intermolecular [3+3] cycloaddition reaction between homoenolate equivalents and 3-oxopyrazolidin-1-ium-2-ides (**I-103**) (known as an azomethine imine) (Scheme 1-30). This cycloaddition process would provide a direct synthesis of bicyclic

pyridazinones (**I-104**); to our knowledge, this structural motif has not yet been reported in the literature.

Scheme 1-30. NHC catalyzed homoenolate addition to azomethine imines



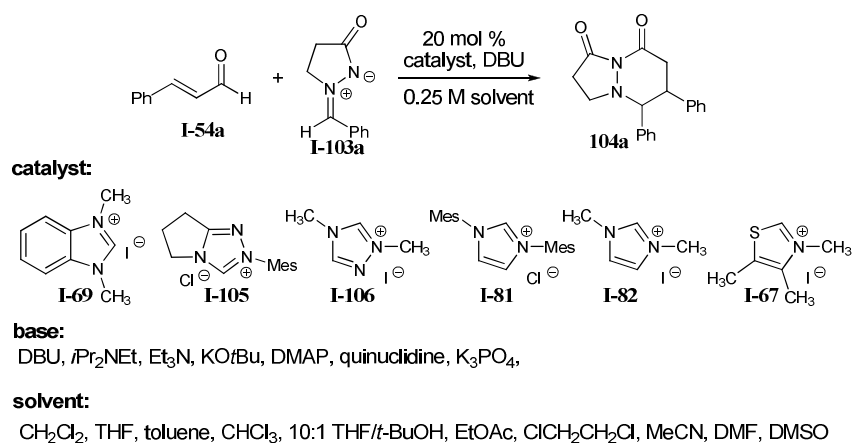
Intermolecular cycloadditions are powerful methods for the convergent synthesis of cyclic compounds from simple precursors.^{74, 75} While major advances have been made in the area of metal-catalyzed cycloadditions over the past decade,⁷⁶⁻⁸¹ there is a great potential for these reactions using organic molecules as catalysts.⁸²⁻⁸⁶ In 1968, Dorn and co-workers demonstrated that 3-oxopyrazolidin-1-ium-2-ides (**I-103**) are stable and easily handled compounds.⁸⁷⁻⁸⁹ Fu,^{90, 91} Hayashi,⁹² and Suga⁹³ have separately shown that these compounds are efficient substrates in metal-catalyzed cycloadditions to furnish five- and six-membered heterocycles.

1.6.1 Optimization of Homoenolate Additions to Azomethine Imines

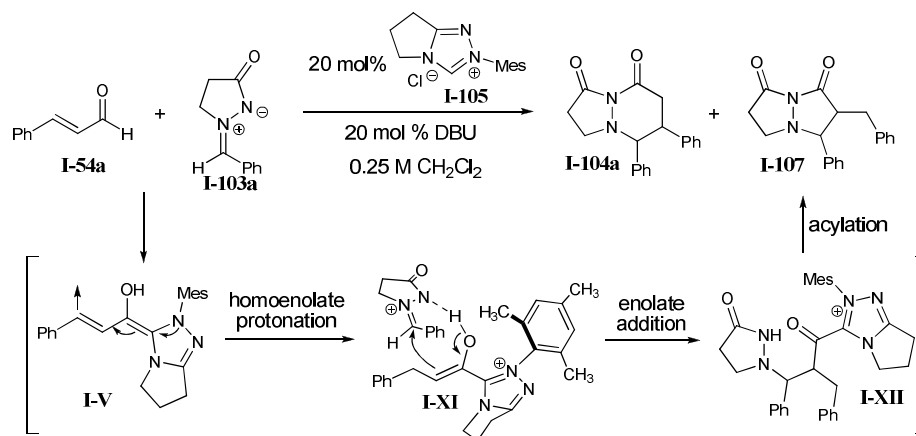
Our investigation of NHC-catalyzed homoenolate additions to azomethine imines began with a survey of reaction conditions by varying the catalyst, base and solvent of the reaction (Scheme 1-31). The azomethine imine **1-103** was easily accessible by following methods disclosed by Fu^{90, 91} and Hayashi⁹² in which benzaldehyde and 3-pyrazolidinone are condensed

in a concentrated solution of methanol. An intensive investigation of the three variables revealed that the best combination was with catalyst **I-69**, DBU as base and CH_2Cl_2 as solvent to produce the bicyclic product **I-104a** in a 37% yield as a single diastereomer.

Scheme 1-31. Early examination of formal [3+3] cycloaddition reactions between homoenolates and azomethine imine **I-103a**



While surveying the different catalysts, we observed that catalyst **I-105** not only catalyzed the formation of the homoenolate cyclized product **I-104a** but also the enolate cyclized product **I-107** (Scheme 1-32). X-ray crystallography was used to confirm the structure of the enolate cyclized product (**I-107**). The NHC-generated homoenolate can be protonated (**I-V**) to subsequently form the enolate intermediate (**I-XI**), which would then add to the azomethine imine to yield the acylazolium intermediate (**I-XII**). Formation of the final product (**I-107**) and regeneration of the catalyst can be achieved by an intramolecular acylation of the amide nitrogen. The amount of observed enolate cyclized product was less than 26%. Further optimization is necessary to selectively synthesize the enolate cyclized product (**I-107**) via this formal [3+2] cycloaddition process.

Scheme 1-32. Observation of formal [3+2] cycloaddition product

Since the best combination of catalyst, base and solvent did not produce an optimal yield of the homoenolate cyclized product (**I-104a**), a thorough examination of the reaction was warranted. An observation made while monitoring the reaction closely was that the reaction stalled after 4 hours. We postulated that the catalyst could have added irreversibly to the azomethine imine, and thus no longer participated in catalyzing the reaction. To test this hypothesis, a ^1H NMR spectroscopy experiment was performed in which the 1,3-dimethylbenzimidazolium iodide salt **I-69**, azomethine imine **I-103a**, and DBU were dissolved in CDCl_3 and cinnamaldehyde was excluded (Figure 1-8). After only 10 minutes, the signal for the imine proton decreased while formation of new peaks was observed on the ^1H NMR spectrum. The data confirm our hypothesis that the carbene is adding to the azomethine imine irreversibly. To exclude the possibility that DBU instead of the carbene was adding to the imine, an additional ^1H NMR experiment was done in which the azomethine imine and DBU were

mixed in CDCl_3 . It was observed that DBU does not interact with the azomethine imine because the ^1H NMR spectrum did not change over 24 h.

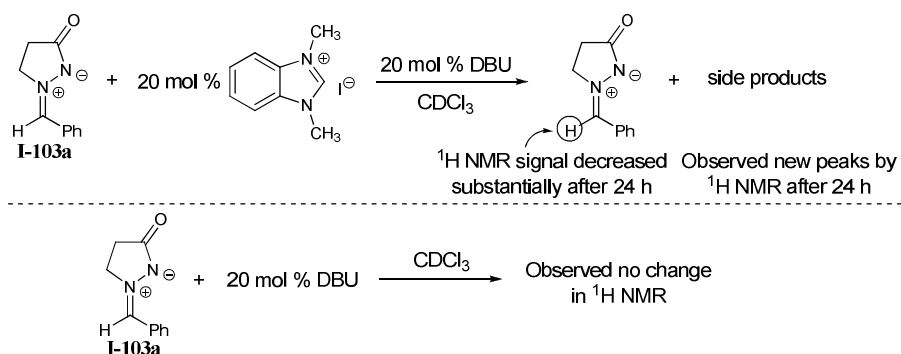


Figure 1-8. ^1H NMR experiments confirmed the irreversible addition of the NHC to the azomethine imine

To minimize the interaction between the carbene and azomethine imine, we thought a larger substituent on the nitrogen of the benzimidazolium salt should favor interaction with the less hindered α,β -unsaturated aldehyde over the azomethine imine (Figure 1-9). Syntheses of three azolium salts were attempted using slightly modified methods (modifications will be discussed in Chapter 3) reported by Diver and coworkers.^{65, 66} Synthesis of benzimidazolium salt **I-108** was not possible because the *N,N'*-dimesityl-1,2-diaminobenzene precursor was too sterically hindered for ring closure to give the salt product. However, syntheses of both 1,3-diphenylbenzimidazolium chloride **I-109** and *N*¹-mesityl-*N*³-methylbenzimidazolium iodide **I-110** proceeded smoothly.

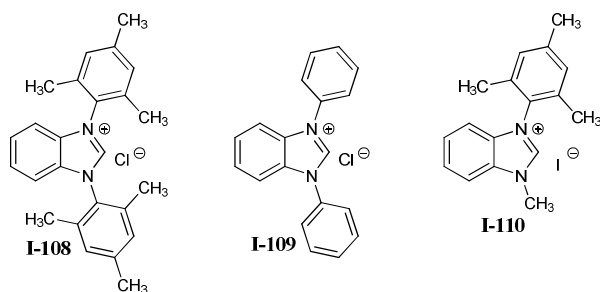


Figure 1-9. New benzimidazolium salts with larger substituents

When we subjected catalysts **I-109** and **I-110** to reaction conditions, catalysts **I-109** did not catalyze the reaction, while catalyst **I-110** produced a 36% yield of the pyridazinedione product **I-104a**. The same ^1H NMR experiment carried out with catalyst **I-69** (Figure 1-8), was performed with the new catalyst **I-110**, and it was found that the addition of the carbene to the azomethine imine does occur but at a slower rate. From the experiment, we concluded that the increased size of the substituent on the catalyst may slow the rate of addition of the carbene to the imine, and the yield still required improvement.

Our next idea was to alter the azomethine imine component to improve the reaction. We hypothesized that if a substituent is placed at C_5 of the pyrazolidinone ring, the aryl group on the imine would be away from the C_5 substituent to minimize steric interactions (Figure 1-10). The additional bulky groups on the azomethine imine can possibly minimize the interactions with the NHC. We then set forth to synthesize azomethine imines with alkyl or aryl substituents at the C_5 position of the pyrazolidinone ring. Unfortunately, alkyl substitution resulted in no reaction (substrates **I-111** to **I-113**). However, with a phenyl group at the C_5 position (**I-114**), a 39% yield of the product was isolated using **I-110** as the catalyst. Since the C_5 -phenyl-substituted azomethine imine is more soluble than other azomethine imines, we decide to further optimize the reaction with substrate **I-114**.

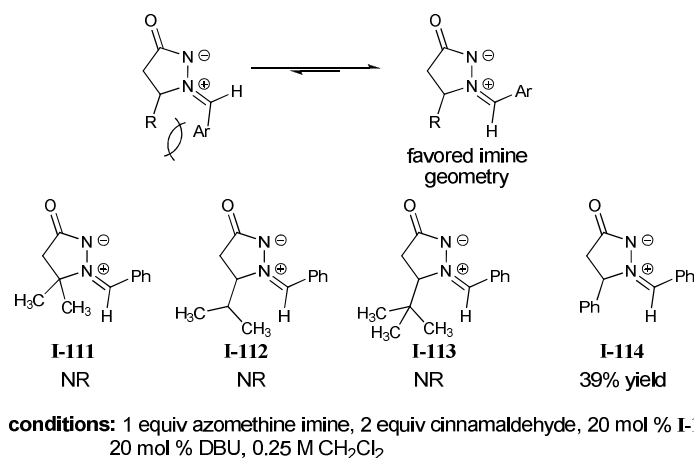


Figure 1-10. Examination of new azomethine imines with substitution at C₅

Examination of azomethine imine **I-114a** with cinnamaldehyde **I-54a**, and heteroazolium salts **I-69**, **I-105** and **I-110** revealed that all three precatalysts produced desired product **I-115a** as a single diastereomer (Table 1-8). While benzimidazolium salt **I-105**, afforded the highest yield (39%, entry 3), the process clearly required improvement. Reactions in THF required heating to induce homogeneity (entries 4 and 5) but did not improve the yields compared to CH₂Cl₂. Careful monitoring of the reaction revealed that shorter times (3 vs. 24 h) significantly improved the yield of **I-115a** because as the reaction progressed, the product may have decomposed (entries 6 and 7). Additionally, increasing the temperature of the reaction to 40 °C favors the [3+3] cycloaddition manifold with a further increase in yield (79%, entry 8). With these temperature parameters identified, an extensive examination of different azolium salts confirmed that the placement of a single *N*-mesityl substituent on the benzimidazole core is necessary for good yields. Decreasing the catalyst loading of **I-110** decreases the yield of **I-115a** to 46% (entry 9).

Table 1-8. Optimization of homoenolate addition to azomethine imine **I-114**

c1ccc(cc1)/C=C/C=O (**I-54a**) + c1ccc(cc1)C2C(=O)N([C-])C2=Cc3ccccc3 (**I-114a**) $\xrightarrow[20\text{ mol \% DBU}]{20\text{ mol \% NHC catalyst}}$ c1ccc(cc1)C2C(=O)N(C2C(=O)N3C(=O)C(=C(c4ccccc4)C3)c5ccccc5)C6C(=O)N([C-])C6=Cc7ccccc7 (**I-115a**)

entry	catalyst	conditions	yield (%)	d.r.
1	I-81	CH ₂ Cl ₂ , 23 °C, 24 h	35	>20:1
2	I-69	CH ₂ Cl ₂ , 23 °C, 24 h	29	>20:1
3	I-110	CH ₂ Cl ₂ , 23 °C, 24 h	39	>20:1
4	I-110	THF, 50 °C, 24 h	15	>20:1
5	I-110	10:1 THF/ <i>t</i> BuOH, 50 °C, 24h	23	>20:1
6	I-110	CH ₂ Cl ₂ , 23 °C, 3 h	45	>20:1
7	I-110	10:1 THF/ <i>t</i> BuOH, 50 °C, 3h	59	>20:1
8	I-110	CH ₂ Cl ₂ , 40 °C, 2 h	79	>20:1
9	I-110	CH ₂ Cl ₂ , 40 °C, 2 h	46	>20:1

catalyst:

I-81

I-69

I-110

1.6.2 Reaction Scope of Homoenolate Additions to Azomethine Imines

With the optimal parameters established for this formal [3+3] cycloaddition process, we turned our attention to investigate the scope of this reaction (Table 1-9). A survey of α,β -unsaturated aldehydes revealed that the process accommodates electron-donating groups on the aryl ring (entries 1-5); however, electron-withdrawing groups on the aryl ring (entry 8) do not yield products. The reaction also tolerates β -alkyl substituents and extended dienylic systems to afford **I-115f** and **I-115g** in moderate yields (entries 6 and 7). An examination of the azomethine imine component indicates that variously substituted aryl groups are competent substrates. Electron withdrawing groups on the aryl ring of the imine afford good to excellent yields of the

pyridazinones (entries 9-12). Placing an electron-donating group on the aryl ring is also a suitable partner (entry 14), albeit in reduced yield (67%). Enolizable substituents, such as cyclohexyl, at R¹ do not afford any pyridazinones and 2-substituted aryl substituents, such as 2-(trifluoromethyl)phenyl, at R¹ resulted in only a moderate yield (41%) of the desired product. However, all productive reactions are highly diastereoselective (>20:1 dr), favoring the all *syn* stereoisomers.

Table 1-9. Examination of the reaction scope of homoenolate addition to azomethine imine

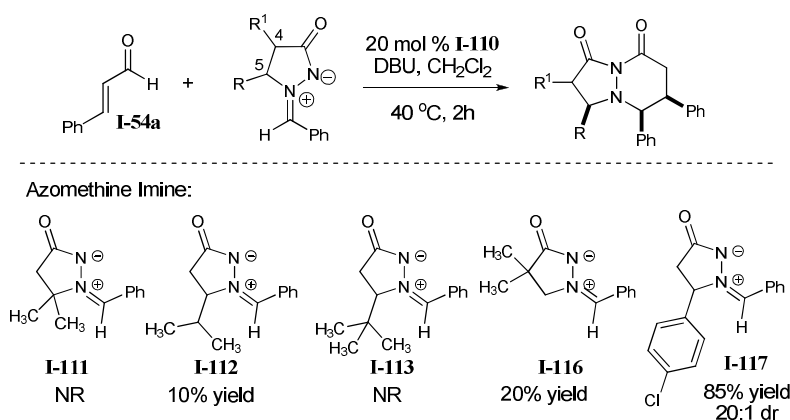
Reaction scheme: $\text{I-54} + \text{I-114} \xrightarrow[40\text{ }^\circ\text{C, 2h}]{20\text{ mol \% I-110, DBU, CH}_2\text{Cl}_2} \text{I-115}$

entry	R	R ¹	product	yield (%)	d.r.
1	Ph	Ph	I-115a	79	>20:1
2	4-OMePh	Ph	I-115b	76	>20:1
3	3-OMePh	Ph	I-115c	79	>20:1
4	2-OMePh	Ph	I-115d	94	>20:1
5	2-naphthyl	Ph	I-115e	77	>20:1
6	CH ₂ CH ₂ CH ₃	Ph	I-115f	67	>20:1
7	HC=CHCH ₃	Ph	I-115g	51	>20:1
8	4-ClPh	Ph	I-115h	0	—
<hr/>					
9	Ph	4-BrPh	I-115i	87	>20:1
10	Ph	4-FPh	I-115j	82	>20:1
11	Ph	3-CF ₃ Ph	I-115k	93	>20:1
12	Ph	3-BrPh	I-115l	78	>20:1
13	Ph	3-CH ₃ Ph	I-115m	76	>20:1
14	Ph	3-OMePh	I-115n	67	>20:1
15	Ph	cyclohexyl	I-115o	0	—

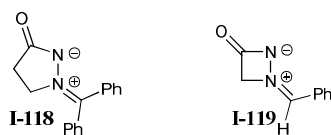
In addition to varying the imine component on the azomethine imine, we also examined azomethine imines with different substituents on the C₄- and C₅-position of the ring under the optimized conditions (Scheme 1-33). With more sterically hindered substituents, such as the geminal dimethyl (**I-111**) or the *tert*-butyl groups (**I-113**) at the C₅-position no pyridazinone was

afforded, while a smaller isopropyl substituent (**I-112**) gave a disappointing 10% yield of the desired bicycle. Placing the geminal dimethyl groups at the C₄-position (**I-116**) resulted in only a 20% yield. However, when an aryl group is at the C₅ position, such as 4-chlorophenyl (**I-117**), the pyridazinone is made in an 85% yield as a single diastereomer. Unfortunately, alkyl substituents on the azomethine imine ring are not favorable for product formation, and further investigation is necessary to understand this result.

Scheme 1-33. Azomethine imine scope with C₄- and C₅-position varied



Azomethine ketimine **I-118** and 1-(phenylmethylene)-3-oxo-1,2 diazetidininium ylide **I-119** were also synthesized and tested under the optimized reaction conditions but resulted in no consumption of starting material (Figure 1-11). The two substrates were synthesized according to a method published by Taylor and coworkers.⁹⁴



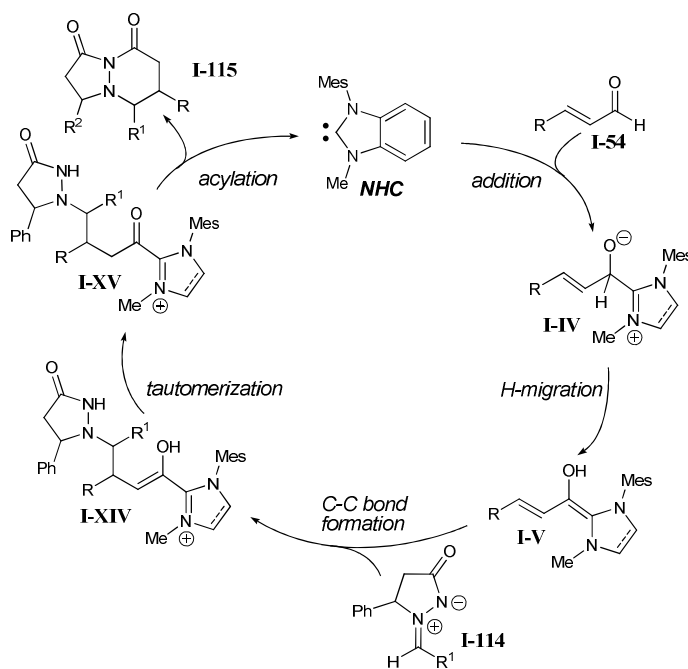
Under optimized conditions with cinnamaldehyde: no reaction

Figure 1-11. Azomethine ketimine and 1,2-diazetidinium ylide

1.6.3 Investigation of Proposed Mechanistic Pathway

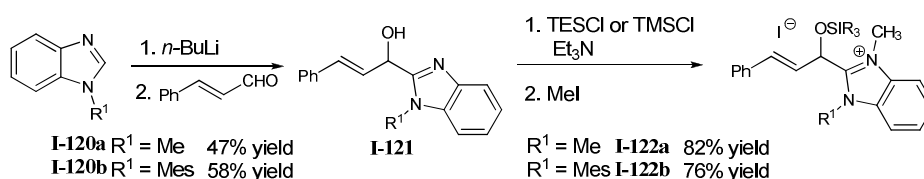
The proposed catalytic pathway for this formal [3+3] cycloaddition reaction involves the addition of an NHC to an α,β -unsaturated aldehyde (**I-54**) to afford the tetrahedral intermediate (**I-IV**), which undergoes proton migration to give the extended Breslow intermediate (**I-V**) (Scheme 1-34). The homoenolate intermediate undergoes addition with the azomethine imine (**I-XIII**) and subsequently generates enol **I-XIV**. After tautomerization of **I-XIV**, the resulting activated heteroazolium species (**I-XV**) releases the NHC catalyst and affords the pyridazinone (**I-115**) by an intramolecular acylation event.

Scheme 1-34. Proposed catalytic pathway of homoenolate addition to azomethine imine



To probe the proposed mechanism of homoenolate additions, we attempted to synthesize a silylated extended Breslow intermediate precursor with a structure similar to **I-IV** in our proposed reaction pathway. Access to compounds similar to **I-IV** would allow us to assess their ability to undergo homoenolate addition reactions and lend support to our proposed catalytic pathway. We postulated that a silylated carbinol should behave similarly to the free hydroxyl carbinol as the precursor to the Breslow intermediate. The synthesis of the silylated extended Breslow intermediate precursor began with lithiation of 1-methylbenzimidazole (**I-120a**) or 1-mesitylbenzimidazole (**I-120b**) at the 2-position using *n*-butyllithium followed by addition of cinnamaldehyde (**I-54a**) (Scheme 1-35).^{95, 96} The resulting purified carbinol (**I-121**) was then protected as a silyl ether. Finally, the benzimidazolium salt was prepared by a straightforward alkylation with neat iodomethane at room temperature. Confirmation of the syntheses of desired silylated carbinol salts, **I-122a** and **I-122b**, was obtained by ¹H and ¹³C NMR spectroscopy.

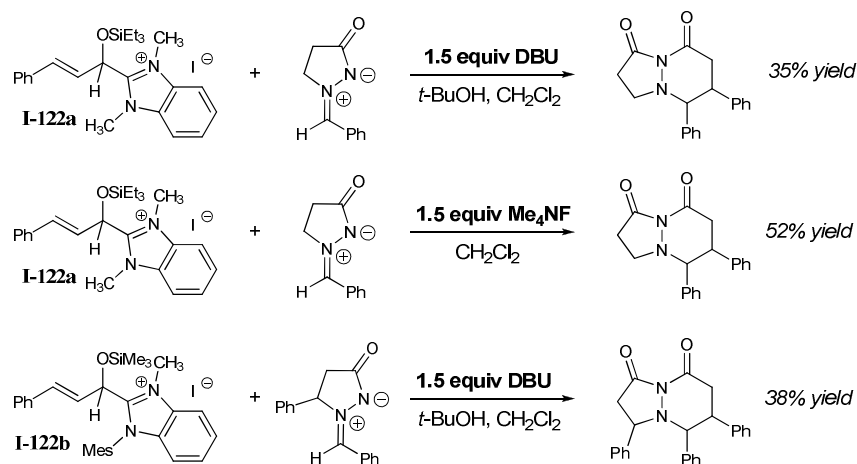
Scheme 1-35. Synthesis of homoenolate intermediate precursor



Conditions for the homoenolate additions with the silylated carbinols were similar to the method developed by Dr. Anita Mattson, who used silylated carbinols as acyl anion precursors. Three experiments were performed in which DBU or tetramethylammonium fluoride (TMAF)

was used to promote the reaction (Scheme 1-36). Under the DBU conditions, *t*-BuOH was added to the reaction to remove the silyl protecting group and DBU would potentially deprotonate the tetrahedral proton to generate the homoenolate intermediate (**I-V**). Under the conditions with tetramethylammonium fluoride, the fluoride source would promote desilylation to give an alkoxide, which would undergo a formal proton migration to afford the extended Breslow intermediate (**I-V**) that subsequently adds to the azomethine imine and undergo the cycloaddition reaction. Gratifyingly, all three reactions gave the desired product. With either DBU or TMAF and **I-122a**, the product was isolated in 35% and 52% yields, respectively, while using **I-122b** under DBU conditions afforded the product in a 38% yield. The success of the experiments provides support for intermediate **I-IV** to participate in the reaction.

Scheme 1-36. Examination of **I-122a** and **122b** in homoenolate addition reactions



1.6.4 Explanation for High Diastereoselectivity for the Formal [3+3] Cycloaddition reaction

The current model for the high levels of *syn* diastereoselectivity for the pyridazinone products invokes a hydrogen bonding assembly between the imine and the carbene-aldehyde

adduct (Figure 1-12). The catalyst structure enforces an extended geometry of the carbene-aldehyde adduct as the *Z*(*O*) enol to minimize interaction between the larger mesityl substituent and the aryl group on the enal (**I-XVI**). To minimize steric interactions, the aryl group on the imine and the phenyl group on the five-membered ring are pointing opposite from one another. Consequently, the nucleophilic intermediate approaches away from the phenyl substituent on the azomethine ring resulting in the overall *syn* diastereoselectivity.

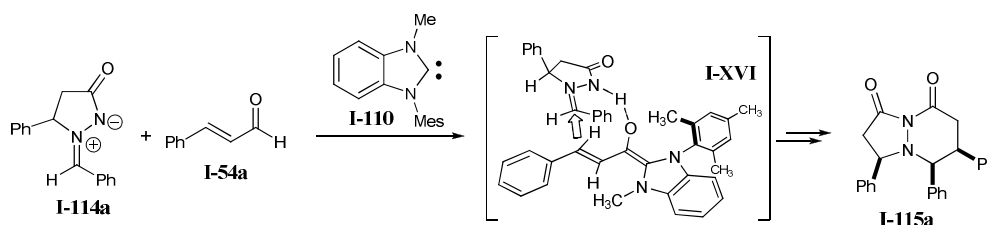
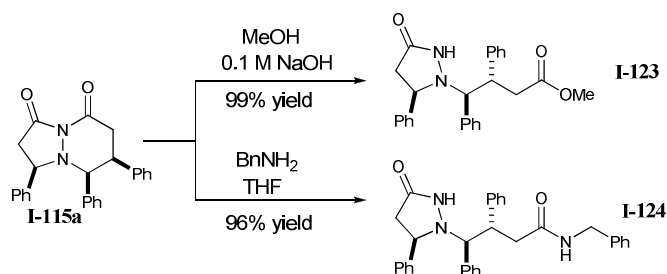


Figure 1-12. Proposed model for homoenolate addition to azomethine imine

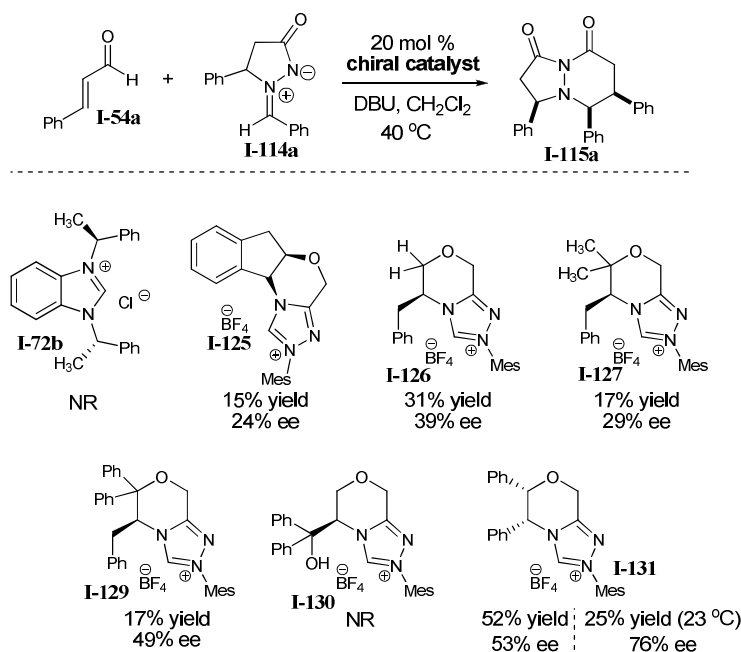
1.6.5 Utility of Pyridazinone Products

Our next goal was to investigate whether we can manipulate the new pyridazinone products into useful synthetic compounds (Scheme 1-37). The first attempt was to cleave the amide bond with a nucleophile. The synthesized pyridazinones can be manipulated to undergo selective 6-membered ring opening products. Accordingly, substituted esters and amides, such as **I-123** and **I-124**, are accessed in excellent yields directly by the addition of methanol or benzyl amine to a solution of the pyridazinones **I-115a**. Only one attempt was made to cleave the *N-N* bond with SmI_2 , and that proved to be unsuccessful. Further processing of these compounds is under investigation.

Scheme 1-37. Selective ring-opening of pyridazinone with nucleophiles

1.6.6 Asymmetric NHC-Catalyzed Homoenolate Addition to Azomethine Imines

The formal [3+3] cycloaddition reaction between NHC-catalyzed generated homoenolates and azomethine imines can be rendered enantioselective by employing a chiral catalyst in the reaction. As shown in Scheme 1-38, several different chiral catalysts were examined. Since the achiral benzimidazolium salt **I-110** was the optimal catalyst for the reaction, we thought the chiral benzimidazolium salt **I-72b** would be an excellent chiral catalyst for the reaction. Disappointingly, catalyst **I-72b** did not afford any product. The synthesis of chiral benzimidazolium salts and imidazolium salts are generally more challenging than the synthesis of chiral triazolium salts. For this reason, our group has a large library of chiral triazolium salts; these were screened under the reaction conditions, and most resulted in product formation with minimal selectivity. Catalyst **I-131** gave the highest selectivity at 76% ee, albeit in a low yield. The requirement to heat the reaction to facilitate catalyst turnover lowers the selectivity, but cooling the reaction to room temperature results in lower yields.

Scheme 1-38. Enantioselective synthesis of pyridazinones

1.7 Amination of Homoenolates Catalyzed by *N*-Heterocyclic Carbenes

The de novo construction of β -amino acids by the direct construction of the C–N bond continues to be an objective because of the continuing utility of these compounds.⁹⁷⁻¹⁰⁴ A conventional method to access these molecules is the conjugate addition of a nucleophilic nitrogen source such as azide or an aliphatic amine to an activated ester or ketone (Figure 1-13).¹⁰⁵⁻¹¹⁵ Alternatively, formal [3+2] reactions with hydroxylamines provide isoxazolidines in which the N–O bond can be easily cleaved.¹¹⁶⁻¹¹⁹ A polarity reversal strategy to access β -amino acid derivatives would employ unusual reactivity patterns, such as homoenolates, in the context of a formal cycloaddition. In this section, we report the catalytic amination of homoenolates by combining α,β -unsaturated aldehydes **I-54** with diazenes in the presence of NHCs to generate pyrazolidinones **I-132** via a formal [3+2] cycloaddition reaction.

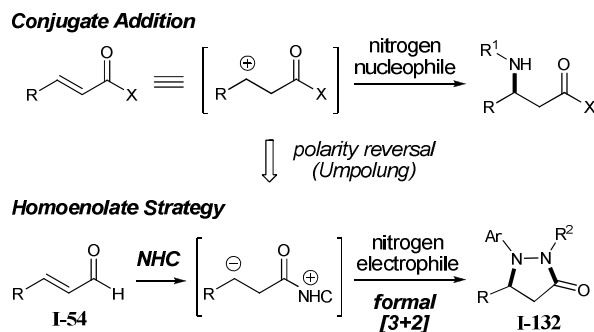
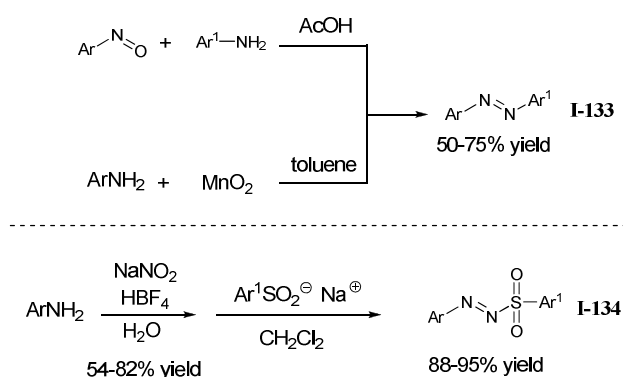


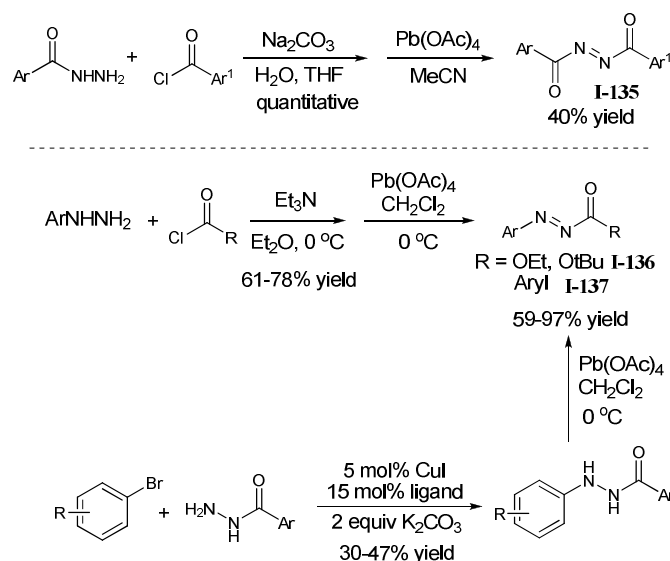
Figure 1-13. Homoenolate amination strategy

1.7.1 Preparation of Diazene Substrates

To begin our investigations on whether diazenes are competent acceptors for homoenolate additions, we first required efficient methods to access a variety of diazenes. Besides diethyl azodicarboxylate (DEAD) which is commercially available, all other diazenes were readily available after one or two step synthetic manipulations (Scheme 1-39). Two methods can be used to synthesize diaryl-substituted diazenes (**I-133**). In the presence of acetic acid, nitrosobenzene can be condensed with arylamines to give diazenes **I-133**.¹²⁰⁻¹²² Additionally, arylamines can be oxidized with MnO₂ and then condensed with itself to give **I-133**.^{123, 124} In the former case the aryl substituents can be different, and in the latter, the aryl groups are the same. The (arenediazosulfonyl)-benzenes **I-134** are remarkably easy to prepare by stirring a suspension of the arenediazonium tetrafluoroborates salt with sodium arylsulfinate in dichloromethane.¹²⁵ The yellow or orange crude solids were obtained in yields ranging from 88-95% and were used without further purification.

Scheme 1-39. Synthesis of azobenzene and (arenediazosulfonyl)-benzene

The preparation of dibenzoyl-substituted diazenes **I-135** was achieved by acylating benzoyl hydrazide with variously substituted benzoyl chlorides followed by oxidation of the disubstituted hydrazine intermediate with $\text{Pb}(\text{OAc})_4$ to the diazene in moderate yield (Scheme 1-40).^{126, 127} The synthesis of 1-carbonyl-2-aryl-substituted diazenes (**I-136** and **I-137**) begins with acylation of an aryl hydrazine followed by oxidation with $\text{Pb}(\text{OAc})_4$.¹²⁸ Since certain aryl hydrazines are not readily available, an alternative method to synthesize 1-benzoyl-2-aryldiazenes was necessary. Utilizing the methodology developed by Buchwald and coworkers, copper can catalyze the *N*-arylation of hydrazide to afford the 1,2-substituted hydrazine intermediate in moderate yields, which can be subsequently oxidized to the corresponding diazenes in good to excellent yields.¹²⁹

Scheme 1-40. Synthesis of acyl-substituted diazenes

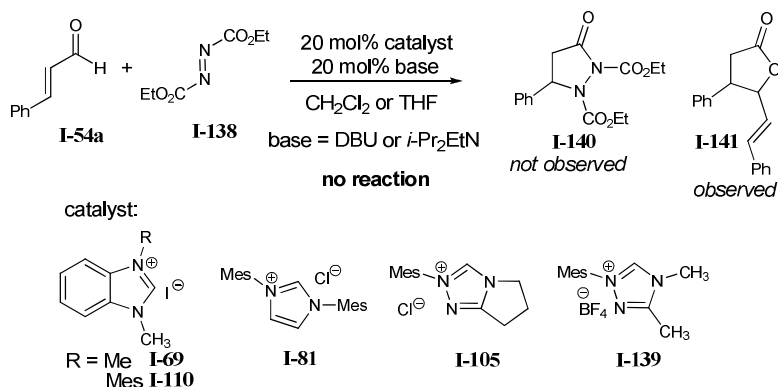
1.7.2 Optimization of the NHC-Catalyzed Amination of Homoenolates

In our previous studies in the area of *N*-heterocyclic carbene catalysis, we have generated new ways to form C-H and C-C bonds by accessing unique homoenolates from α,β -unsaturated aldehydes. In continuing to expand the utility of NHC-catalyzed homoenolate reactions, we also aspired to form a new C-N bond between a homoenolate intermediate and an electrophilic nitrogen source. Homoenolate additions to a nitrogen electrophile would enable the direct preparation of β -amino acid derivatives, which are valuable compounds in synthetic organic and medicinal chemistry.

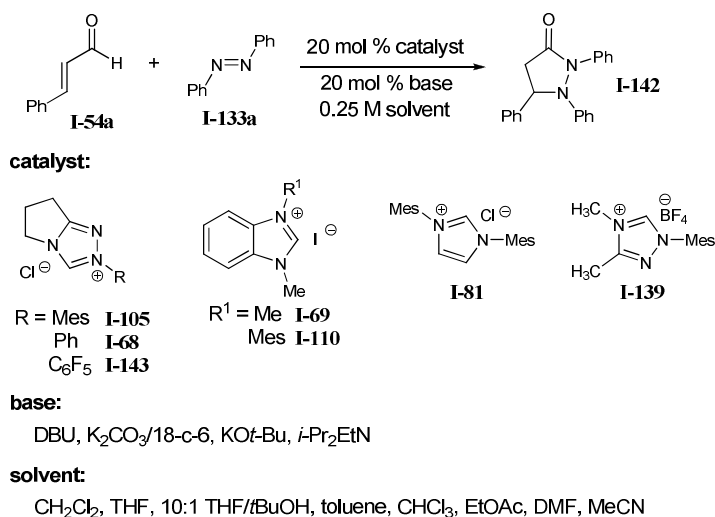
The first goal for the direct amination of homoenolates was to identify a suitable nitrogen-containing electrophile. We began screening cinnamaldehyde (**I-54a**) and DEAD **I-138** with heteroazolium salts **I-69**, **I-81**, **I-105**, **I-110**, and **I-139**, which disappointingly resulted in no desired pyrazolidinone product (**I-140**) (Scheme 1-41). A combination of different solvents

(THF or CH₂Cl₂), bases (DBU or *i*Pr₂Net) and heteroazolium salts resulted in the formation of a small amount of enal-aldehyde cross-condensation γ -lactone (**I-141**) side product.

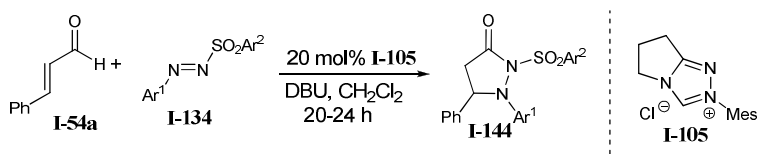
Scheme 1-41. Examination of DEAD as homoenolate acceptor



Following the examination of DEAD as the homoenolate acceptor, 1,2-diphenyl diazene **I-133a**, also known as azobenzene, was investigated (Scheme 1-42). After the first reaction with cinnamaldehyde, azobenzene, heteroazolium salt **I-105** and DBU in dichloromethane, we were delighted to isolate 10% of the desired pyrazolidinone product **I-142**. This encouraging result led us to further investigate the reaction with different heteroazolium salts, bases and solvents. Multiple combinations of the three variables were examined that provided 29% as the best yield when employing catalyst **I-110** and DBU in dichloromethane. Besides phenyl substituted diazene, we also tested 1,2-di(4-methoxyphenyl)diazene and 1,2-di(4-chlorophenyl)diazene, and only the latter afforded desired product in an 18% yield.

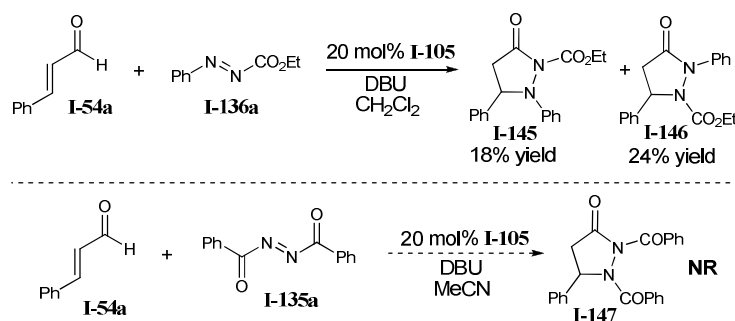
Scheme 1-42. Optimization with 1,2-diphenyl diazene as homoenolate acceptor

The next diazene to be investigated as the homoenolate acceptor is the 1-aryl-2-sulfonyldiazene (**I-134**) (Table 1-10). Diazenes with variously substituted aryl groups were synthesized and subjected to reaction conditions with catalyst **I-105**, cinnamaldehyde **I-54a** and DBU in dichloromethane. The highest yielding case was 16% when both aryl groups were phenyl. Cooling the reaction temperature to 0 °C lowered the yields. Examination of other catalysts, such as the benzimidazolium salts **I-69** and **I-110**, resulted in no product formation, while triazolium salt **I-139** gave comparable yields to **I-105**.

Table 1-10. Optimization with sulfonyl-substituted diazenes


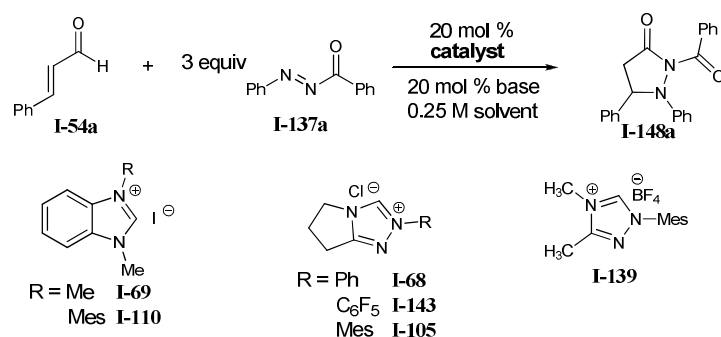
Ar ¹	Ar ²	temp (°C)	yield (%)
Ph	Ph	23	16
Ph	4-MePh	23	<10
4-OMePh	Ph	23	NR
4-ClPh	Ph	23	<5
Ph	Ph	0	<5
Ph	4-MePh	0	<5

We also tested diazene substrates **I-136a** with cinnamaldehyde **I-54a**, DBU and heteroazolium salt **I-105** and isolated the two regiosomers **I-145** and **I-146** in 18% and 24% yield, respectively (Scheme 1-43). Because of the poor regioselectivity, we decided to abandon this substrate and examine other diazenes. Diazene **I-135a** was subjected to the same conditions as **I-136a**, but it only resulted in decomposition of the dibenzoyldiazene to benzyl, and no product was observed by ¹H NMR spectroscopy of the crude mixture.

Scheme 1-43. Examination of Diazenes **I-135a** and **I-136a** as homoenolate acceptors

Lastly, acylaryldiazenes **I-137** were examined with varying conditions (Table 1-11). Initially, six different catalysts were tested in the presence of DBU and cinnamaldehyde. We

found that benzimidazolium salts **I-69** and **I-110**, which were competent catalysts for the previous homoenolate protonation and formal [3+3] cycloaddition reactions, were not productive catalysts for this reaction (entry 1-2). Surprisingly, triazolium salts with different *N*-substituents gave varying results with catalyst **I-68** and **I-143**, giving minimal to no product formation (entry 3-4), while catalyst **I-105** produced an encouraging 42% yield of the desired pyrazolidinone product (entry 5). In continuing to build our library of *N*-heterocyclic carbenes, we set forth to synthesize triazolium salt **I-139**, since it is structurally similar to **I-105**. A disadvantage of using triazolium salt **I-105** as a catalyst is that it is hygroscopic and decomposes at a much faster rate compared to other NHC precursors. The synthesis of catalyst **I-139** was successful, and it was observed to be less hygroscopic and more stable than **I-105**. Not only was **I-139** easier to work with, but it also catalyzed the reaction to give a higher yield (49%, entry 6) when subjected to the reaction conditions.

Table 1-11. Optimization with acylaryldiazenes as homoenolate acceptor

entry	catalyst	conditions	yield (%)
1	I-69	DBU, CH ₂ Cl ₂ , 23 °C, 24 h	0
2	I-110	DBU, CH ₂ Cl ₂ , 23 °C, 24 h	0
3	I-68	DBU, CH ₂ Cl ₂ , 23 °C, 24 h	0
4	I-143	DBU, CH ₂ Cl ₂ , 23 °C, 24 h	<5
5	I-105	DBU, CH ₂ Cl ₂ , 23 °C, 2 h	42
6	I-139	DBU, CH ₂ Cl ₂ , 23 °C, 5 h	49
7	I-139	DBU MeCN, 23 °C, 20 h	36
8	I-139	DBU, THF, 23 °C, 24 h	40
9	I-139	DBU, toluene, 23 °C, 19 h	44
10	I-139	<i>i</i> Pr ₂ EtN, CH ₂ Cl ₂ , 23 °C, 43 h	<5
11	I-139	K ₂ CO ₃ /18-c-6, CH ₂ Cl ₂ , 23 °C, 24 h	<20
12	I-139	KOtBu, CH ₂ Cl ₂ , 23 °C, 24 h	<10
13 ^a	I-139	DBN, CH ₂ Cl ₂ , 23 °C, 5h	53
14 ^a	I-139	DBU, CH ₂ Cl ₂ , 23 °C, 4h	61
15 ^b	I-139	DBU, CH ₂ Cl ₂ , 23 °C, 4h	50
16 ^c	I-139	DBU, CH ₂ Cl ₂ , 23 °C, 24h	<20
17 ^a	I-139	DBU, CH ₂ Cl ₂ , 0 °C, 24h	63
18 ^e	I-139	DBU, CH ₂ Cl ₂ , 0 °C, 24h	54

^a 30 mol % base, 4Å molecular sieves ^b 50 mol % base, 4Å molecular sieves ^c 10 mol % base, 4Å molecular sieves
^e 30 mol % base, 4Å molecular sieves, 0 °C, 2 equiv **I-139**

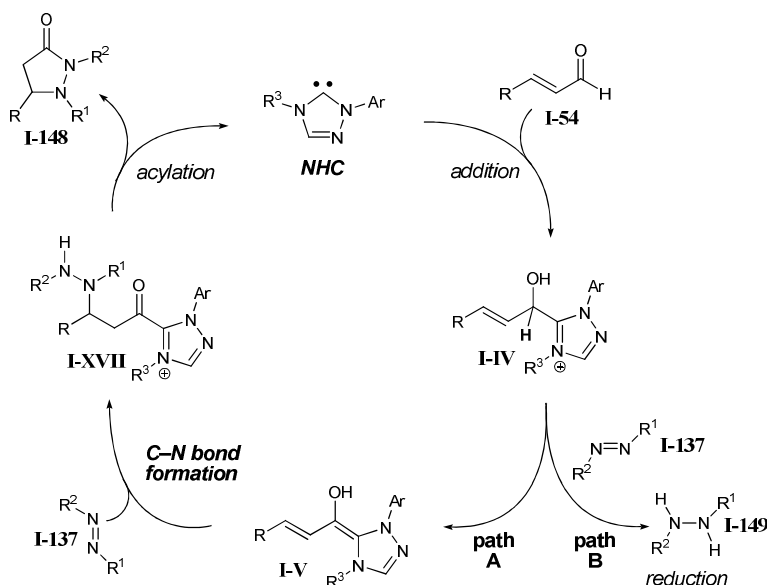
With the optimal catalyst determined for the reaction, we began to optimize the other variables in the reaction. The first variable investigated was solvent. As shown in Table 1-11, CH₂Cl₂, CH₃CN, THF and toluene facilitated product formation with dichloromethane as the best solvent (entry 6-9). Additionally, 1,4-dioxane, glyme and 10:1 THF/*t*-BuOH (not shown) were also examined and only produced minimal product. A large number of bases were examined that included DBU, *i*Pr₂NEt, K₂CO₃/18-crown-6, KO*t*-Bu, and DBN, which facilitated minor to moderate product formation (entries 6, 10-13). Bases such as KHMDS, Cs₂CO₃,

DMAP, Et₃N, quinuclidine, Proton Sponge, NaH, and sodium *t*-pentoxide were not competent bases for the reaction (not shown).

All five components of the reaction have been identified but further optimization was necessary. The amount of base used in the reaction and drying the reaction with 4Å molecular sieves turned out to be important factors for the success of the reaction. When employing 30 mol % of DBU and 4Å molecular sieves, a 61% yield of pyrazolidinone was isolated (Table 1, entry 14), while using an increased amount of DBU (50 mol %, entry 15) decreased the yield to 50%. However, when using substoichiometric amounts of DBU compared to the catalyst loading (10 mol %, entry 16), less than 20% of desired the product was observed by ¹H NMR spectroscopy of the crude mixture. Lastly, cooling the reaction to 0 °C and allowing the reaction to stir for 24 h improved the yield slightly (entry 17). It is also important to note that 3.0 equivalents of the diazene are required for this reaction because when 2.0 equivalents are used, only a 54% yield of pyrazolidinone **I-148** was isolated (entry 18).

1.7.3 Examination of Proposed Reaction Pathway and Reductive Side Product Formation

The anticipated catalytic pathway for our amination involves the addition of an NHC to α,β-unsaturated aldehyde **I-54** to afford tetrahedral intermediate **I-IV** (Scheme 1-42). Upon rearrangement, the extended diene homoenolate intermediate equivalent **I-V** was generated, which underwent addition to the diazene **I-137** and subsequently generated ketone **I-XVII** after tautomerization. This activated carbonyl species facilitated catalyst turnover by intramolecular acylation to produce pyrazolidinone **I-148**.

Scheme 1-44. Proposed catalytic pathway for NHC-catalyzed amination of homoenolates

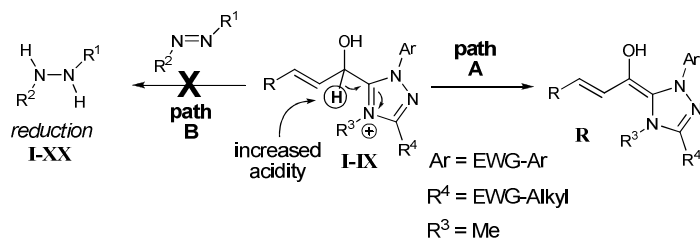
During our optimization studies, we isolated varying amounts of 1-benzoyl-2-phenylhydrazine (**I-149**), when employing diazene (**I-137a**) as the electrophile. On the basis of our carbene-catalyzed hydroacylation studies (discussed in the following chapter),¹³⁰ we postulated that tetrahedral intermediate **I-IV** (Scheme 1-44) can form the desired homoenolate intermediate (path A) or collapse to afford an acyl heteroazolium species with concomitant hydride transfer to the diazene (path B). The undesired reaction reduced **I-137a** to the observed hydrazine and sacrificed an equivalent of unsaturated aldehyde. Therefore, by lowering the reaction temperature, we can maximize the desired homoenolate amination.

A major effort was made to eliminate the reductive pathway by altering the electronics of the substrates used in the reaction. Our initial hypothesis was that if we used diazenes with electron-poor substituents on the aryl groups, then it would be a better homoenolate acceptor. However, exposure of the electron-withdrawing substituted aryl diazenes to reaction conditions

resulted in an increase in the undesired diazene reduced product. With an electron withdrawing group on the diazene, it should be a better homoenolate acceptor as well as an enhanced oxidant. We thought that using an enal with an electron-poor substituent on the aryl group should help stabilize the homoenolate intermediate, but again, this did not improve yields.

Lastly, an exhaustive attempt was made to synthesize new catalysts to improve the reaction. We recognized that it is crucial to control the fate of intermediate **I-IV** to undergo formal proton migration to generate the homoenolate intermediate (**I-V**, path A) instead of collapsing to effect a hydride transfer to the diazene (path B). To tune the reaction towards the desired reactivity, we set forth to synthesize new triazolium salts with electron withdrawing aryl or alkyl substituents on the ring (Scheme 1-45). We postulated that with electron poor substituents, it would cause the tetrahedral proton of intermediate **I-IV** to be more acidic, and, therefore, more likely to deprotonate, facilitating proton migration to generate the homoenolate intermediate (**I-V**) instead of the undesired pathway (path B).

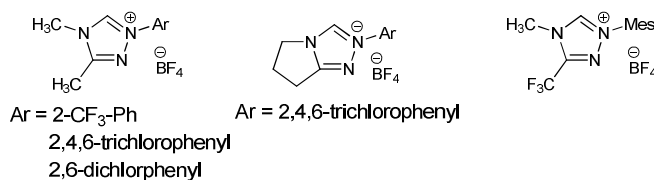
Scheme 1-45. Attempt to turn reactivity towards homoenolate formation



The syntheses of the electron poor substituted triazolium salts were synthetically challenging (Figure 1-14). Triazolium salts with aryl substituents, including 2-trifluoromethyl, 2,4,6-trichloro or 2,4-dichloro, were not able to be synthesized because the ring closure could not

be effected with triethyl orthoformate in chlorobenzene. This could be explained by the decreased nucleophilicity of the nitrogen as well as the sterically demanding groups on the nitrogen, which prevents ring closure to occur. Additionally, the triazolium salt with a trifluoromethyl substituent on C₅ was not successfully synthesized. Gratifyingly, triazolium salts with 4-trifluoromethyl substituted aryl groups were successfully synthesized, tested under homoenolate amination conditions, and it was found that **I-150** and **I-151** gave 42% and 35% yields of the pyrazolidinone product, respectively. To test the other extreme with an electron-donating aryl group on the triazolium salt, catalyst **I-152** was synthesized and subjected to homoenolate amination conditions. Triazolium salt **I-152** gave a disappointing 25% yield of the desired product. Even though our efforts to improve the reaction by altering the electronics of the catalyst were fruitless, we continued to expand the scope of the reaction with catalyst **I-139**, DBU, and 4 Å molecular sieves at 0 °C.

Unsuccessful Catalyst Synthesis:



New Catalysts:

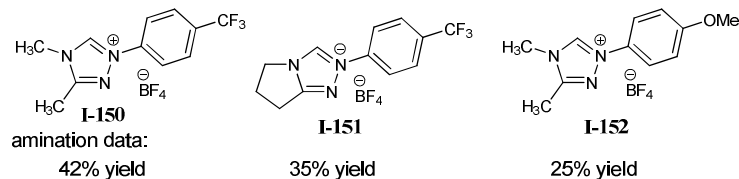


Figure 1-14. New triazolium salts to improve the homoenolate amination reaction

1.7.4 Reaction Scope of NHC-Catalyzed Amination of Homo-enolates

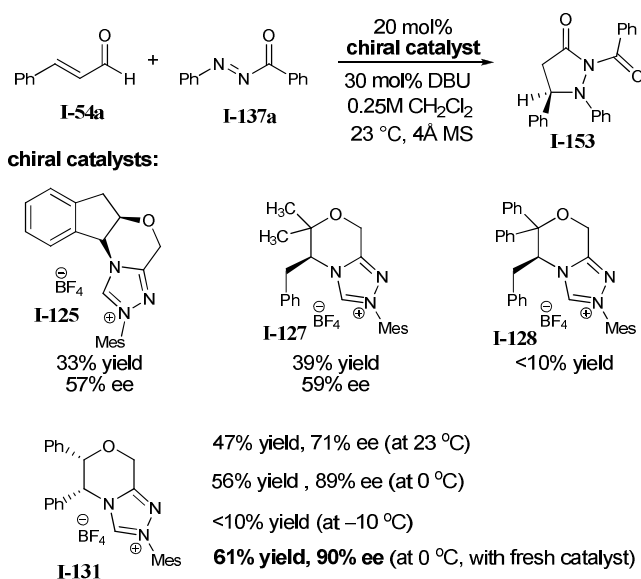
The reaction scope (Table 1-12) accommodates a variety of substituted α,β -unsaturated aldehydes, including electron-rich and electron-poor systems (entries 2-6), and importantly, β -alkyl substituted aldehydes provided excellent yields of **I-148g** and **I-148h** (entries 7-8). An examination of the acylaryldiazene component of the reaction reveals that variously substituted aryl groups are competent substrates. Electron-withdrawing and electron-donating groups on the aryl ring of the benzoyl portion of the diazene afforded good yields of the pyrazolidinone (entries 9-11). However, only electron-rich substituents on the aryl component of the diazene resulted in product formation (entries 12, 13), while electron poor substituents on the aryl group (i.e. Ar = 4-Br-Ph) gave a low yield (25%).

Table 1-12. Reaction Scope of NHC-catalyzed amination of homo-enolates

entry	R	Ar	R ¹	yield (%)
1	Ph	Ph	Ph	63 (I-148a)
2	3-OMe-Ph	Ph	Ph	60 (I-148b)
3	2-OMe-Ph	Ph	Ph	66 (I-148c)
4	2-Naphthyl	Ph	Ph	64 (I-148d)
5	4-Cl-Ph	Ph	Ph	61 (I-148e)
6	2-OMe-Ph	Ph	3-Me-Ph	64 (I-148f)
7	Me	Ph	3-Me-Ph	82 (I-148g)
8	CH ₂ CH ₂ CH ₃	Ph	3-Me-Ph	84 (I-148h)
9	Ph	Ph	4-Cl-Ph	68 (I-148i)
10	Ph	Ph	4-F-Ph	61 (I-148j)
11	Ph	Ph	3-Me-Ph	73 (I-148h)
12	Ph	3-Me-Ph	Ph	71 (I-148k)
13	Ph	4-Me-Ph	Ph	63 (I-148l)

1.7.5 Asymmetric Synthesis of Pyrazolidinones via NHC-Catalyzed Amination of Homoenolates

Once the reaction scope had been established, a new potential direction was the development of an asymmetric variant of this reaction (Scheme 1-46). The NHC-catalyzed asymmetric amination of homoenolates would allow a novel method to synthesize enantioenriched β -amino acid derivatives. Several chiral triazolium salts were tested under the optimized reaction conditions, and the reaction did proceed with all of the catalysts, but both the yield and selectivity were superior with catalyst **I-131**. To improve the selectivity using catalyst **I-131**, the reaction was cooled to 0 °C, which did indeed improve the selectivity to 89% ee. A further decrease in temperature to –10 °C resulted in reduced reaction rate with less than 10% product formation as observed by ^1H NMR spectroscopy after 7 days. When fresh catalyst **I-131** was used in the reaction at 0 °C, the yield and selectivity improved to 61% yield and 90% ee, respectively. We have previously observed that catalyst **I-131** decomposes over time even if kept in an anhydrous and inert atmosphere.

Scheme 1-46. Investigation of asymmetric amination of homoenolates

In addition to using cinnamaldehyde as the enal component, 2-hexenal was also examined. Although switching to a β -alkyl substituted aldehyde gave a higher yield, 71%, the enantioselectivity suffered (51% ee). Another diazene that was tested was the 1-phenyl-2-(3-methylphenyl)-diazene with cinnamaldehyde, and the yield was 57% while the selectivity was 79% ee. Further investigation in this area is necessary and can provide a useful method to access chiral pyrazolidinones.

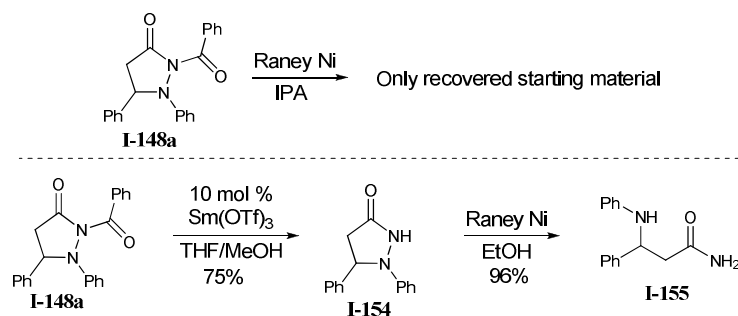
1.7.6 Conversion of Pyrazolidinones to β -Amino Acid Derivatives

As mentioned previously, an important application to develop this method is that it allows facile access to β -amino acid derivatives. To investigate whether this was plausible, we set forth to reductively cleave the *N-N* bond. In the first attempt, the pyrazolidinone product **I-148a** was dissolved in isopropanol and allowed to react with Raney nickel. However, when heated to 50 °C, only starting material was recovered (Scheme 1-47). A search in the literature

revealed limited examples of successful reductive cleavage of highly substituted *N-N* bonds.

Therefore, our next goal was to first break an amide bond followed by cleavage of the *N-N* bond that should occur readily under Raney nickel conditions. Two amide bonds are present in the molecule, and conditions must be chosen carefully to selectively cleave one amide bond over the other. An initial attempt was made with 0.1 M NaOH in methanol (same conditions to selectively ring-open the six-membered ring of pyridazinones), but an unidentifiable side product was isolated instead. Finally, using a catalytic amount of Sm(OTf)₃ in THF/MeOH, the benzoyl functionality was selectively removed to **I-148a** in a 75% yield.¹³¹ A clean reductive cleavage of the *N-N* bond of pyrazolidinone **I-154** with Raney nickel and H₂ in ethanol produced the β-amino amide **I-155** in excellent yield.

Scheme 1-47. Synthesis of β-amino amides from pyrazolidinone



1.8 Summary

The combination of α,β-unsaturated aldehydes and a *N*-heterocyclic carbene accesses unique homoenolate reactivity. These nucleophilic species possess subsequent electrophilic character at the carbonyl carbon that can be trapped by a secondary nucleophile such as an alcohol. The combination of a proton donor and a separate nucleophile afforded saturated esters

in high yields. The use of a chiral imidazoyleidene carbene as a catalyst in the protonation reaction allowed for the kinetic resolution of chiral secondary alcohols, thereby implicating a chiral activated ester as an intermediate in the process.

Additionally, we have developed the first formal [3+3] cycloaddition reaction catalyzed by NHCs. The addition of an *N*-mesityl benzimidazol carbene to an α,β -unsaturated aldehyde generates a homoenolate intermediate that undergoes an addition/acylation sequence with an azomethine imine to afford new bicyclic heterocycles with excellent diastereoselectivity. The pyridazinone products can be manipulated to provide esters and amides in excellent yields upon addition of alcohols or amines.

Lastly, the direct amination of homoenolates can be catalyzed by NHCs. The addition of a carbene derived from *N*²-mesityl-*N*⁴-methyl-5-methyl triazolium salt to an α,β -unsaturated aldehyde generates a homoenolate intermediate, which undergoes a formal [3+2] cycloaddition with 1-acyl-2-aryldiazene to afford pyrazolidinones as a single regioisomer. A chiral triazolium salt can be used to control the newly formed stereocenter of the product, which results in good selectivity. The pyrazolidinone products can be converted to β -amino acid derivatives in excellent yields.

This new NHC-catalyzed method to generate homoenolate equivalents is a powerful addition to *umpolung* strategies, since it utilizes neutral carbenes as catalysts and eliminates the production of wasteful by-products that are produced when generating homoenolate equivalents via metal catalysis. This NHC-catalyzed approach to homoenolates enables the use of new electrophiles to produce valuable organic compounds. It also allows for the development of enantioselective variants by employing chiral NHCs.

1.9 Experimental Section

General Information. All reactions were carried out under a nitrogen atmosphere in flame-dried glassware with magnetic stirring. THF, Et₂O, CH₂Cl₂, DMF and toluene were purified by passage through a bed of activated alumina.¹³² Reagents were purified prior to use unless otherwise stated following the guidelines of Perrin and Armarego.¹³³ Purification of reaction products was carried out by flask chromatography using EM Reagent silica gel 60 (230-400 mesh). Analytical thin layer chromatography was performed on EM Reagent 0.25 mm silica gel 60-F plates. Visualization was accomplished with UV light and anisaldehyde, ceric ammonium nitrate stain, potassium permanganate, or phosphomolybic acid followed by heating. Melting points were obtained on a Thomas Hoover capillary melting point apparatus and are uncorrected. Infrared spectra (**IR**) were obtained on a Bio-Rad FTS-40 FTIR spectrophotometer. ¹H-NMR spectra were recorded on a Varian Inova 500 (500 MHz) or Mercury 400 (400 MHz) spectrometer and are reported in ppm using solvent as an internal standard (CDCl₃ at 7.26). Data are reported as (ap = apparent, s = singlet, d = doublet, t = triplet, q = quartet, m = multiplet, b = broad; coupling constant(s) in Hz, integration. Proton-decoupled ¹³C-NMR spectra were recorded on a Varian Inova 500 (125 MHz) or Mercury 400 (100 MHz) spectrometer and are reported in ppm using solvent as an internal standard (CDCl₃ at 77.0 ppm). Electrospray mass spectra (ESI-MS) were obtained using a Micromass Quattro II Triple Quadrupole HPLC/MS/MS Mass Spectrometer.

1.9.1 Preparations of α,β -Unsaturated Aldehydes

3-(4-chlorophenyl)cinnamaldehyde was prepared according to a method developed by Kirsch.^{134, 135} 4-Chlorocinnamaldehyde was prepared according to a procedure analogous to Moloney.¹³⁶ 3-methylcinnamaldehyde, 3-(naphthalene-5-yl)acrylaldehyde 3-(naphthalene-6-yl)acrylaldehyde, and 3-methoxycinnamaldehyde were synthesized according to a procedure disclosed by Cacchi and coworkers¹³⁷ 4-Methoxycinnamaldehyde was purchased from Acros Chemical Company and the remaining aldehydes were commercially available from Sigma-Aldrich Chemical Company and purified before use.

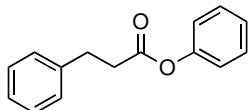
1.9.2 Experimental for NHC-Catalyzed Protonation of Homoenolates

1.9.2.1 General Procedure for NHC-Catalyzed Protonation of Homoenolates

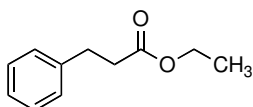
A screw-capped tube was charged with the benzimidazolium salt (11 mg, 0.04 mmol) in a nitrogen-filled dry box. The tube was removed from the box and placed under a positive pressure of nitrogen. The tube was charged with toluene (1.0 mL), DBU (6 μ L, 0.04 mmol) and lastly, distilled cinnamaldehyde (104 mg, 0.79 mmol). The reaction mixture was allowed to stir for 5 minutes after which phenol (150mg, 1.6 mmol) in toluene (0.6 ml) was added via syringe followed by the addition of benzyl alcohol (429 mg, 4 mmol). The reaction was heated at 110 °C for 2-6 hours until cinnamaldehyde was consumed (as judged by GC). The reaction was cooled to room temperature, diluted with methylene chloride (20 mL) and washed with water (20 mL). The aqueous layer was washed with methylene chloride (3x30 mL) and the combined organic extracts were dried over anhydrous sodium sulfate, filtered, and concentrated *in vacuo*. The resulting residue was purified by flash column chromatography on silica gel.

1.9.2.2 Characterization of Saturated Esters

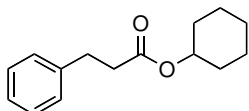
Known compounds:



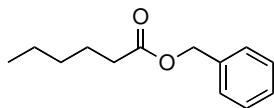
phenyl 3-phenylpropanoate (I-66c)¹³⁸



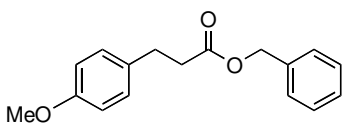
ethyl 3-phenylpropanoate (I-66a)¹³⁹



cyclohexyl 3-phenylpropanoate (I-66f)¹⁴⁰

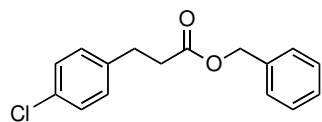


benzyl hexanoate (I-66l)¹⁴¹



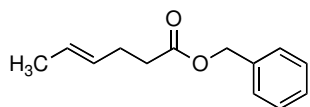
Benzyl 3-(4-methoxyphenyl)propanoate (I-66j): Purified with 10% Et₂O/hexanes yielding 127 mg (76%) of **I-66j** as a light yellow oil. R_f = 0.6 (1:4 Et₂O/hexanes); IR (film) 3448, 3033, 2951, 2835,

1734, 1247 cm⁻¹; ¹H NMR (500 MHz, CDCl₃) δ 7.40-7.30 (m, 5H); 7.10 (d, J = 7.94, 2H); 6.82 (d, J = 7.63, 2H); 5.11 (s, 2H); 3.79 (s, 3H); 2.92 (t, J = 7.63, 2H); 2.65 (t, J = 7.63, 1H); ¹³C NMR (125 MHz, CDCl₃) δ 173.3, 158.5, 136.4, 132.9, 129.7, 129.0, 128.7, 128.6, 114.3, 66.7, 55.7, 36.7, 30.6; LRMS (APCI): Mass calculated for C₁₇H₁₈O₃ [M+H]⁺ 271.3. Found 271.4.



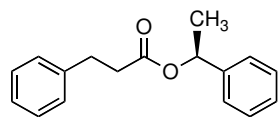
Benzyl 3-(4-chlorophenyl)propanoate (I-66k): Purified with 10%

Et₂O/hexanes yielding 118 mg (71%) of **I-66k** as a yellow oil. $R_f = 0.75$ (1:4 Et₂O/hexanes); IR (film) 3452, 3033, 2949, 1735 cm⁻¹; ¹H NMR (500 MHz, CDCl₃) δ 7.37-7.22 (m, 7H); 7.11 (d, $J = 8.2$, 2H); 5.10 (s, 2H); 2.94 (t, $J = 7.6$, 2H); 2.66 (t, $J = 7.6$, 2H); ¹³C NMR (125 MHz, CDCl₃) δ 172.9, 139.3, 136.2, 132.5, 130.2, 129.1, 128.8, 128.7, 66.8, 36.2, 30.7; LRMS (APCI): Mass calculated for C₁₆H₁₅ClO₂ [M+5H]⁺ 279.7. Found 279.5.



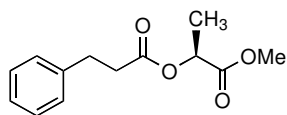
(E)-Benzyl hex-4-enoate (I-66m): Purified with 10% Et₂O/hexanes

yielding 129 mg (70%) of **I-66m** as a clear oil. $R_f = 0.77$ (1:4 Et₂O/hexanes); IR (film) 3455, 3040, 2959, 2936, 1736 cm⁻¹; ¹H NMR (500 MHz, CDCl₃) δ 7.40-7.32 (m, 5H); 5.50-5.39 (m, 2H); 5.12 (s, 2H); 2.41 (m, 2H); 2.33 (t, $J = 6.4$, 2H); 1.62 (t, $J = 5.8$, 3H); ¹³C NMR (125 MHz, CDCl₃) δ 173.3, 136.3, 129.3, 128.7, 128.4, 126.5, 66.3, 34.5, 28.1, 22.6, 18.1; LRMS (APCI): Mass calculated for C₁₃H₁₆O₂ [M+H]⁺ 205.2. Found 205.2.



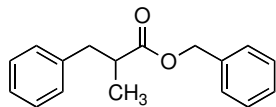
(S)-1-Phenylethyl 3-phenylpropanoate (I-66g): Purified with 10%

Et₂O/hexanes yielding 155 mg (77%) of **I-66g** as a yellow oil. $R_f = 0.70$ (1:4 Et₂O/hexanes); IR (film) 3446, 3030, 2981, 2868, 1732, 1248 cm⁻¹; ¹H NMR (500 MHz, CDCl₃) δ 7.36-7.17 (m, 10H); 5.89 (q, $J = 6.7$, 1H); 2.96 (t, $J = 7.3$, 2H); 2.66 (t, $J = 5.7$, 2H); 1.51 (d, $J = 6.7$, 3H); ¹³C NMR (125 MHz, CDCl₃) δ 172.4, 141.8, 140.7, 129.6, 128.8, 128.7, 128.5, 128.0, 126.4, 126.3, 36.3, 31.1, 22.4; LRMS (ACPI): Mass calculated for C₁₇H₁₈O₂ [M+H]⁺ 255.3. Found 255.4.



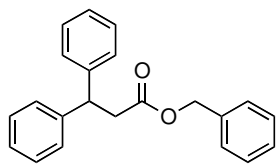
(S)-(Methoxycarbonyl)methyl 3-phenylpropanoate (I-66h): Purified

with 10% Et₂O/hexanes yielding 114 mg (61%) of **I-66h** as a light yellow oil. $R_f = 0.54$ (1:4 Et₂O/hexanes); IR (film) 3463, 3029, 2994, 2951, 1744, 1215 cm⁻¹; ¹H NMR (500 MHz, CDCl₃) δ 7.31-7.20 (m, 5H); 5.10 (q, $J = 7.0$, 1H); 3.74 (s, 3H); 2.98 (t, $J = 7.9$, 2H); 2.75-2.70 (m, 2H); 1.47 (d, $J = 7.3$, 3H); ¹³C NMR (125 MHz, CDCl₃) δ 172.5, 171.5, 140.5, 128.7, 128.5, 126.5, 68.7, 52.5, 35.7, 30.9, 17.1; LRMS (APCI): Mass calculated for C₁₃H₁₆O₄ [M+H]⁺ 237.1. Found 237.1.



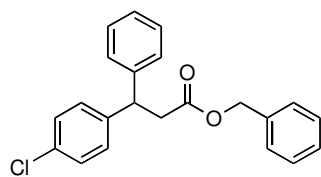
Benzyl 2-benzylpropanoate (I-66n): Purified with 10% Et₂O/hexanes

yielding 150 mg (82%) of **I-66n** as light tan oil. $R_f = 0.71$ (1:4 EtOAc/hexanes); IR (film) 3448, 3064, 3030, 3974, 2936, 1735, 1245 cm⁻¹; ¹H NMR (500 MHz, CDCl₃) δ 7.35-7.14 (m, 10H); 5.07 (s, 2H); 3.04 (dd, $J = 13.3$, 7.0, 1H); 2.80 (q, $J = 7.3$, 1H); 2.69 (dd, $J = 13.4$, 7.3, 1H); 1.18 (d, $J = 6.7$, 3H); ¹³C NMR (125 MHz, CDCl₃) δ 176.4, 139.7, 136.5, 129.5, 129.0, 128.8, 128.6, 128.5, 126.8, 66.6, 42.0, 40.2, 17.3; LRMS (APCI): Mass calculated for C₁₇H₁₈O₂ [M+H]⁺ 255.3. Found 255.3.



Benzyl 3,3-diphenylpropanoate (I-66o): Purified with 10%

Et₂O/hexanes yielding 113 mg (82%) of **I-66o** as a light yellow oil. $R_f = 0.70$ (1:4 Et₂O/hexanes); IR (film) 3448, 3061, 3030, 2953, 2921, 1735, 1258 cm⁻¹; ¹H NMR (500 MHz, CDCl₃) δ 7.38-7.14 (m, 15H); 5.02 (s, 2H); 4.56 (t, $J = 8.2$, 1H); 3.12 (d, $J = 7.9$, 2H); ¹³C NMR (125 MHz, CDCl₃) δ 172.1, 143.8, 136.2, 129.6, 129.0, 128.9, 128.8, 128.7, 128.6, 128.5, 128.4, 128.1, 127.0, 66.8, 47.5, 41.3.



Benzyl 3-(4-chlorophenyl)-3-phenylpropanoate (I-66p): Purified

with 60% CH₂Cl₂/hexanes yielding 94 mg (86%) of **I-66p** as a light yellow oil. R_f = 0.85 (5:1 CH₂Cl₂/hexanes); IR (film) 3449, 3030,

2955, 1735, 1254 cm⁻¹; ¹H NMR (500 MHz, CDCl₃) δ 7.31-7.14 (m, 14H); 5.02 (s, 2H); 4.54 (t, J = 7.9, 1H); 3.08 (d, J = 7.7, 2H); ¹³C NMR (125 MHz, CDCl₃) δ 171.9, 143.3, 142.2, 136.1, 132.8, 129.5, 129.2, 129.0, 128.7, 128.6, 128.0, 127.2, 114.6, 66.9, 46.9, 41.2.

1.9.3 Kinetic Resolution of Secondary Alcohol Data

A screw-capped tube was charged with the chiral benzimidazolium salt **I-72a** (42 mg, 0.09 mmol) in a nitrogen-filled dry box. The tube was removed from the box and placed under a positive pressure of nitrogen. The tube was charged with toluene (0.6 mL), DBU (14 μ L, 0.09 mmol) and lastly, distilled cinnamaldehyde (247 mg, 1.87 mmol). The reaction mixture was allowed to stir for 5 minutes after which 2,6-dimethylphenol (76 mg, 0.62 mmol) in toluene (0.6 mL) was added via syringe followed by the addition of 1-phenylethanol (429 mg, 0.62 mmol) and dodecane (106 mg, 0.62 mmol) that served as an internal standard for GC analysis. The reaction was heated at 80°C 6 days and monitored by standard analytical techniques (GC and HPLC) for % conversion and enantiomeric excess values. Aliquots of the reaction mixture (50 μ L) were collected after 24 h, 48 h, 72 h, 96 h, 120 h, and 144 h. Each aliquot was filtered through a small silica gel plug (1:1 EtOAc/hexanes) and analyzed. Percent conversions were measured by GC integration of the sec-phenethyl alcohol and the dodecane peaks.

Table 1-13. Summarized data for kinetic resolution study

Methods utilized for the determination of enantiomeric excess					
Entry	Catalyst	ee Assay	Condition	Retention Time of (S) Isomer (min)	Retention Time of (R) Isomer (min)
1	I-72a	HPLC Chiralcel OD-H	0.5% IPA/hexane 0.75 mL/min	9.76	11.14

Methods utilized for the determination of % conversion				
Entry	Catalyst	GC Condition	Retention Time of sec-phenethanol (min)	Retention Time of dodecane (min)
1	I-72a	70 °C, 1 min; 35 °C/min to 285 °C; 285 °C, 3 min	4.44	5.39

Selected Experimental Data for the Determination of Conversion, Enantiomeric Excess, and Selectivity (s).					
Entry	Catalyst	time (h)	% conversion	Measured % ee	s
1	I-72a	54	32.4	34.2	8.25
		76	33.2	32.3	7.08
		100	38.7	25.3	2.93
		124	40.1	24.2	2.66
		150	41.0	28.9	3.15

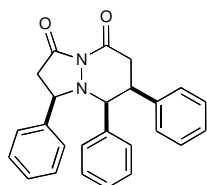
1.9.4 NHC-Catalyzed Formal [3+3] Cycloaddition Reaction between Homoenolates and Azomethine Imines

Azomethine imines were prepared according to the general procedure of by Fu and coworkers⁹⁰,⁹¹ and Hayashi and coworkers.⁹² 4-Chloro-cinnamaldehyde was prepared according to a procedure analogous to Moloney.¹³⁶ 3-methyl-cinnamaldehyde, 3-(naphthalene-5-yl)acrylaldehyde 3-(naphthalene-6-yl)acrylaldehyde, and 3-methoxy-cinnamaldehyde were synthesized according to a procedure disclosed by Cacchi and coworkers¹³⁷ 4-Methoxy-cinnamaldehyde was purchased from Acros Chemical Company and the remaining aldehydes were commercially available from Sigma-Aldrich Chemical Company and purified before use.

1.9.5 General Procedure for NHC-Catalyzed Protonation of Homo-enolates

Into an oven-dried screw-capped test tube (SCTT) equipped with a stirbar was charged with the *N*-mesityl-*N*-methylbenzimidazolium iodide salt **I-110** (16.6 mg, 0.044 mmol) and the 1-benzylidene-3-oxo-5-phenylpyrazolidin-1-ium-2-ide **I-114a** (55 mg, 0.22 mmol), capped and then purged with N₂. The two solids were then dissolved in CH₂Cl₂ (880 μ L) and into it was added distilled cinnamaldehyde **I-54a** (55 μ L, 0.44 mmol). The SCTT was heated to 45 °C and into it was added DBU (6.6 μ L, 0.044 mmol). Upon DBU addition, the reaction turned immediately green then orange/red. After 2 h at reflux, a TLC showed no further progress. The dark green or deep red (depending on the substrates) reaction mixture was allowed to cool to room temperature. The reaction was diluted with CH₂Cl₂, washed with water (1 x 5 mL) and saturated NaCl (1 x 5 mL). The layers were separated and the aqueous layer was extracted two additional times with CH₂Cl₂ (2 x 10 mL). The organic layers were combined, dried over Na₂SO₄, filtered and concentrated. The resulting residue was purified by flash column chromatography on silica gel.

1.9.5.1 Characterization of Pyridazinones



tetrahydro-3,5,6-triphenyl-5H-pyrazolo[1,2-*a*]pyridazine-1,8-dione (I-

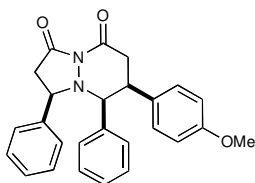
115a): Purified with 8% ethyl acetate/dichloromethane, yielding 66 mg (79%)

of **I-115a** as a white foam. R_f = 0.63 (96/2/2 dichloromethane/ethyl

acetate/methanol); IR (film) 3031.2, 2920.7, 1773.6, 1299.9, 698.2 cm⁻¹; ¹H NMR (400 MHz, CDCl₃) δ 7.13-7.04 (m, 8H); 6.94-6.91 (m, 1H); 6.81 (m, 4H); 6.69-6.67 (d, J = 7.6 Hz, 2H); 4.48 (d, J = 7.6 Hz, 1H); 4.26 (t, J = 8.2, 1H); 3.67-3.61 (m, 1H); 3.34-3.22 (m, 2H); 2.85-2.74 (m, 2H); ¹³C NMR (100 MHz, CDCl₃) δ 169.1, 168.7, 140.1, 138.5, 136.2, 129.2, 128.9, 128.8,

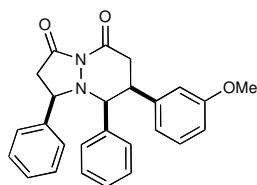
128.7, 128.2, 127.9, 127.6, 127.2, 126.9, 72.2, 63.6, 44.6, 40.4, 37.6; LRMS (electrospray):

Mass calculated for $C_{25}H_{22}N_2O_2$ $[2M + 23]^+$, 787.9. Found 787.5.



**tetrahydro-6-(4-methoxyphenyl)-3,5-diphenyl-5Hpyrazolo-
[1,2a]pyridazine-1,8-dione (I-115b):** Purified with 8% ethyl
acetate/dichloromethane, yielding 75 mg (76%) of **I-115b** as a yellow

foam. R_f = 0.60 (96/2/2 dichloromethane/ethyl acetate/methanol); IR (film) 3033.2, 2931.8, 2836.8, 1773.0, 1296.7, 699.8 cm^{-1} ; 1H NMR (400 MHz, $CDCl_3$) δ 7.13-7.11 (m, 3H); 7.03-7.02 (m, 2H); 6.93 (t, J = 7.0 Hz, 1H); 6.82 (t, J = 7.6 Hz, 2H); 6.74-6.71 (m, 2H); 6.67-6.60 (m, 4H); 4.42 (d, J = 7.0 Hz, 1H); 4.24 (t, J = 8.2 Hz, 1H); 3.70 (s, 3H); 3.59-3.53 (m, 1H); 3.26-3.20 (m, 2H); 2.83-2.73 (m, 2H); ^{13}C NMR (100 MHz, $CDCl_3$) δ 169.0, 168.6, 158.6, 140.1, 136.3, 130.6, 129.9, 129.3, 128.7, 128.6, 127.9, 127.6, 126.9, 113.5, 72.3, 63.9, 55.4, 43.9, 40.5, 38.0; LRMS (electrospray): Mass calculated for $C_{26}H_{24}N_2O_3$ $[2M + 23]^+$, 847.9. Found 847.2.

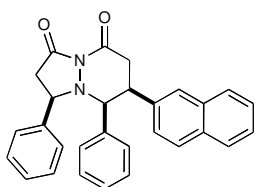


**tetrahydro-6-(3-methoxyphenyl)-3,5-diphenyl-5Hpyrazolo[1,2-
a]pyridazine-1,8-dione (I-115c):** Purified with 8% ethyl
acetate/dichloromethane, yielding 78 mg (79%) of **I-115c** as a light tan

foam. R_f = 0.65 (96/2/2 dichloromethane/ethyl acetate/methanol); IR (film) 3031.6, 2919.6, 2836.7, 1773.6, 1297.7, 699.9 cm^{-1} ; 1H NMR (400 MHz, $CDCl_3$) δ 7.15-7.13 (m, 3H); 7.06-7.04 (m, 2H); 7.01-6.93 (m, 2H); 6.85 (t, J = 7.6 Hz, 2H); 6.74 (d, J = 7.6 Hz, 2H); 6.61-6.59 (m, 1H); 6.44 (d, J = 7.6 Hz, 1H); 6.29 (s, 1H); 4.48 (d, J = 7.6 Hz, 1H); 4.27 (t, J = 8.8 Hz, 1H); 3.68-3.55 (m, 4H); 3.33-3.23 (m, 2H); 2.82-2.73 (m, 2H); ^{13}C NMR (100 MHz, $CDCl_3$) δ 169.1, 168.6, 159.3, 140.1, 139.9, 136.3, 129.2, 129.1, 128.7, 127.9, 127.6, 126.9, 126.8, 121.3, 114.7,

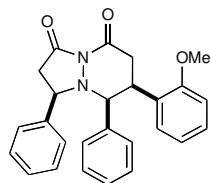
112.6, 72.0, 63.5, 55.3, 44.6, 40.3, 37.5; LRMS (electrospray): Mass calculated for $C_{26}H_{24}N_2O_3$ $[2M + 23]^+$, 847.9. Found 847.4.

tetrahydro-6-(2-methoxyphenyl)-3,5-diphenyl-5H-pyrazolo[1,2-a]pyridazine-1,8-dione (I-115d): Purified with 8% ethyl acetate/dichloromethane, yielding 93 mg (94%) of **I-115d** as a light yellow foam. $R_f = 0.62$ (96/2/2 dichloromethane/ethyl acetate/methanol); IR (film) 3036.4, 2921.5, 2843.8, 1773.6, 1297.2, 699.1 cm^{-1} ; 1H NMR (400 MHz, $CDCl_3$) δ 7.18-7.16 (m, 3H); 7.07-6.97 (m, 3H); 6.93-6.84 (m, 5H); 6.65-6.61 (m, 2H); 6.57 (d, $J = 8.2$ Hz, 1H); 4.67 (d, $J = 8.8$ Hz, 1H); 4.30-4.27 (m, 1H); 4.11-4.05 (m, 1H); 3.76 (s, 3H); 3.45-3.32 (m, 2H); 2.79-2.63 (m, 2H); ^{13}C NMR (100 MHz, $CDCl_3$) δ 169.6, 169.4, 156.4, 140.4, 137.2, 128.8, 128.7, 128.1, 127.9, 127.8, 127.5, 127.4, 127.3, 126.7, 120.3, 109.7, 69.7, 62.4, 55.2, 39.9, 37.5, 36.4; LRMS (electrospray): Mass calculated for $C_{26}H_{24}N_2O_3$ $[2M + 23]^+$, 847.9. Found 847.3.



tetrahydro-6-(naphthalene-3-yl)-3,5-diphenyl-5H-pyrazolo[1,2-a]pyridazine-1,8-dione (I-115e): Purified with 8% ethyl acetate/dichloromethane, yielding 80 mg (77%) of **I-115e** as a light brown

foam. $R_f = 0.60$ (96/2/2 dichloromethane/ethyl acetate/methanol); IR (film) 3052.51, 2921.1,



1773.3, 1298.3, 699.1 cm^{-1} ; 1H NMR (400 MHz, $CDCl_3$) δ 7.71-7.63 (m, 2H);

7.53 (d, $J = 8.2$ Hz, 1H); 7.42-7.39 (m, 2H); 7.30 (s, 1H); 7.12-7.11 (m, 3H);

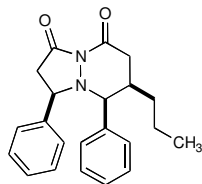
7.04-6.99 (m, 2H); 6.93-6.91 (m, 1H); 6.87-6.83 (m, 1H); 6.75-6.68 (m, 4H);

4.56 (d, $J = 7.0$ Hz, 1H); 4.28 (t, $J = 8.2$ Hz, 1H); 3.81-3.75 (m, 1H); 3.43-

3.23 (m, 2H); 2.94-2.76 (m, 2H); ^{13}C NMR (100 MHz, $CDCl_3$) δ 169.1, 168.5, 140.1, 136.1,

136.0, 133.1, 132.4, 129.2, 128.7, 128.6, 128.0, 127.9, 127.8, 127.8, 127.7, 127.7, 127.6, 126.9,

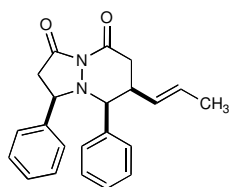
126.3, 126.1, 72.2, 63.8, 44.8, 40.5, 37.9; LRMS (electrospray): Mass calculated for $C_{25}H_{22}N_2O_2$ $[2M + 23]^+$, 888.0. Found 888.2.



tetrahydro-3,5-diphenyl-6-propyl-5H-pyrazolo[1,2-a]pyridazine-1,8-dione

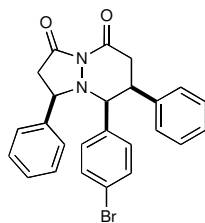
(I-115f): Purified with 8% ethyl acetate/dichloromethane, yielding 54 mg

(70%) of **I-115f** as a white foam. $R_f = 0.57$ (96/2/2 dichloromethane/ethyl acetate/methanol); IR (film) 3030.9, 2957.2, 1774.4, 1308.9, 699.7 cm^{-1} ; 1H NMR (400 MHz, $CDCl_3$) δ 7.16-7.11 (m, 8H); 7.03-7.01 (m, 2H); 4.27 (d, $J = 8.8$ Hz, 1H); 4.22-4.18 (m, 1H); 3.30-3.23 (m, 1H); 2.80-2.67 (m, 2H); 2.59-2.55 (m, 1H); 2.37-2.30 (m, 1H); 1.31-1.22 (m, 1H); 1.20-1.03 (m, 1H); 1.01-0.92 (m, 1H); 0.86-0.76 (m, 1H); 0.71 (t, $J = 7.0$ Hz; 3H); ^{13}C NMR (100 MHz, $CDCl_3$) δ 169.6, 169.3, 140.5, 137.3, 129.5, 128.7, 128.4, 128.3, 127.9, 126.7, 71.2, 62.3, 39.8, 37.9, 37.4, 34.4, 20.9, 14.1; LRMS (electrospray): Mass calculated for $C_{29}H_{24}N_2O_2$ $[2M + 23]^+$, 719.9. Found 719.3.



tetrahydro-3,5-diphenyl-6-((E)-prop-1-enyl)-5H-pyrazolo[1,2-a]pyridazine-1,8-dione (I-115g):

Purified with 8% ethyl acetate/dichloromethane, yielding 39 mg (51%) of **I-115g** as a white foam. $R_f = 0.58$ (96/2/2 dichloromethane/ethyl acetate/methanol); IR (film) 3030.9, 2918.0, 1774.6, 1696.9, 1297.7, 699.4 cm^{-1} ; 1H NMR (400 MHz, $CDCl_3$) δ 7.17-7.03 (m, 10H); 5.35-5.26 (m, 1H); 4.91-4.80 (m, 1H); 4.29-4.18 (m, 2H); 3.27-3.20 (m, 1H); 2.95-2.88 (m, 2H); 2.73-2.68 (m, 1H); 2.54-2.49 (m, 1H); 1.46 (d, $J = 7.0$ Hz, 3H); ^{13}C NMR (100 MHz, $CDCl_3$) δ 169.2, 168.8, 140.5, 136.9, 129.4, 129.3, 129.1, 128.7, 128.2, 128.1, 127.8, 126.8, 71.6, 62.7, 42.4, 40.0, 38.8, 36.3; LRMS (electrospray): Mass calculated for $C_{22}H_{22}N_2O_2$ $[2M + 23]^+$, 715.8. Found 715.4.

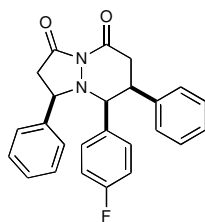


5-(4-bromophenyl)-tetrahydro-3,6-diphenyl-5H-pyrazolo[1,2-a]pyridazine-

1,8-dione (I-115i): Purified with 8% ethyl acetate/dichloromethane, yielding 85 mg (87%) of **I-115i** as a light tan foam. $R_f = 0.59$ (96/2/2 dichloromethane/ethyl acetate/methanol); IR (film) 3047.5, 2919.6, 1773.3,

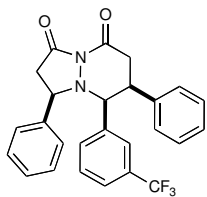
1300.0, 698.5 cm^{-1} ; ^1H NMR (400 MHz, CDCl_3) δ 7.14-7.11 (m, 6H); 7.00-6.98 (m, 2H); 6.87 (m, 2H); 6.82 (m, 2H); 6.48 (m, 2H); 4.41 (d, $J = 7.0$ Hz, 1H); 4.19 (t, $J = 8.2$ Hz, 1H); 3.62-3.57 (m, 1H); 3.26-3.17 (m, 2H); 2.88-2.76 (m, 2H); ^{13}C NMR (100 MHz, CDCl_3) δ 168.7, 168.2, 138.0, 135.2, 130.8, 130.6, 128.9, 128.8, 128.7, 128.4, 128.1, 127.5, 127.0, 121.9, 71.8, 64.7, 44.3, 40.6, 37.5; LRMS (electrospray): Mass calculated for $\text{C}_{25}\text{H}_{21}\text{BrN}_2\text{O}_2$ $[2\text{M} + 23]^+$, 945.7. Found 944.8.

5-(4-fluorophenyl)-tetrahydro-3,6-diphenyl-5H-pyrazolo[1,2-a]pyridazine-1,8-dione (I-



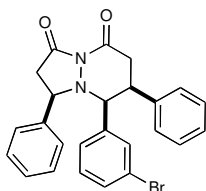
115j): Purified with 8% ethyl acetate/dichloromethane, yielding 73 mg (82%) of **I-115j** as a yellow foam. $R_f = 0.65$ (96/2/2 dichloromethane/ethyl acetate/methanol); IR (film) 3037.5, 2921.6, 1773.8, 1300.7, 699.3 cm^{-1} ; ^1H NMR (400 MHz, CDCl_3) δ 7.13-7.09 (m, 6H); 7.00-6.98 (m, 2H); 6.82-6.80

(m, 2H); 6.62-6.58 (m, 2H); 6.49-6.45 (m, 2H); 4.44 (d, $J = 7.6$ Hz, 1H); 4.20 (t, $J = 8.2$ Hz, 1H); 3.63-3.57 (m, 1H); 3.29-3.19 (m, 2H); 2.87-2.75 (m, 2H); ^{13}C NMR (100 MHz, CDCl_3) δ 168.8, 168.4, 139.9, 138.3, 130.9, 130.8, 128.9, 128.7, 128.3, 128.0, 127.4, 126.9, 114.5, 114.3, 71.8, 64.5, 44.6, 40.6, 37.5; LRMS (electrospray): Mass calculated for $\text{C}_{25}\text{H}_{21}\text{FN}_2\text{O}_2$ $[2\text{M} + 23]^+$, 823.9. Found 823.1.

5-(3-trifluoromethylphenyl)-tetrahydro-3,6-diphenyl-5H-pyrazolo[1,2-**a]- pyridazine-1,8-dione (I-115k):** Purified with 8% ethylacetate/dichloromethane, yielding 92 mg (93%) of **I-115k** as a yellow foam. $R_f = 0.63$ (96/2/2 dichloromethane/ethyl acetate/methanol); IR (film) 3032.8,2920.8, 1774.7, 1326.6, 1300.9, 1122.8, 699.4 cm^{-1} ; ^1H NMR (400 MHz, CDCl_3) δ 7.14-7.06 (m,7H); 7.00-6.97 (m, 1H); 6.93-6.76 (m, 6H); 4.50 (d, $J = 7.0$ Hz, 1H); 4.20 (t, $J = 8.8$ Hz, 1H);3.67-3.62 (m, 1H); 3.29-3.17 (m, 2H); 2.89-2.81 (m, 2H); ^{13}C NMR (100 MHz, CDCl_3) δ 168.5,

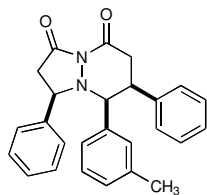
168.3, 139.2, 137.7, 137.3, 132.4, 132.3, 128.8, 128.7, 128.4, 128.3, 127.9, 127.6, 127.1, 126.2,

126.2, 124.6, 72.5, 65.5, 44.5, 40.7, 37.3; LRMS (electrospray): Mass calculated for

 $\text{C}_{26}\text{H}_{21}\text{F}_3\text{N}_2\text{O}_2$ $[2\text{M} + 23]^+$, 923.9. Found 923.2.**5-(3-bromophenyl)-tetrahydro-3,6-diphenyl-5H-pyrazolo[1,2-****a]pyridazine-1,8-dione (I-115l):** Purified with 8% ethylacetate/dichloromethane, yielding 76 mg (78%) of **I-115l** as a white foam. R_f $= 0.65$ (96/2/2 dichloromethane/ethyl acetate/methanol); IR (film) 3035.2, 2921.5, 1774.2,1296.2, 698.9 cm^{-1} ; ^1H NMR (400 MHz, CDCl_3) δ 7.14-7.11 (m, 6H); 7.03-7.01 (m, 3H); 6.82-6.80 (m, 2H); 6.73 (s, 1H); 6.68-6.64 (m, 1H); 6.59-6.57 (m, 1H); 4.39 (d, $J = 7.6$ Hz, 1H); 4.21(t, $J = 8.2$ Hz, 1H); 3.63-3.58 (m, 1H); 3.28-3.17 (m, 2H); 2.87-2.79 (m, 2H); ^{13}C NMR (100MHz, CDCl_3) δ 168.7, 168.3, 139.4, 138.4, 137.9, 132.6, 130.9, 129.0, 128.8, 128.7, 128.4,

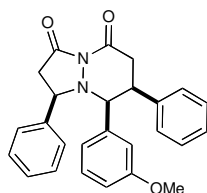
128.3, 127.7, 127.5, 127.0, 121.6, 72.1, 65.0, 44.4, 40.5, 37.3; LRMS (electrospray): Mass

calculated for $\text{C}_{25}\text{H}_{21}\text{BrN}_2\text{O}_2$ $[2\text{M} + 23]^+$, 945.7. Found 945.1.

5-(3-methylphenyl)-tetrahydro-3,6-diphenyl-5H-pyrazolo[1,2-

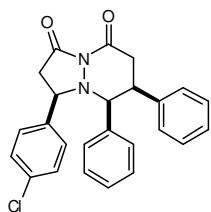
a]pyridazine-1,8-dione (I-115m): Purified with 8% ethyl acetate/dichloromethane, yielding 68 mg (76%) of **I-115m** as a tan solid. $R_f = 0.66$ (96/2/2 dichloromethane/ethyl acetate/methanol); Mp: 169-171 °C; IR

(film) 3033.6, 2919.7, 1770.7, 1298.0, 698.7 cm^{-1} ; ^1H NMR (400 MHz, CDCl_3) δ 7.12-7.08 (m, 6H); 7.02-7.00 (m, 2H); 6.84-6.82 (m, 2H); 6.76-6.70 (m, 2H); 6.55-6.53 (d, $J = 6.4$ Hz, 1H); 6.28 (s, 1H); 4.41 (d, $J = 7.0$ Hz, 1H); 4.23 (t, $J = 8.2$ Hz, 1H); 3.60-3.55 (m, 1H); 3.31-3.19 (m, 2H); 2.88-2.73 (m, 2H); 1.89 (s, 3H); ^{13}C NMR (100 MHz, CDCl_3) δ 169.0, 168.5, 140.3, 138.3, 136.9, 135.8, 130.5, 129.0, 128.6, 128.5, 128.0, 127.9, 127.4, 127.2, 126.9, 126.2, 72.4, 63.8, 44.6, 40.4, 37.8, 21.2; LRMS (electrospray): Mass calculated for $\text{C}_{26}\text{H}_{24}\text{N}_2\text{O}_2$ $[2\text{M} + 23]^+$, 815.9. Found 815.5.

5-(3-methoxyphenyl)-tetrahydro-3,6-diphenyl-5H-pyrazolo[1,2-

a]pyridazine-1,8-dione (I-115n): Purified with 8% ethyl acetate/dichloromethane, yielding 59 mg (67%) of **I-115n** as a yellow foam.

$R_f = 0.61$ (96/2/2 dichloromethane/ethyl acetate/methanol); IR (film) 3047.4, 2920.9, 2836.1, 1770.7, 1296.2, 698.5 cm^{-1} ; ^1H NMR (400 MHz, CDCl_3) δ 7.13-7.11 (m, 6H); 7.05-7.03 (m, 2H); 6.88-6.80 (m, 3H); 6.48-6.43 (m, 2H); 5.96 (s, 1H); 4.44 (d, $J = 7.0$ Hz, 1H); 4.25 (t, $J = 8.2$ Hz, 1H); 3.61-3.58 (m, 1H); 3.29-3.21 (m, 5H); 2.91-2.73 (m, 2H); ^{13}C NMR (100 MHz, CDCl_3) δ 168.9, 168.1, 159.5, 140.5, 138.8, 137.4, 129.1, 128.7, 128.6, 128.2, 127.9, 127.3, 126.8, 121.7, 114.7, 114.1, 72.3, 63.7, 54.8, 44.8, 40.5, 38.0; LRMS (electrospray): Mass calculated for $\text{C}_{26}\text{H}_{24}\text{N}_2\text{O}_3$ $[2\text{M} + 23]^+$, 847.9. Found 847.3.



3-(4-chlorophenyl)-tetrahydro-5,6-diphenyl-5H-pyrazolo[1,2-a]pyridazine-1,8-dione (I-117): Purified with 8% ethyl

acetate/dichloromethane, yielding 74 mg (85%) of **I-117** as a yellow foam. R_f = 0.63 (96/2/2 dichloromethane/ethyl acetate/methanol); IR (film) 3032,

2920, 1773, 1302, 699 cm^{-1} ; ^1H NMR (400 MHz, CDCl_3) δ 7.10-7.08 (m, 5H); 6.95-6.93 (m, 3H); 6.85-6.81 (m, 4H); 6.65-6.63 (m, 2H); 4.45 (d, J = 7.0, 1H); 4.22 (t, J = 8.2 Hz, 1H); 3.64-3.59 (m, 1H); 3.32-3.20 (m, 2H); 2.88-2.68 (m, 2H); ^{13}C NMR (100 MHz, CDCl_3) δ 168.6, 168.4, 138.7, 138.4, 135.9, 133.7, 129.3, 128.9, 128.8, 128.3, 128.2, 128.1, 127.7, 127.3, 72.5, 63.2, 44.6, 40.3, 37.8; LRMS (electrospray): Mass calculated for $\text{C}_{21}\text{H}_{24}\text{ClN}_2\text{O}_3$ $[2\text{M} + 23]^+$, 856.8. Found 857.1.

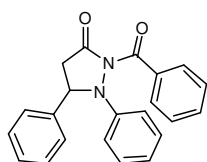
1.9.6 Amination of Homoenolates Catalyzed by *N*-Heterocyclic Carbenes

1.9.6.1 General Procedure for the Amination of Homoenolates Catalyzed by NHC

Into an oven-dried screw-capped glass tube equipped with a stir bar was charged with the *N*2-mesityl-*N*4-methyl-5-methyltriazolium tetrafluoroborate salt **I-139** (14.4 mg, 0.0476 mmol) and 4 Å molecular sieves (150 mg) and capped in a nitrogen-filled drybox. The tube with the reagents was removed from the drybox and then purged with N_2 . Into the tube was added a solution of 1-benzoyl-1-phenyldiazene **I-137a** (150 mg, 0.714 mmol) dissolved in CH_2Cl_2 (950 μL , 0.25 M). Next, distilled cinnamaldehyde **I-54a** (30 μL , 0.238 mmol) was added and the reaction mixture was cooled to 0 °C and DBU was added (10.7 μL , 0.0714 mmol). Upon DBU addition, the reaction turned brown then orange. After 24 h at 0 °C, the orange suspension was warmed to room temperature. The mixture was diluted with CH_2Cl_2 and filtered through a pad

of silica gel and washed with CH_2Cl_2 and Et_2O . The resulting residue was purified by flash column chromatography on silica gel.

1.9.6.2 Characterization of Pyrazolidinones



2-Benzoyl-1,5-diphenylpyrazolidin-3-one (I-148a): Purified with 10-15%

ethyl acetate/hexanes, yielding 51 mg (63%) of **I-148a** as a light tan foam. R_f

= 0.40 (25% ethyl acetate/hexanes); Mp: 135-137 °C; IR (film) 3061, 2920,

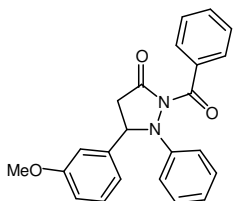
1759, 1694, 1492, 1279, 1230, 696 cm^{-1} ; ^1H NMR (500 MHz, CDCl_3) δ 7.63-7.59 (m, 4H); 7.53-

7.50 (m, 1H); 7.47-7.44 (m, 2H); 7.40-7.33 (m, 5H); 7.12-7.09 (m, 3H); 5.11 (d, J = 8.3 Hz, 1H);

3.47 (dd, J = 17.1, 8.3 Hz, 1H); 2.82 (d, J = 17.1 Hz, 1H); ^{13}C NMR (125 MHz, CDCl_3) δ 172.2,

166.3, 149.7, 139.7, 133.5, 132.5, 129.7, 129.3, 129.2, 128.5, 128.1, 126.3, 124.1, 117.2, 67.7,

38.6; LRMS (electrospray): Mass calculated for $\text{C}_{44}\text{H}_{36}\text{N}_4\text{O}_4\text{Na}$ [$2\text{M} + \text{Na}$] $^+$, 707. Found 707.



2-Benzoyl-5-(3-methoxyphenyl)-1-phenylpyrazolidin-3-one (I-148b):

Purified with 10-15% ethyl acetate/hexanes, yielding 69mg (60%) of **I-148b**

as a yellow foam. R_f = 0.39 (25% ethyl acetate/hexane); Mp: 45-47 °C; IR

(film) 3061, 2922, 1759, 1695, 1598, 1491, 1275, 1230, 1194, 696 cm^{-1} ; ^1H NMR (500 MHz,

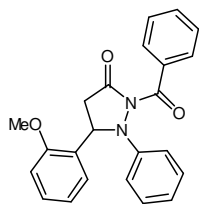
CDCl_3) δ 7.66 (d, J = 7.8 Hz, 2H); 7.53 (t, J = 7.3 Hz, 1H); 7.42-7.34 (m, 6H); 7.11 (d, J = 7.8

Hz, 4H); 6.92-6.90 (m, 1H); 5.11 (d, J = 8.3 Hz, 1H); 3.83 (s, 3H); 3.47 (dd, J = 17.1, 8.8 Hz,

1H); 2.80 (d, J = 17.1 Hz, 1H); ^{13}C NMR (125 MHz, CDCl_3) δ 172.1, 166.3, 160.4, 149.6, 141.5,

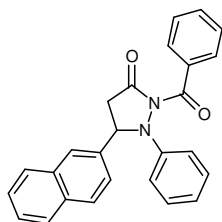
133.5, 132.5, 130.3, 129.7, 129.3, 128.1, 123.9, 118.3, 116.9, 114.1, 111.6, 67.5, 55.5, 38.9;

LRMS (electrospray): Mass calculated for $\text{C}_{46}\text{H}_{40}\text{N}_4\text{O}_6\text{Na}$ [$2\text{M} + \text{Na}$] $^+$, 767, Found 767.

2-Benzoyl-5-(2-methoxyphenyl)-1-phenylpyrazolidin-3-one (I-148c):

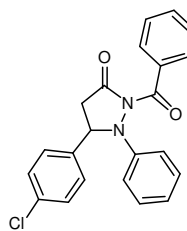
Purified with 5/25/70 ethyl acetate/dichloromethane/hexane, yielding 53 mg (66%) of **I-148c** as a yellow foam. $R_f = 0.30$ (5/35/60 ethyl acetate/dichloromethane/hexane); Mp: 70-72 °C; IR (film) 3060, 2922, 1759,

1694, 1599, 1491, 1281, 1240, 1192, 696 cm^{-1} ; ^1H NMR (500 MHz, CDCl_3) δ 7.77 (d, $J = 6.8$ Hz, 1H); 7.66 (d, $J = 6.8$ Hz, 2H); 7.51 (t, $J = 7.3$ Hz, 1H); 7.41-7.32 (m, 5H); 7.11-7.03 (m, 4H); 6.95 (d, $J = 7.8$ Hz, 1H); 5.27 (d, $J = 8.8$ Hz, 1H); 3.86 (s, 3H); 3.44 (dd, $J = 17.6, 8.8$ Hz, 1H); 2.73 (d, $J = 17.6$ Hz, 1H); ^{13}C NMR (125 MHz, CDCl_3) δ 173.0, 166.5, 156.5, 150.2, 133.8, 132.4, 129.7, 129.5, 129.3, 128.3, 128.1, 127.1, 123.6, 121.2, 116.8, 110.7, 64.5, 55.4, 38.0; LRMS (electrospray): Mass calculated for $\text{C}_{22}\text{H}_{20}\text{N}_4\text{O}_3$ [2M + Na] $^+$, 767. Found 767.

2-Benzoyl-5-(naphthalene-3-yl)-1-phenylpyrazolidin-3-one (I-148d):

Purified with 5/25/70 ethyl acetate/dichloromethane/hexane, yielding 55 mg (64%) of **I-148d** as a light tan solid. $R_f = 0.30$ (5/35/60 ethyl acetate/dichloromethane/hexane); Mp: 205-207 °C; IR (film) 3055, 2920,

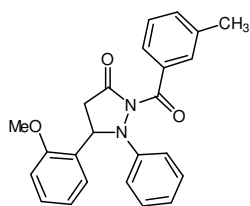
1759, 1693, 1593, 1492, 1275, 1231, 696 cm^{-1} ; ^1H NMR (500 MHz, CDCl_3) δ 8.14 (s, 1H); 7.93 (d, $J = 8.8$ Hz, 1H); 7.88-7.87 (m, 2H); 7.63-7.57 (m, 3H); 7.54-7.49 (m, 3H); 7.38-7.35 (m, 4H); 7.16-7.11 (m, 3H); 5.25 (d, $J = 8.3$ Hz, 1H); 3.53 (dd, $J = 17.1, 8.3$ Hz, 1H); 2.93 (d, $J = 17.1$ Hz, 1H); ^{13}C NMR (125 MHz, CDCl_3) δ 172.1, 166.4, 149.8, 136.9, 133.6, 133.5, 133.3, 132.5, 129.8, 129.3, 129.2, 128.5, 128.1, 127.9, 126.8, 126.7, 125.3, 124.2, 124.1, 117.3, 67.9, 38.5; LRMS (electrospray): Mass calculated for $\text{C}_{26}\text{H}_{20}\text{N}_4\text{O}_3$ [2M + Na] $^+$, 808. Found 808.



2-Benzoyl-5-(4-chlorophenyl)-1-phenylpyrazolidin-3-one (I-148e):

Purified with 5/25/70 ethyl acetate/dichloromethane/hexane, yielding 55 mg (61%) of **I-148e** as a light yellow solid. $R_f = 0.31$ (5/35/60 ethyl acetate/dichloromethane/hexane); Mp: 197-198 °C; IR (film) 3061, 2920, 1759,

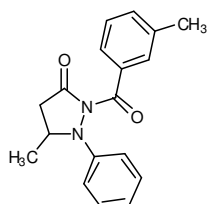
1694, 1593, 1491, 1277, 1230, 696 cm^{-1} ; ^1H NMR (500 MHz, CDCl_3) δ 7.65-7.63 (m, 2H); 7.55-7.52 (m, 3H); 7.42-7.39 (m, 4H); 7.37-7.33 (m, 2H); 7.25-7.08 (m, 3H); 5.07 (d, $J = 8.3$ Hz, 1H); 3.48 (dd, $J = 17.1, 8.8$ Hz, 1H); 2.75 (d, $J = 17.1$ Hz, 1H); ^{13}C NMR (125 MHz, CDCl_3) δ 171.7, 166.2, 149.5, 138.3, 134.4, 133.4, 132.7, 129.8, 129.4, 129.3, 128.2, 127.8, 124.3, 117.2, 67.1, 38.8; LRMS (electrospray): Mass calculated for $\text{C}_{44}\text{H}_{34}\text{ClN}_4\text{O}_4\text{Na}$ $[2\text{M} + \text{Na}]^+$, 777. Found 777.



2-(3-Methylbenzoyl)-5-(2-methoxyphenyl)-1-phenylpyrazolidin-3-one

(I-148f): Purified with 5/25/70 ethyl acetate/dichloromethane/hexane, yielding 53 mg (64%) of **I-148f** as a light yellow foam. $R_f = 0.28$ (5/35/60

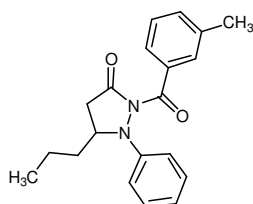
ethyl acetate/dichloromethane/hexane); Mp: 61-64 °C; IR (film) 3060, 2921, 1760, 1693, 1597, 1491, 1285, 1236, 1200, 695 cm^{-1} ; ^1H NMR (500 MHz, CDCl_3) δ 7.77 (d, $J = 7.8$ Hz, 1H); 7.46-7.44 (m, 2H); 7.38-7.27 (m, 5H); 7.11-7.03 (m, 4H); 6.95 (d, $J = 8.3$ Hz, 1H); 5.28 (d, $J = 8.8$ Hz, 1H); 3.86 (s, 3H); 3.43 (dd, $J = 17.6, 9.3$ Hz, 1H); 2.72 (d, $J = 17.6$ Hz, 1H); 2.36 (s, 3H); ^{13}C NMR (125 MHz, CDCl_3) δ 172.9, 166.6, 156.5, 150.2, 137.9, 133.8, 133.2, 129.8, 129.7, 129.5, 128.3, 127.9, 127.1, 126.4, 123.5, 121.2, 116.8, 110.7, 64.4, 55.4, 38.0, 21.5; LRMS (electrospray): Mass calculated for $\text{C}_{48}\text{H}_{44}\text{N}_4\text{O}_6\text{Na}$ $[2\text{M} + \text{Na}]^+$, 796. Found 796.



2-(3-Methylbenzoyl)-1-phenyl-5-methylpyrazolidin-3-one (I-148g):

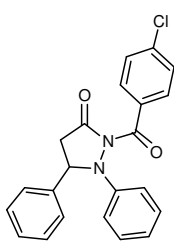
Purified with 5/25/70 ethyl acetate/dichloromethane/hexane, yielding 73 mg

(82%) of **I-148g** as a light orange solid. $R_f = 0.33$ (5/35/60 ethyl acetate/dichloromethane/hexane); Mp: 135-137 °C; IR (film) 3051, 2974, 1760, 1694, 1593, 1490, 1287, 1187, 696 cm^{-1} ; ^1H NMR (500 MHz, CDCl_3) δ 7.56-7.54 (m, 2H); 7.33-7.28 (m, 4H); 7.09-7.05 (m, 3H); 4.09-4.06 (m, 1H); 3.06 (dd, $J = 17.1, 7.3$ Hz, 1H); 2.38 (s, 3H); 2.26 (d, $J = 17.1$ Hz, 1H); 1.56 (d, $J = 6.8$ Hz, 3H); ^{13}C NMR (125 MHz, CDCl_3) δ 172.9, 166.9, 149.9, 137.9, 133.6, 133.2, 129.8, 129.5, 127.9, 126.4, 124.1, 117.7, 61.4, 37.9, 21.5, 21.0; LRMS (electrospray): Mass calculated for $\text{C}_{36}\text{H}_{36}\text{N}_4\text{O}_4\text{Na}$ $[2\text{M} + \text{Na}]^+$, 611. Found 611.



2-(3-Methylbenzoyl)-1-phenyl-5-propylpyrazolidin-3-one (I-148h):

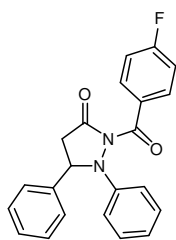
Purified with 5/25/70 ethyl acetate/dichloromethane/hexane, yielding 70 mg (84%) of **I-148h** as a yellow oil. $R_f = 0.32$ (5/35/60 ethyl acetate/dichloromethane/hexane); IR (film) 3047, 2958, 1760, 1694, 1593, 1490, 1284, 1232, 694 cm^{-1} ; ^1H NMR (500 MHz, CDCl_3) δ 7.51-7.49 (m, 2H); 7.33-7.28 (m, 4H); 7.05 (t, $J = 7.3$ Hz, 1H); 7.02 (d, $J = 7.8$ Hz, 2H); 3.90-3.85 (m, 1H); 3.07 (dd, $J = 17.1, 7.8$ Hz, 1H); 2.37 (s, 3H); 2.28 (d, $J = 17.6$ Hz, 1H); 1.96-1.90 (m, 1H); 1.76-1.69 (m, 1H); 1.63-1.55 (m, 2H); 1.04 (t, $J = 6.8$ Hz, 3H); ^{13}C NMR (125 MHz, CDCl_3) δ 173.3, 167.0, 150.4, 137.9, 133.7, 133.1, 129.7, 129.6, 127.9, 126.3, 123.9, 117.5, 65.9, 36.9, 36.7, 21.5, 19.7, 14.1; LRMS (electrospray): Mass calculated for $\text{C}_{40}\text{H}_{44}\text{N}_4\text{O}_4\text{Na}$ $[2\text{M} + \text{Na}]^+$, 667. Found 667.



2-(4-Chlorobenzoyl)-1,5-diphenylpyrazolidin-3-one (I-148i):

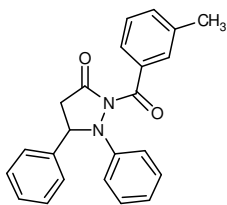
Purified with 5/25/70 ethyl acetate/dichloromethane/hexane, yielding 61 mg (68%) of **I-148i** as an yellow solid. $R_f = 0.31$ (5/35/60 ethyl acetate/dichloromethane/hexane); Mp: 173-175 °C; IR (film) 3062, 2921, 1760, 1694, 1595, 1489, 1274, 1230,

738, 696 cm^{-1} ; ^1H NMR (500 MHz, CDCl_3) δ 7.58-7.53 (m, 4H); 7.46-7.39 (m, 2H); 7.38-7.30 (m, 5H); 7.12-7.07 (m, 3H); 5.09 (d, $J = 8.3$ Hz, 1H); 3.46 (dd, $J = 17.1, 8.3$ Hz, 1H); 2.83 (d, $J = 17.1$ Hz, 1H); ^{13}C NMR (125 MHz, CDCl_3) δ 172.3, 165.3, 149.6, 139.5, 138.9, 131.8, 130.8, 129.8, 129.3, 128.6, 128.5, 126.4, 124.3, 117.3, 67.8, 38.4; LRMS (electrospray): Mass calculated for $\text{C}_{44}\text{H}_{34}\text{ClN}_4\text{O}_4\text{Na}$ $[2\text{M} + \text{Na}]^+$, 777. Found 777.



2-(4-Fluorobenzoyl)-1,5-diphenylpyrazolidin-3-one (I-148j): Purified with 5/25/70 ethyl acetate/dichloromethane/hexane, yielding 52 mg (61%) of **I-148j** as a light tan solid. $R_f = 0.30$ (5/35/60 ethyl acetate/dichloromethane/hexane); Mp: 156-159 $^{\circ}\text{C}$; IR (film) 3063, 2924, 1760, 1184, 1600, 1494, 1276, 1233,

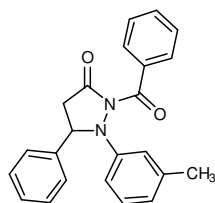
847, 698 cm^{-1} ; ^1H NMR (500 MHz, CDCl_3) δ 7.66-7.63 (m, 2H); 7.58 (d, $J = 7.8$ Hz, 2H); 7.45 (t, $J = 7.3$ Hz, 2H); 7.39-7.32 (m, 3H); 7.11-7.03 (m, 5H); 5.09 (d, $J = 8.3$ Hz, 1H); 3.47 (dd, $J = 17.1, 8.8$ Hz, 1H); 2.83 (d, $J = 17.1$ Hz, 1H); ^{13}C NMR (125 MHz, CDCl_3) δ 172.3, 165.2, 149.7, 139.6, 132.2, 132.1, 129.8, 129.3, 128.6, 126.4, 124.2, 117.2, 115.5, 115.3, 67.7, 38.5; LRMS (electrospray): Mass calculated for $\text{C}_{44}\text{H}_{34}\text{FN}_4\text{O}_4\text{Na}$ $[2\text{M} + \text{Na}]^+$, 744. Found 744.



2-(3-Methylbenzoyl)-1,5-diphenylpyrazolidin-3-one (I-148h): Purified with 5/25/70 ethyl acetate/dichloromethane/hexane, yielding 62 mg (73%) of **I-148h** as a light tan foam. $R_f = 0.30$ (5/35/60 ethyl acetate/dichloromethane/hexane); Mp: 52-53 $^{\circ}\text{C}$; IR (film) 3050, 2921,

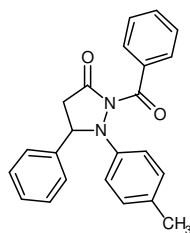
1760, 1693, 1598, 1492, 1282, 1204, 696 cm^{-1} ; ^1H NMR (500 MHz, CDCl_3) δ 7.59 (d, $J = 7.3$ Hz, 2H); 7.45 (t, $J = 7.8$ Hz, 2H); 7.40-7.27 (m, 7H); 7.10 (d, $J = 7.3$ Hz, 3H); 5.11 (d, $J = 8.3$ Hz, 1H); 3.46 (dd, $J = 17.1, 8.8$ Hz, 1H); 2.81 (d, $J = 17.1$ Hz, 1H); 2.34 (s, 3H); ^{13}C NMR (125

MHz, CDCl₃) δ 172.2, 166.5, 149.8, 139.8, 137.9, 133.5, 133.3, 129.8, 129.7, 129.3, 128.5, 127.9, 126.4, 126.3, 124.0, 117.2, 67.7, 38.6, 21.5; LRMS (electrospray): Mass calculated for C₄₆H₄₀N₄O₄Na [2M + Na]⁺, 736. Found 736.



2-Benzoyl-1-(3-methylphenyl)-5-phenylpyrazolidin-3-one (I-148k):

Purified with 5/25/70 ethyl acetate/dichloromethane/hexane, yielding 59 mg (66%) of **I-148k** as a light tan foam. R_f = 0.30 (5/35/60 ethyl acetate/dichloromethane/hexane); Mp: 104-106 °C; IR (film) 3059, 2921, 1759, 1694, 1601, 1490, 1279, 1221, 697 cm⁻¹; ¹H NMR (500 MHz, CDCl₃) δ 7.60 (t, J = 6.8 Hz, 4H); 7.51 (t, J = 7.8 Hz, 1H); 7.45 (t, J = 7.3, 2H); 7.40-7.34 (m, 3H); 7.25-7.21 (m, 1H); 6.93-6.91 (m, 3H); 5.10 (d, J = 8.3 Hz, 1H); 3.47 (dd, J = 17.1, 8.8 Hz, 1H); 2.80 (d, J = 17.1 Hz, 1H); 2.34 (m, 3H); ¹³C NMR (125 MHz, CDCl₃) δ 172.3, 166.3, 149.9, 139.8, 139.7, 133.6, 132.4, 129.5, 129.3, 129.2, 128.4, 128.1, 126.3, 125.0, 118.2, 114.1, 67.7, 38.6, 21.8; LRMS (electrospray): Mass calculated for C₄₆H₄₀N₄O₄Na [2M + Na]⁺, 736. Found 736.



2-Benzoyl-1-(4-methylphenyl)-5-phenylpyrazolidin-3-one (I-148l):

Purified with 5/25/70 ethyl acetate/dichloromethane/hexane, yielding 53 mg (63%) of **I-148l** as a light yellow solid. R_f = 0.30 (5/35/60 ethyl acetate/dichloromethane/hexane); Mp: 151-152 °C; IR (film) 3047, 2921, 1757, 1691, 1599, 1493, 1276, 1231, 696 cm⁻¹; ¹H NMR (500 MHz, CDCl₃) δ 7.60-7.56 (m, 4H); 7.44 (t, J = 7.8 Hz, 2H); 7.39-7.32 (m, 3H); 7.19 (d, J = 7.8 Hz, 2H); 7.09 (d, J = 7.8 Hz, 3H); 5.10 (d, J = 8.3 Hz, 1H); 3.47 (dd, J = 17.1, 8.8 Hz, 1H); 2.81 (d, J = 17.1 Hz, 1H); 2.39 (s, 3H); ¹³C NMR (125 MHz, CDCl₃) δ 172.1, 166.2, 149.8, 143.4, 139.9, 130.6, 129.7, 129.6, 129.3, 128.9,

128.4, 126.3, 123.9, 117.1, 67.7, 38.9, 21.9; LRMS (electrospray): Mass calculated for $C_{46}H_{40}N_4O_4Na$ $[2M + Na]^+$, 736. Found 736.

1.9.7 *Enantioselective Amination of Enals with 1-Acyl-2-Aryldiazenes*

Into an oven-dried screw-capped glass tube equipped with a stir bar was charged with the triazolium salt **I-131** (15.3 mg, 0.0317 mmol) and 4 Å molecular sieves (150 mg) and capped in a nitrogen-filled drybox. The tube with the reagents was removed from the drybox and then purged with N_2 . Into the tube was added a solution of 1-benzoyl-1-phenyldiazene **I-137a** (100 mg, 0.476 mmol) dissolved in CH_2Cl_2 (635 μ L, 0.25 M). Next, distilled cinnamaldehyde **I-54a** (20 μ L, 0.159 mmol) was added and the reaction mixture was cooled to 0 °C. Lastly, DBU (7.1 μ L, 0.0476 mmol) was added to the reaction which turned the solution brown then orange. After 96 h at 0 °C, the orange suspension was allowed to warm to room temperature. The reaction was diluted with CH_2Cl_2 and filtered through a pad of silica gel and washed with CH_2Cl_2 and Et_2O . The resulting residue was purified by flash column chromatography on silica gel, 10-15% ethyl acetate/hexanes, yielding 33.1 mg (61%) of **I-153** as a light tan solid. R_f = 0.40 (25% ethyl acetate/hexanes).

Enantiomeric excess determined by HPLC on a Chiralcel AD-H column (20% IIPA/Hexanes, 1mL/min).

HPLC Trace of racemic I-53:

Data File C:\HPCHEM\2\DATA\ACHAN\AC7-0230.D

Sample Name: AC7-023

AC7-037 racemic phenyl

```

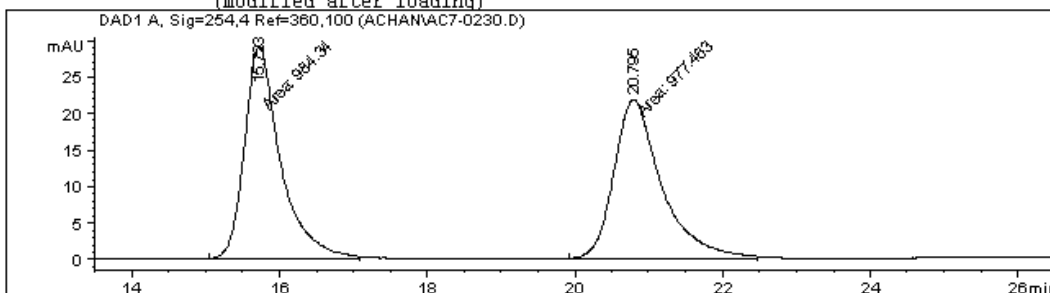
=====
Injection Date   : 12/11/2007 11:20:04 AM
Sample Name      : AC7-023
Acq. Operator    : mmb
Location         : Vial 31
Inj Volume       : 5 µl

```

```

Acq. Method      : C:\HPCHEM\2\METHODS\ACHAN.M
Last changed     : 12/11/2007 11:16:35 AM by mmb
                  (modified after loading)
Analysis Method   : C:\HPCHEM\2\METHODS\ACHAN.M
Last changed     : 12/11/2007 11:53:31 AM by mmb
                  (modified after loading)

```



```

=====
Area Percent Report
=====

```

```

Sorted By      :      Signal
Multiplier     :      1.0000
Dilution       :      1.0000
Use Multiplier & Dilution Factor with ISTDs

```

Signal 1: DAD1 A, Sig=254,4 Ref=360,100

Peak #	RetTime [min]	Type	Width [min]	Area [mAU*s]	Height [mAU]	Area %
1	15.723	MM	0.5656	984.34033	29.00793	50.1753
2	20.795	MM	0.7493	977.46326	21.74290	49.8247

```
Totals :                1961.80359  50.75082
```

Results obtained with enhanced integrator!

```

=====
*** End of Report ***

```


HPLC Trace of enantioenriched I-53:

Data File C:\HPCHEM\2\DATA\ACHAN\AC7-2360.D

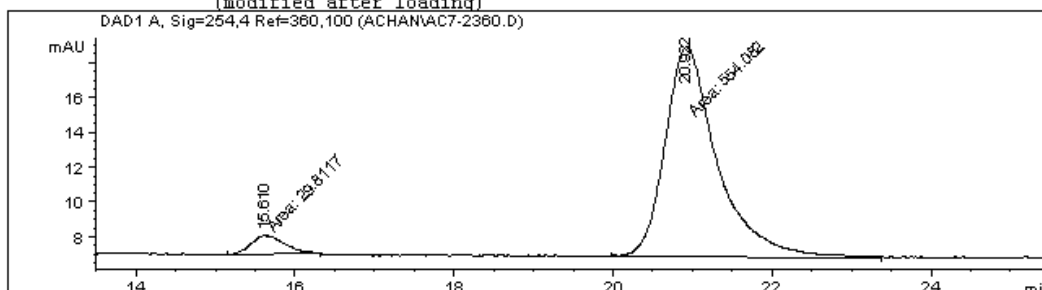
Sample Name: AC7-236-1

AC7-236 chiral phenyl

```

=====
Injection Date   : 12/14/2007 12:40:32 PM
Sample Name     : AC7-236-1                Location : Vial 31
Acq. Operator   : mmb                      Inj Volume : 5 µl
Acq. Method     : C:\HPCHEM\2\METHODS\ACHAN.M
Last changed    : 12/11/2007 10:49:54 AM by mmb
Analysis Method : C:\HPCHEM\2\METHODS\ACHAN.M
Last changed    : 12/14/2007 1:13:17 PM by mmb
                  (modified after loading)
=====

```



Area Percent Report

```

=====
Sorted By      :      Signal
Multiplier     :      1.0000
Dilution      :      1.0000
Use Multiplier & Dilution Factor with ISTDs
=====

```

Signal 1: DAD1 A, Sig=254,4 Ref=360,100

Peak #	RetTime [min]	Type	Width [min]	Area [mAU*s]	Height [mAU]	Area %
1	15.610	MM	0.4711	29.81166	1.05478	5.1057
2	20.922	MM	0.7658	554.08221	12.05952	94.8943

Totals : 583.89388 13.11430

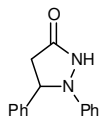
Results obtained with enhanced integrator!

```

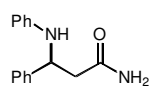
=====
*** End of Report ***
=====

```

1.9.8 Procedure for the Synthesis of β -Amino Acid Derivatives



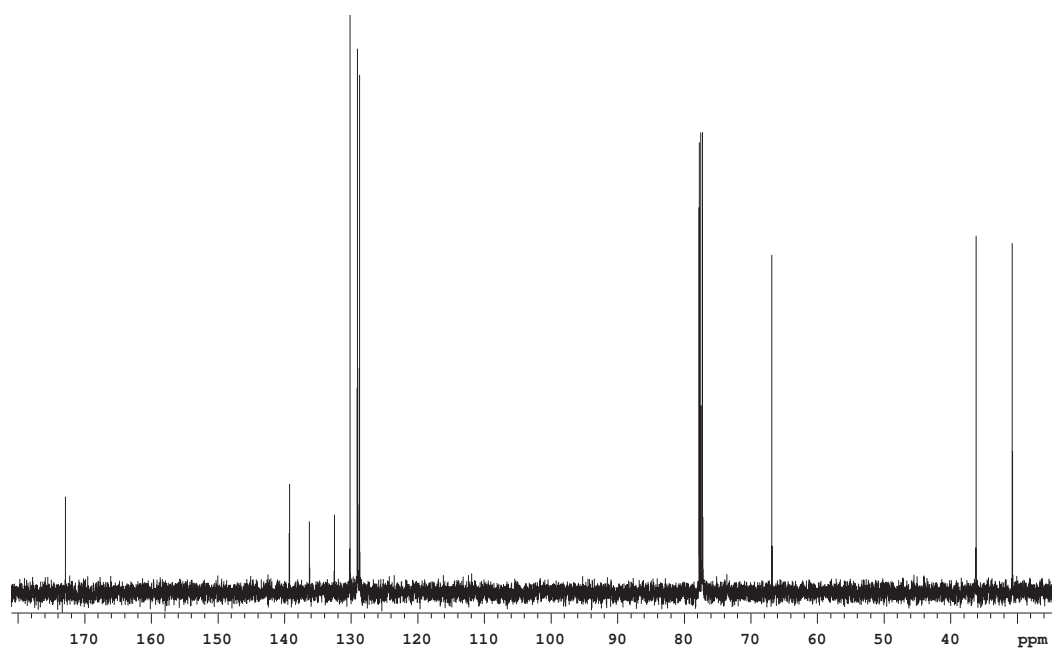
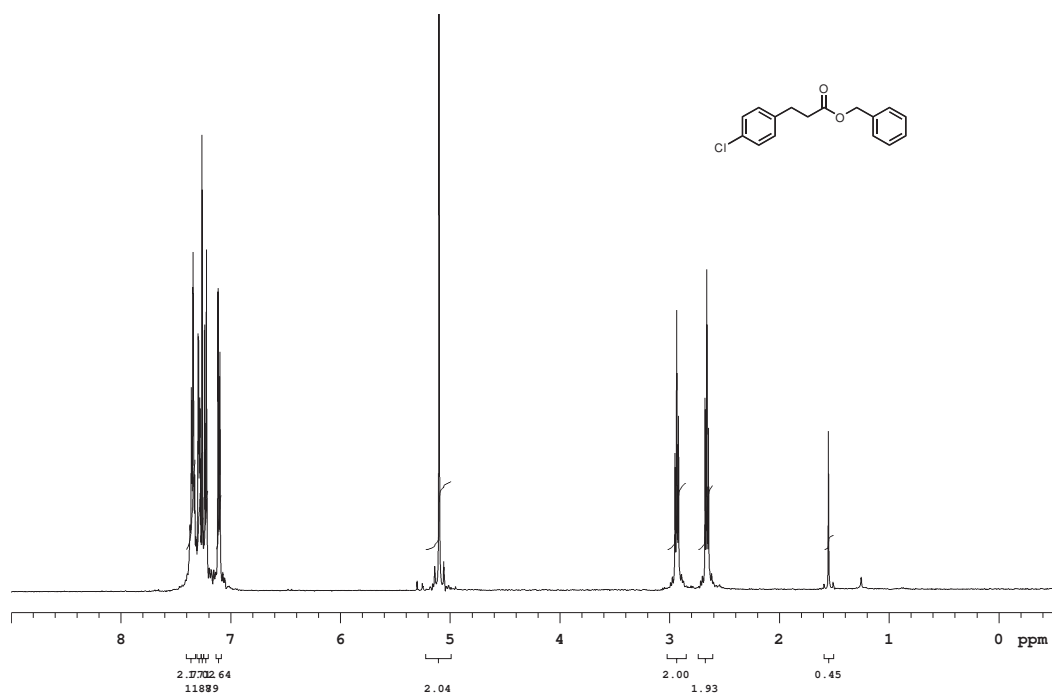
1,5-Diphenylpyrazolidin-3-one (I-154): Into a flame-dried 25 mL round-bottom flask equipped with a stir bar was added the 2-benzoyl-1,5-diphenylpyrazolidin-3-one (**I-148a**) (100 mg, 0.292 mmol) and dissolved in THF/MeOH (3 mL, 1:2, 0.05 M). It was purged with N₂ and into it was added Sm(OTf)₃ (17.5 mg, 0.029 mmol). The reaction mixture was allowed to stir at room temperature under a positive pressure of N₂. After 1 h, the solvent was removed in vacuo and the residue was purified via flash chromatography, 25-40% ethyl acetate/hexanes, yielding 52 mg (75%) of **19** as a white solid. R_f = 0.23 (40% ethyl acetate/hexanes); Mp: 154-156 °C; IR (film) 3173, 3063, 2853, 1693, 1593, 1452, 1209, 696 cm⁻¹; ¹H NMR (500 MHz, CDCl₃) δ 7.77 (s, 1H); 7.48 (d, J = 7.81 Hz, 2H); 7.42 (t, J = 7.3 Hz, 2H); 7.36-7.29 (m, 3H); 7.06 (d, J = 8.3 Hz, 3H); 4.94 (dd, J = 8.8, 2.9 Hz, 1H); 3.29 (dd, J = 16.6, 9.2 Hz, 1H); 2.53 (dd, J = 16.6, 2.9 Hz, 1H); ¹³C NMR (125 MHz, CDCl₃) δ 173.9, 151.4, 141.6, 129.5, 129.2, 128.2, 126.2, 123.2, 116.5, 70.1, 38.0; LRMS (electrospray): Mass calculated for C₁₅H₁₅N₂O [M+H]⁺, 239 Found 239.

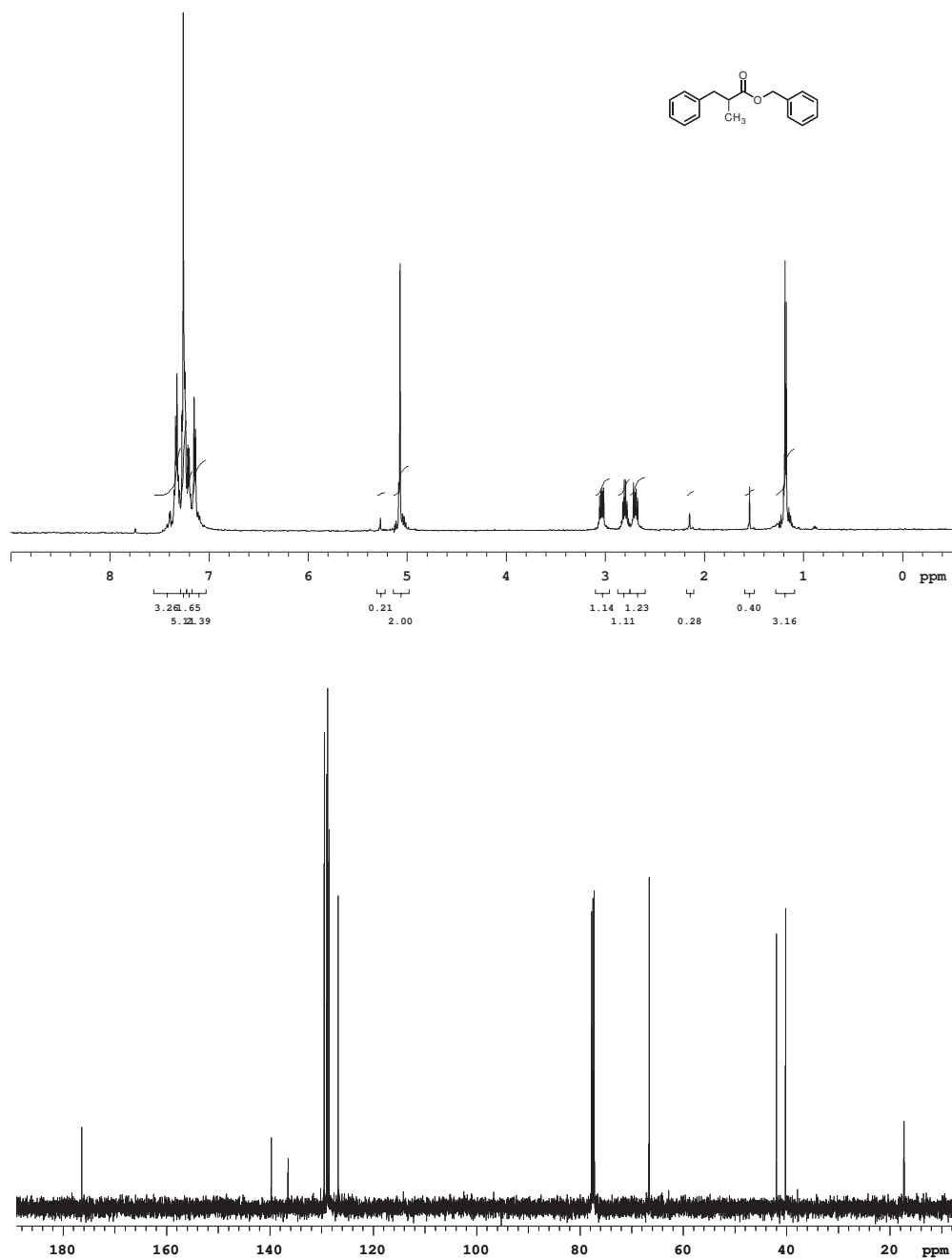


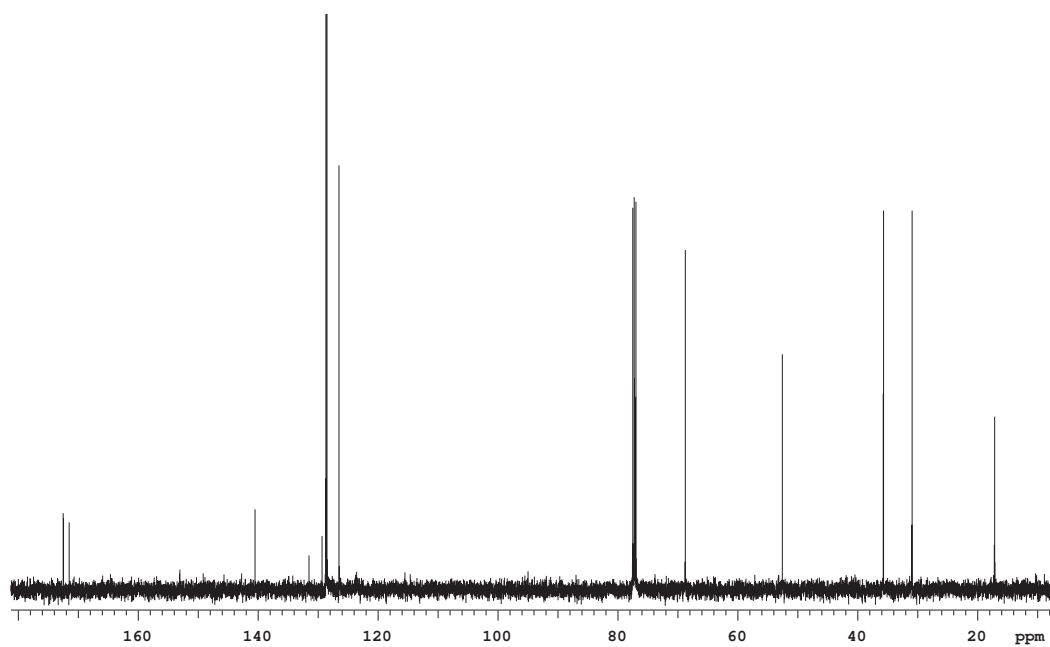
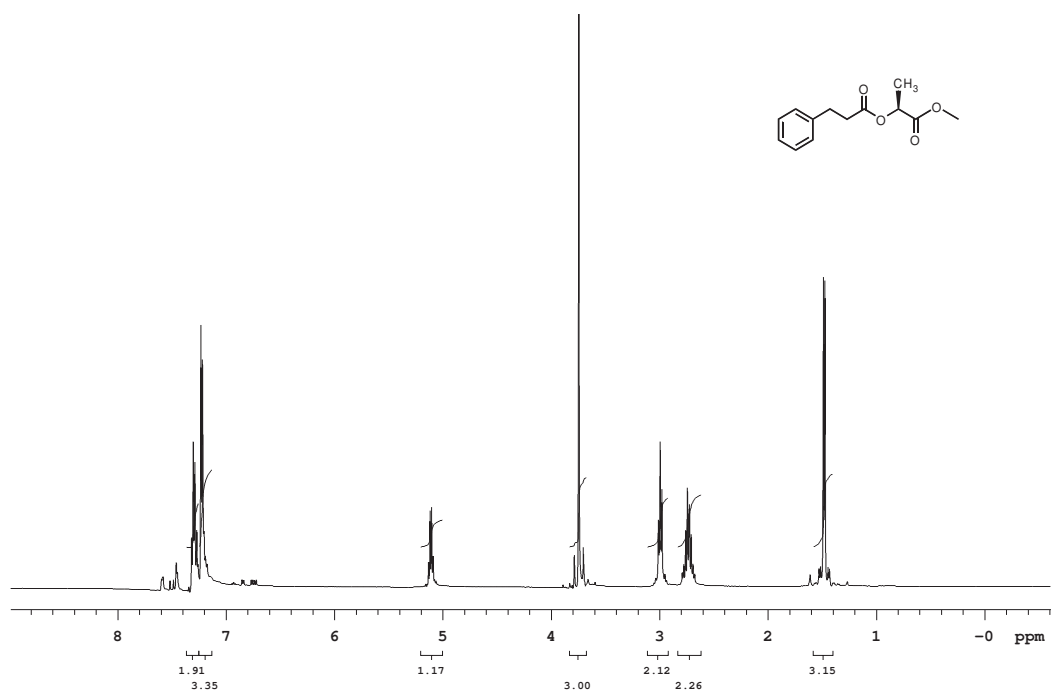
3-Phenyl-3-(phenylamino)propanamide (I-155): Into a flame-dried 25 mL round-bottom flask equipped with a stirbar was added 1,5-diphenylpyrazolidin-3-one (**I-154**) (43.5 mg, 0.183 mmol) and dissolved in EtOH (3.65 mL, 0.05 M). Into it was added a slurry of Raney 2800 nickel (approx. 325 mg, 5.5 mmol, previously washed 2 times with EtOH) and the reaction was allowed to stir at room temperature under an atmosphere of H₂ via a gas-filled double balloon. After 1 h, the reaction was deemed complete (as determined by thin layer chromatography) and it was filtered through a pad of Celite with EtOH. Solvent was removed

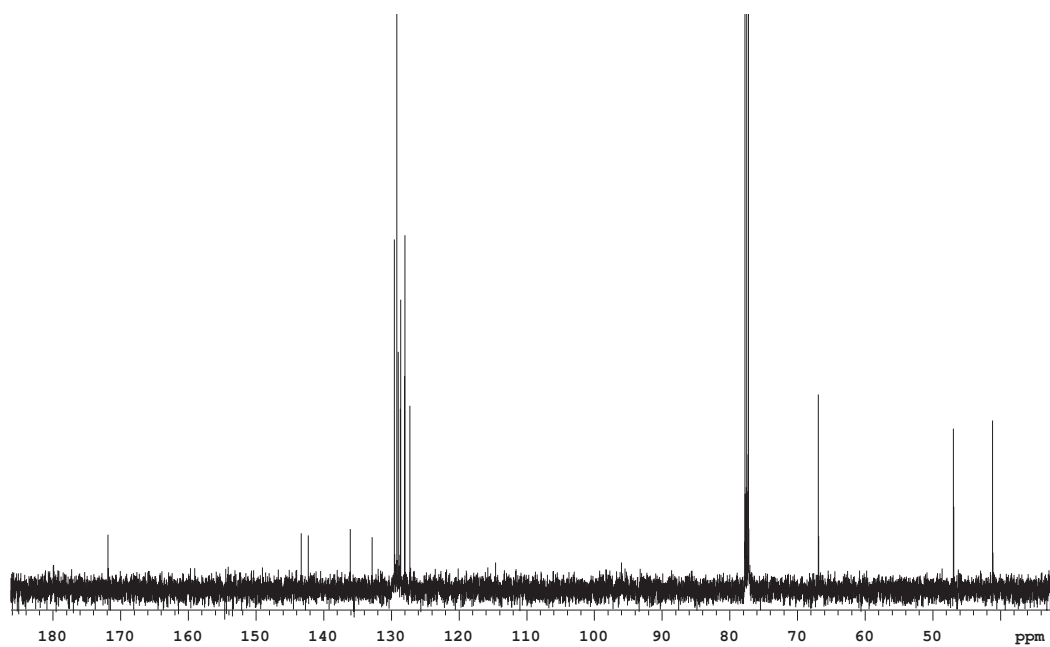
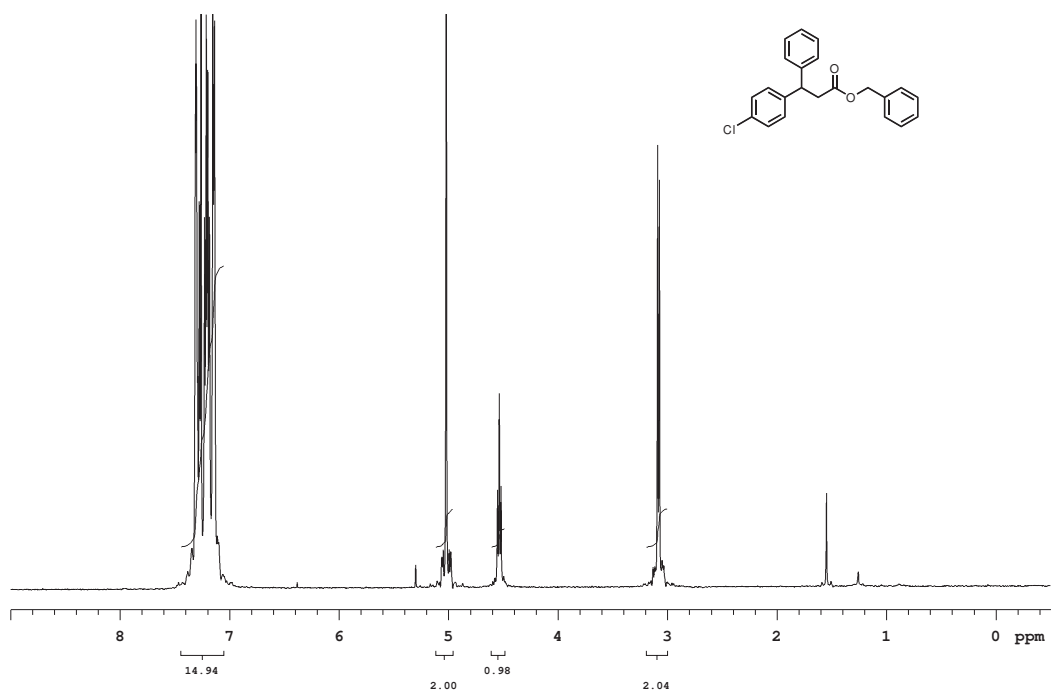
and the residue was purified via flash chromatography, 50-90% ethyl acetate/hexane, yielding 42 mg (96%) of 20 as a white solid. $R_f = 0.21$ (50% ethyl acetate/hexanes); Mp: 122-124 °C; IR (film) 3453, 3350, 3189, 3051, 2924, 1666, 1602, 1503, 1400, 748, 698 cm^{-1} ; ^1H NMR (500 MHz, CDCl_3) δ 7.36 (t, $J = 7.3$ Hz, 2H); 7.33-7.31 (m, 2H); 7.20 (d, $J = 7.3$ Hz, 1H); 7.10 (t, $J = 7.3$ Hz, 2H); 6.68 (t, $J = 7.3$ Hz, 1H); 6.53 (d, $J = 7.8$ Hz, 2H); 5.60 (s, b, 1H); 5.35 (s, br, 1H); 4.84 (s, br, 1H); 4.79 (t, $J = 5.9$ Hz, 1H); 2.75-2.66 (m, 2H); ^{13}C NMR (125 MHz, CDCl_3) δ 173.2, 146.9, 142.5, 129.3, 129.0, 127.6, 126.4, 118.1, 114.1, 55.5, 44.2; LRMS (electrospray): Mass calculated for $\text{C}_{15}\text{H}_{17}\text{N}_2\text{O}$ $[\text{M} + \text{H}]^+$, 241, Found 241.

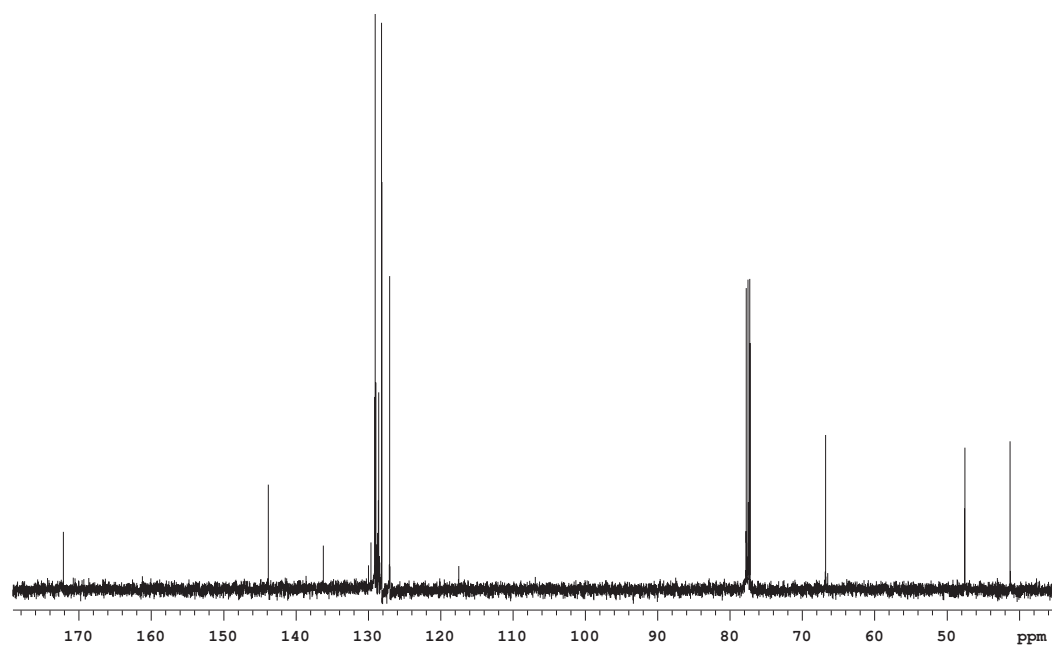
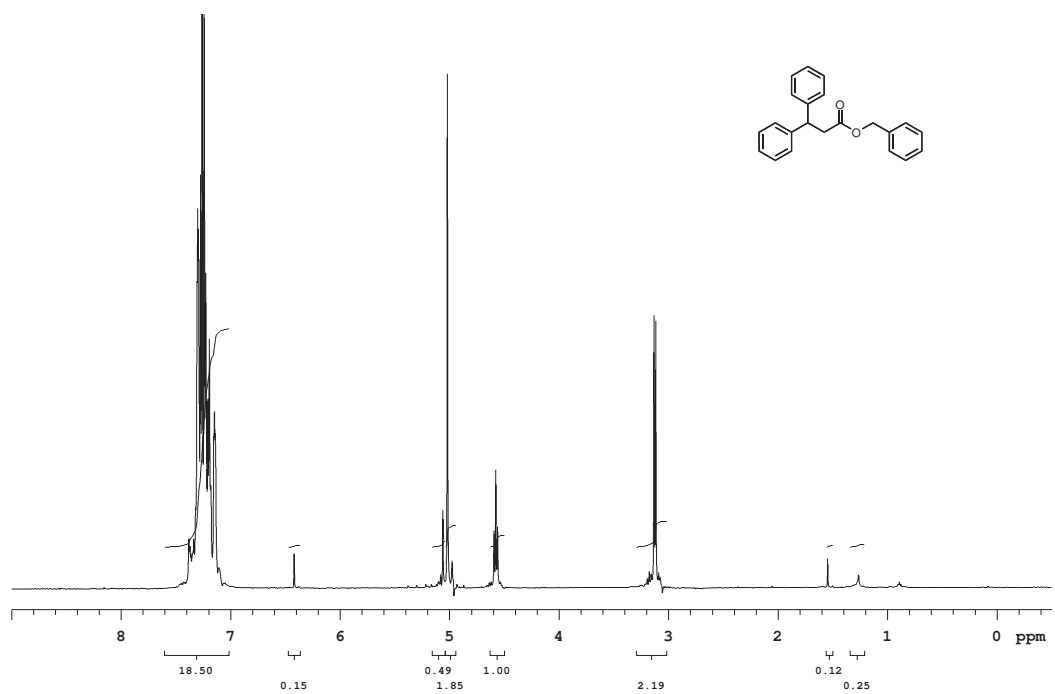
1.9.9 Selected NMR Spectra

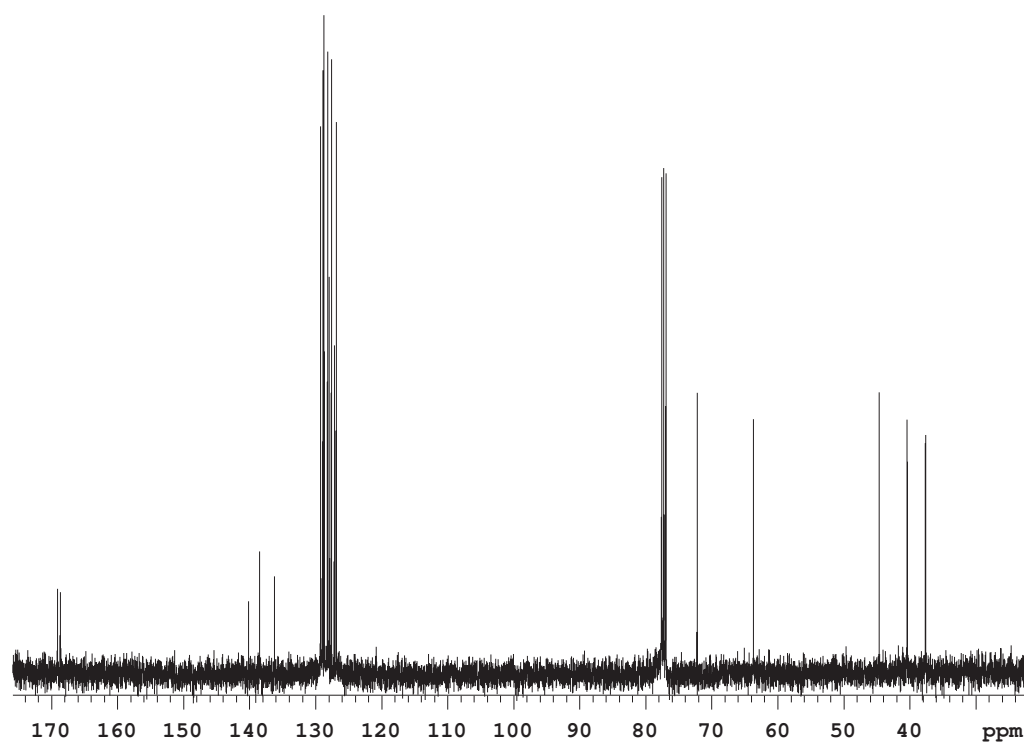
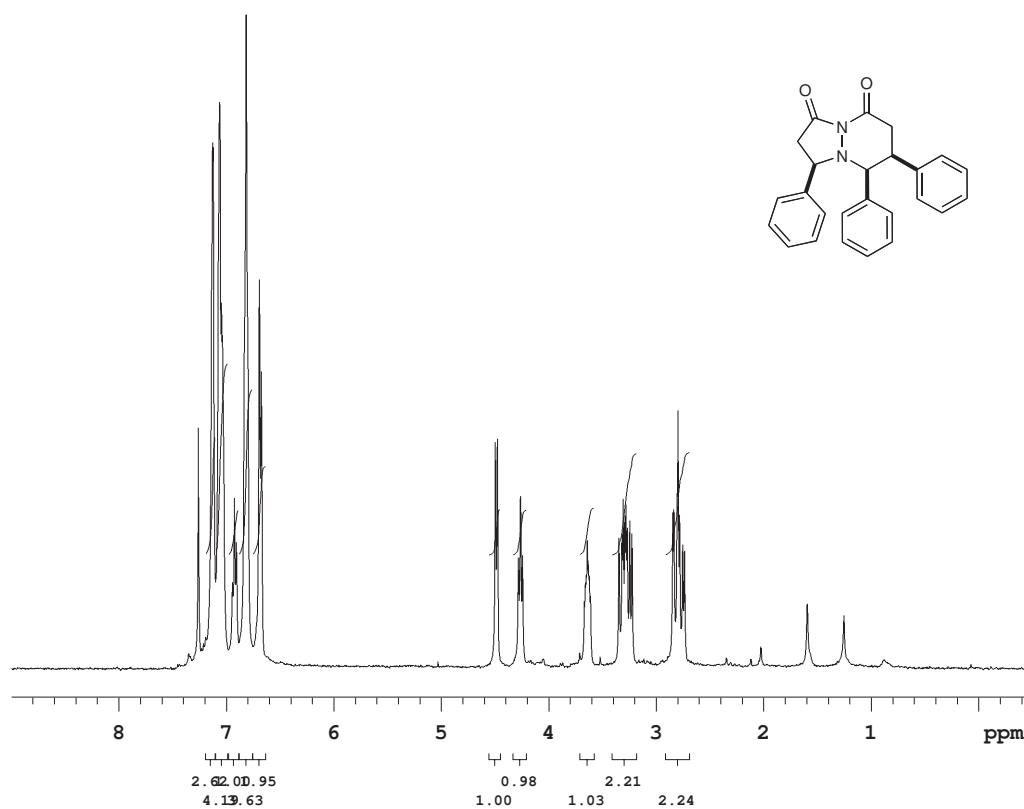


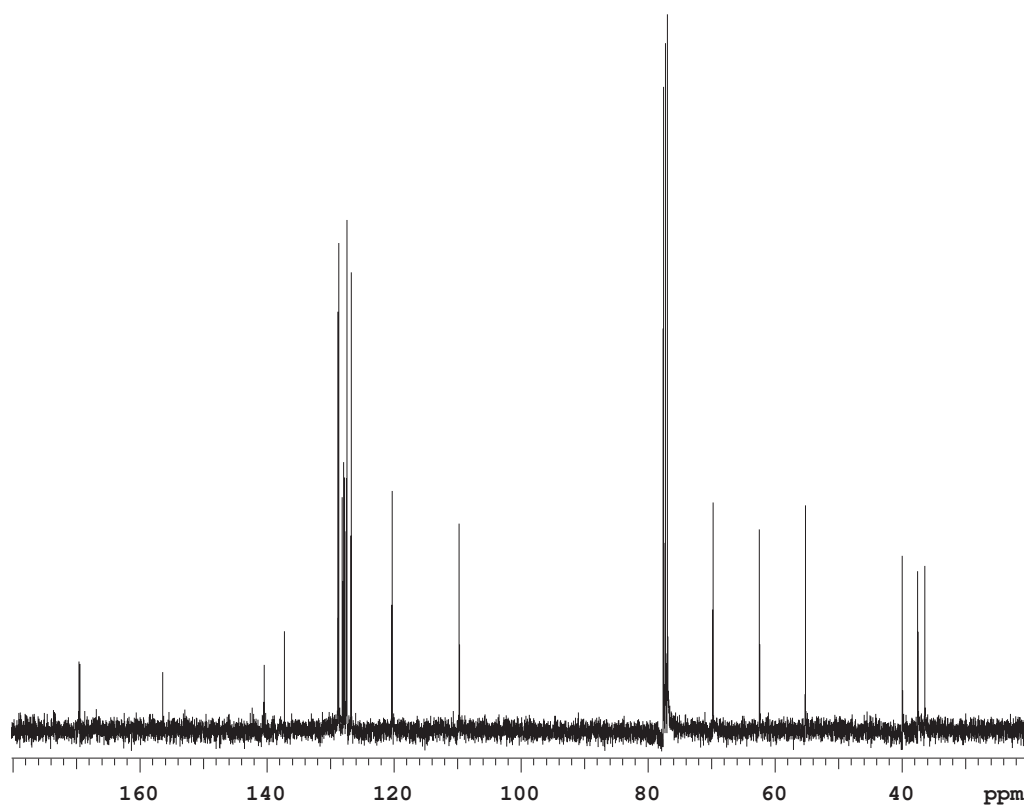
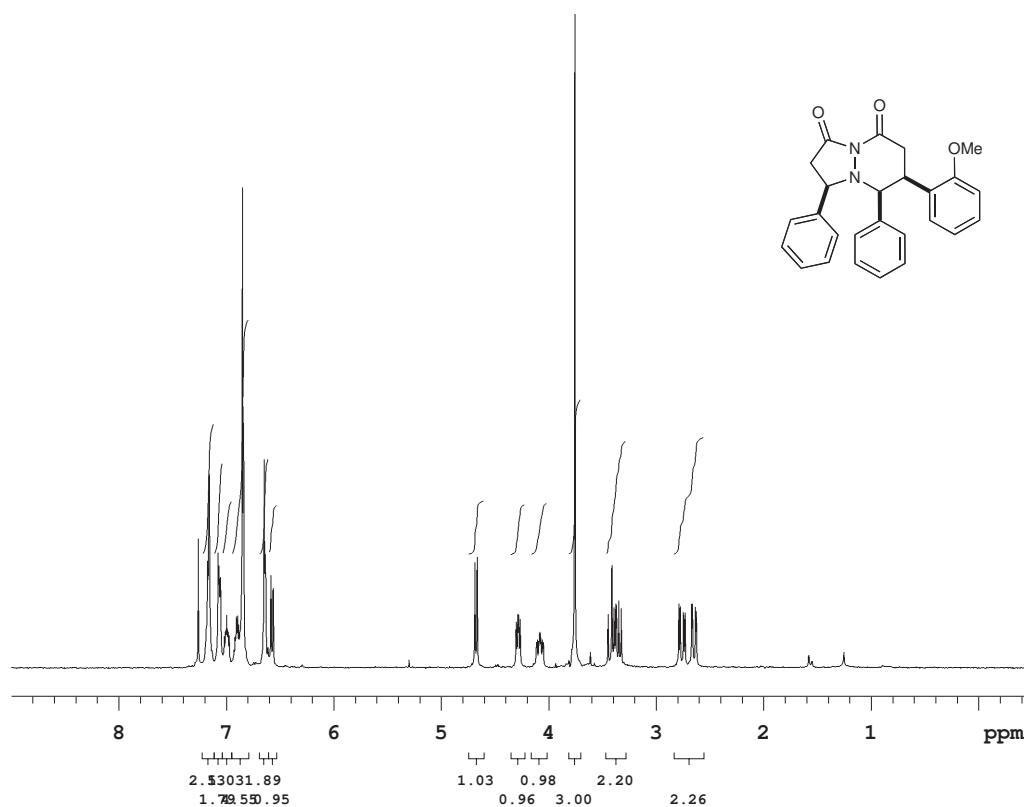


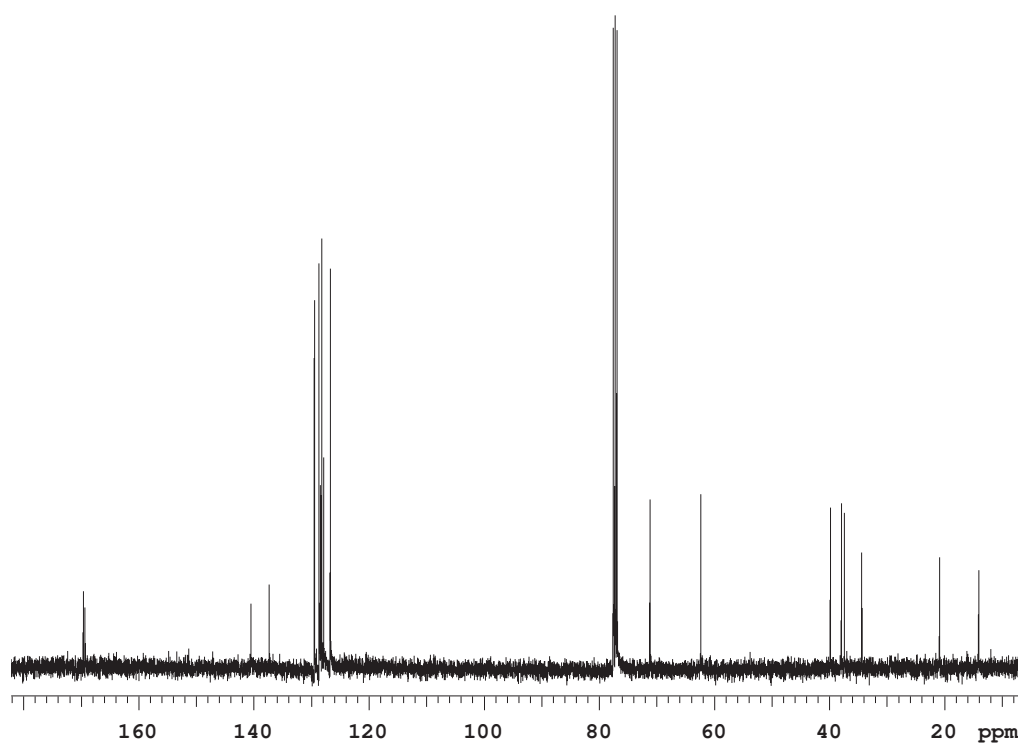
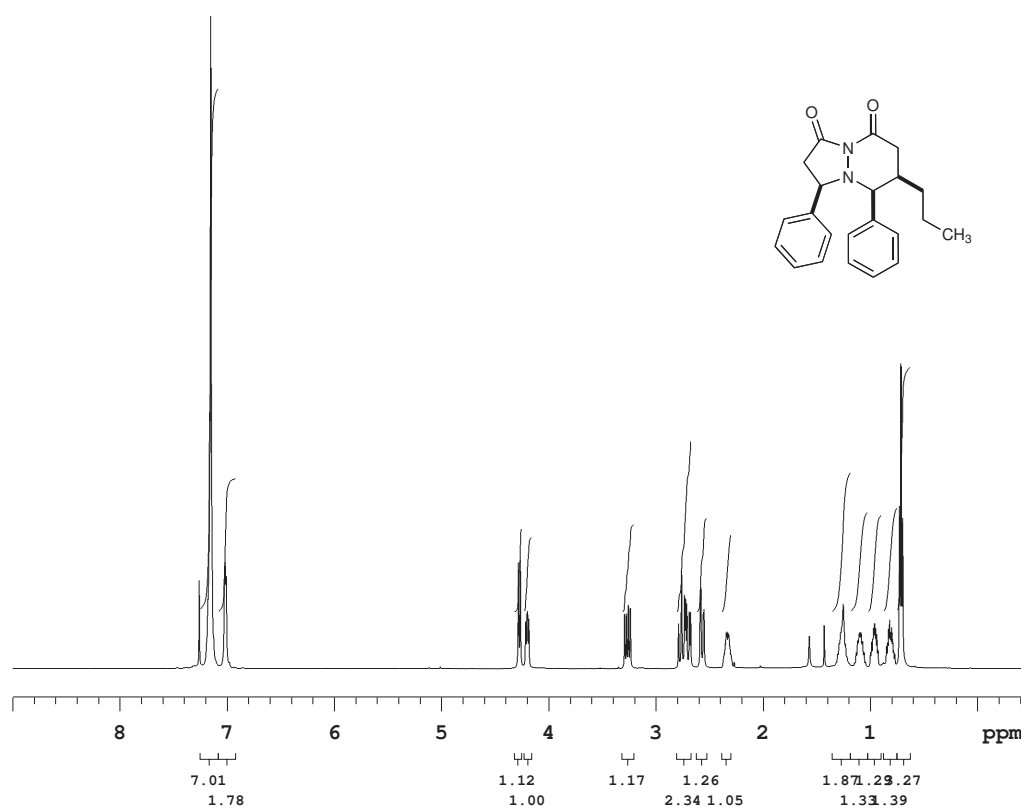


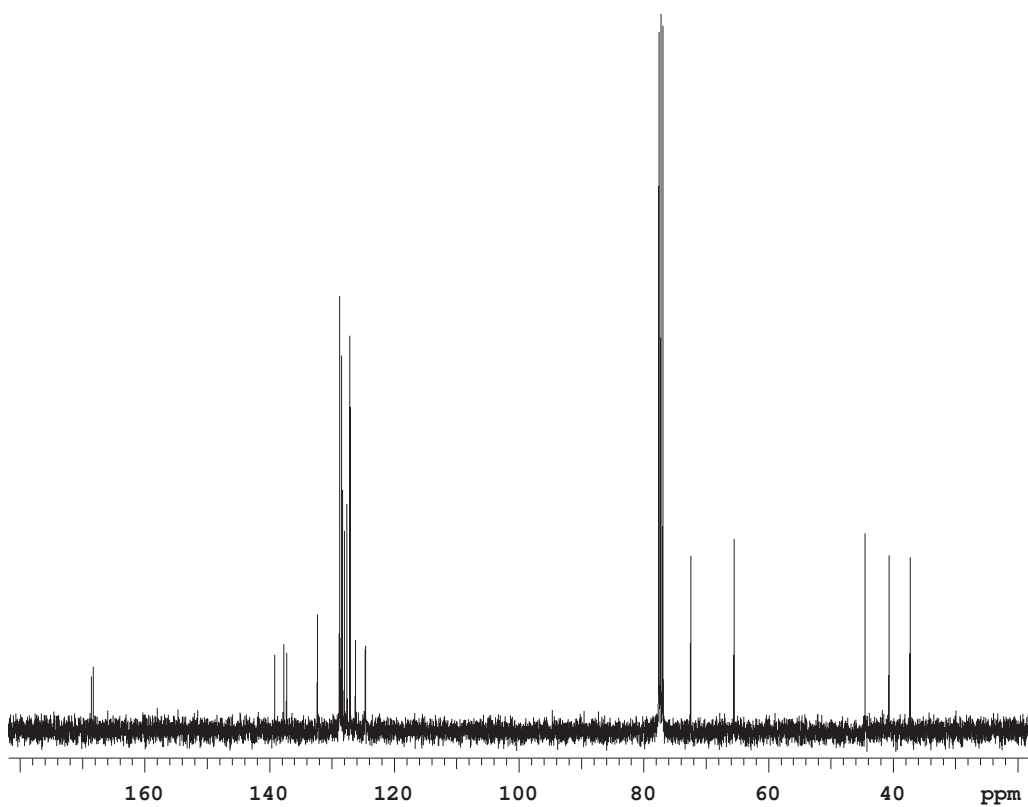
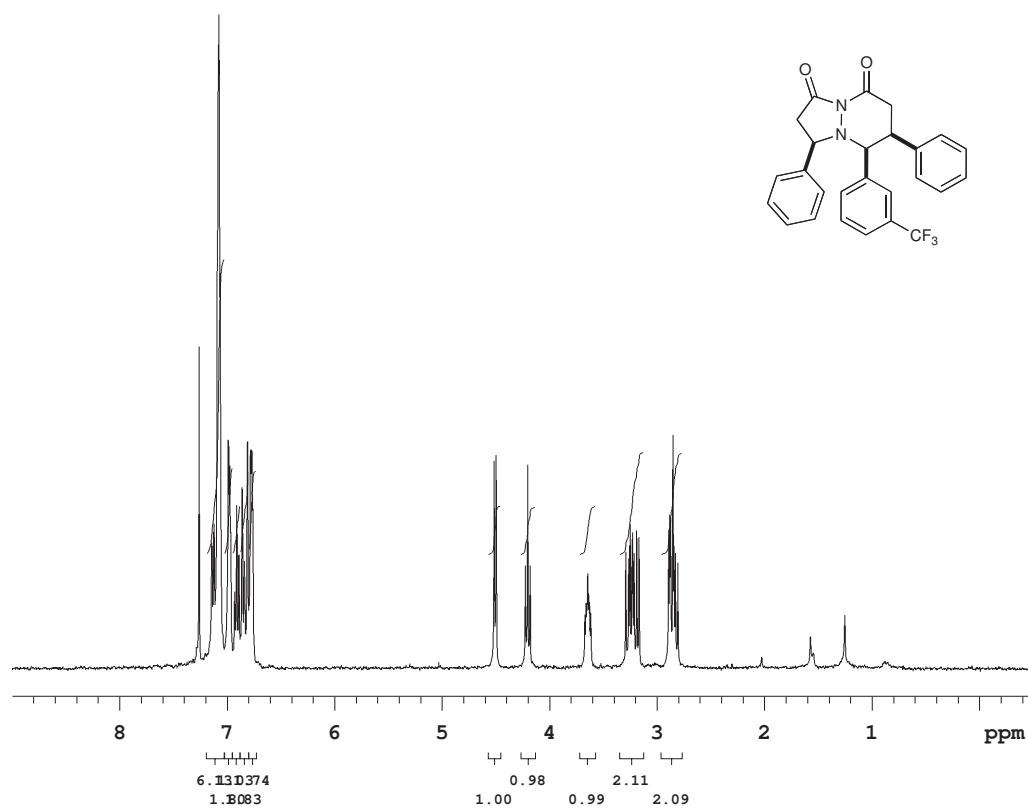


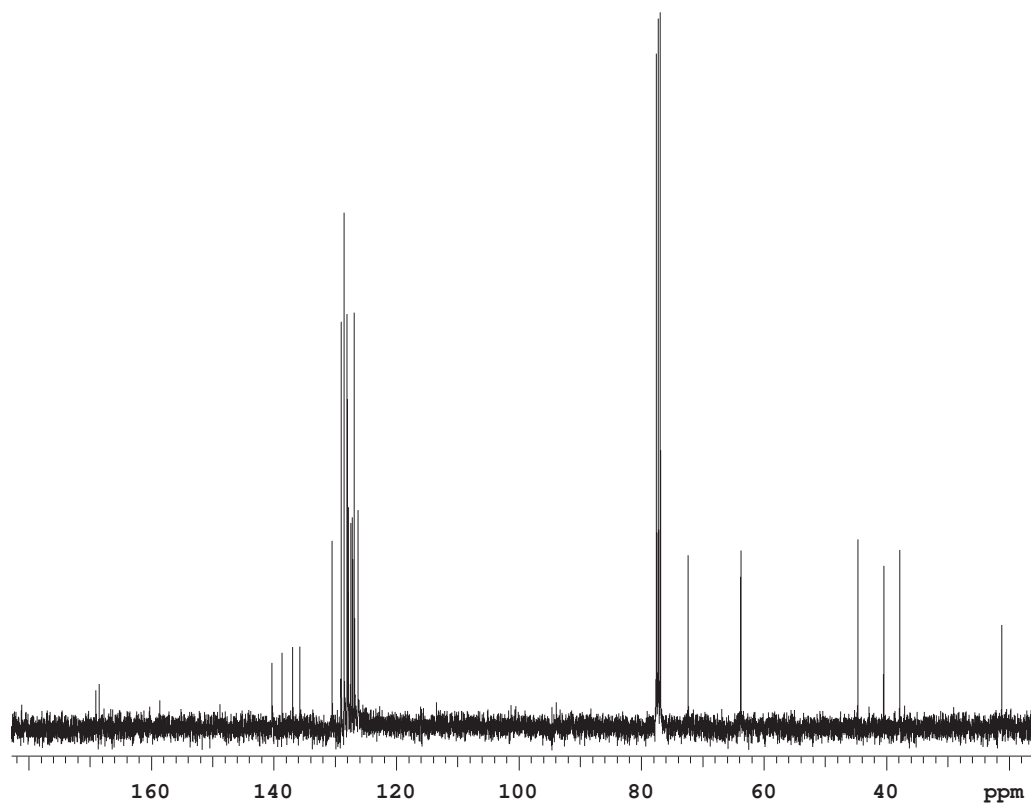
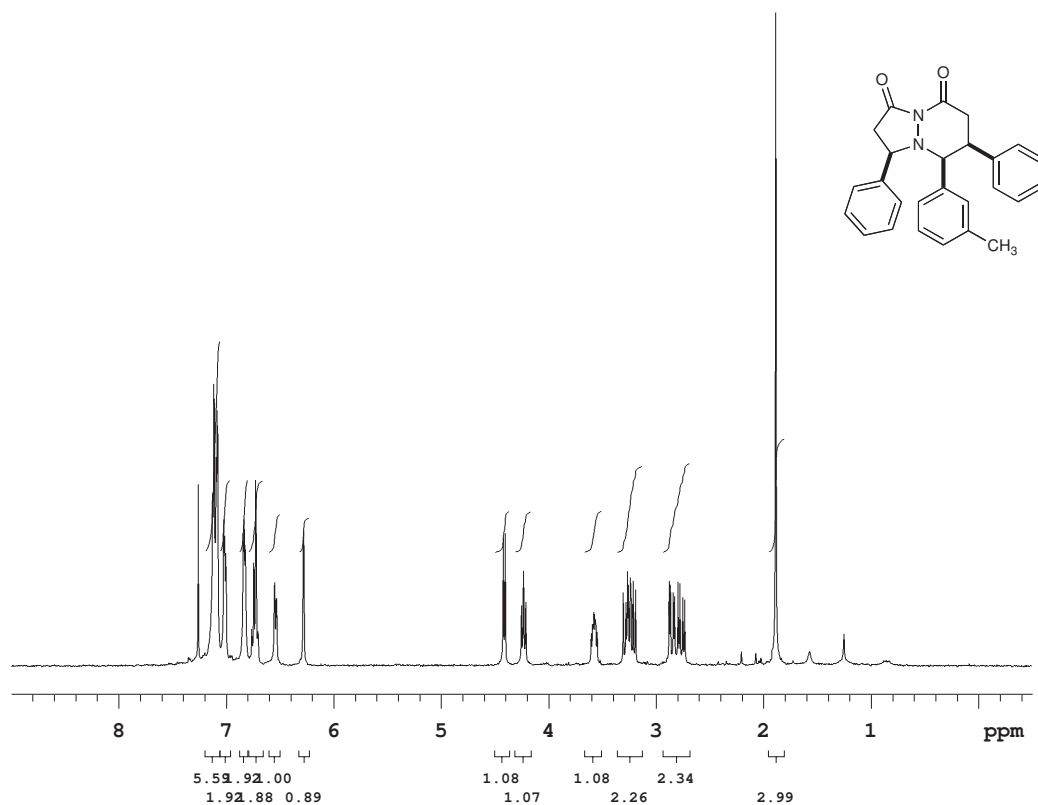


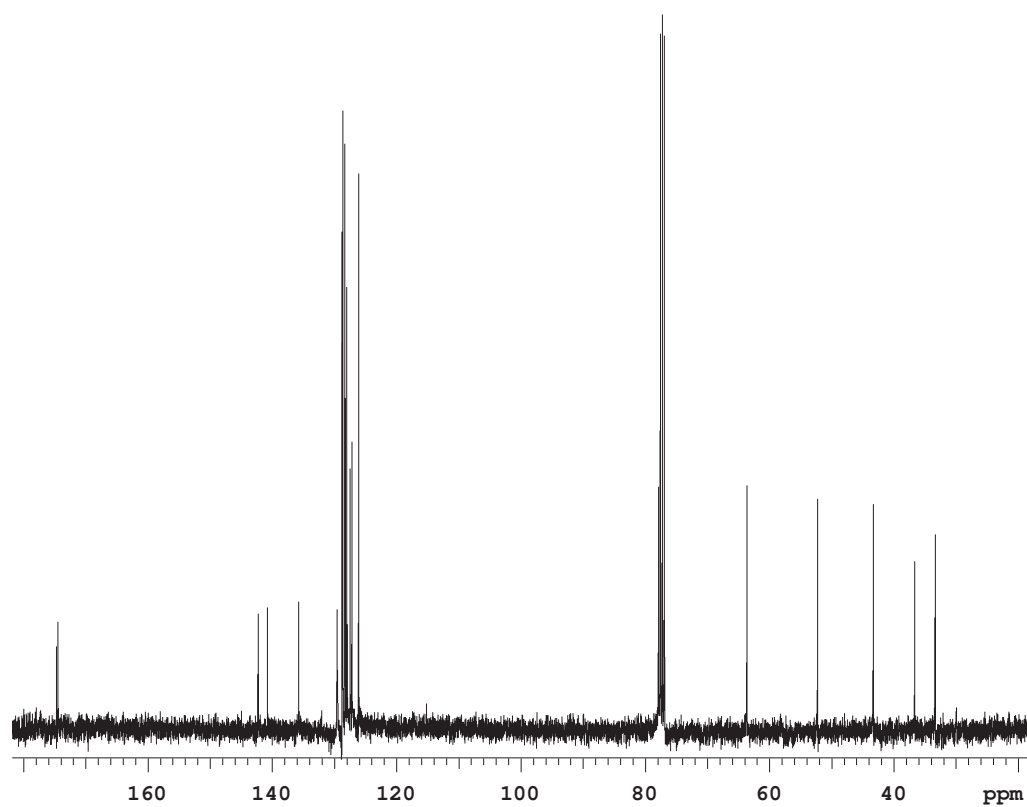
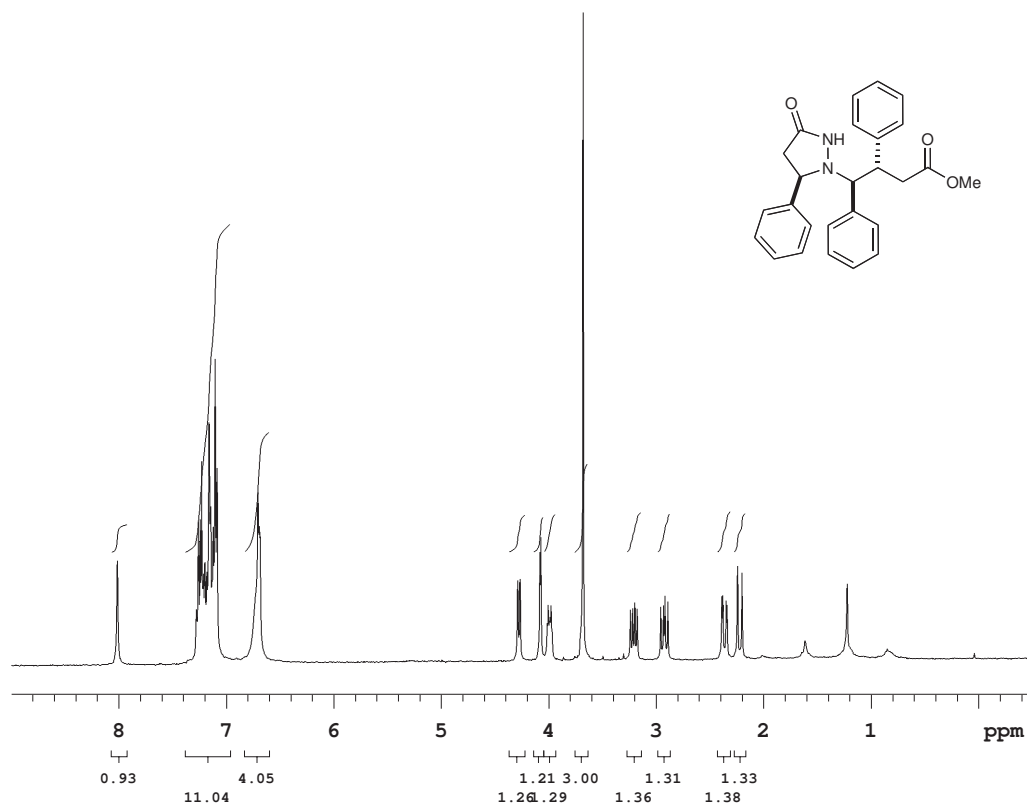


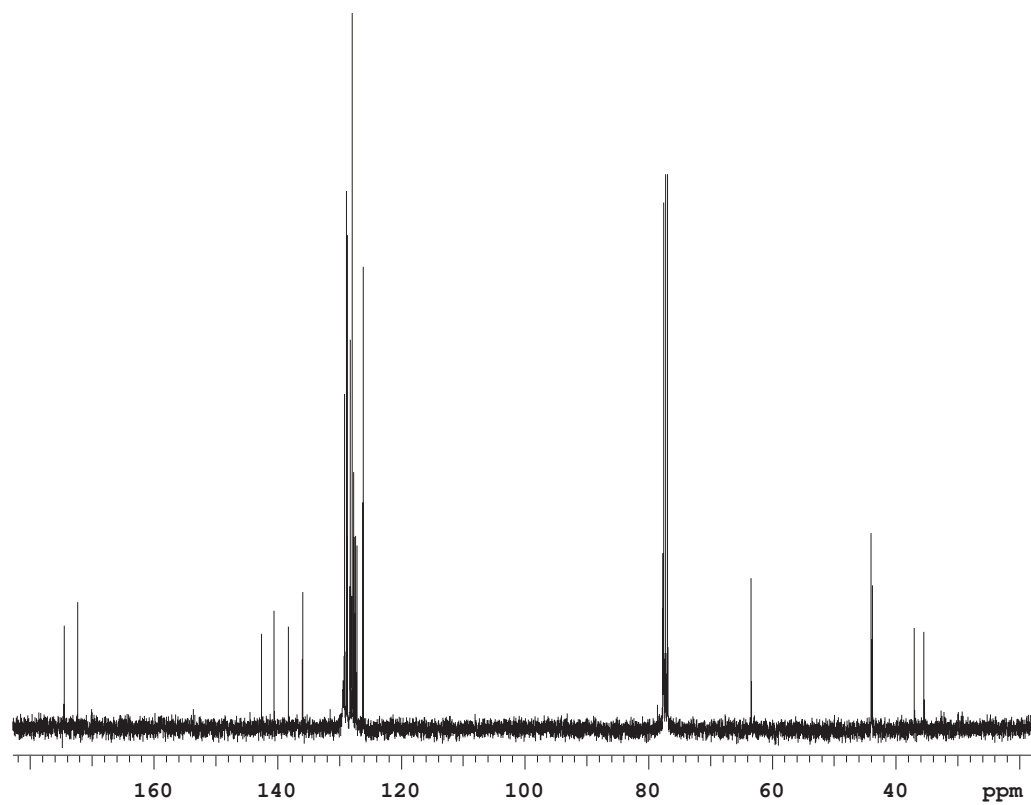
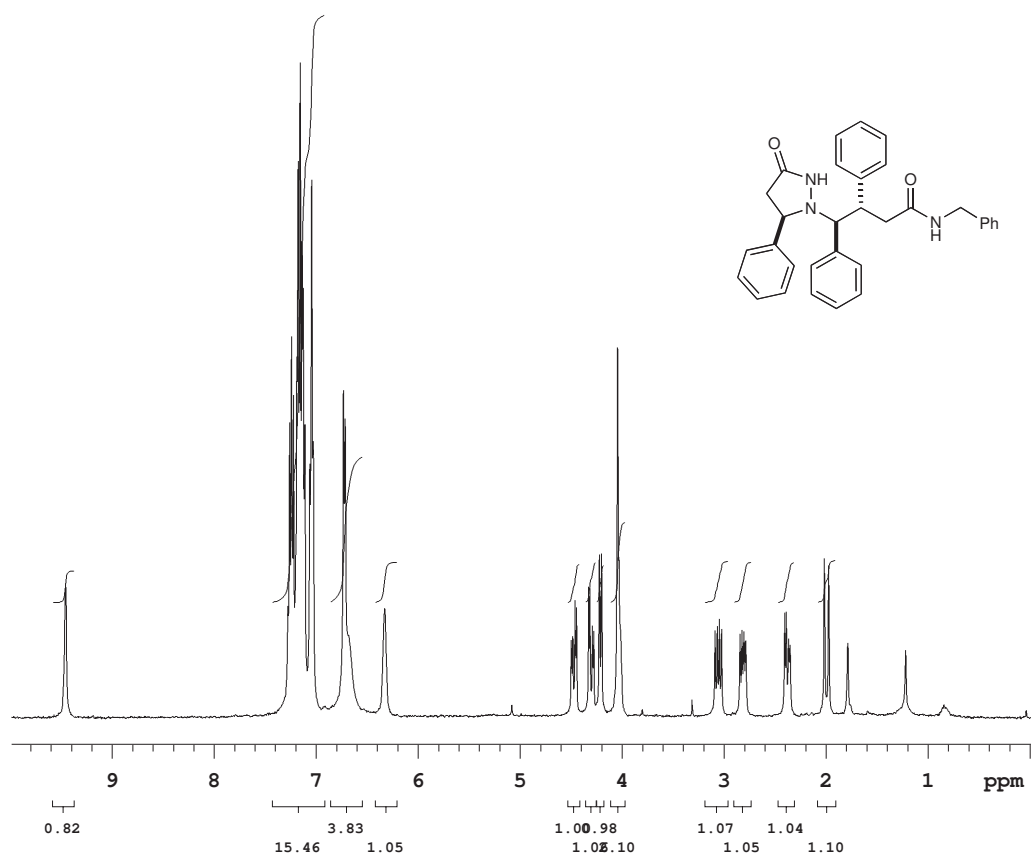


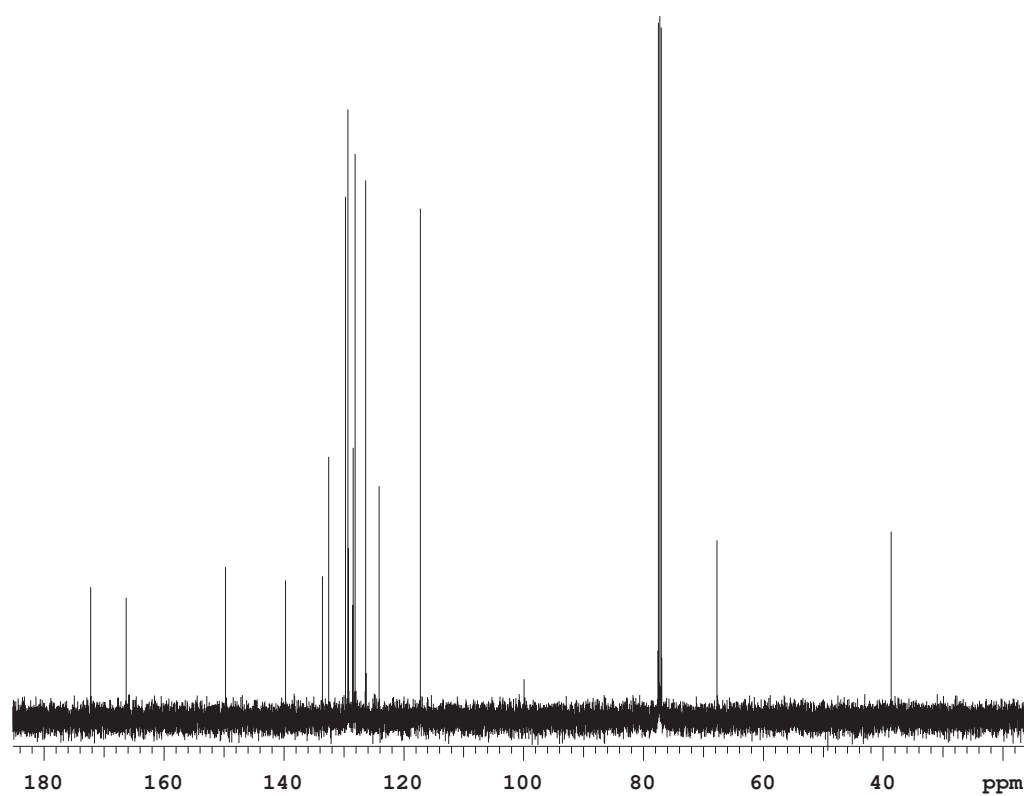
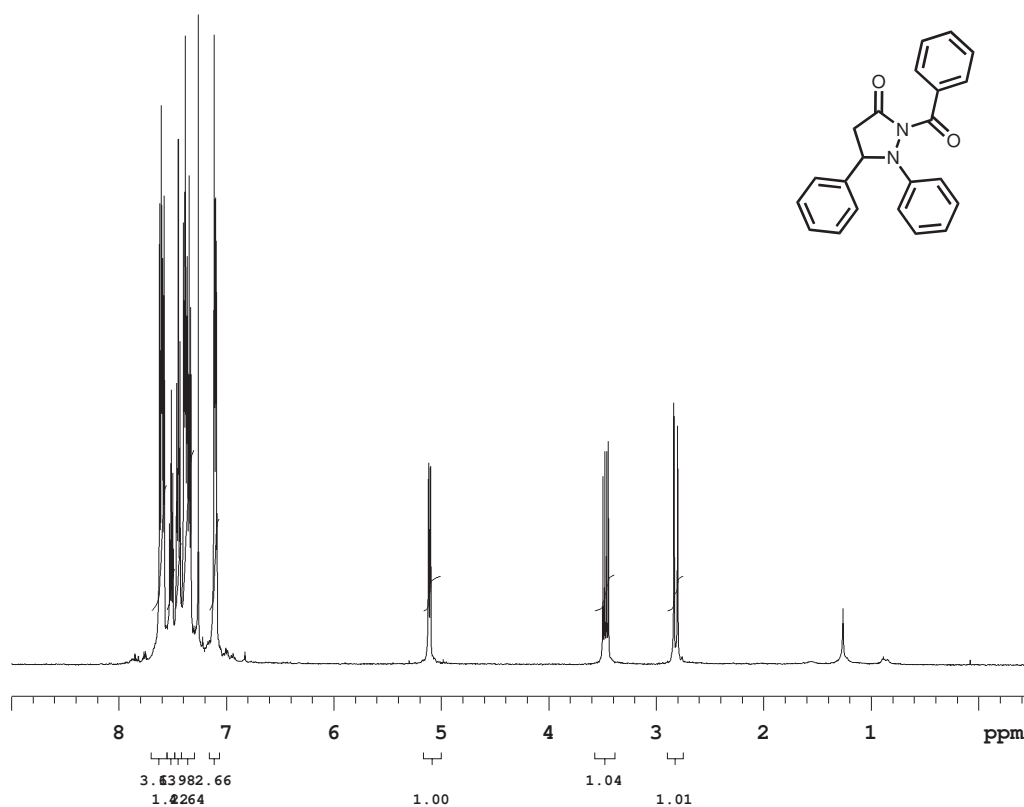
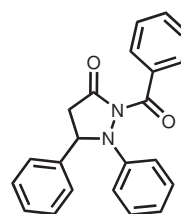


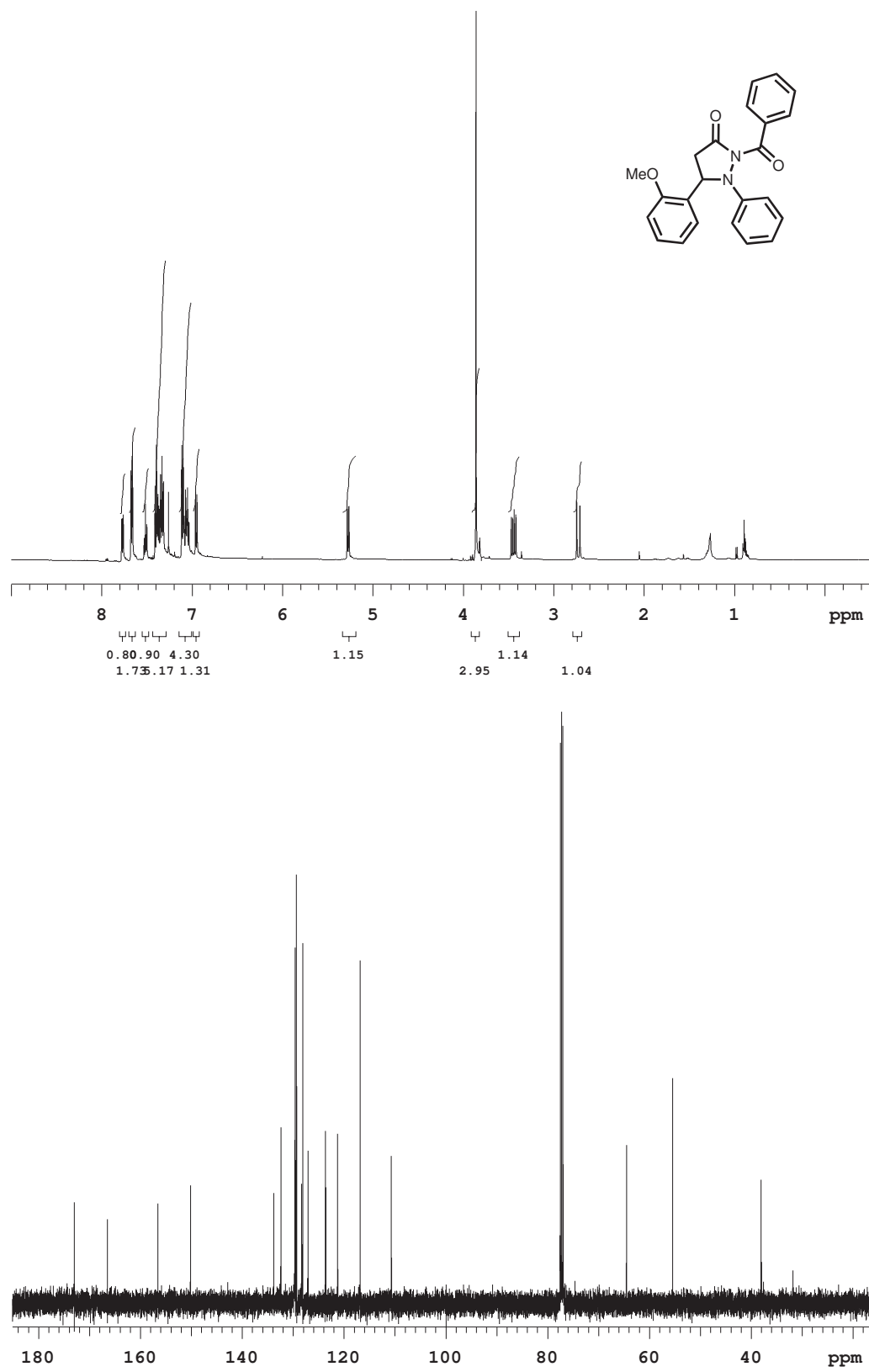


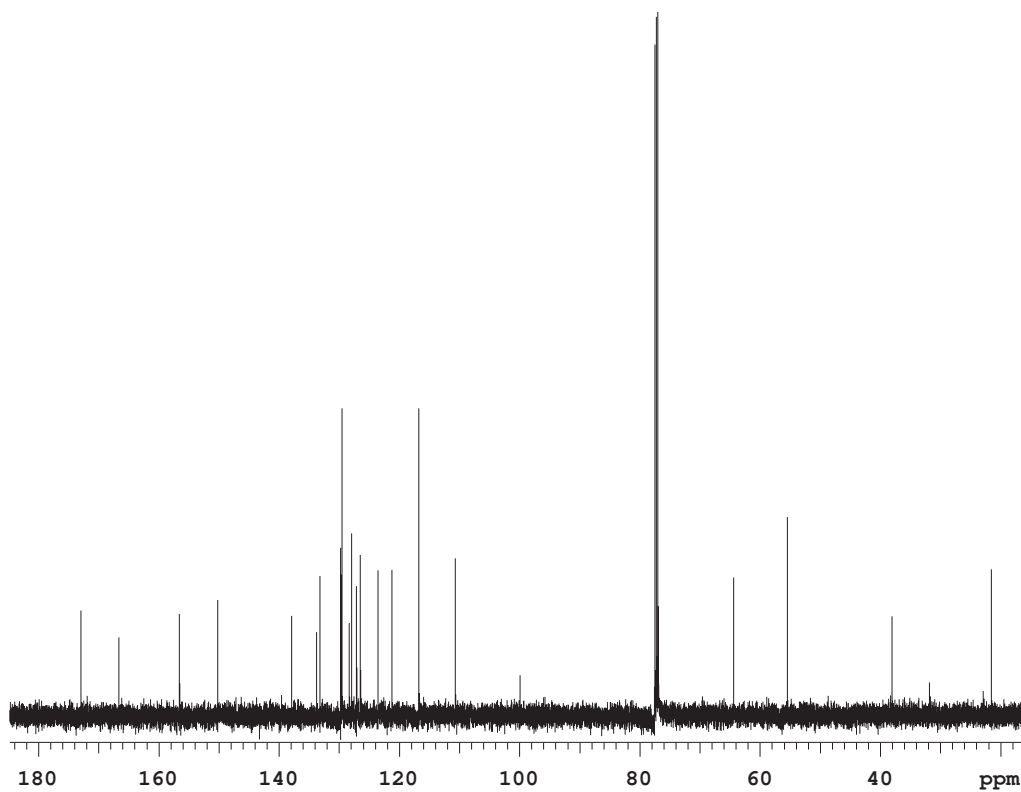
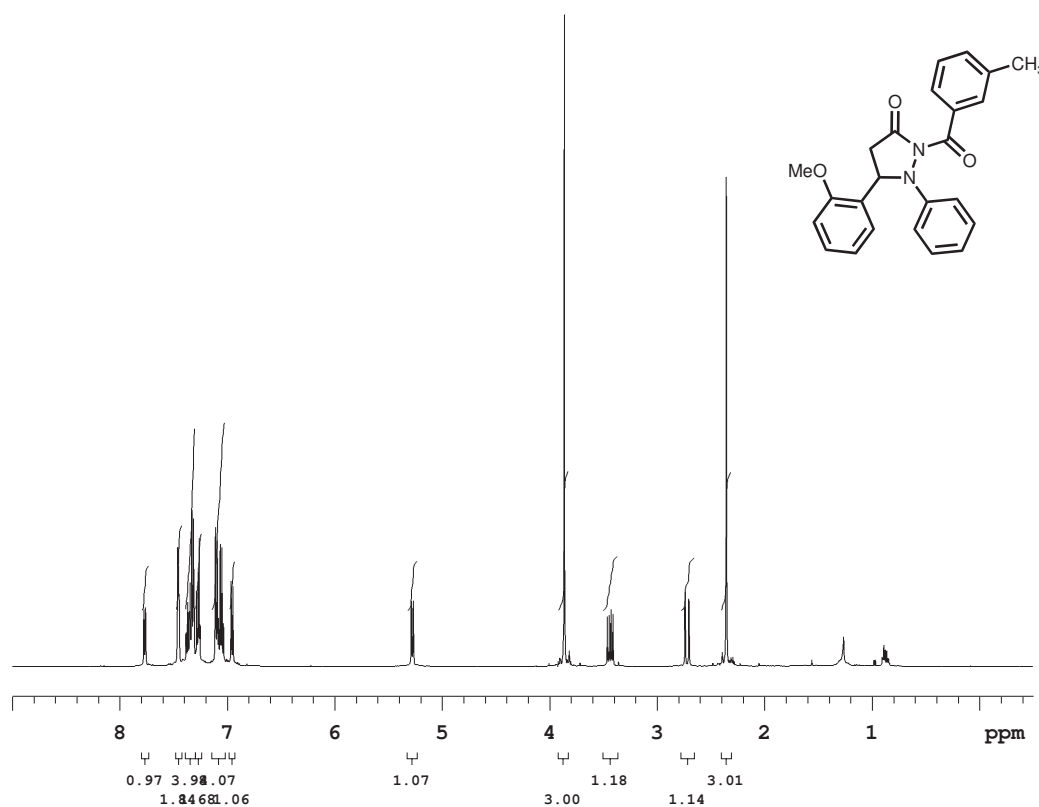


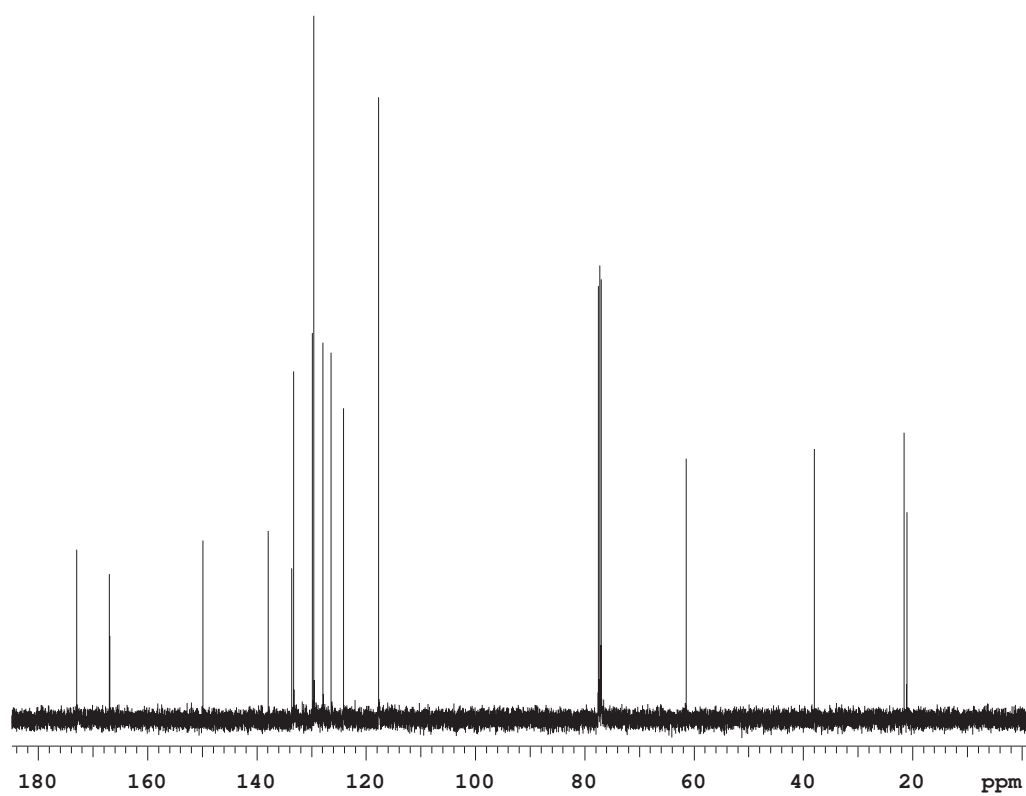
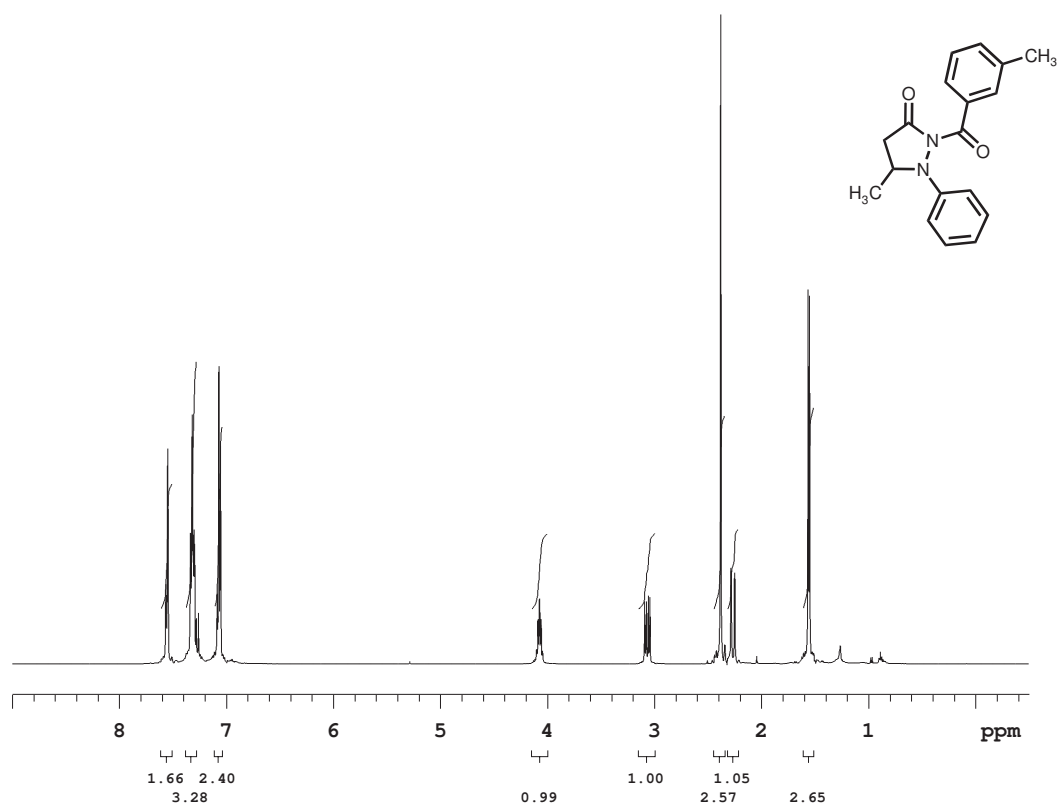


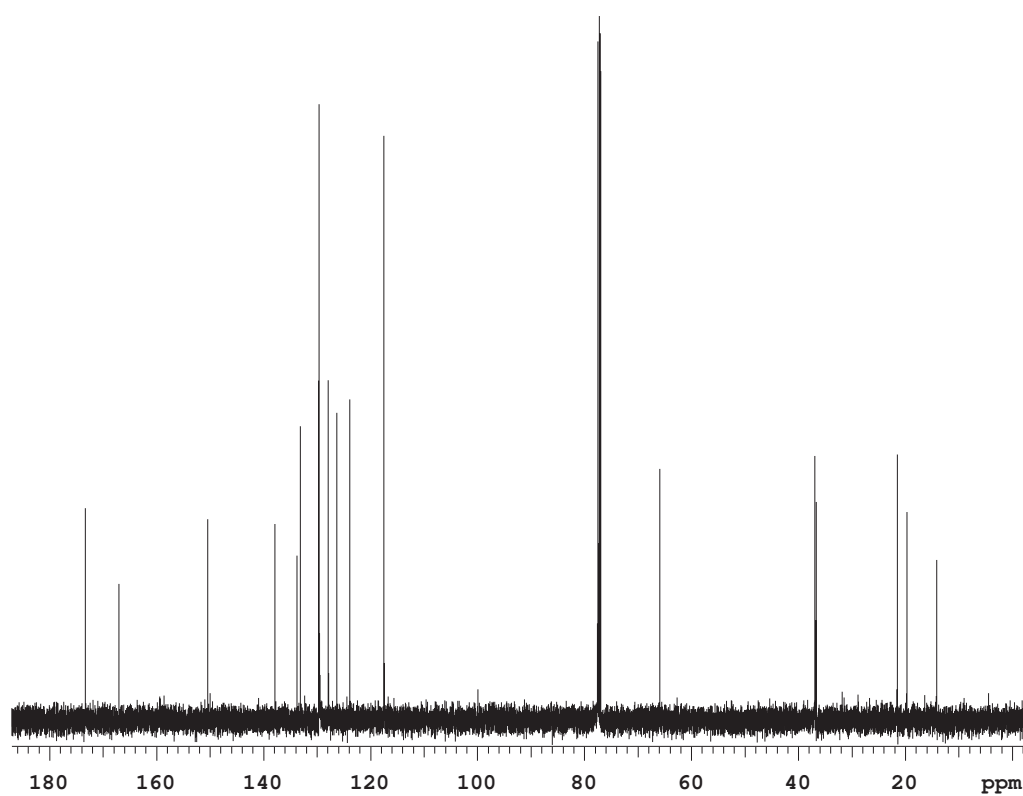
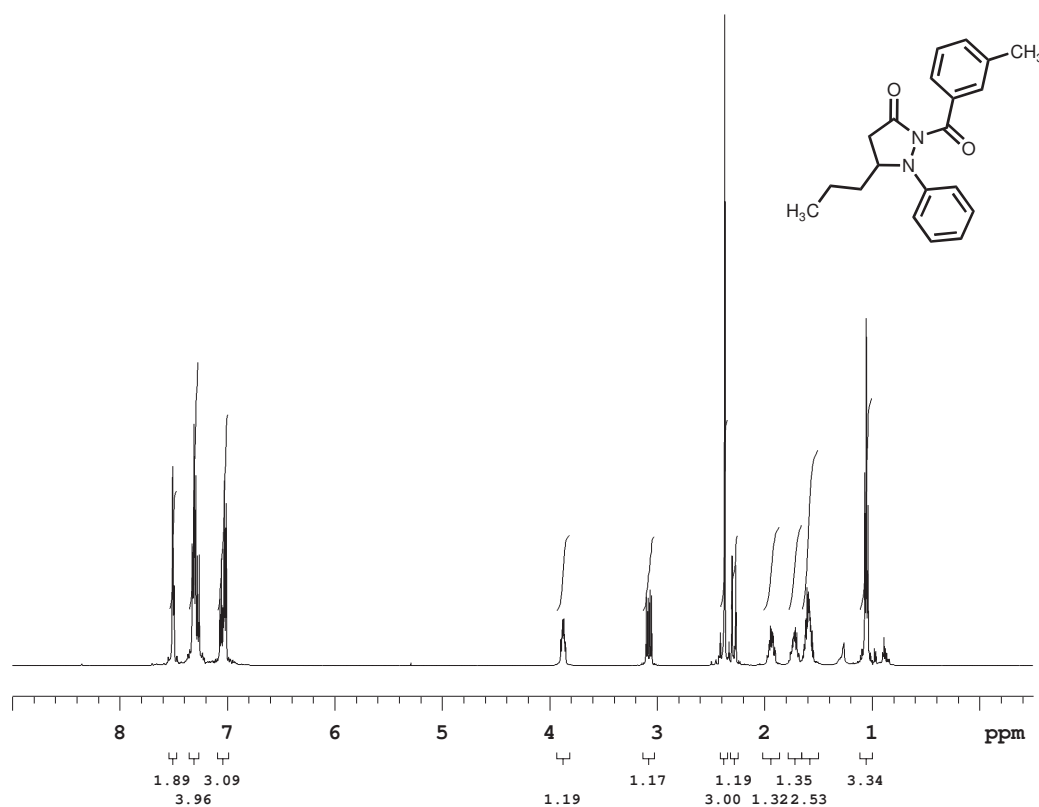


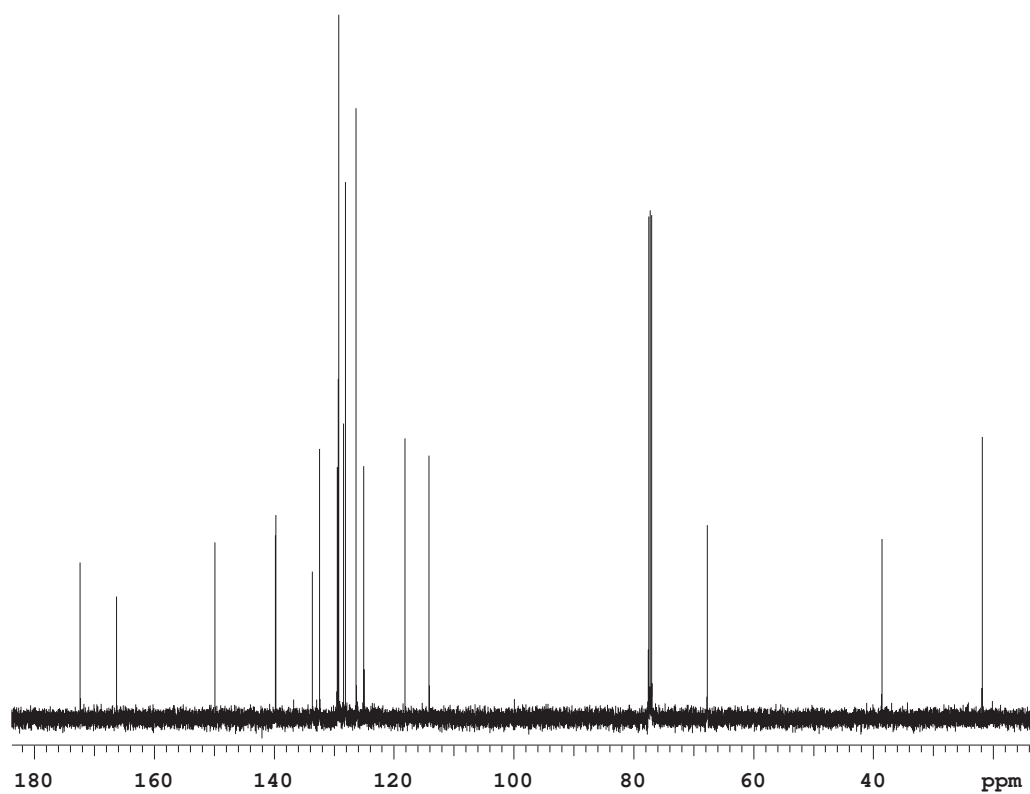
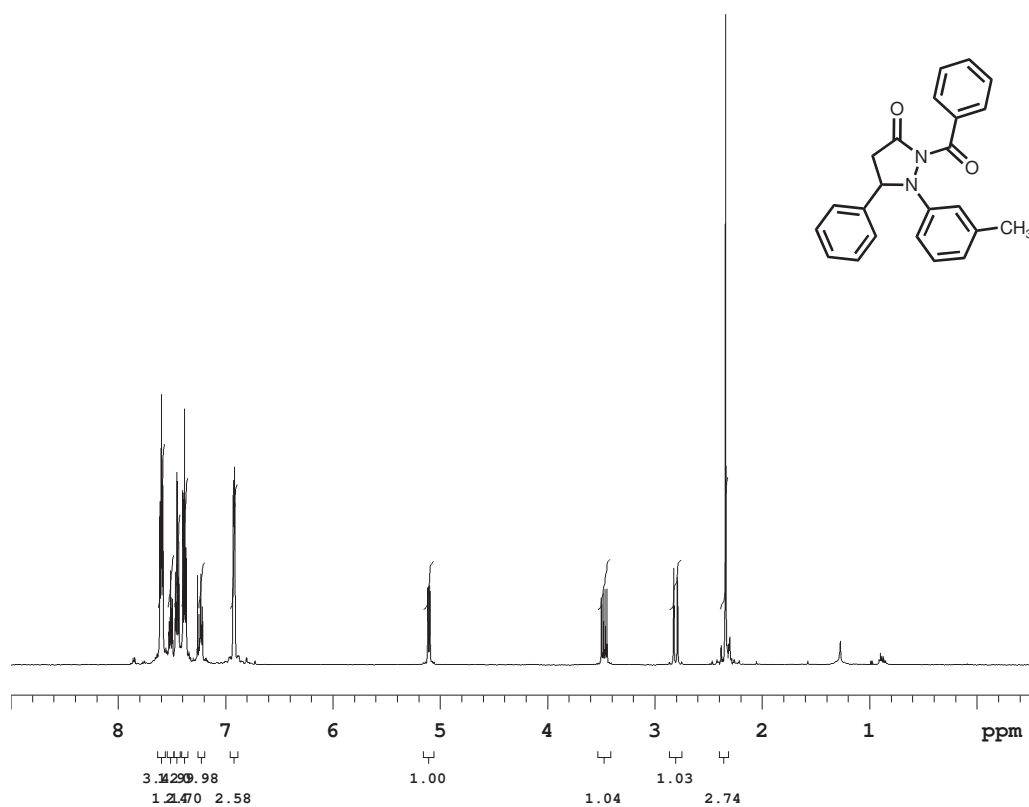
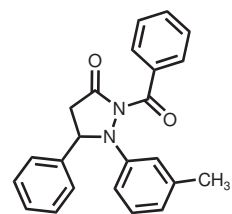


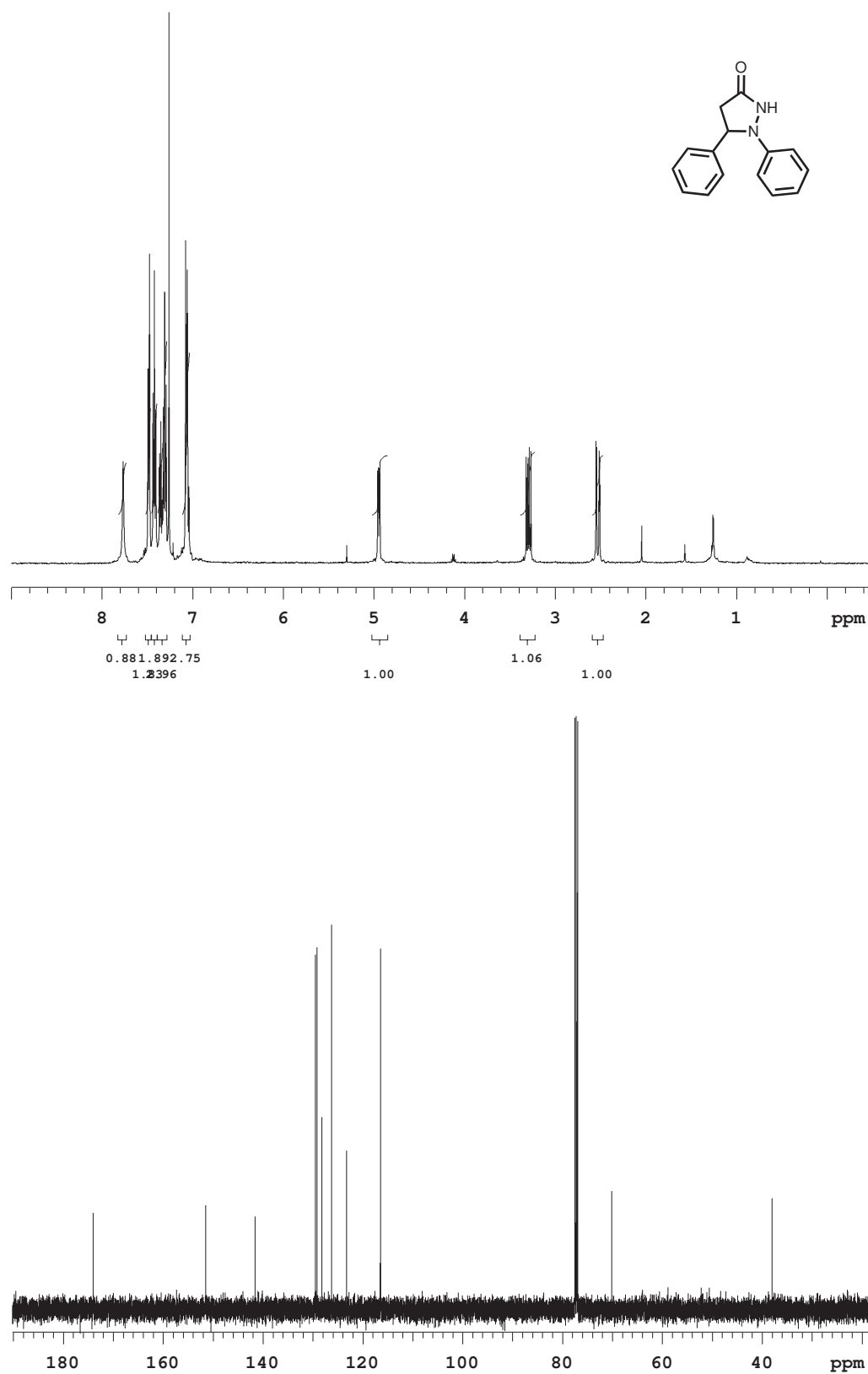


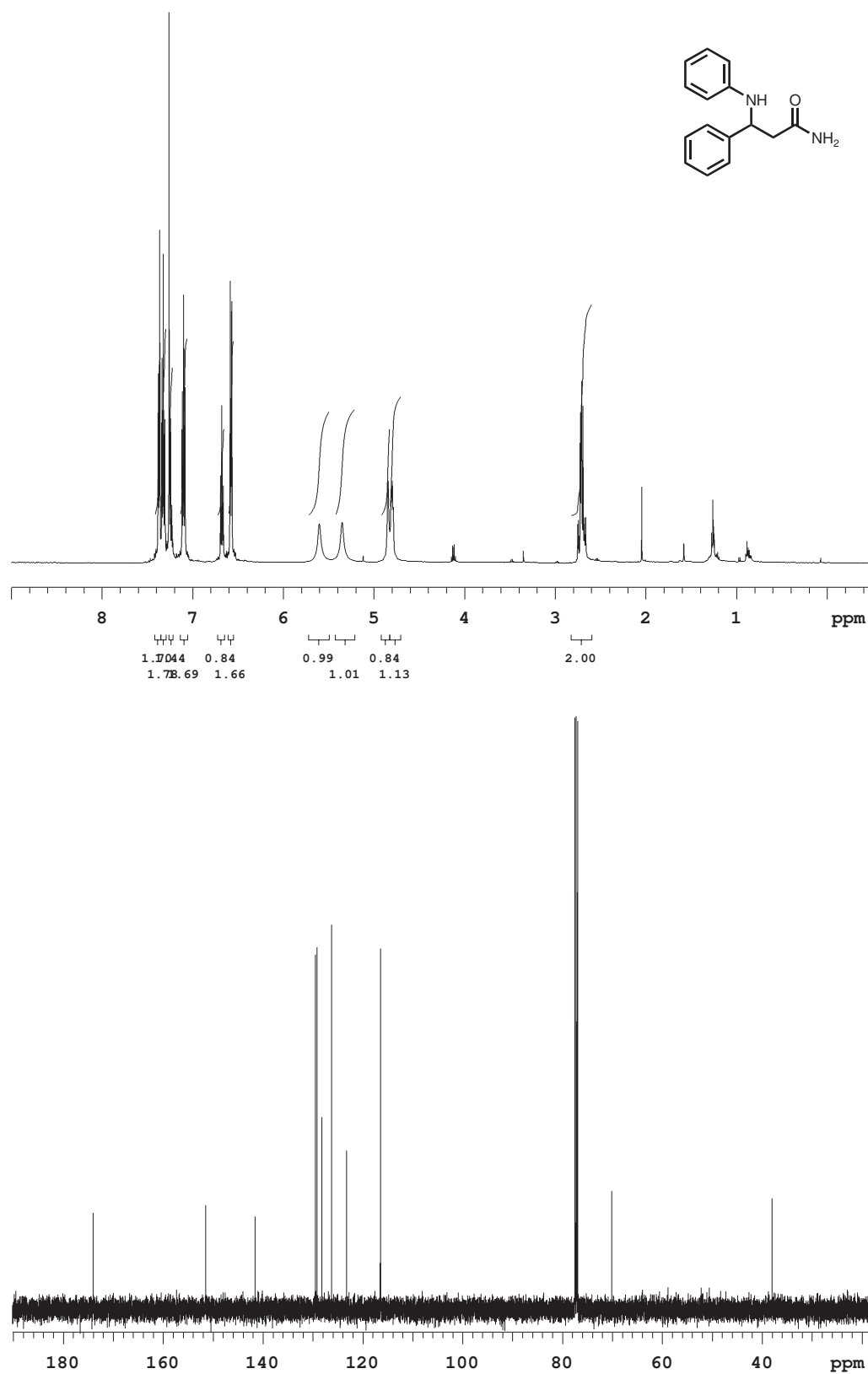












Chapter 2

N-Heterocyclic Carbene-Catalyzed Hydroacylation Processes

Portions of this chapter appear in the following publications:

Maki, B. E.; Chan, A.; Phillips, E. M.; Scheidt, K. A. "Tandem Oxidation of Allylic and Benzylic Alcohols to Esters Catalyzed by *N*-Heterocyclic Carbenes," *Org. Lett.* **2007**, 9, 371-374.

Chan, A; Scheidt, K. A. "Hydroacylation of Activated Ketones Catalyzed by *N*-Heterocyclic Carbenes," *J. Am. Chem. Soc.* **2006**, 128, 4558-4559.

Chapter 2

2.1 Introduction

Direct methods for the selective oxidation of σ bonds are powerful bond-forming strategies in organic synthesis. Hydroacylation is an established reaction that selectively oxidizes the C-H bond of an aldehyde by utilizing transition metals capable of undergoing oxidative addition processes.¹⁴²⁻¹⁴⁶ This is a multiple bond-forming process (Figure 2-1), which makes it an attractive method to create complex organic molecules in a single operation.

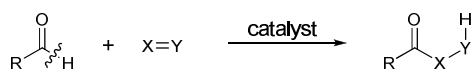
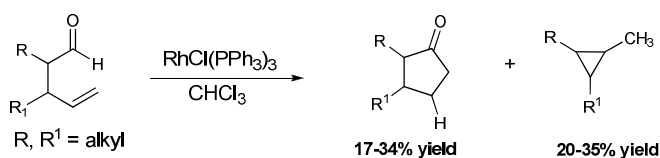


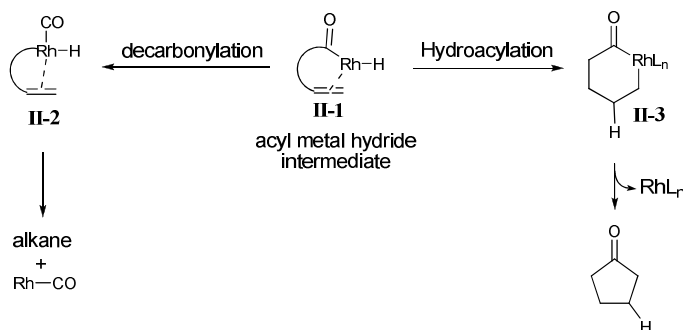
Figure 2-1 Hydroacylation across a π -bond

2.1.1 Metal-Catalyzed Hydroacylation of Aldehydes across Olefins

In 1972, Sakai and coworkers¹⁴⁷ were the first to discover that the treatment of 2,3-disubstituted 4-pentenals with a stoichiometric amount of the Wilkinson complex $\text{RhCl}(\text{PPh}_3)_3$ in CHCl_3 affords cyclopentanones in 17-34% yield, together with a cyclopropane byproduct in 20-35% yield (Scheme 2-1). After this discovery, Miller and coworkers¹⁴⁸ reported that the cyclization could proceed by using a catalytic amount of $\text{RhCl}(\text{PPh}_3)_3$ under ethylene pressure. The mechanism of the process was studied and reported by several groups.¹⁴⁹⁻¹⁵²

Scheme 2-1. First reported hydroacylation process by Sakai and coworkers

The proposed catalytic pathway begins with the activation and cleavage of the C-H bond of an aldehyde by a transition metal complex to generate acyl-metal hydride intermediate **II-1** (Scheme 2-2). Complex **II-1** can then react in two distinct pathways. Complex **II-1** can undergo decarbonylation to give intermediate **II-2**, which would produce an alkane and a metal carbonyl complex upon reductive elimination. Alternatively, **II-1** could proceed through hydrometallation of the olefin to give acylmetal alkyl complex **II-3**, followed by subsequent reductive elimination to produce the ketone.

Scheme 2-2. Proposed catalytic pathway for transition metal-promoted hydroacylation

The generality of this cyclization was studied subsequently by Larock and coworkers using various substrates and neutral rhodium-complexes with trialkyl- or triarylphosphines and phosphites.¹⁵³ The development of the asymmetric rhodium-catalyzed hydroacylation reaction

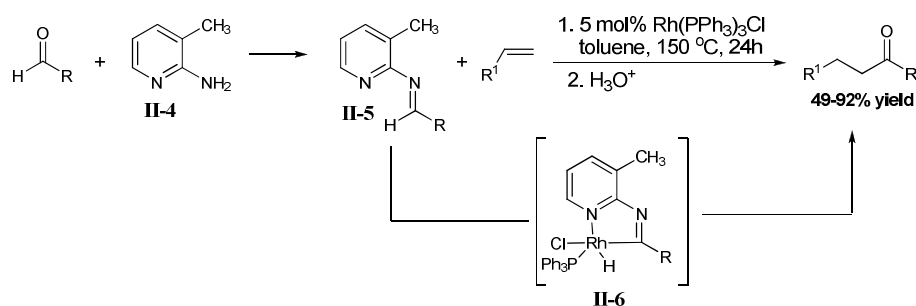
was first reported by James's group, which used rhodium-complex with chiralphos as a chiral phosphine ligand and synthesized 2-methyl-2-phenylcyclopentanone in 52% ee and 40-50% yield by kinetic resolution of racemic 4-pentenals.^{154, 155} In 1988, Bosnich's group^{156, 157} revealed that a cationic rhodium-complex, $[\text{Rh}(\text{diphosphine})]^+$, was the most effective catalyst for the intramolecular cyclization. This finding prompted the groups of Bosnich¹⁵⁸⁻¹⁶³ and Tanaka¹⁶⁴⁻¹⁶⁶ to independently study the asymmetric intramolecular hydroacylation process using the cationic rhodium-complex with chiral ligands. The method has been further studied by several other groups including the laboratories of Brookhart,¹⁶⁷ Shair,¹⁶⁸ Fu¹⁶⁹ and Morehead.¹⁷⁰ These groups have independently expanded the concept with new catalysts and conditions to generate various cyclic alkyl ketones from enals or cyclic enones from ynals.

Although intramolecular hydroacylation has been studied in detail, the intermolecular reaction is not well preceded. Marder and coworkers were the first to develop an intermolecular hydroacylation reaction, which employed a rhodium complex $[\text{Rh}(\eta^5\text{-C}_9\text{H}_7)(\eta^2\text{-C}_2\text{H}_4)_2]$, 1000 psi of ethylene and high temperature (100 °C) to hydroacylate benzaldehyde across ethylene, affording propiophenone.¹⁷¹ The high pressure of ethylene has been devised to stabilize the acyl-metal hydride complex, which is essential to avoid decarbonylation. Although the system produces the desired product, it lacks generality and efficiency. The harsh reaction conditions and the limited olefin scope encouraged the discovery of new methods.

Jun and coworkers^{172, 173} cleverly developed a new process that eliminates the need for harsh conditions to avoid decarbonylation side products. Their method is known as the chelation-assisted hydroacylation reaction, which utilizes 2-amino-3-picoline (**II-4**) (Scheme 2-3). Condensation between the aldehyde and **II-4** gives rise to aldimine **II-5**, which has no carbonyl group to undergo decarbonylation. Additionally, this strategy provides a stable five-

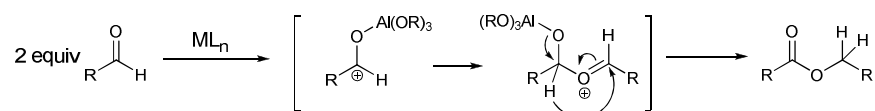
membered metallocycle (**II-6**) that forms between the metal catalyst and the nitrogen on the picoline ring that prevents decarbonylation. Coordination of an alkene and subsequent hydride insertion followed by reductive elimination produces a ketimine, which can undergo hydrolysis with H₂O to give the ketone product and regenerate **II-4**.

Scheme 2-3. Chelation-assisted intermolecular hydroacylation process

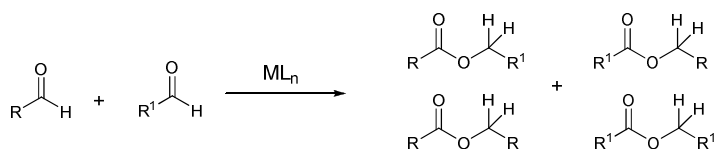


2.1.2 The Tishchenko Reaction

The catalytic dimerization of aldehydes giving the corresponding esters was first discovered by Claisen¹⁷⁴ in 1887, and is now well known as the “Tishchenko reaction” (Scheme 2-4). The Tishchenko reaction is essentially a metal-promoted hydroacylation of an aldehyde onto itself or another carbonyl species. In 1906, the Russian chemist, Tishchenko, reported that aluminum alkoxides are superior catalysts for the reaction that provides a much wider applicability than Claisen’s method with sodium alkoxides.¹⁷⁵⁻¹⁷⁸ It has since been discovered that a wide variety of catalysts promote this transformation including alkali- and alkali earth metal oxides and alkoxides, transition metal-based catalysts (Ru, Rh, Ir, and Fe complexes), metallocenes of group IV metals (Cp₂MH₂, M = Hf, Zr), lanthanide amides (Ln[NSiMe₂]₃], Ln = La, Sm, Y), organolanthanoid halides (alkylLnX, Ln = Pr, Nd, Sm, X = I) and SmI₂.¹⁷⁹

Scheme 2-4. The Tishchenko reaction

A major limitation of the Tishchenko reaction is that only one aldehyde can be used in the reaction. When two different carbonyl species are used, the reaction is no longer selective (Scheme 2-5). With two different aldehydes, all four possible hydroacylation products are produced. Slight improvement on the selectivity has been demonstrated when using one aldehyde in excess.¹⁸⁰

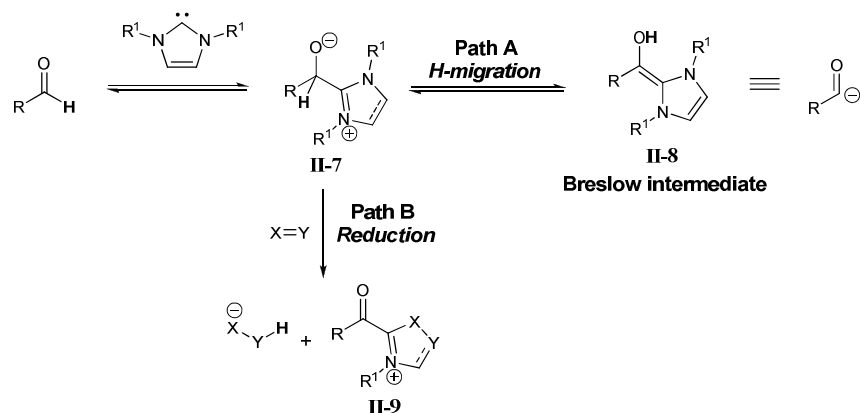
Scheme 2-5. Mixed Tishchenko reaction

2.1.3 NHC-Promoted Redox Reactions with an Aldehyde

It is well known that the addition of an NHC to an aldehyde generates the Breslow intermediate (**II-8**) that has been shown to react with aldehydes (benzoin reaction) and conjugate acceptors (Stetter reaction). Tetrahedral intermediate **II-7** leads to the generation of the Breslow structure (**II-8**) through proton migration (Path A, Scheme 2-6). In contrast to the usual pathway to generate the Breslow species (Path A), an alternative course potentially involves the collapse

of the tetrahedral intermediate to afford an acyl heteroazolium species (**II-9**) and concurrent formation of a hydride equivalent that can be used to reduce organic substrates (Path B).

Scheme 2-6. Divergent reactivity of tetrahedral intermediate **II-7**

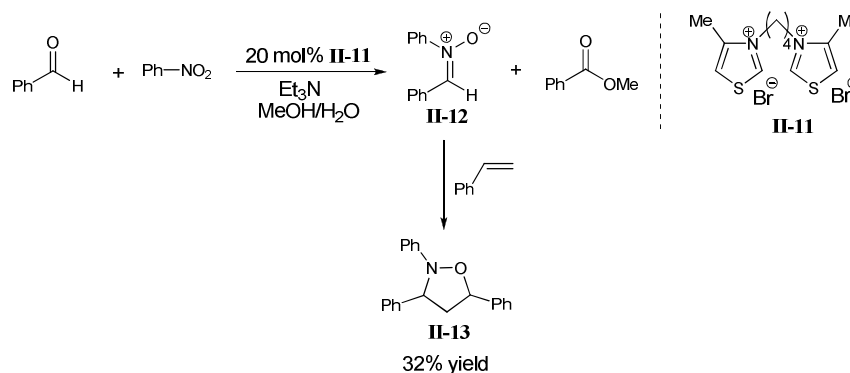


In 1980, Inoue and coworkers reported the use of thiazolium catalysis to perform electron-transfer reductions by active aldehydes in the presence of triethylamine (Table 2-1).¹⁸¹ This transformation allows aldehydes to be oxidized to methyl esters in up to an 87% yield (entries 1-2) with subsequent reduction of organic oxidants. With an excess of aldehyde used in the reaction, the desired methyl ester product as well as an α -hydroxy-ketone by-product, formed by the benzoin condensation, are isolated. The nature of the organic oxidant was varied, and includes several aromatic compounds as well as activated aromatic species that are depicted in Table 2-1. It is noteworthy that the reduction of nitrobenzene gave both *N*-benzoyl-*N*-phenylhydroxylamine and aniline as products (entry 5).

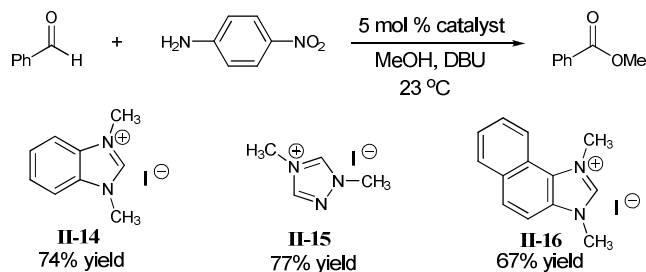
Table 2-1. Inoue's NHC-catalyzed redox reactions with aldehydes

entry	Organic oxidant	Ester (% yield)	reduced substrate (% yield)
1		87	9,9'-acridan (93)
2		87	10,10'-dimethyl-9,9'-biacridan (88)
3		84	5,10-dihydrophenazine (83)
4		65	benzidine (66) aniline (6)
5		60	aniline (25) <i>N</i> -benzoyl- <i>N</i> -phenylhydroxylamine (22)

In a later communication, Inoue and coworkers showed that NHC-catalyzed reduction of nitrobenzenes by aldehydes provides nitrones (Scheme 2-7).¹⁸¹ In contrast to *N*-benzylthiazolium bromide (**II-10**) as precatalyst, 3,3'-tetramethylene-bridged-4-methylthiazolium bromide (**II-11**) favored the formation of nitrone with decreased yield of aniline and *N*-benzoyl-*N*-phenylhydroxylamine. Catalyst **II-11** also retards the formation of the benzoin. The presence of water as co-solvent in the reaction depresses the reduction of nitrobenzene. Styrene can be added to the reaction system after the generation of the nitrone **II-12** to afford the cycloaddition product **II-13** in moderate yield.

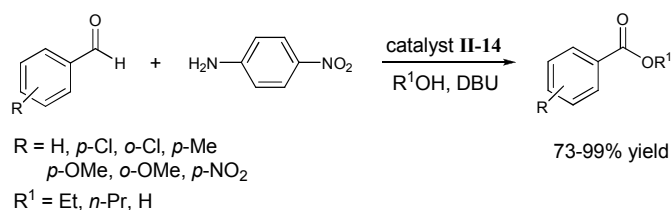
Scheme 2-7. NHC-catalyzed reduction of nitrobenzenes with aldehydes

In 1997, Miyashita and coworkers reported the use of several different NHCs as catalyst in the oxidation of aldehydes to esters with concomitant reduction of *p*-nitroaniline.¹⁸² As depicted in Scheme 2-8, 1,3-dimethylbenzimidazolium salt **II-14**, 1,3-dimethyltriazolium salt **II-15** and 1,3-dimethylnaphtholimadazolium salt **II-16** catalyzed the oxidation of benzaldehyde to methyl benzoyl ester in good yields. The authors proposed a mechanism that involves a NHC-generated acyl anion addition to the nitroaniline followed by fragmentation to give nitrosobenzene and the activated acyl heteroazolium salt (**II-9**) that is trapped by methanol to give methyl benzoate.

Scheme 2-8. NHC-catalyzed oxidation of aldehydes to esters

The scope of the reaction was investigated and was found that the reaction is able to produce high yields of a variety of different esters by varying the aldehyde and the nucleophilic alcohol (Scheme 2-9). A survey of the aldehydes revealed that the reaction is compatible with electron poor as well as electron rich substituents on the aromatic component of the aldehydes. Only primary alcohols and water were shown to be competent nucleophilic sources to yield the corresponding primary alkyl ester and benzoic acid product.

Scheme 2-9. Aldehydes and alcohol scope of Miyashita's oxidation reactions

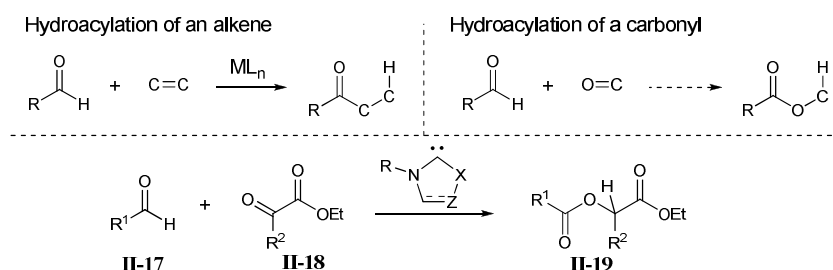


2.2 *N*-Heterocyclic Carbene-Catalyzed Hydroacylation of Activated Ketones

As discussed above, the rhodium(I)-catalyzed intramolecular hydroacylations of alkenes, reported from many laboratories, including Bosnich, Larock, Jun, Brookhart, Shair, Fu, and Morehead, functionalize aldehydic C–H bonds for the synthesis of carbocycles. However, the development of analogous catalytic hydroacylation processes involving aldehydes and carbonyl π systems has not received the same attention. The Scheidt group has been interested in developing approaches in which an organic molecule promotes multiple bond-forming steps in a single catalytic cycle. Therefore, we began to investigate *N*-heterocyclic carbene-catalyzed hydroacylation of α -keto esters (**II-18**) with aldehydes (**II-17**). In this process, the NHC facilitates selective catalytic oxidation of C–H bond with concomitant reduction of a ketone.

The use of an organic molecule to catalyze the hydroacylation of π -bonds combined with employing an aldehyde as a hydride source eliminates the production of wasteful by-products that are produced with metal catalysis.

Scheme 2-10. NHC-catalyzed hydroacylation of ketones

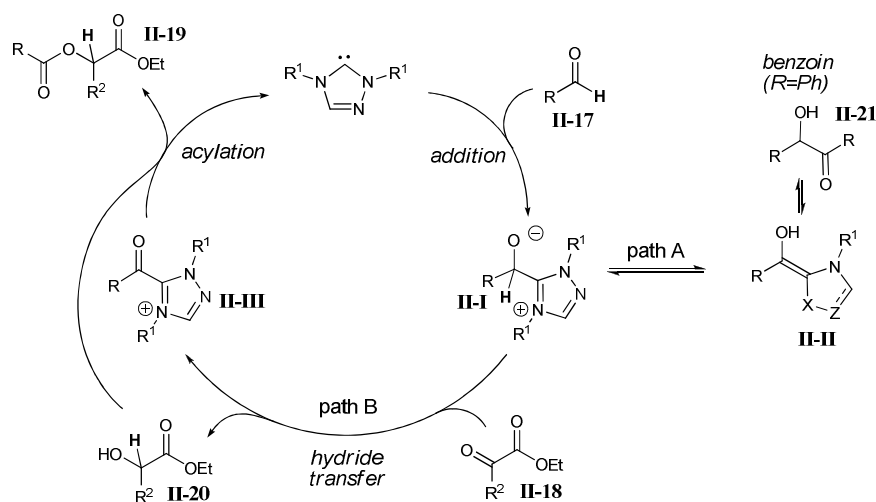


2.2.1 Proposed Catalytic Pathway for NHC-Catalyzed Hydroacylation Process

The interaction of *N*-heterocyclic carbenes with aldehydes has been extensively employed in the generation of carbonyl anions, mainly in the additions of these *umpolung* species to aldehydes (benzoin reaction) and conjugate acceptors (Stetter reaction). A common premise in these processes is that the tetrahedral intermediate (**II-I**) resulting from the addition of the NHC to an aldehyde (**II-17**) usually generates a “Breslow intermediate” structure (**II-II**, path A, Scheme 2-11). However, an alternative course potentially involves the collapse of this intermediate to afford an acyl heteroazolium species (**II-III**) with concomitant formation of a hydride equivalent (path B). We envisioned that this Cannizzaro-type reducing equivalent could be harnessed to reduce ketones (**II-19**). The resulting alcohol (**II-20**) produced after a reduction step can undergo an acylation event with the acyl iminium species formed *in situ* (**II-III**), thus promoting catalyst turnover and yielding an overall hydroacylation process catalyzed by an

organic molecule. Importantly, the aldehyde and activated ketone are separate components, thereby providing for a metal-free reaction with broader potential reaction scope than the related Al(III)-promoted Tishchenko disproportionation reaction.

Scheme 2-11. Proposed catalytic pathway for NHC-catalyzed hydroacylation reaction

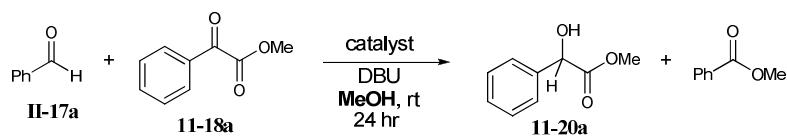
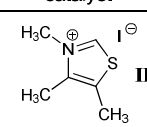
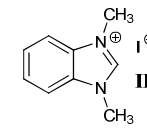
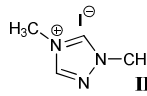


2.2.2 Optimization of NHC-Catalyzed Hydroacylation of Activated Ketones

To explore this transformation, a protic solvent (MeOH) was employed to decouple the reduction and acylation events (Table 2-2). The use of a protic solvent serves two purposes. The first is that it protonates the alkoxide (**II-20**) that is generated upon the reduction of the ketone, while the second purpose is to regenerate the catalyst via acylation of methanol by the activated acylazolium species (**II-III**). A screen of three different catalysts (**II-14**, **II-15**, **II-22**) demonstrated that NHCs can, in fact, catalyze the reduction of α -ketoesters **II-18a** to the corresponding methyl mandelate **II-20a** and methyl benzoate. Thiazolium salt **II-22** gave good yields of the mandelate product (entry 1) while benzimidazolium salt **II-14** gave the least

promising result (entry 2). Triazolium salt **II-15** is the superior catalyst of the three, yielding 96% of the desired product at only 15 mol % catalyst loading (entry 4). Decreasing the catalyst loading to 10 mol % decreased the reaction yield (entry 5).

Table 2-2. Survey of NHCs for hydroacylation reaction

			
entry	catalyst	catalyst loading	yield(%)
1	 II-22	30 mol%	76
2	 II-14	30 mol%	15
3	 II-15	30 mol%	95
4		15 mol%	96
5		10 mol%	80

Utilizing an aprotic solvent should result in the production of the hydroacylated product (**II-19**), since the alkoxide generated from the reduction of the ketone should undergo an acylation event with the activated acylazolium species (**II-III**) to regenerate the catalyst. Three different solvents were examined when using benzaldehyde as the hydroacylating agent (Table 2-3). THF, toluene and dichloromethane were all competent solvents for the reaction with dichloromethane, resulting in the highest yield when 10 mol % of 1,3-dimethyltriazolium salt was employed (entries 1-3). Increasing the catalyst loading to 15 mol % in dichloromethane did not have significant impact on the yield (79% yield, not shown). Decreasing the catalyst loading to 5 mol % proved unfavorable, as the product was isolated in only 36% yield (entry 4). As

expected, aldehydes with electron-rich substituents are better hydride donors than aldehydes with electron-poor substituents (entries 5-6).

Table 2-3. Survey of solvent for hydroacylation process

entry	aldehyde	solvent	time (hr)	yield(%)
1		THF	19	63
2		toluene	19	74
3		CH₂Cl₂	2.5	78
4		CH ₂ Cl ₂	24	36 ^a
5		CH ₂ Cl ₂	9	77
6		CH ₂ Cl ₂	24	28

a. 5 mol % catalyst and DBU loadings

2.2.3 Substrate Scope of the Hydroacylation Reaction

With the optimized conditions for both the reduction and hydroacylation processes established, we proceeded to examine the scope of the aldehyde (**II-17**) as the hydride donor and methyl benzoyl formate (**II-18a**) as the α -keto ester (Table 2-4). The reaction accommodates aromatic substituted aldehydes to provide the desired ester (**II-19a-f**) resulting from the overall hydroacylation process, when dichloromethane is used as the solvent. Switching the medium to methanol, the corresponding methyl mandelate (**II-20a**) is produced directly in the reaction along with methyl benzoate. Both processes are tolerant of electron rich substituents (entries 5-12), while the yields are generally lower when electron-deficient systems are employed (i.e. 4-Cl-Ph, yield = 28% for ester formation). The yields are usually higher for the reduction reaction than

the hydroacylation process. To date, the use of enolizable aldehydes yields predominantly benzoin products (entries 13-16).

Table 2-4. Examination of the aldehyde scope

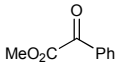
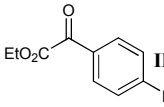
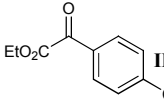
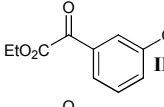
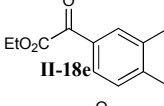
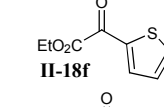
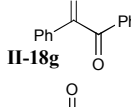
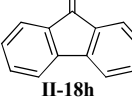
Entry	Aldehyde	solvent	product	yield (%)
1 2	II-17a	CH ₂ Cl ₂ MeOH	ester (II-19a) alcohol (II-20a)	78 96
3 4	II-17b	CH ₂ Cl ₂ MeOH	ester (II-19b) alcohol (II-20a)	71 98
5 6	II-17c	CH ₂ Cl ₂ MeOH	ester (II-19c) alcohol (II-20a)	72 79
7 8	II-17d	CH ₂ Cl ₂ MeOH	ester (II-19d) alcohol (II-20a)	77 77
9 10	II-17e	CH ₂ Cl ₂ MeOH	ester (II-19e) alcohol (II-20a)	70 78
11 12	II-17f	CH ₂ Cl ₂ MeOH	ester (II-19f) alcohol (II-20a)	73 83
13 14	II-17g	CH ₂ Cl ₂ MeOH	ester (II-19g) alcohol (II-20a)	0 0
15 16	II-17h	CH ₂ Cl ₂ MeOH	ester (II-19h) alcohol (II-20a)	0 0

We also examined the scope of the reaction with regard to the activated ketone component (Table 2-5). Substituted aromatic keto esters provided the desired esters resulting from overall hydroacylation in good yield when dichloromethane was used as the solvent (entries 1, 3, 5, 7, 9, and 11). By switching the medium to ethanol, the corresponding alcohols were

produced directly in the reaction along with the benzoic ester (entries 2, 4, 6, 8, 10, and 12).

Currently, the conditions do not generate hydroacylation/reduction products with enolizable keto esters. Benzil was also a productive substrate that gave the hydroacylated product **II-19n** (entry 13) in good yields. Under protic conditions, benzoin **II-21** was isolated in excellent yield (entry 14). For less active ketones, only protic conditions were successful in the reduction of the keto ester (entry 16).

Table 2-5. Examination of the keto ester scope

$ \begin{array}{c} \text{R}-\text{CHO} + \text{R}^1-\text{C}(=\text{O})-\text{C}(=\text{O})-\text{OR}^2 \\ \text{II-17a, Ar = Ph} \quad \text{II-18} \\ \text{II-17d, Ar = 4-MeOPh} \end{array} \xrightarrow[10-15 \text{ mol \% DBU, solvent, rt}]{10-15 \text{ mol \% } \text{H}_3\text{C}-\text{N}^+\text{C}(\text{CH}_3)=\text{N}^-\text{I}^- \text{II-15}} \begin{array}{c} \text{R}-\text{C}(=\text{O})-\text{O}-\text{CH}(\text{R}^1)-\text{C}(=\text{O})-\text{OR}^2 \\ \text{ester} \end{array} \text{ or } \begin{array}{c} \text{HO}-\text{CH}(\text{R}^1)-\text{C}(=\text{O})-\text{OR}^2 \\ \text{alcohol} \end{array} $				
entry	ketone	solvent	product ^a	yield (%)
1 2	 II-18a	CH ₂ Cl ₂ MeOH	ester (II-19a) alcohol (II-20a)	77 96
3 4	 II-18b	CH ₂ Cl ₂ EtOH	ester (II-19i) alcohol (II-20b)	87 80
5 6	 II-18c	CH ₂ Cl ₂ EtOH	ester (II-19j) alcohol (II-20c)	81 75
7 8	 II-18d	CH ₂ Cl ₂ EtOH	ester (II-19k) alcohol (II-20d)	72 84
9 10	 II-18e	CH ₂ Cl ₂ EtOH	ester (II-19l) alcohol (II-20e)	78 89
11 12	 II-18f	CH ₂ Cl ₂ EtOH	ester (II-19m) alcohol (II-20f)	73 71
13 14	 II-18g	CH ₂ Cl ₂ EtOH	ester (II-19n) ^b alcohol (II-21)	83 93
15 16	 II-18h	CH ₂ Cl ₂ EtOH	ester (II-19p) alcohol (II-20h)	0 75 ^c

a. Protic solvent reactions employed **II-17a** and aprotic solvent reaction used **II-17d**b. Aldehyde **II-17a** was used c. Performed at 40 °C

Several other substrates were subjected to reaction conditions with the intention to induce hydroacylation across the carbonyl π -bond, which did not provide the desired product (Figure 2-2). As mentioned previously, alkyl substituted α -keto esters that can undergo enolization (**II-23** and **II-24**) were not competent substrates, but non-enolizable alkyl substituted α -keto esters (**II-25**, **II-26**) also resulted in no reaction. We postulated that the 2-methyl-substituted aryl keto ester

(**II-27**) is too sterically hindered to provide product formation. Indole-, alkenyl-, and alkynyl-substituted α -keto esters (**II-28**, **II-30**, **II-31**) may be too electron-rich for productive reactivity while surprisingly, the highly electrophilic α -(phosphoryl-ketimine) ester (**II-29**) also did not produce any desired product but only produced benzoin side product. We also examined 1,2-diketones with either alkyl or aryl substitution (**II-32** to **II-35**) and found that these less reactive species when compared to α -keto esters are also not competent substrates. Additionally, α -keto amides (**II-36** to **II-39**) and acyl phosphonates (**II-40**) only produced benzoin side products under the reaction conditions. The main side product isolated from most of these unsuccessful reactions is benzoin.

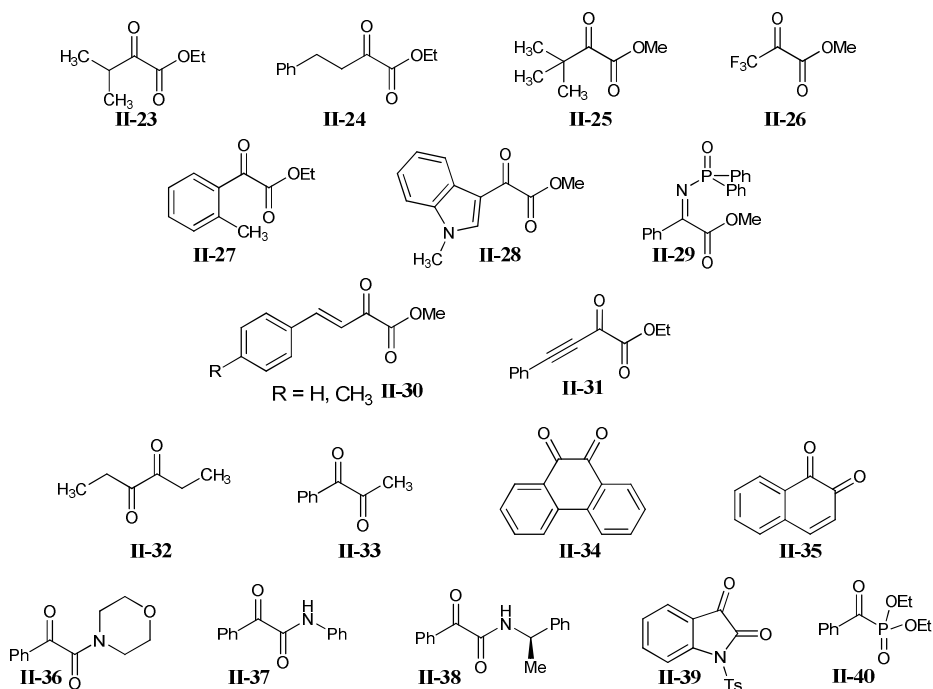
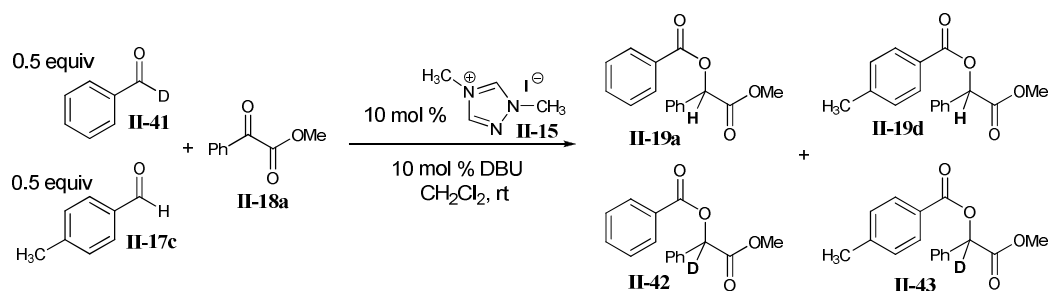


Figure 2-2. Unsuccessful hydroacylation substrates

2.2.4 Mechanistic Studies for Hydroacylation Reaction

To provide further insight into the operative reaction pathway, we performed a crossover experiment (Scheme 2-12). The experiment would provide evidence to suggest whether reduction and acylation occur at the same time or as two separate events. The experiment using deuterium-labeled benzaldehyde **II-41**, 4-methyl benzaldehyde **II-17c**, α -keto ester **II-18a**, triazolium salt **II-15** and DBU in dichloromethane would result in one of two outcomes. First, if crossover does not occur, then only two products, **II-42** and **II-19d**, should be observed, which would lead us to conclude that the reduction and acylation steps occur together. However, if we observe four different products (**II-19a**, **II-19d**, **II-42**, and **II-43**) then crossover does occur, which lends supporting evidence to the theory that the reduction and acylation steps are separate events.

Scheme 2-12. Cross-over experiment



The experiment was performed under the developed hydroacylation conditions. After purification, a ^1H NMR spectroscopy experiment revealed that multiple products were present but could not be identified. However, mass spectrometry verified that the four possible products (**II-19a**, **II-19d**, **II-42**, and **II-43**) were, in fact, produced to confirm that cross over between the

deuterium-labeled benzaldehyde and tolualdehyde did occur (Figure 2-3). The observed crossover suggests that reduction and acylation steps occur as two separate events.

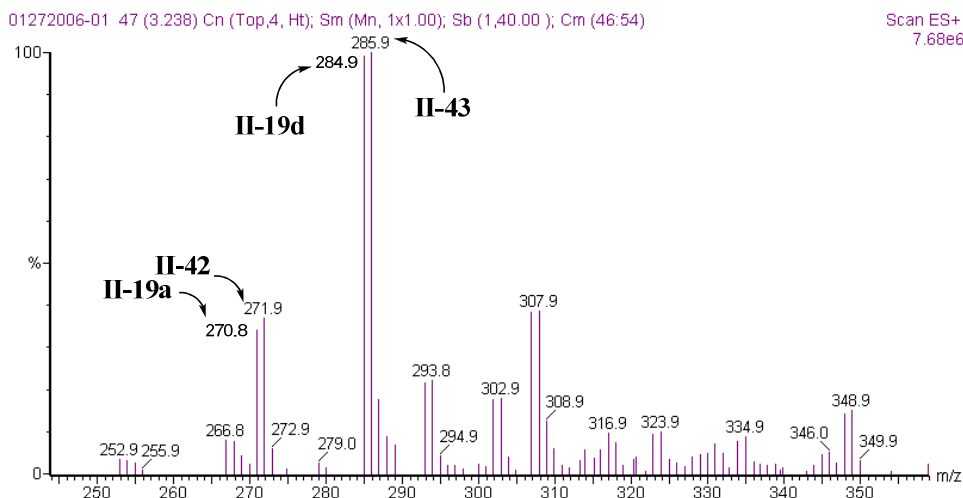
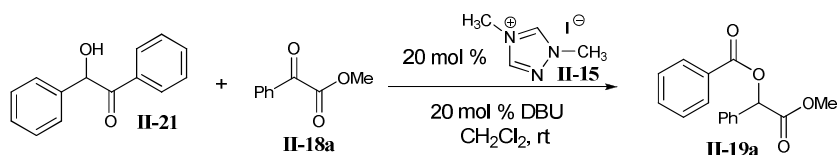


Figure 2-3. Mass spectrometry spectrum for crossover experiment

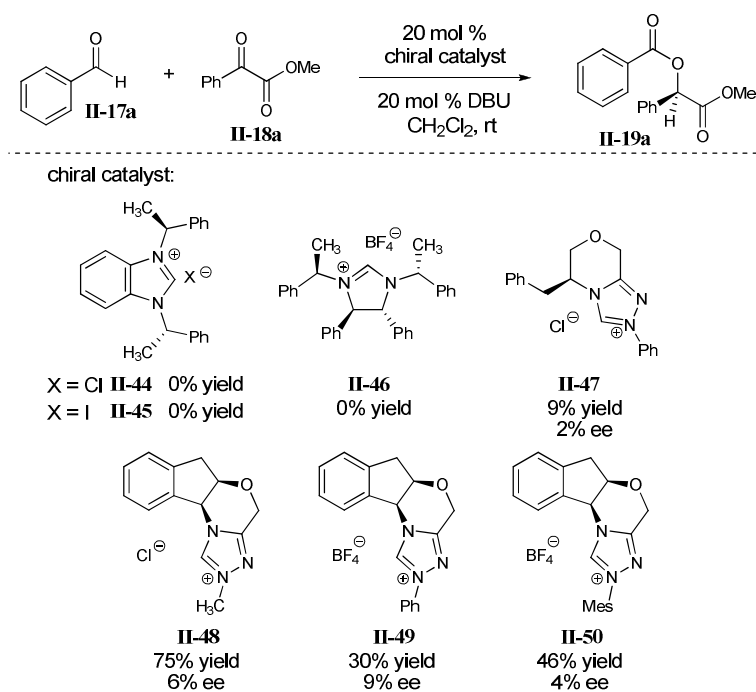
The combination of benzoin (**II-21**, Scheme 2-13) and keto ester (**II-18a**) in the presence of **II-15** and DBU affords the hydroacylated product **II-19a** in a 63% yield, indicating path A is reversible (Scheme 2-11), and potential intermediates such as **II-I** and **II-II** can enter into the catalytic cycle (path B).

Scheme 2-13. Benzoin as hydride donor to hydroacylate ketones



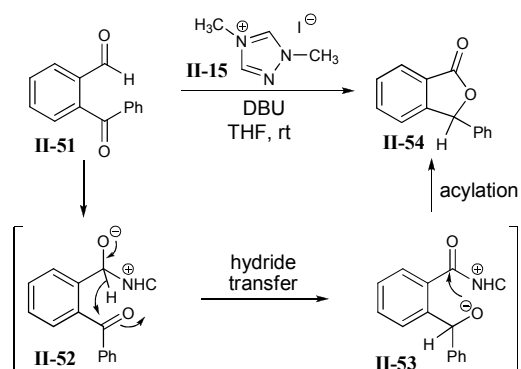
2.2.5 *NHC-Catalyzed Asymmetric Hydroacylation Reactions*

An attempt was made to render the NHC-catalyzed hydroacylation of activated ketones enantioselective. Several different chiral heteroazolium salts as NHC precursors were employed in the reaction (Scheme 2-14). Since we had the chiral imidazolium salts (**II-44** to **II-46**) available in our laboratory, we began our investigation using them as the chiral catalysts. Not surprisingly, none of three imidazolium catalysts facilitated the reaction. Since the reaction has been shown to work best with triazolium salts as the precatalysts, chiral triazolium salt **II-47** was tested, resulting in a low yield of the desired product and essentially no selectivity. Switching to chiral triazolium salts **II-48**, **II-49** and **II-50** resulted in encouraging yields, but the selectivity was still poor. The highest observed enantiomeric excess was only 9%. A reason for the low observed selectivity can be that the stereogenic center has a proton that is α to an ester functionality, which could easily epimerize under the basic reaction condition. An alternative explanation is that the chirality on the carbene does not provide any substantial selectivity when the keto ester is reduced by the chiral tetrahedral intermediate. Due to the low selectivity, we moved on to development an intramolecular hydroacylation reaction.

Scheme 2-14. NHC-catalyzed asymmetric hydroacylation

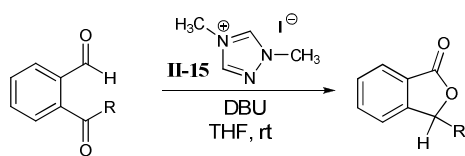
2.3 Intramolecular Hydroacylation Processes

This NHC-catalyzed hydroacylation is also successful in an intramolecular manifold. We chose to examine 1,2-diacylbenzene **II-51** in this reaction because it is easily accessible after two synthetic manipulations (Scheme II-15).¹⁸³⁻¹⁸⁵ Another reason to examine this reaction is that the successful intramolecular hydroacylation process would provide benzofuranones **II-54**, which are important structural motifs present in many biologically-active compounds (i.e. spirolaxine which exhibits cholesterol-lowering activity).¹⁸⁶

Scheme 2-15. NHC-catalyzed intramolecular hydroacylation to give benzofuranones

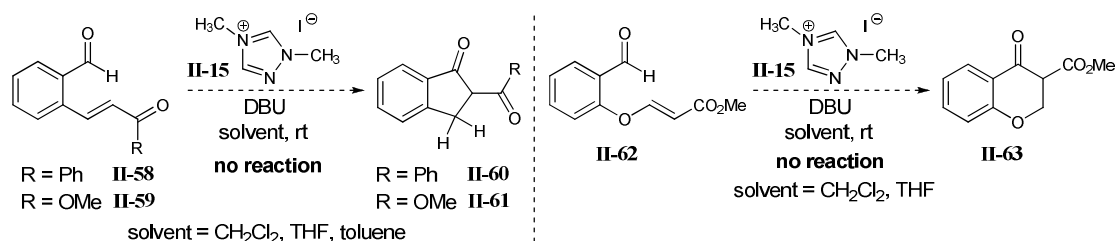
We envisioned that upon addition of the carbene to the aldehyde, the tetrahedral intermediate **II-52** would collapse to transfer the hydride to the pendant ketone with subsequent acylation of the alkoxide **II-53** to produce the benzofuranone **II-54** and regenerate the carbene (Scheme 2-15). Optimization of the reaction began with a screen of heteroazolium salts, bases, and solvents. We found that the exposure of **II-51** to a stoichiometric amount of **II-15** delivers the benzofuranone **II-54** in moderate yield under aprotic conditions. When using a catalytic amount of **II-15**, the reaction was very slow and resulted in formation of polymerized side products that could not be identified after ^1H NMR spectroscopic analysis. One possible side reaction begins with an alkoxide intermediate that can be either generated after the addition of the NHC to the aldehyde or after the hydride transfer. The alkoxide intermediate can add to carbonyl species to give another alkoxide and polymerization continues. Alternatively, the intermolecular benzoin condensation is another possible reaction pathway.

An examination of the substrate scope showed that the reaction can accommodate a limited number of substrates (Table 2-6). Moderate yields were obtained with 4-methoxy- and 4-chlorophenyl on the ketone component (entries 2, 3). No desired product was isolated when an alkyl-substituted ketone (entry 4) was subjected to reaction conditions.

Table 2-6. Substrate scope of NHC-catalyzed synthesis of benzofuranones


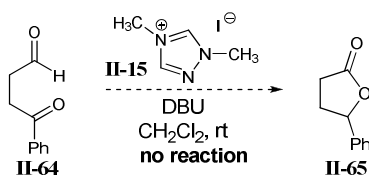
entry	R		yield (%)
1	Ph	II-54	60
2	4-OMe-Ph	II-55	58
3	4-Cl-Ph	II-56	64
4	Me	II-57	0

Additionally, we examined the intramolecular hydroacylation of α,β -unsaturated carbonyl species to give indanones (Scheme 2-16). Both phenyl ketone **II-58** and methyl ester **II-59** were synthesized by heating 1,2-phthalaldehyde with the corresponding Wittig reagent. When both substrates were independently subjected to intramolecular hydroacylation reaction conditions in THF, CH_2Cl_2 or toluene as solvent, only unidentified side products were observed. Salicylaldehyde derived substrate **II-62** was also tested to potentially give 2-(methyl carboxylate)-4-chromanone **II-63**, but only a small amount of unidentified side product was observed.

Scheme 2-16. NHC-catalyzed intramolecular hydroacylation to give indanones

Thus far, we have only examined intramolecular substrates with the diaryl functionalities bound to an aryl group. We continued our investigations with a substrate that has an alkyl backbone that is tethered to both the aldehyde and ketone groups. Due to the previous unsuccessful intermolecular attempts with alkyl substrates, we did not anticipate substrate **II-64** to undergo a NHC-catalyzed intramolecular hydroacylation reaction to produce γ -lactone **II-65**. The result of treating substrate **II-64** with triazolium salt **II-15** and DBU in dichloromethane confirmed our assessment, and no reaction was observed after 20 hours.

Scheme 2-17. NHC-catalyzed intramolecular hydroacylation to give γ -lactones



2.4 Attempted NHC-Catalyzed Hydroacylation Reactions

We also attempted to utilize NHCs to catalyze the hydroacylation of new electrophiles (Table 2-7). The reactivity of various imines was examined under both protic and aprotic conditions. Both phosphoryl aldimine (**II-66**) and sulfonyl aldimines (**II-67**) (entries 1-2) were subjected to protic conditions to test whether reduction of the imine would occur; however, only benzoin formation was observed. A more thorough screen for optimal conditions was done for phosphoryl ketimine (**II-68**). Both protic and aprotic solvents were examined to give either the amine as the reduced product or the hydroacylated amine (entries 3-9). Unfortunately, we only observed either unconsumed aldehyde and imine or a small amount of benzoin side product.

Sulfonyl-substituted ketimine **II-69** was also not a competent substrate under methanol conditions (entries 10-12). Lastly, alkylidene malonates (**II-70**) were also examined in both ethanol and dichloromethane (entries 13-14). After 24 hours, only benzoin was observed. From these investigations, we can conclude that any electrophile that is less reactive than an aldehyde would result in benzoin formation. It is crucial that the electrophile is electronically compatible with the reaction conditions to suppress benzoin formation and/or addition of the NHC to the electrophile.

Table 2-7. Attempted NHC-catalyzed hydroacylation reactions with new electrophiles

$\text{Ar}-\text{CHO} + \text{X}=\text{Y} \xrightarrow[\text{conditions}]{20-30 \text{ mol } \% \text{ II-15}}$

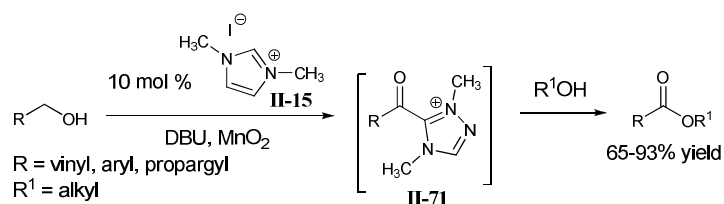
$\text{Ar} = \text{Ph} \quad \text{II-17a}$
 $\text{Ar} = 4\text{-OMe-Ph} \quad \text{II-17d}$

hydroacylated or reduced

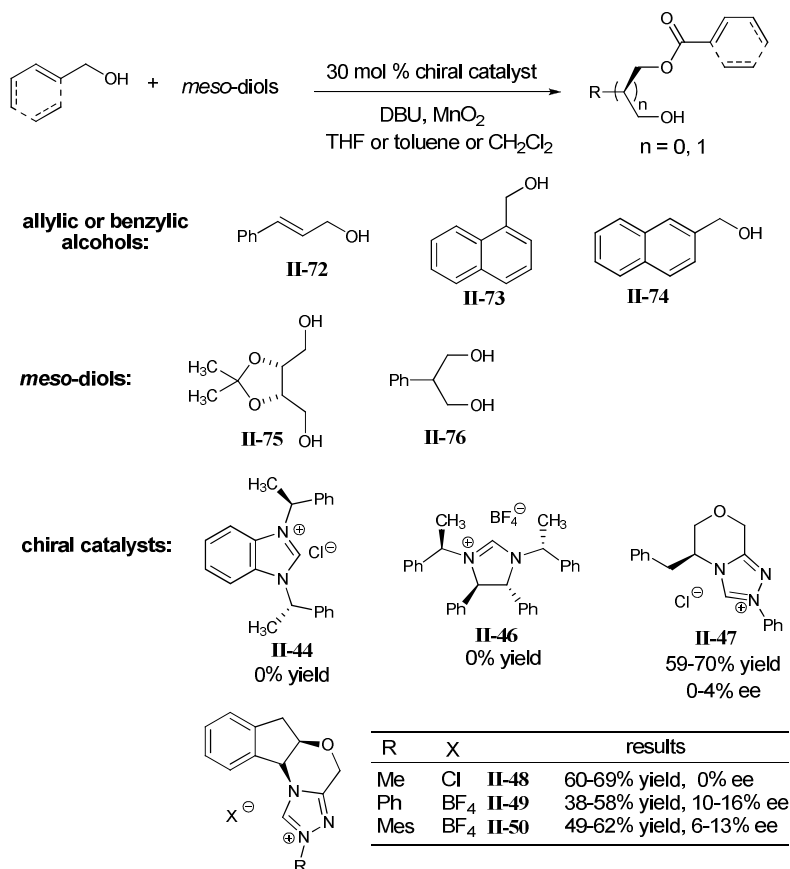
entry	substrate	conditions	anticipated product
1	 II-66	20 mol % II-15 , 20 mol % DBU, 0.5 M MeOH	
2	 II-67	20 mol % II-15 , 20 mol % DBU, 0.5 M MeOH	
3	 II-68	30 mol % II-15 , 30 mol % DBU, 0.3 M MeOH	 or
4		30 mol % II-15 , 30 mol % DBU, 0.3 M <i>t</i> -BuOH	
5		30 mol % II-14 , 30 mol % DBU, 0.3 M <i>t</i> -BuOH	
6		100 mol % II-15 , 100 mol % DBU, 0.25 M MeOH	
7		30 mol % II-15 , 30 mol % K_2CO_3 , 20 mol % 18-c-6, 0.3 M CH_2Cl_2	
8	 II-69	30 mol % II-14 , 30 mol % K_2CO_3 , 20 mol % 18-c-6, 0.3 M CH_2Cl_2	
9		30 mol % II-22 , 30 mol % K_2CO_3 , 20 mol % 18-c-6, 0.3 M CH_2Cl_2	
10	 II-69	30 mol % II-15 , 30 mol % DBU, 0.3 M MeOH	
11		30 mol % II-14 , 30 mol % DBU, 0.3 M MeOH	
12		30 mol % II-22 , 30 mol % DBU, 0.3 M MeOH	
13	 II-70	15 mol % II-15 , 15 mol % DBU, 0.3 M EtOH	 or
14		15 mol % II-15 , 15 mol % DBU, 0.3 M CH_2Cl_2	

2.5 NHC-Catalyzed Desymmetrization of Meso-Diols

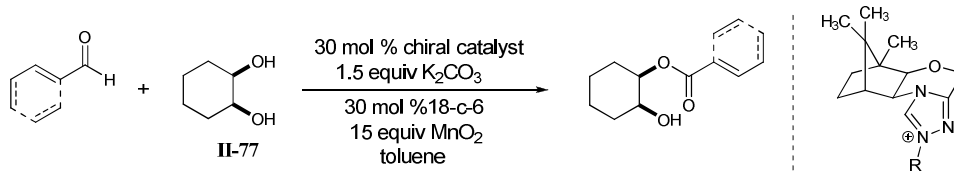
The development of mild and efficient oxidation methods remains an important goal in chemistry. Our group has demonstrated that NHC derived from triazolium salt **II-15** promotes the tandem oxidation of allylic, benzylic and propargylic alcohols to esters (Scheme 2-18). An oxidant, MnO_2 , was employed in the reaction to initially oxidize the alcohol to the aldehyde. Upon carbene addition to the aldehyde, a tetrahedral intermediate is generated and is oxidized by MnO_2 to the activated acyltriazolium species (**II-71**). The activated acyltriazolium species **II-71** can acylate an alcohol to produce an ester and regenerate the catalyst.

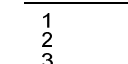
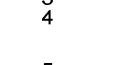
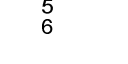
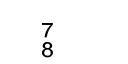
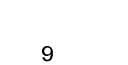
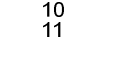



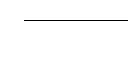

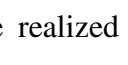
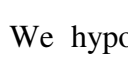
Scheme 2-18. NHC-catalyzed tandem oxidation of alcohols to esters

This methodology can be expanded to asymmetric applications by creating a chiral environment around the activated carbonyl. A chiral NHC can be used to generate a chiral acylating agent, similar to **II-71**, and applied towards the desymmetrization of *meso*-diols. Initial investigations into the selective acylation of *meso*-diols began with easily accessible diols **II-75**¹⁸⁷ and **II-76**¹⁸⁸ (Scheme 2-19). Different allylic and benzylic alcohols (**II-72** to **II-74**) were tested as the acylating agents to selectively acylate the two *meso*-alcohols catalyzed by various chiral NHCs. Chiral imidazolium salts **II-44** and **II-46** did not promote the reaction, while chiral triazolium salts (**II-47** to **II-50**) produced moderate yields of the desired product but minimal to no selectivities.

Scheme 2-19. Meso-diols examined for NHC-catalyzed desymmetrization

We next focused our attention on the selective acylation of *cis*-1,2-cyclohexane diol **II-77** (Table 2-8). Again, we surveyed a variety of substituted cinnamaldehydes and aryl aldehydes with chiral catalysts **II-49**, **II-50** and newly synthesized **II-78** and **II-79** that are derived from camphor. The four chiral catalysts promoted the reaction to give moderate yields and poor selectivities. Surprisingly, the rigid camphor-derived catalysts **II-78** and **II-79** were not effective at blocking one face of the intermediate. The highest selectivity resulting from either catalysts **II-78** or **II-79**, was only 9% ee (entry 4). Treating cinnamaldehyde with chiral catalyst **II-50** resulted in the highest selectivity observed at 41% ee (entry 2).

Table 2-8. NHC-catalyzed desymmetrization of *cis*-1,2-cyclohexane diol


entry	aldehyde	chiral catalysts	yield (%)	ee (%)
1		II-49	53	20
2		II-50	47	41
3		II-78	43	5
4		II-79	40	9
5		II-49	41	0
6		II-50	77	2
7		II-49	48	19
8		II-50	36	22
9		II-49	65	6
10		II-50	56	2
11		II-78	49	7
12		II-50	28	0
13		II-50	57	6

We realized that with prolonged reaction times, the enantioselectivity of the product suffered. We hypothesized that the excess base employed in the reaction may cause the decreased enantioselectivity by a base-catalyzed acyl transfer.^{189, 190} To test this hypothesis, the enantioenriched product **II-80** (at 20% ee) was treated with base, 0.5 equivalents of K_2CO_3 and 20 mol % 18-crown-6 in toluene. After 1.5 hours, we observed a racemic mixture, confirming that base promoted the undesired acyl group transfer (Figure 2-4)

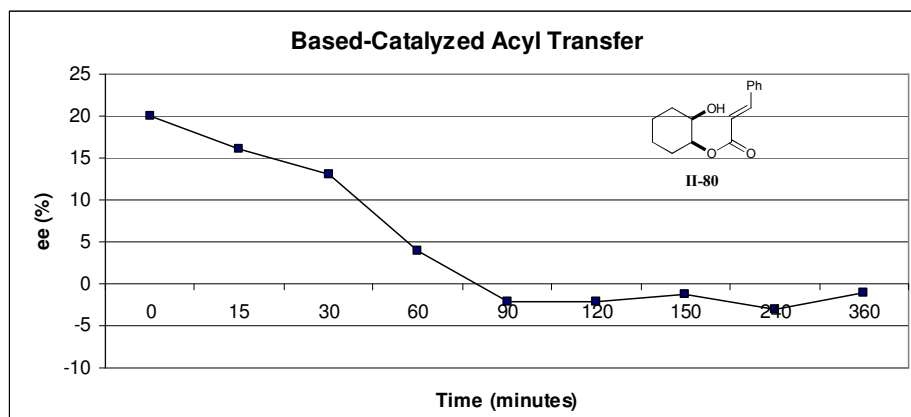
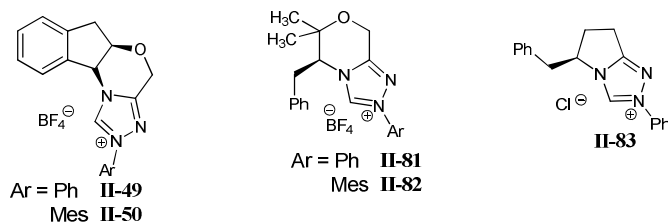


Figure 2-4. Chart summarizing the based-catalyzed acyl transfer data

Armed with this knowledge, we chose to employ a milder base, Proton Sponge®, to suppress the acyl transfer. The switch to Proton Sponge® resulted in isolation of **II-80** in >60% yield with ~60% ee (Table 2-9). A survey of solvents for this desymmetrization indicates that methylene chloride provides the best combination of yield and selectivity (entry 7). More chiral triazolium salts were screened in this reaction. Triazolium salt **II-50** in the presence of both potassium carbonate and Proton Sponge® provides the highest selectivity and reactivity with **II-77** and cinnamaldehyde (entry 7). When this reaction was conducted at -30 °C, chiral triazolium salt **II-50** catalyzed the oxidation of cinnamaldehyde and subsequently selectively acylated cis-1,2-cyclohexane diol in 58% yield and 80% ee (entry 12). This strategy of accessing activated acylating agents from aldehydes and an oxidant only in the presence of an NHC has potential applications with nucleophiles that undergo fast background reactions with acid chlorides and anhydrides.

Table 2-9. Desymmetrization of *cis*-1,2-cyclohexane diol

entry	catalyst	conditions ^a	yield (%)	ee (%)
1 ^b	II-49	toluene, 23 °C	53	20
2 ^b	II-50	toluene, 23 °C	47	41
3	II-49	Proton Sponge, toluene, 23 °C	66	52
4	II-50	Proton Sponge, toluene, 23 °C	62	60
5	II-50	Proton Sponge, 4-CF ₃ -Ph, 23 °C	39	63
6	II-50	Proton Sponge, THF, 23 °C	53	54
7	II-50	Proton Sponge, CH ₂ Cl ₂ , 23 °C	78	59
8	II-81	Proton Sponge, CH ₂ Cl ₂ , 23 °C	76	23
9	II-82	Proton Sponge, CH ₂ Cl ₂ , 23 °C	57	20
10	II-83	Proton Sponge CH ₂ Cl ₂ , 23 °C	76	37
11	II-50	Proton Sponge, CH ₂ Cl ₂ , 0 °C	67	65
12	II-50	Proton Sponge, CH ₂ Cl ₂ , -30 °C	58	80
13	II-50	Proton Sponge, CH ₂ Cl ₂ , -40 °C	38	73



a. Reactions performed with 30 mol % K₂CO₃, 15 mol % 18-crown-6, 1 equiv of Proton Sponge @, and 0.25 M solvent. b. Reaction performed with 1.5 equiv K₂CO₃, 20 mol % of 18-crown-6, and 0.25 M solvent. Proton Sponge @ = N,N,N',N'-tetramethyl-1,8-naphthalene-diamine

2.6 Summary

We have demonstrated that the hydroacylation of activated ketones can be catalyzed by *N*-heterocyclic carbenes. This process occurs via separate reduction and acylation steps in which the organocatalyst is responsible for two key bond-forming steps of the catalytic cycle. An intramolecular variant was also developed to deliver benzofuranones as products. An asymmetric desymmetrization of *meso*-diols can be achieved using chiral heteroazolium salts.

We have also shown that NHCs can be used to catalyze new redox processes. This new reactivity offers significant potential to expand to other redox systems. The use of an aldehyde

as a hydride source is a unique and mild method to reduce π -bonds that eliminates wasteful by-products that are produced when using conventional hydride sources or metal catalysis.

2.7 *Experimental*

General Information. All reactions were carried out under a nitrogen atmosphere in flame-dried glassware with magnetic stirring. THF, Et₂O, CH₂Cl₂, DMF and toluene were purified by passage through a bed of activated alumina.¹³² Reagents were purified prior to use unless otherwise stated following the guidelines of Perrin and Armarego.¹³³ Purification of reaction products was carried out by flash chromatography using EM Reagent silica gel 60 (230-400 mesh). Analytical thin layer chromatography was performed on EM Reagent 0.25 mm silica gel 60-F plates. Visualization was accomplished with UV light and anisaldehyde, ceric ammonium nitrate stain, potassium permanganate, or phosphomolybic acid followed by heating. Infrared spectra were recorded on a Perkin Elmer 1600 series FT-IR spectrometer. ¹H-NMR spectra were recorded on a Varian Inova 500 (500 MHz) or Mercury 400 (400 MHz) spectrometer and are reported in ppm using solvent as an internal standard (CDCl₃ at 7.26 ppm). Data are reported as (ap = apparent, s = singlet, d = doublet, t = triplet, q = quartet, m = multiplet, b = broad; coupling constant(s) in Hz; integration. Proton-decoupled ¹³C-NMR spectra were recorded on a Varian Inova 500 (125 MHz) or Mercury 400 (100 MHz) spectrometer and are reported in ppm using solvent as an internal standard (CDCl₃ at 77.0 ppm). Mass spectra data were obtained on a Varian 1200 Quadrupole Mass Spectrometer and Micromass Quadro II Spectrometer.

2.7.1 *Preparations of α -Ketoesters*

Ethyl 2-(4-bromophenyl)-2-oxoacetate was prepared according to Imoto¹⁹¹ and ethyl 2-(4-chlorophenyl)-2-oxoacetate was prepared according to Mills.¹⁹² Ethyl 2-(naphthalene-6-yl)-2-oxoacetate and ethyl 2-(3-methoxyphenyl)-2-oxoacetate were prepared according to procedure

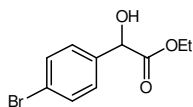
analogous to Seebach.¹⁹³ Ethyl 2-oxo-2-(thiophen-2-yl)acetate was purchased from Alfa Aesar Chemical Company. Methyl benzoyl formate, benzil, 9-fluorenone and all aldehydes were commercially available from Sigma-Aldrich Chemical Company and all aldehydes were purified before use.

2.7.2 NHC-Catalyzed Hydroacylation of Activated Ketones

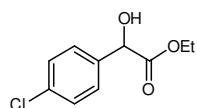
2.7.2.1 General Procedure for Triazolium-Catalyzed Reaction with Protic Solvent

A screw-capped tube was charged with the triazolium salt (25 mg, 0.111 mmol) in a nitrogen-filled dry box. The tube was removed from the box and placed under a positive pressure of nitrogen. The tube was charged with methanol (1.5 mL), DBU (17 μ L, 0.111 mmol), distilled benzaldehyde (75 μ L, 0.74 mmol) and lastly, methyl benzoyl formate (213 mg, 1.3 mmol). The reaction was stirred at 23 °C for 24 hours until benzaldehyde was consumed (as judged by GC). The reaction mixture was concentrated *in vacuo*. The resulting residue was purified by flash column chromatography on silica gel.

2.7.2.2 2-Hydroxyacetate Characterization



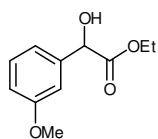
Ethyl 2-(4-bromophenyl)-2-hydroxyacetate (II-20b): Purified with 20% EtOAc/hexanes yielding 153 mg (80%) of **II-20b** as a white solid. R_f = 0.35 (1:3 EtOAc/hexanes); IR (film) 3460, 2982, 1734, 1477, 1396, 1256, 763 cm^{-1} ; ^1H NMR (500 MHz, CDCl_3) δ 7.49 (d, J = 8.3, 2H); 7.31 (d, J = 8.3, 2H); 5.11 (d, J = 5.2, 1H); 4.22 (dq, J = 33.3, 7.0, 2H); 3.49 (d, J = 5.2, 1H); 1.23 (t, J = 7.0, 3H); ^{13}C NMR (125 MHz, CDCl_3) δ 173.2, 137.3, 131.6, 128.2, 122.4, 72.1, 62.5, 14.0.



Ethyl 2-(4-chlorophenyl)-2-hydroxyacetate (II-20c): Purified with 20%

EtOAc/hexanes yielding 118 mg (75%) of **II-20c** as a white solid. $R_f = 0.36$

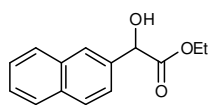
(1:3 EtOAc/hexanes); IR (film) 3458, 2983, 1736, 1400, 1257, 768 cm^{-1} ; ^1H NMR (500 MHz, CDCl_3) δ 7.38-7.33 (m, 4H); 5.13 (d, $J = 5.2$, 1H); 4.12 (dq, $J = 32.1$, 7.3, 2H); 3.48 (d, $J = 5.5$, 1H); 1.23 (t, $J = 7.0$, 3H); ^{13}C NMR (125 MHz, CDCl_3) δ 173.8, 137.3, 134.7, 129.2, 128.3, 72.6, 62.9, 14.5.



Ethyl-2-hydroxy-2-(3-methoxyphenyl)acetate (II-20d): Purified with 20%

EtOAc/hexanes yielding 131 mg (84%) of **II-20d** as a light tan solid. $R_f = 0.31$

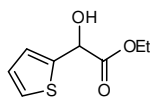
(1:3 EtOAc/hexanes); IR (film) 3472, 2938, 2935, 1734, 1369, 1261, 782, 738 cm^{-1} ; ^1H NMR (500 MHz, CDCl_3) δ 7.28 (t, $J = 7.9$, 1H); 7.01 (d, $J = 7.6$, 1H); 6.98 (s, 1H); 6.86 (m, 1H); 5.13 (s, 1H); 4.22 (dq, $J = 36.9$, 7.3, 2H); 3.81 (s, 3H); 3.51 (s, 1H); 1.24 (t, $J = 7.0$, 3H); ^{13}C NMR (125 MHz, CDCl_3) δ 173.8, 159.9, 140.1, 129.8, 119.1, 114.3, 112.0, 72.9, 62.5, 55.4, 14.1; LRMS (electrospray): Mass calculated for $\text{C}_{11}\text{H}_{14}\text{O}_4$ $[2\text{M}+\text{Na}]^+$ 443.5. Found 443.3.



Ethyl-2-hydroxy-2-(naphthalen3-yl)acetate (II-20e): Purified with 15%

EtOAc/hexanes yielding 151 mg (89%) of **II-20e** as a white solid. $R_f = 0.26$

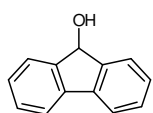
(1:3 EtOAc/hexanes); IR (film) 3462, 3051, 2982, 1734, 1367, 1258 cm^{-1} ; ^1H NMR (500 MHz, CDCl_3) δ 7.91 (s, 1H); 7.85 (m, 3H); 7.51 (m, 3H); 5.33 (d, $J = 4.6$, 1H); 4.23 (dq, $J = 43.7$, 7.0, 2H); 3.85 (d, $J = 5.2$, 1H); 1.22 (t, $J = 7.0$, 3H); ^{13}C NMR (125 MHz, CDCl_3) δ 174.2, 139.8, 136.2, 133.7, 133.6, 128.9, 128.6, 128.2, 126.8, 126.3, 124.6, 73.5, 62.9, 14.5; LRMS (electrospray): Mass calculated for $\text{C}_{14}\text{H}_{14}\text{O}_3$ $[2\text{M}+\text{Na}]^+$ 483.5. Found 483.4



Ethyl-2-hydroxy-2-(thiophen-2-yl)acetate (II-20f): Purified with 15%

EtOAc/hexanes yielding 98 mg (71%) of **II-20f** as a light yellow oil. $R_f = 0.49$ (1:3

EtOAc/hexanes); IR (film) 3466, 3102, 2983, 1736, 1369, 1267, 706 cm^{-1} ; ^1H NMR (500 MHz, CDCl_3) δ 7.29 (d, $J = 5.2$, 1H); 7.11 (s, 1H); 6.99 (m, 1H); 5.40 (s, 1H); 4.29 (m, 2H); 3.49 (s, 1H); 1.29 (t, $J = 7.3$, 3H); ^{13}C NMR (125 MHz, CDCl_3) δ 172.7, 141.7, 127.2, 125.9, 125.5, 69.3, 62.8, 14.3; LRMS (electrospray): Mass calculated for $\text{C}_{13}\text{H}_{16}\text{O}_2$ $[2\text{M}]^+$ 372.4. Found 372.4.



9H-fluoren-9-ol (II-20h): Purified with 12.5% EtOAc/hexanes yielding 102 mg

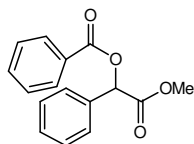
(75%) of **II-20h** as a light tan solid. $R_f = 0.42$ (1:3 EtOAc/hexanes); IR (film)

3199, 3054, 2986, 1265 cm^{-1} ; ^1H NMR (500 MHz, CDCl_3) δ 7.65 (m, 4H); 7.40 (t, $J = 7.6$, 2H); 7.33, (t, $J = 7.3$, 2H); 5.60 (sb, 1H); 1.82 (d, $J = 5.8$, 1H); ^{13}C NMR (125 MHz, CDCl_3) δ 146.1, 140.5, 129.6, 128.3, 125.6, 120.5, 75.7.

2.7.2.3 General Procedure for Triazolium-Catalyzed Reaction with Aprotic Solvent

A screw-capped tube was charged with the triazolium salt (17 mg, 0.074 mmol) in a nitrogen-filled dry box. The tube was removed from the box and placed under a positive pressure of nitrogen. The tube was charged with CH_2Cl_2 (1.5 mL), DBU (11 μL , 0.074 mmol), distilled *p*-anisaldehyde (90 μL , 0.74 mmol) and lastly, methyl benzoyl formate (213 mg, 1.3 mmol). The reaction was stirred at 23 $^\circ\text{C}$ for 9 hours or until benzaldehyde was consumed (as judged by GC). The reaction mixture was concentrated *in vacuo*. The resulting residue was purified by flash column chromatography on silica gel.

2.7.2.4 Alkyl Benzoate Characterizations



(Methoxycarbonyl)(phenyl)methyl benzoate (II-19a): Purified with 30-50%

CH₂Cl₂/hexanes yielding 155 mg (78%) of **II-19a** as a white solid. R_f = 0.39

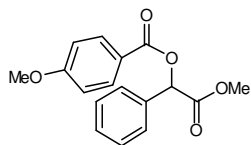
(1:1 CH₂Cl₂/hexanes); IR (film) 3035, 2951, 1753, 1719, 1259 cm⁻¹; ¹H NMR

(500 MHz, CDCl₃) δ 8.13 (d, J = 7.9, 2H); 7.59 (m, 3H); 7.43 (m, 5H); 6.17 (s, 1H); 3.76 (s,

3H); ¹³C NMR (125 MHz, CDCl₃) δ 169.5, 166.1, 134.2, 133.7, 130.2, 129.5, 129.4, 129.1,

128.7, 128.9, 75.1, 52.9; LRMS (electrospray): Mass calculated for C₁₆H₁₄O₄ [2M+Na]⁺ 563.6.

Found 563.2.



(Methoxycarbonyl)(phenyl)methyl 4-methoxybenzoate (II-19d):

Purified with 15% EtOAc/hexanes yielding 170 mg (77%) of **II-19d** as a

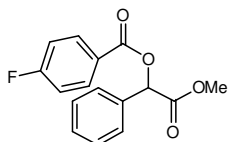
colorless oil. R_f = 0.56 (1:3 EtOAc/hexanes); IR (film) 2951, 1753, 1718,

1450, 1257, 845 cm⁻¹; ¹H NMR (500 MHz, CDCl₃) δ 8.08 (d, J = 8.9, 2H); 7.57 (m, 2H); 7.42

(m, 3H); 6.93 (d, J = 8.6, 2H); 6.014 (s, 1H); 3.87 (s, 3H); 3.75 (s, 3H); ¹³C NMR (125 MHz,

CDCl₃) δ 169.5, 165.5, 163.8, 134.1, 132.1, 129.2, 128.8, 127.6, 121.5, 113.7, 74.6, 55.4, 52.6;

LRMS (electrospray): Mass calculated for C₁₇H₁₆O₅ [2M+Na]⁺ 623.6 Found 623.29.



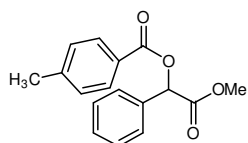
(Methoxycarbonyl)(phenyl)methyl 4-fluorobenzoate (II-19b): Purified

with 45% CH₂Cl₂/hexanes yielding 152 mg (71%) of **II-19b** as a white solid.

R_f = 0.39 (1:1 CH₂Cl₂/hexanes); IR (film) 2955, 1761, 1726, 1259, 849 cm⁻¹; ¹H NMR (500

MHz, CDCl₃) δ 8.14 (m, 2H); 7.58 (m, 2H); 7.45 (m, 4H); 7.13 (t, J = 8.6, 1H); 6.15 (s, 1H);

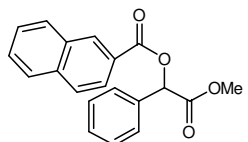
3.76 (s, 3H); ^{13}C NMR (125 MHz, CDCl_3) δ 169.7, 165.4, 133.8, 133.1, 129.9, 129.4, 129.3, 128.9, 128.1, 116.2, 75.4, 53.2.



(Methoxycarbonyl)(phenyl)methyl 4-methylbenzoate (10): Purified with

40-50% CH_2Cl_2 /hexanes yielding 155 mg (72%) of **10** as a white solid. R_f = 0.34 (1:1 CH_2Cl_2 /hexanes); IR (film) 2954, 1753, 1723, 1261, 840 cm^{-1} ;

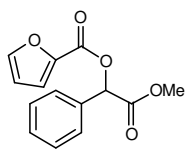
^1H NMR (500 MHz, CDCl_3) δ 8.01 (d, J = 8.3, 2H); 7.59 (m, 2H); 7.42 (m, 3H); 7.25 (m, 2H); 6.15 (s, 1H); 3.75 (s, 3H); 2.42 (s, 3H); ^{13}C NMR (125 MHz, CDCl_3) δ 169.7, 166.2, 144.6, 134.3, 133.8, 130.3, 129.5, 129.4, 129.1, 127.9, 75.0, 52.9, 22.0; LRMS (electrospray): Mass calculated for $\text{C}_{17}\text{H}_{16}\text{O}_4$ $[\text{M}+\text{H}]^+$ 591.6. Found 591.2.



(Methoxycarbonyl)(phenyl)methyl 2-naphthoate (II-19e): Purified with

45% CH_2Cl_2 /hexanes yielding 171 mg (70%) of **II-19e** as a colorless oil. R_f = 0.31 (1:1 CH_2Cl_2 /hexanes); IR (film) 3051, 2947, 1753, 1721, 1263 cm^{-1} ;

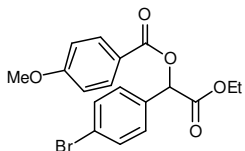
^1H NMR (500 MHz, CDCl_3) δ 8.71 (s, 1H); 8.13 (m, 2H); 7.97 (d, J = 8.3, 1H); 7.89 (m, 1H); 7.59 (m, 3H); 7.45 (m, 4H); 6.24 (s, 1H); 3.78 (s, 3H); ^{13}C NMR (125 MHz, CDCl_3) δ 169.6, 166.3, 136.0, 133.7, 132.6, 129.7, 129.6, 129.1, 129.0, 128.7, 128.6, 128.5, 128.0, 127.9, 127.8, 127.0, 75.2, 52.9; LRMS (electrospray): Mass calculated for $\text{C}_{20}\text{H}_{16}\text{O}_4$ $[2\text{M}+\text{Na}]^+$ 663.7. Found 663.9.



(Methoxycarbonyl)(phenyl)methyl furan-2-carboxylate (II-19f): Purified

with 10% EtOAc/hexanes yielding 138 mg (73%) of **II-19f** as a colorless oil. R_f = 0.57 (1:3 EtOAc/hexanes); IR (film) 3136, 2956, 1753, 1730, 1285 cm^{-1} ; ^1H

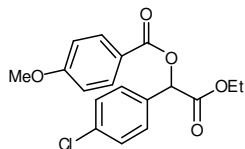
NMR (500 MHz, CDCl_3) δ 7.57 (m, 2H); 7.41 (m, 4H); 7.31 (m, 1H); 6.53 (sb, 1H); 6.15 (s, 1H); 3.76 (s, 3H); ^{13}C NMR (125 MHz, CDCl_3) δ 169.3, 158.0, 147.2, 144.0, 133.8, 129.6, 129.1, 128.0, 119.5, 112.3, 74.8, 53.0; LRMS (electrospray): Mass calculated for $\text{C}_{14}\text{H}_{12}\text{O}_5$ $[2\text{M}+\text{Na}]^+$ 543.4. Found 543.2.



(Ethoxycarbonyl)(4-bromophenyl)methyl 4-methoxybenzoate (II-19i):

Purified with 7.5% EtOAc/hexanes yielding 251 mg (87%) of **II-19i** as a colorless oil. R_f = 0.58 (1:3 EtOAc/hexanes); IR (film) 2974, 1746, 1719,

1257, 837, 770 cm^{-1} ; ^1H NMR (500 MHz, CDCl_3) δ 8.06 (d, J = 8.9, 2H); 7.55 (d, J = 8.6, 2H); 7.46 (d, J = 8.6, 2H); 6.93 (d, J = 8.9, 2H); 6.07 (s, 1H); 4.21 (dq, J = 25.0, 7.0, 2H); 3.87 (s, 3H); 1.23 (t, J = 7.3, 3H); ^{13}C NMR (125 MHz, CDCl_3) δ 169.0, 165.9, 164.3, 133.8, 132.5, 129.7, 123.8, 121.9, 114.2, 74.5, 62.3, 55.9, 14.5; LRMS (electrospray): Mass calculated for $\text{C}_{18}\text{H}_{17}\text{BrO}_5$ $[2\text{M}+\text{Na}]^+$ 809.4. Found 808.7.



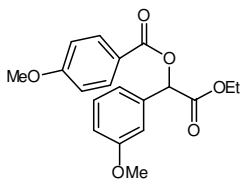
(Ethoxycarbonyl)(4-chlorophenyl)methyl 4-methoxybenzoate (II-19j):

Purified with 10% EtOAc/hexanes yielding 206 mg (81%) of **II-19j** as a colorless oil. R_f = 0.54 (1:3 EtOAc/hexanes); IR (film) 2974, 1753, 1719,

1257, 837, 770 cm^{-1} ; ^1H NMR (500 MHz, CDCl_3) δ 8.06 (d, J = 8.9, 2H); 7.52 (d, J = 8.3, 2H); 7.39 (d, J = 8.3, 2H); 6.93 (d, J = 8.9, 2H); 6.08 (s, 1H); 4.21 (dq, J = 24.1, 7.0, 2H); 3.87 (s, 3H); 1.23 (t, J = 7.0, 3H); ^{13}C NMR (125 MHz, CDCl_3) δ 169.1, 165.9, 164.3, 135.6, 133.3,

132.5, 129.5, 121.9, 114.2, 74.5, 62.3, 55.9, 14.5; LRMS (electrospray): Mass calculated for $C_{18}H_{17}ClO_5$ $[2M+Na]^+$ 719.5. Found 719.1.

(Ethoxycarbonyl)(naphthalene-3-yl)methyl 4-methoxybenz oate (II-19k): Purified with 9%

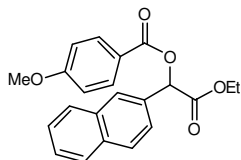


EtOAc/hexanes yielding 183 mg (72%) of **II-19k** as a colorless oil. $R_f =$

0.41 (1:3 EtOAc/hexanes); IR (film) 2951, 1753, 1718, 1260, 849, 771, 687 cm^{-1} ; 1H NMR (500 MHz, $CDCl_3$) δ 8.08 (d, $J = 8.6$, 2H); 7.33 (m,

1H); 7.16 (m, 1H); 7.12 (s, 1H); 6.93 (d, $J = 8.6$, 2H); 6.08 (s, 1H); 4.21 (m, 2H); 3.86 (s, 3H); 3.84 (s, 3H); 1.24 (t, $J = 7.0$, 3H); ^{13}C NMR (125 MHz, $CDCl_3$) δ 169.1, 165.8, 163.9, 160.0, 135.8, 132.2, 130.0, 121.8, 120.1, 114.8, 113.9, 113.3, 74.9, 61.9, 55.7, 55.5, 14.2; LRMS (electrospray): Mass calculated for $C_{19}H_{20}O_6$ $[2M+Na]^+$ 711.7. Found 711.1.

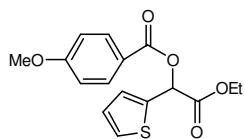
(Ethoxycarbonyl)(naphthalene-3-yl)methyl 4-methoxybenz oate (II-



19l): Purified with 10% EtOAc/hexanes yielding 208 mg (78%) of **II-19l**

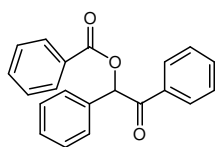
as a colorless oil. $R_f = 0.57$ (1:3 EtOAc/hexanes); IR (film) 2972, 2911,

1746, 1717, 1258, 747 cm^{-1} ; 1H NMR (500 MHz, $CDCl_3$) δ 8.11 (d, $J = 8.6$, 2H); 8.05 (s, 1H); 7.88 (d, $J = 7.9$, 1H); 7.53 (m, 2H); 6.94 (d, $J = 8.6$, 2H); 4.22 (dq, $J = 34.2$, 7.0, 2H); 3.87 (s, 3H); 1.23 (d, $J = 7.33$, 3H); ^{13}C NMR (125 MHz, $CDCl_3$) δ 169.2, 165.9, 164.0, 133.8, 133.4, 132.4, 131.9, 128.9, 128.5, 128.0, 127.6, 127.0, 126.8, 125.0, 121.9, 114.0, 75.2, 62.0, 55.7, 14.3; LRMS (electrospray): Mass calculated for $C_{22}H_{20}O_5$ $[2M+Na]^+$ 751.7. Found 751.1



(Ethoxycarbonyl)(thiophen-2-yl)methyl 4-methoxybenzoate (II-19m):

19m): Purified with 5.0% EtOAc/hexanes yielding 170 mg (73%) of **II-19m** as a light yellow oil. R_f = 0.67 (1:3 EtOAc/hexanes); IR (film) 2974, 1742, 1718, 1259, 849, 709 cm^{-1} ; ^1H NMR (500 MHz, CDCl_3) δ 8.07 (d, J = 8.6, 2H); 7.38 (d, J = 4.9, 1H); 7.25 (d, J = 4.3, 1H); 7.04 (t, J = 4.3, 1H); 6.93 (d, J = 8.6, 2H); 6.38 (s, 1H); 4.26 (m, 2H); 3.87 (s, 3); 1.27 (t, J = 7.0, 3H); ^{13}C NMR (125 MHz, CDCl_3) δ 128.6, 165.8, 164.3, 136.4, 132.6, 128.0, 127.4, 121.8, 114.2, 71.0, 62.5, 55.9, 14.5; LRMS (electrospray): Mass calculated for $\text{C}_{16}\text{H}_{16}\text{O}_5\text{S}$ $[2\text{M}+\text{Na}]^+$ 663.7. Found 663.1.



2-oxo-1,2-diphenylethyl benzoate (II-19n): Purified with 45%

CH_2Cl_2 /hexanes yielding 195 mg (83%) of **II-19n** as a white solid. R_f = 0.44 (1:1 CH_2Cl_2 /hexanes); IR (film) 3064, 1711, 1696, 1277, 1251 cm^{-1} ; ^1H NMR (500 MHz, CDCl_3) δ 8.13 (d, J = 7.3, 2H); 8.00 (d, J = 7.3, 2H); 7.57 (m 3H); 7.54 (t, J = 7.3, 1H); 7.43 (m, 7H); 7.09 (s, 1H); ^{13}C NMR (125 MHz, CDCl_3) δ 194.2, 166.5, 135.2, 134.2, 134.0, 133.9, 133.8, 130.5, 129.9, 129.8, 129.6, 129.3, 129.2, 128.9, 78.4; LRMS (electrospray): Mass calculated for $\text{C}_{21}\text{H}_{16}\text{O}_3$ $[2\text{M}+\text{Na}]^+$ 655.7. Found 655.0.

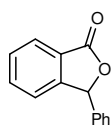
2.7.2.5 General Procedure for the Crossover Experiment

Into a 25 mL sealed-tube equipped with stir bar was added 4Å molecular sieves and flame-dried under vacuum and purged with N_2 (3x). Into it was charged with the triazolium salt (22 mg, 0.1 mmol) in a nitrogen-filled dry box. The tube was removed from the box and placed under a positive pressure of nitrogen. The tube was charged with CH_2Cl_2 (2.0 mL), DBU (15 μL , 0.1 mmol), benzaldehyde- α - d_1 (50 μL , 0.49 mmol), *p*-tolualdehyde (58 μL , 0.49 mmol) and lastly,

methyl benzoyl formate (245 μ L, 1.7 mmol). The reaction was stirred at 23 °C for 24 hours (as judged by GC). The reaction mixture was concentrated *in vacuo*. The resulting residue was purified by flash chromatography on silica gel and the 4 products were isolated.

2.7.2.6 General Procedure for NHC-catalyzed Intramolecular Hydroacylation Reaction

A flame-dried 10 mL round bottom flask equipped with stir bar was charged with the triazolium salt (54 mg, 0.238 mmol) and placed under a positive pressure of nitrogen. Into the flask was then added 1,2-diacylbenzene (50 mg, 0.238 mmol) and purged with nitrogen followed by addition of THF (1.2 mL) and DBU (36 μ L, 0.238 mmol) via syringe. The reaction was stirred at 23 °C for 24 hours until the 1,2-diacylbenzene was consumed (as judged by GC). The reaction was diluted with ethyl acetate (10 mL) and washed with water (2x10 mL). The aqueous layer was washed with ethyl acetate (2x10 mL) and the combined organic extracts were dried over anhydrous sodium sulfate, filtered, and concentrated *in vacuo*. The resulting residue was purified by flash column chromatography on silica gel.

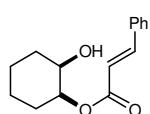


3-phenylisobenzofuran-1(3H)-one (II-54): Purified with 0.5:3.5:6 EtOAc/CH₂Cl₂/hexanes yielding 29.4 mg (59%) of **II-54** as a white solid. R_f = 0.45 (0.5:3.5:6 EtOAc/CH₂Cl₂/hexanes); IR (film) 3033, 2920, 1765, 1285 cm⁻¹; ¹H NMR (500 MHz, CDCl₃) δ 7.97 (d, J = 7.6, 1H); 7.65 (t, J = 7.3, 1H); 7.56 (t, J = 7.3, 1H); 7.38 (m, 3H); 7.34 (d, J = 7.6, 1H); 7.28 (m, 2H); 6.41 (s, 1H); ¹³C NMR (125 MHz, CDCl₃) δ 149.9, 136.6, 134.5, 129.6, 129.5, 129.2, 127.3, 127.2, 125.9, 125.8, 123.1, 82.9. LRMS (electrospray): Mass calculated for C₁₄H₁₀O₂ [2M+Na]⁺ 443.5. Found 443.4.

2.7.3 NHC-Catalyzed Desymmetrization of Meso-Diols

2.7.3.1 General Procedure for NHC-Catalyzed Desymmetrization of Meso-Diols

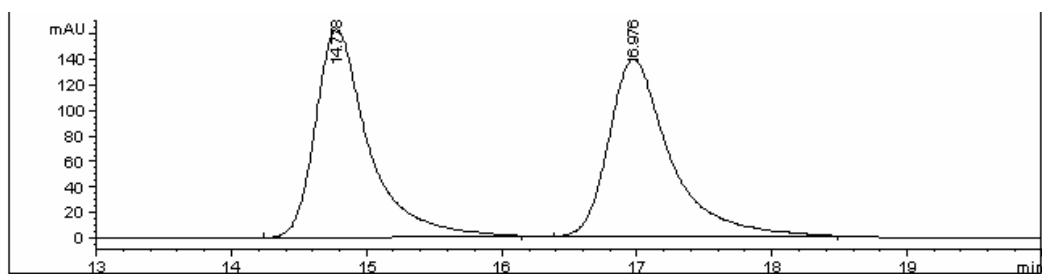
A flame-dried 10 ml round bottom flask equipped with stirbar was charged with the chiral triazolium salt **II-50** (50 mg, 0.119 mmol), K₂CO₃ (16.4 mg, 0.119 mmol), and 18-crown-6 (15.7 mg, 0.06 mmol). The flask was sealed with a septum and placed under a positive pressure of nitrogen. Into it was then added the *meso* diol (115 mg, 0.99 mmol), proton sponge (85 mg, 0.397 mmol), and MnO₂ (517 mg, 5.95 mmol). Dichloromethane (1.6 mL, 0.25 M) was added resulting in a black suspension. Lastly, cinnamaldehyde (50 μ L, 0.397 mmol) was added via syringe. The reaction was allowed to stir at -30 °C under a positive pressure of nitrogen until the aldehyde was consumed as determined by TLC. Upon consumption of the aldehyde, the mixture was filtered through a thin pad of celite and washed with ethyl acetate (25 mL). The filtrate was then concentrated *in vacuo* and the resulting residue was purified by flash chromatography on silica gel.



(E)-(1S,2R)-2-hydroxycyclohexyl cinnamate (II-80): Purified by column chromatography (25% EtOAc/hexane) yielding 57 mg (58%) of **II-80** as a white solid. Mp: 61-63 °C; IR (film) 3464, 3048, 2936, 2861, 2351, 1701, 1281 cm⁻¹; ¹H NMR (400 MHz, CDCl₃) δ 7.10 (d, *J*=15.8, 1H, CH); 7.53 (m, 2H); 7.39 (m, 3H); 6.58 (d, *J*=16.4, 1H, CH); 5.07 (m, 1H); 3.95 (m, 1H); 1.98-1.95 (m, 2H); 1.84-1.82 (m, 1H); 1.69-1.65 (m, 3H); 1.57 (s, 1H); 1.43-1.39 (m, 2H); ¹³C NMR (100 MHz, CDCl₃) δ 166.9, 145.4, 134.5, 130.6, 129.1, 128.3, 118.3, 74.5, 69.5, 30.6, 27.3, 22.3, 21.3; LRMS (electrospray): Mass calculated for C₁₅H₁₈O₃ [2M+Na]⁺ 515.6 Found 515.4

2.7.3.2 Determination of Enantiomeric Excess

The desymmetrization of *cis*-1,2-cyclohexanediol was carried out using cinnamaldehyde and the chiral catalyst **II-50** to yield **II-80** with an enantiomeric excess of 80%. Enantiomeric excess determined by HPLC on a Chiralcel AD-H column. 10% IPA/Hexanes, 1mL/min.

Racemic II-80:

```

=====
                        Area Percent Report
=====
  
```

```

Sorted By      :      Signal
Multiplier     :      1.0000
Dilution      :      1.0000
Use Multiplier & Dilution Factor with ISTDs
  
```

```

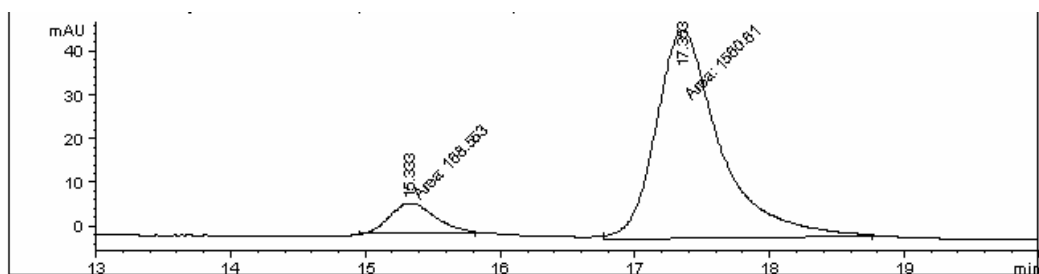
Signal 1: DAD1 A, Sig=254,4 Ref=360,100
  
```

Peak #	RetTime [min]	Type	Width [min]	Area [mAU*s]	Height [mAU]	Area %
1	14.778	BB	0.4061	4483.20117	163.41731	50.5538
2	16.976	PB	0.4681	4384.97656	138.98174	49.4462

```

Totals :                      8868.17773  302.39905
  
```

Enantioenriched II-80:



```

=====
                        Area Percent Report
=====
  
```

```

Sorted By      :      Signal
Multiplier     :      1.0000
Dilution      :      1.0000
Use Multiplier & Dilution Factor with ISTDs
  
```

```

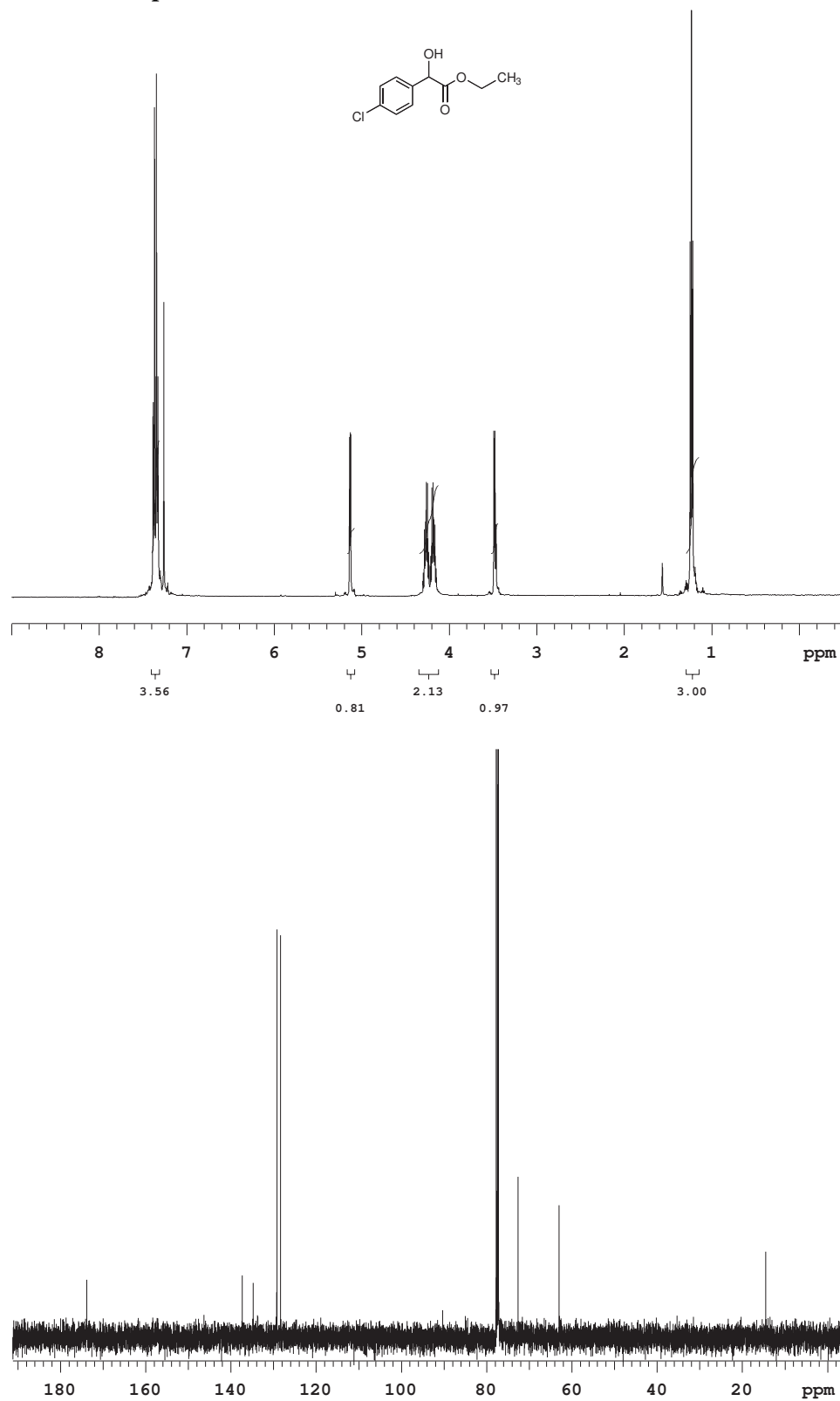
Signal 1: DAD1 A, Sig=254,4 Ref=360,100
  
```

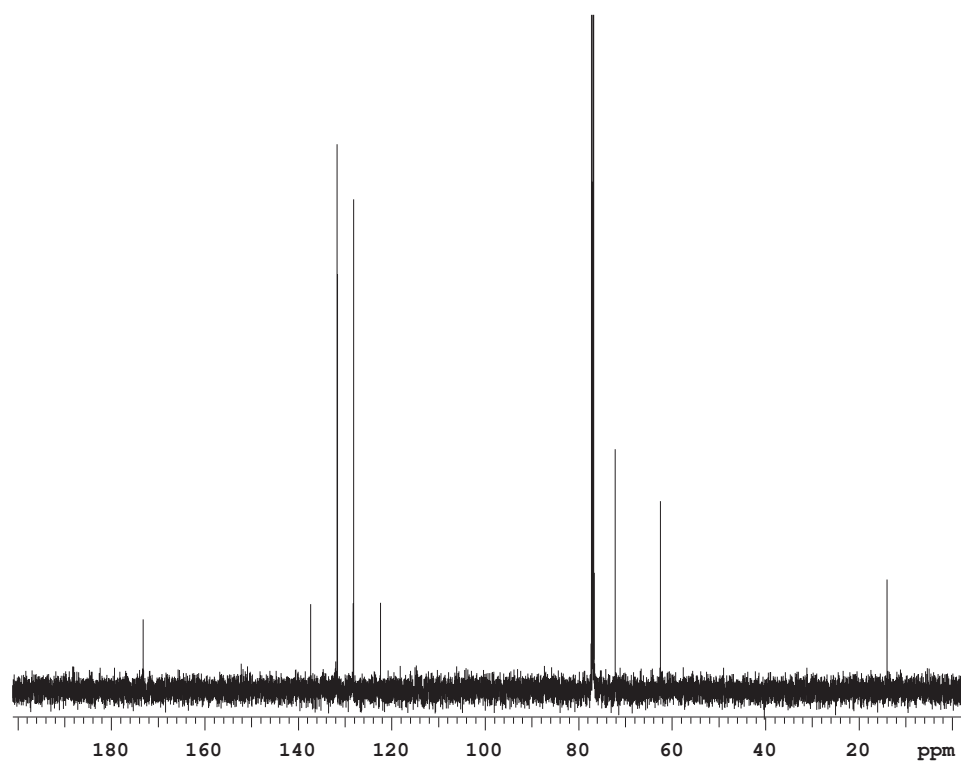
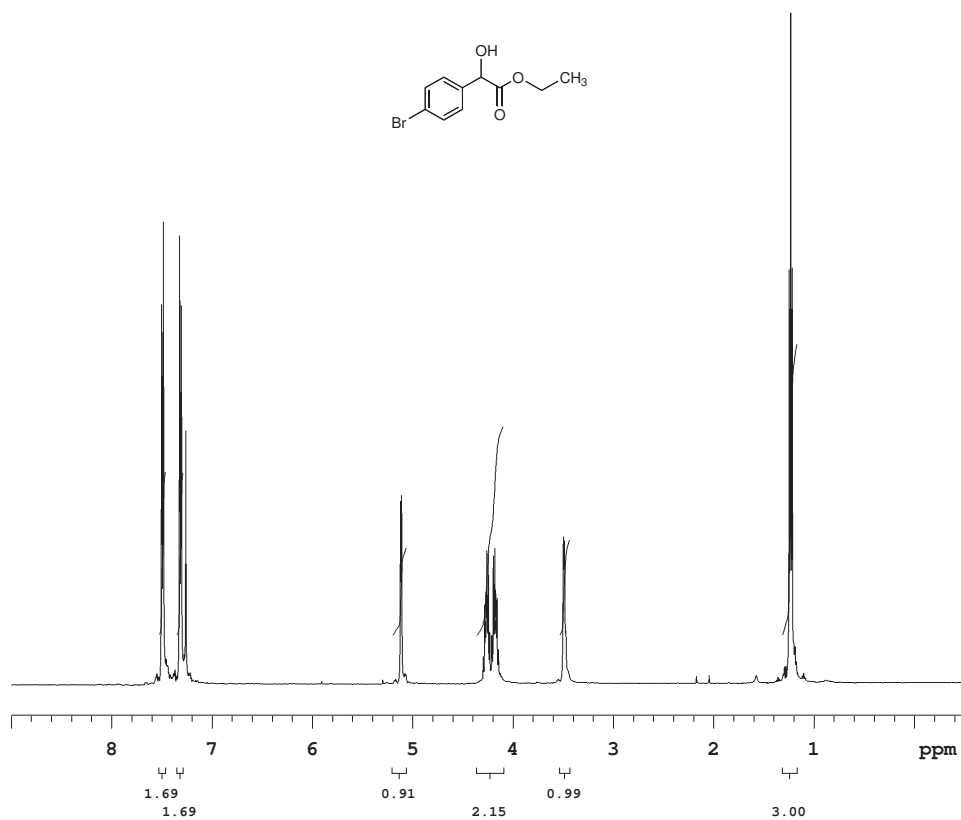
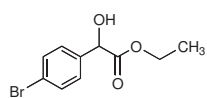
Peak #	RetTime [min]	Type	Width [min]	Area [mAU*s]	Height [mAU]	Area %
1	15.333	MM	0.3977	168.55333	7.06430	9.7477
2	17.353	MM	0.5499	1560.61377	47.29740	90.2523

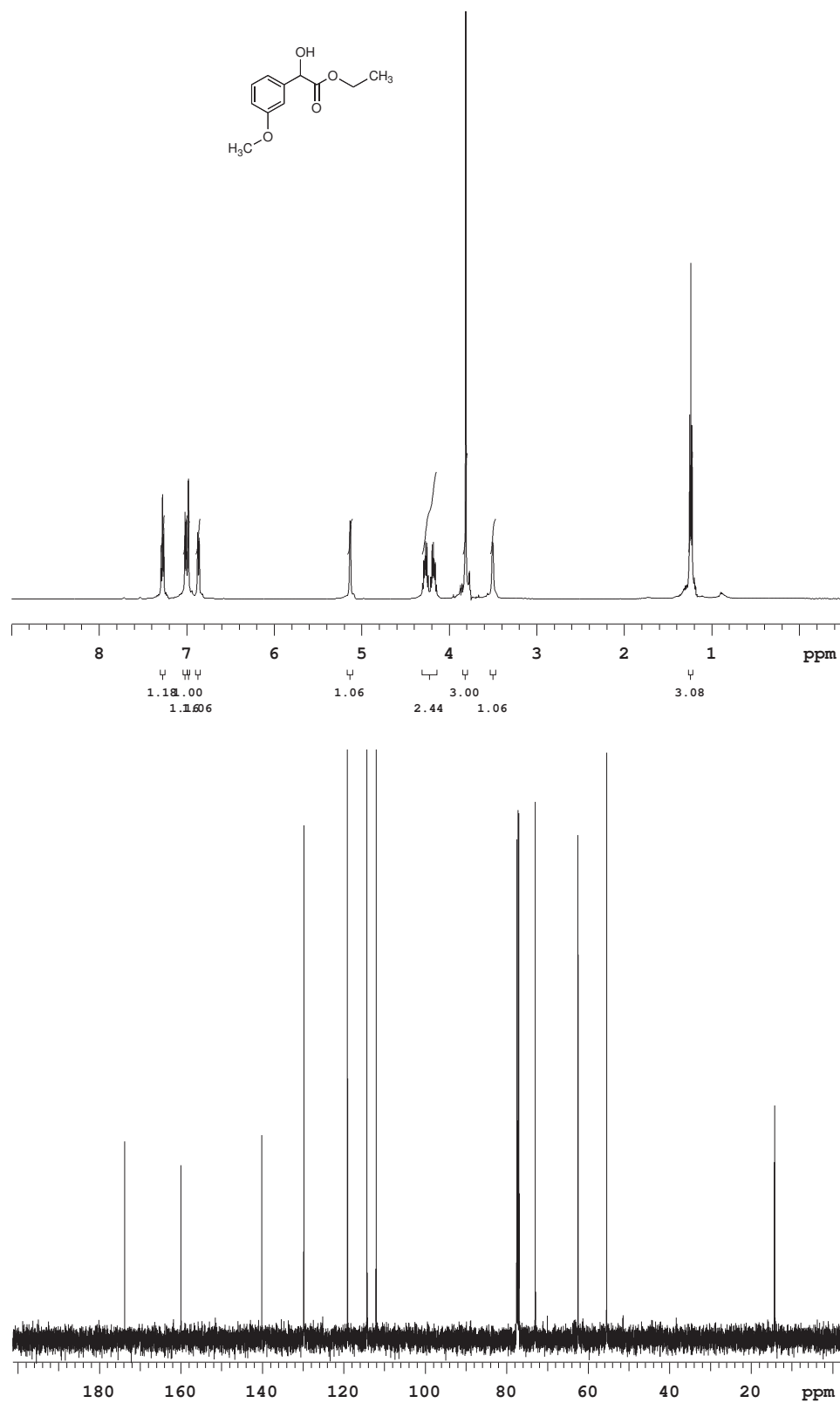
```

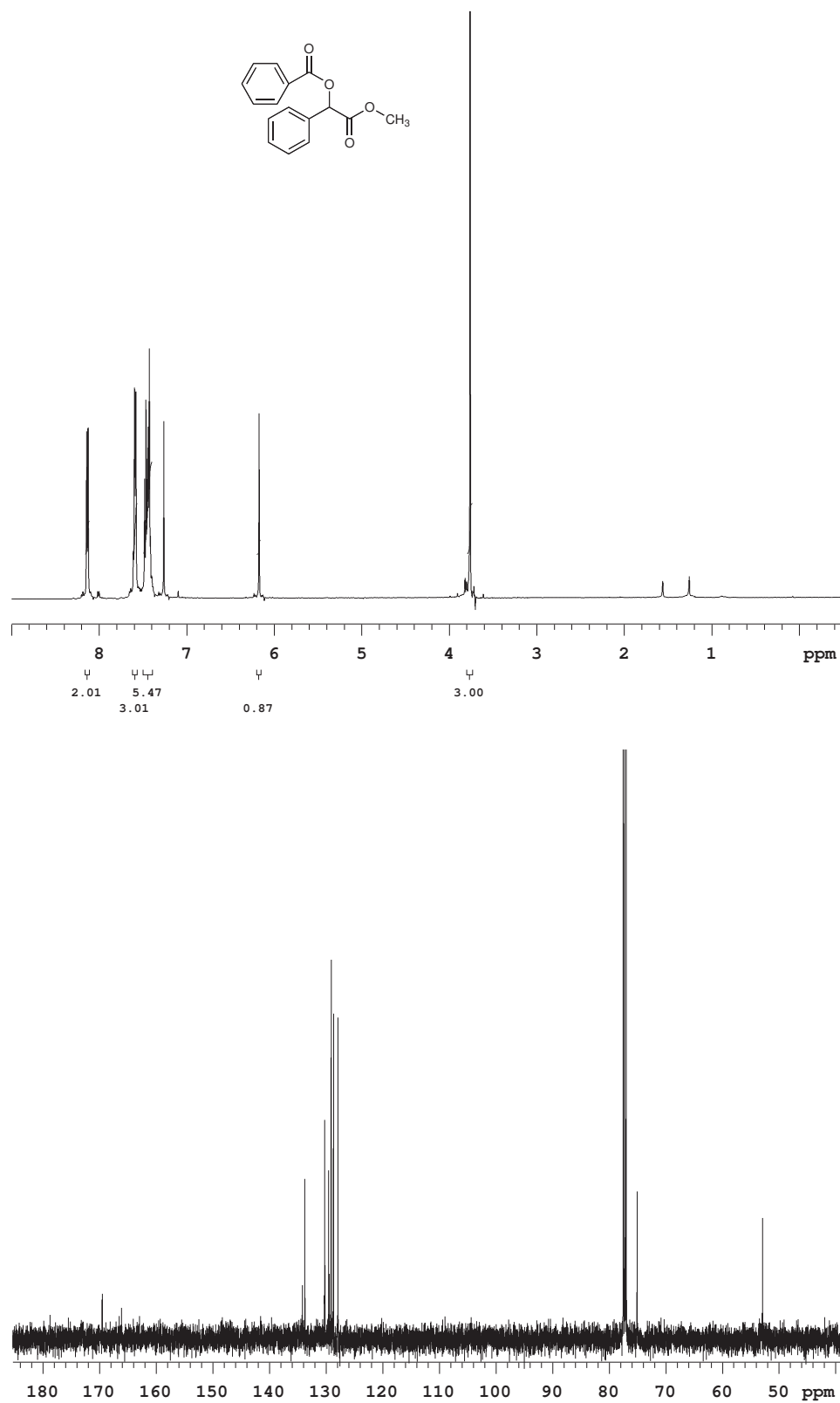
Totals :                      1729.16710  54.36171
  
```

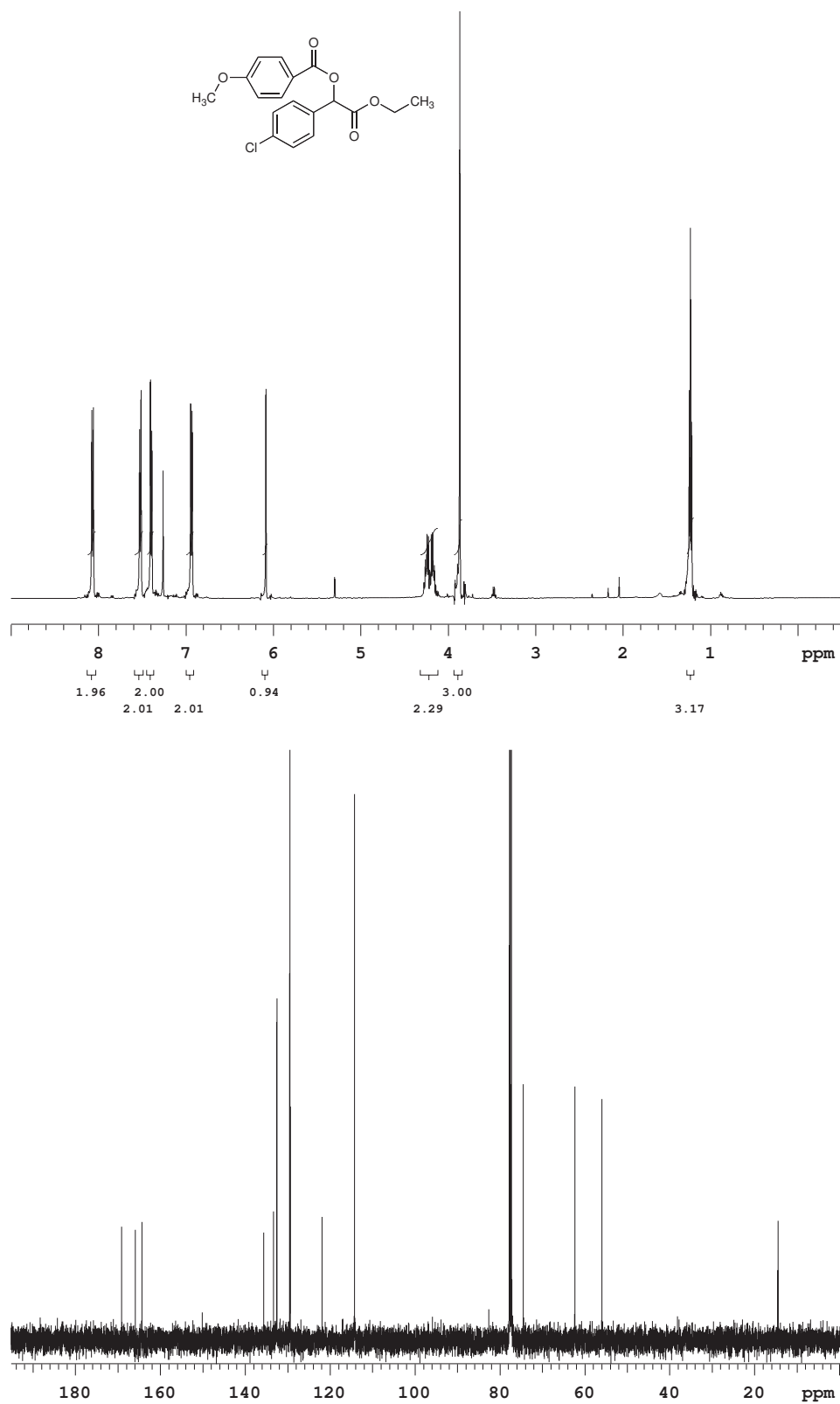
2.7.4 Selected NMR Spectra

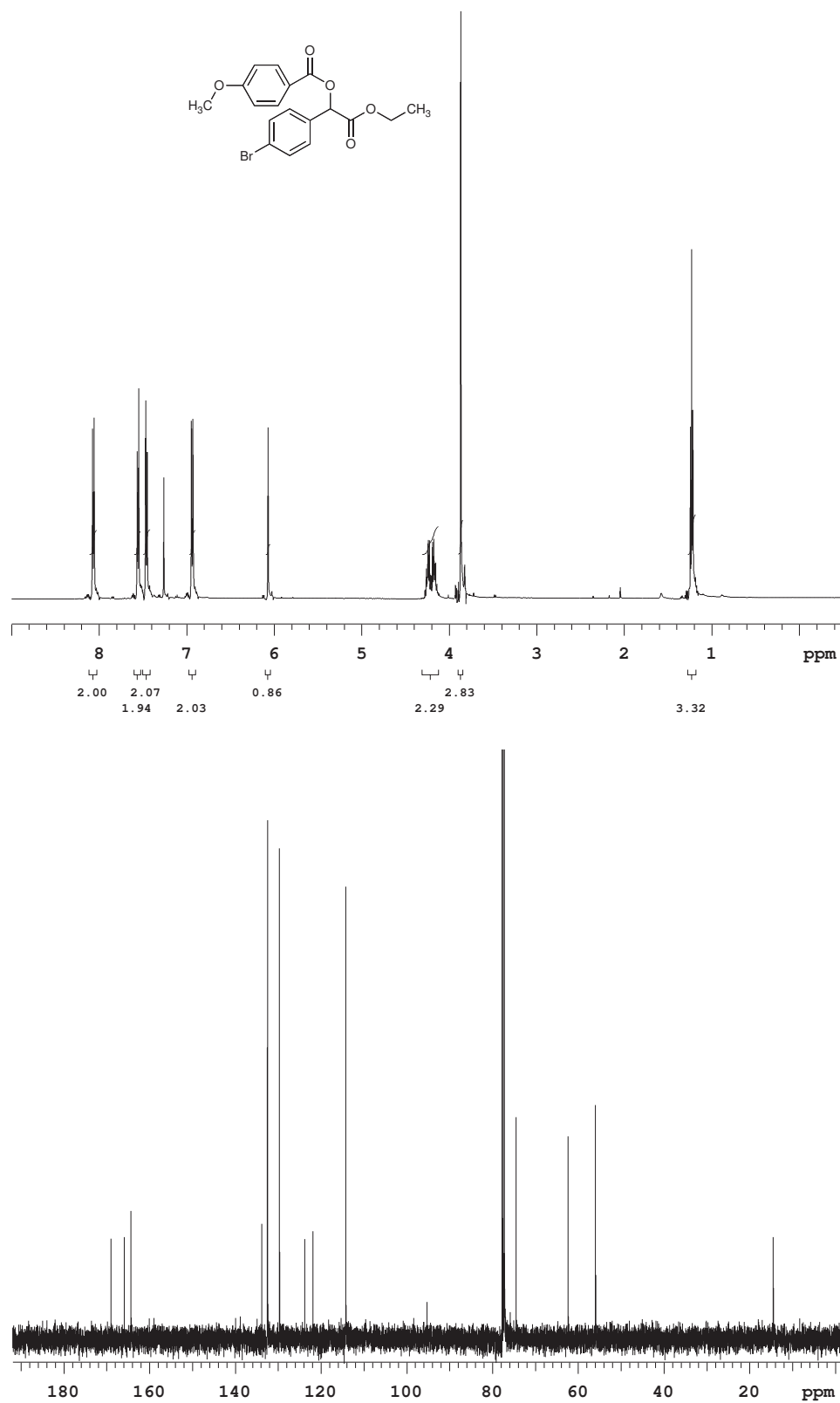


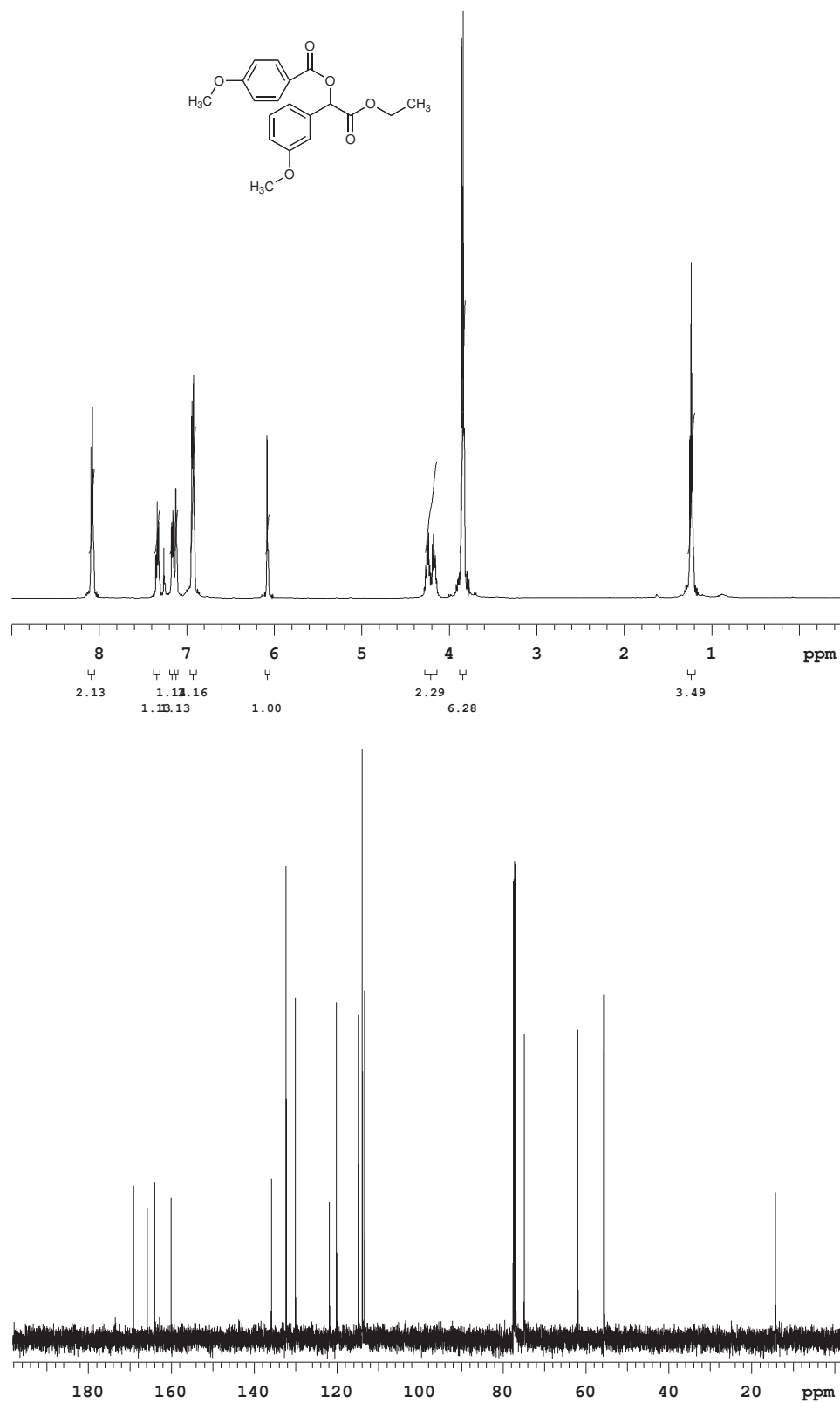


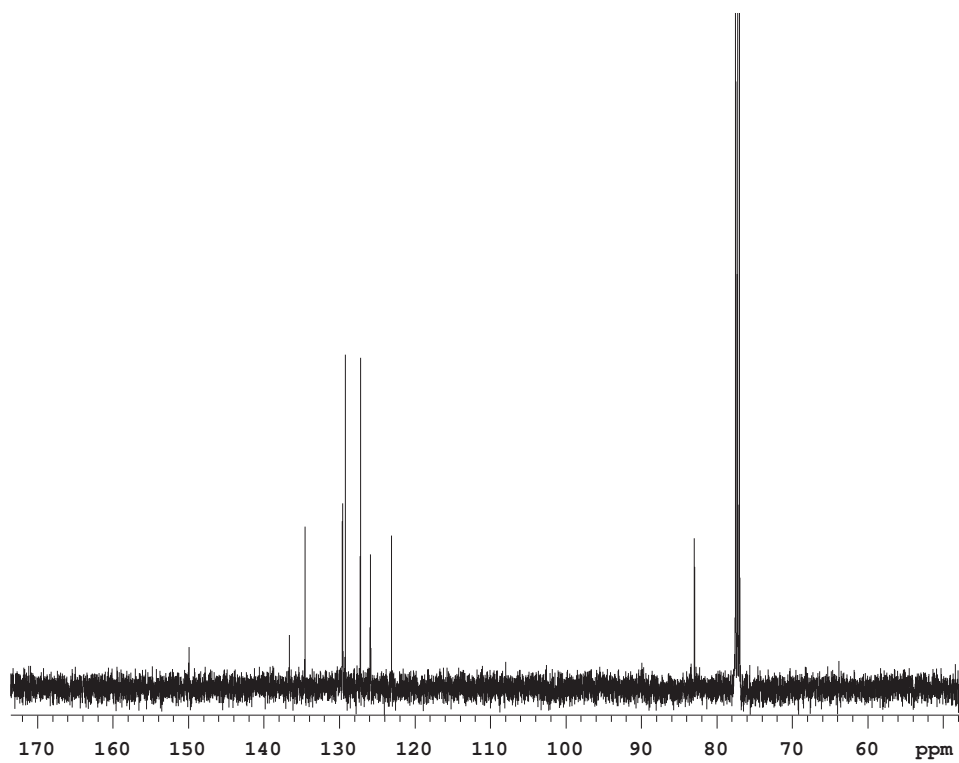
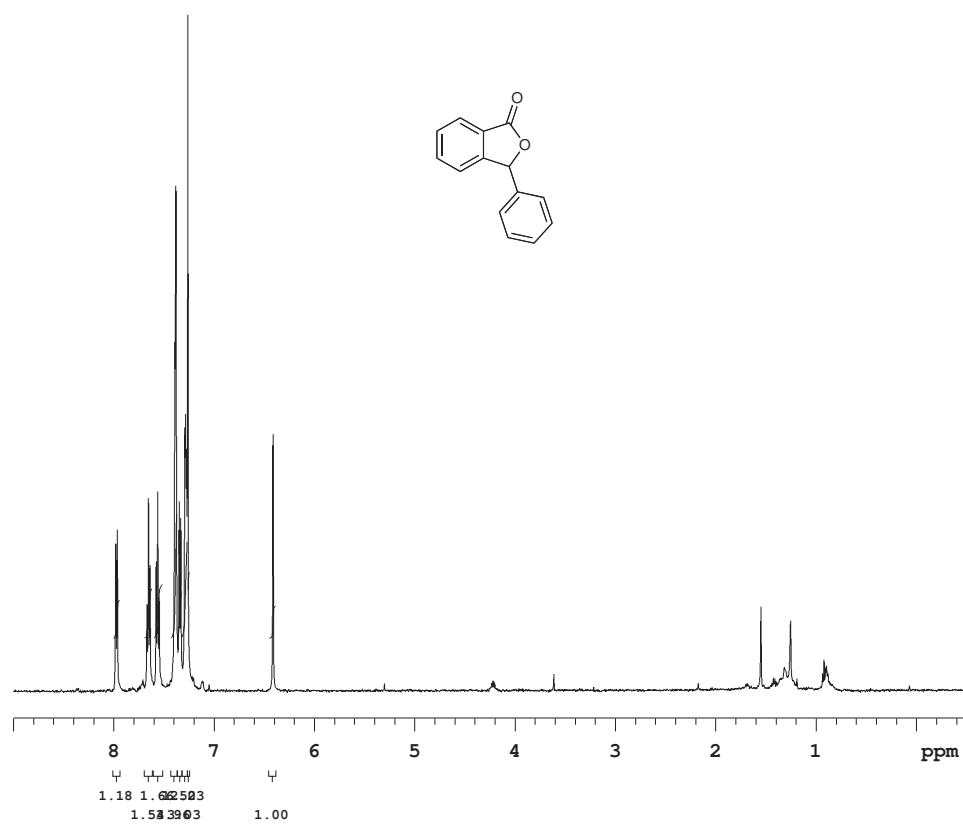


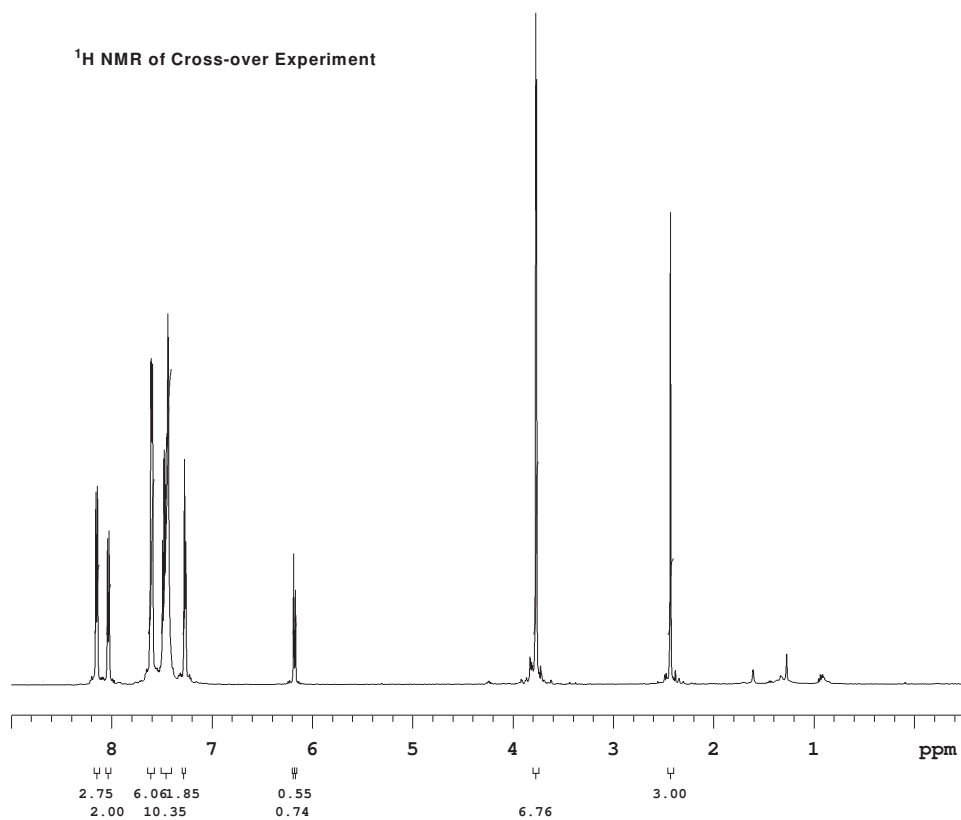
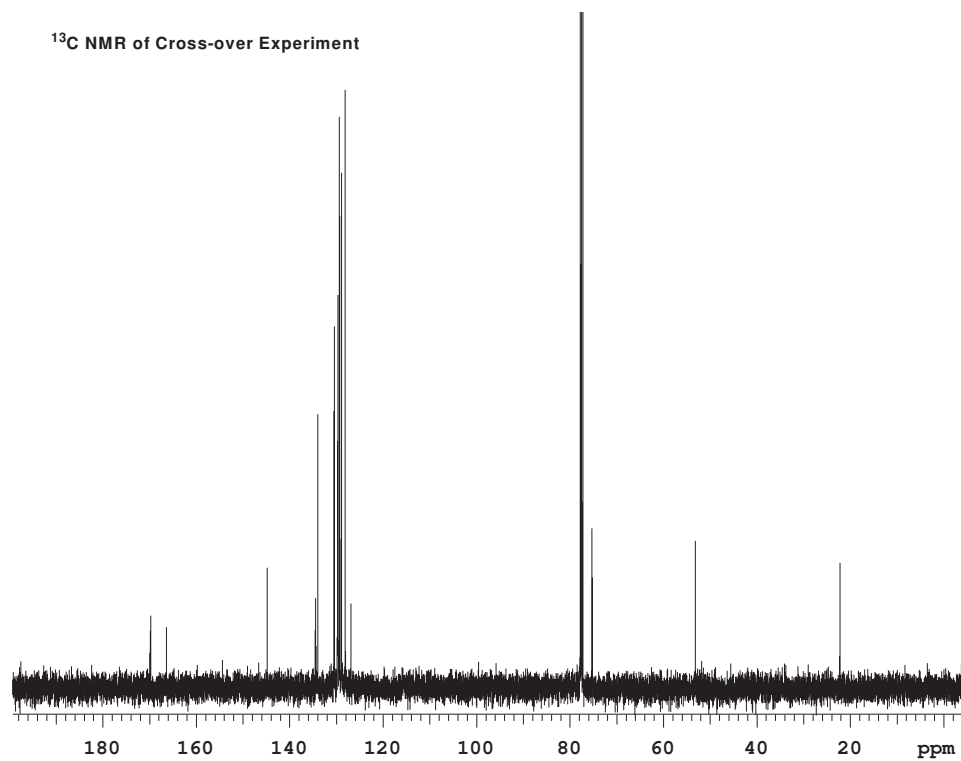


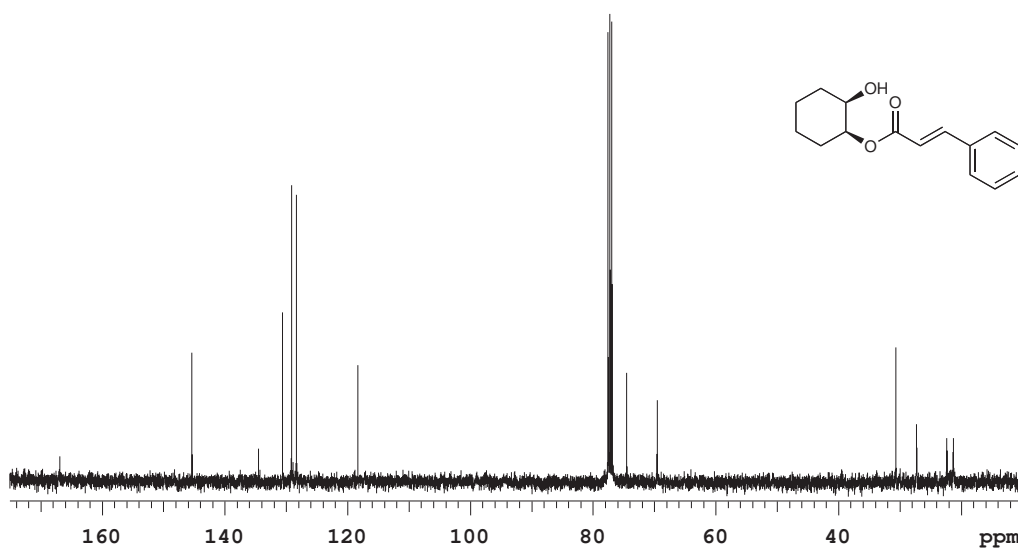
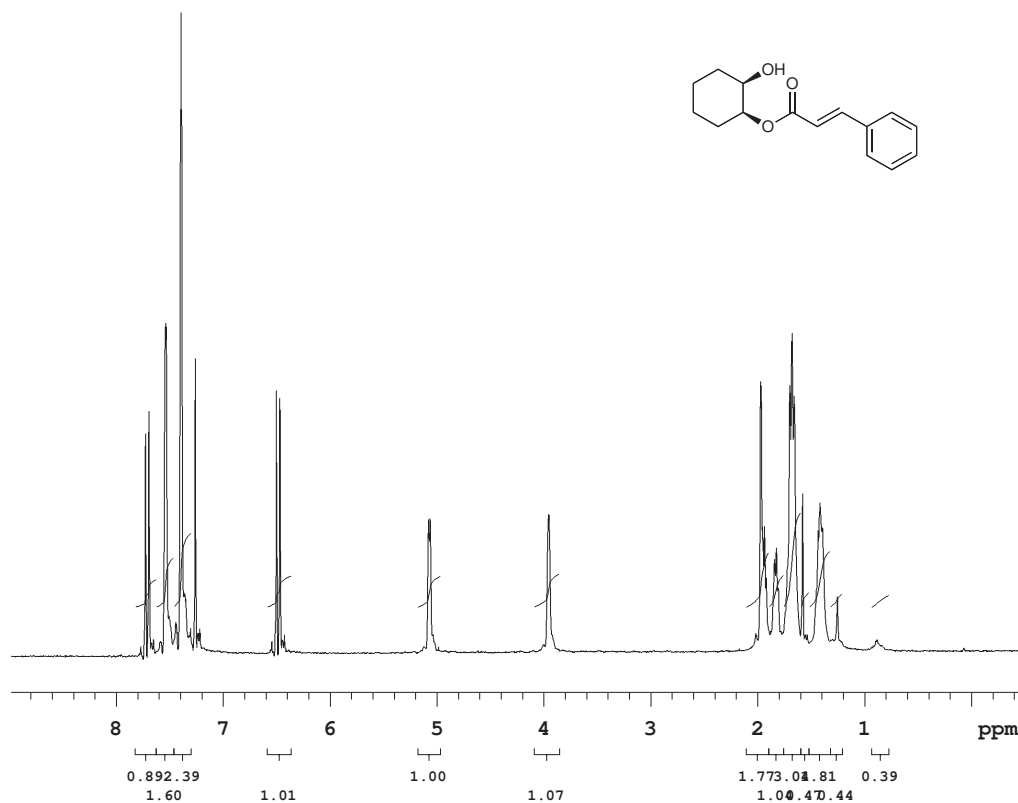








¹H NMR of Cross-over Experiment¹³C NMR of Cross-over Experiment



Chapter 3

Synthesis of Achiral and Chiral Heteroazolium salts as Precursors to *N*-Heterocyclic Carbenes

Portions of this chapter appear in the following publications:

Chan, A.; Scheidt, K. A. "Direct Amination of Homoenolates Catalyzed by *N*-heterocyclic Carbenes," *J. Am. Chem. Soc.* **2008**, *130*, 2740-2741.

Phillips, E. M.; Wadamoto, M.; Chan, A.; Scheidt, K. A. "Highly Enantioselective Intramolecular Michael Reaction Catalyzed by *N*-Heterocyclic Carbenes" *Angew. Chem. Int. Ed.* **2007**, *46*, 3107-3110.

Chan, A.; Scheidt, K. A. "Highly Stereoselective Formal [3+3] Cycloaddition of Enals and Azomethine Imines Catalyzed by *N*-Heterocyclic Carbenes," *J. Am. Chem. Soc.* **2007**, *129*, 5334-5335.

Maki, B. E.; Chan, A.; Phillips, E. M.; Scheidt, K. A. "Tandem Oxidation of Allylic and Benzylic Alcohols to Esters Catalyzed by *N*-Heterocyclic Carbenes," *Org. Lett.* **2007**, *9*, 371-374.

Chapter 3

3.1 Introduction

N-Heterocyclic carbenes (NHCs) have become a notable area of research since the first isolation of a stable carbene derived from an imidazolium salt reported by Arduengo and coworkers in 1991.¹² Over the next 20 years, researchers have synthesized a number of novel heteroazolium salts as NHC precursors that are used as ligands in metal-based catalysis and as organic catalysts in Lewis base catalysis. The promising utility of NHCs as catalysts in a number of different transformations requires straightforward and reliable syntheses from readily available starting materials. This chapter will focus on the syntheses of a variety of novel NHC precursors that were employed as precatalysts in the previous chapters.

The success of a new NHC-catalyzed reaction depends significantly on determining the optimal catalyst. Therefore, it is important to have a large library of heteroazolium salts to examine. The NHC-catalyzed reactions discussed in the previous chapters were successful mainly because the optimal catalyst for each system was determined after screening a number of different heteroazolium salts. The protonation of NHC-generated homoenolates required 1,3-dimethylbenzimidazolium iodide while a benzimidazolium salt with a bulkier substituent such as a mesityl group was necessary for the formal [3+3] cycloaddition between NHC-generated homoenolates and azomethine imines. Conversely, to achieve the amination of NHC-generated homoenolates as well as the NHC-catalyzed hydroacylation of activated ketones, it was essential to employ a triazolium salt as the NHC precursor. The desymmetrization of *meso*-diols required a chiral triazolium salt.

While the NHCs derived from the three classes of heterocycles are closely related, it is important to note that their stability and reactivity differ significantly. These differences in

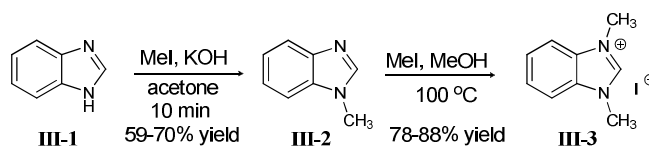
reactivity enable certain carbenes to be more suitable for one type of reaction versus another, and it is still difficult to predict the optimal catalyst for a new reaction. It is still necessary to screen a large number of heteroazolium salts to establish the optimal precatalyst for a new reaction. Therefore, it is imperative to develop general and dependable synthetic routes to access these heteroazolium salts.

3.2 *Synthesis of Benzimidazolium Salts*

3.2.1 *Synthesis of 1, 3-DimethylBenzimidazolium Iodide*

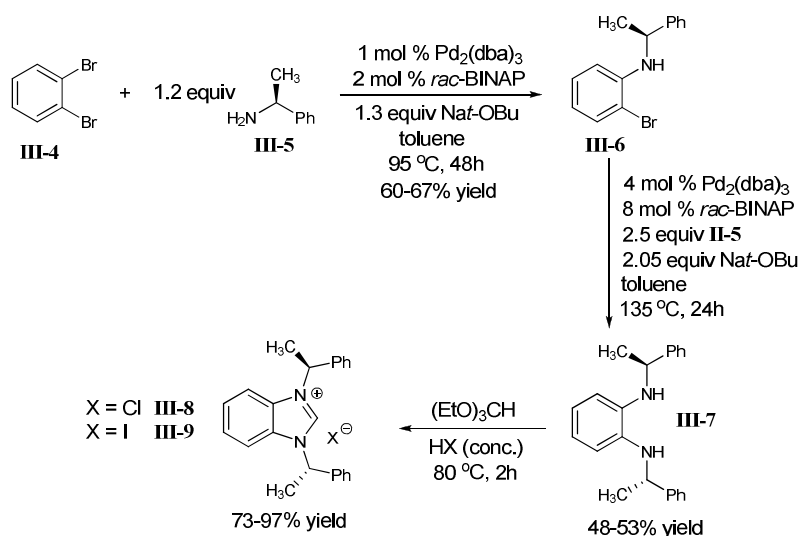
The use of 1,3-dimethylbenzimidazolium iodide (**III-3**) as a precatalyst successfully catalyzes the protonation of NHC-generated homoenolates. The synthesis of **III-3** is straightforward in which benzimidazole **III-1** can be methylated successively with iodomethane (Scheme 3-1). We followed the method developed by Kikugawa to do the initial methylation with iodomethane, which required an excess of KOH in acetone.¹⁹⁴ This method was chosen among others because the reaction provided the desired mono-methylated benzimidazole **III-2** in only 10 minutes. The final bis-methylated benzimidazolium iodide **III-3** was accomplished in a sealed tube with iodomethane in methanol heated to 100 °C.¹⁹⁵

Scheme 3-1. Synthesis of 1, 3-dimethylbenzimidazolium iodide

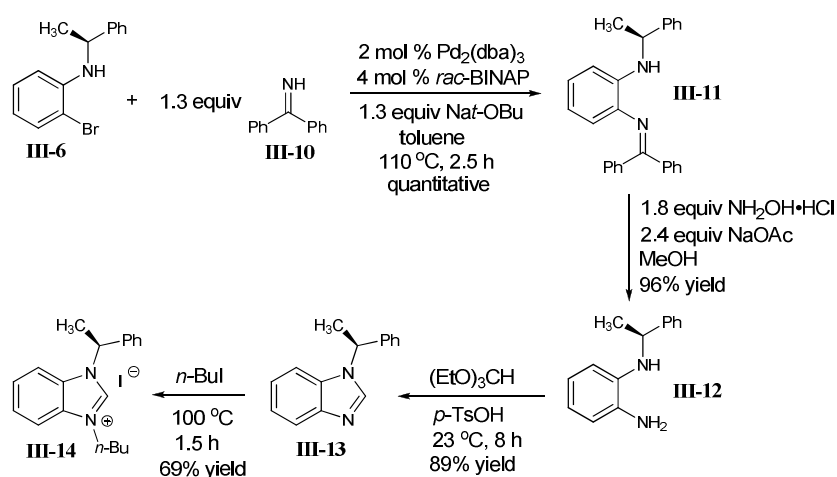


3.2.2 *Synthesis of N,N' -Bis (S)- α -methylbenzyl-benzimidazolium salts and 1-(S)- α -methylbenzyl-2-phenyl-3- n -butyl-benzimidazolium chloride*

The synthesis of N,N' -Bis (S)- α -methylbenzyl-benzimidazolium salts and 1-(S)- α -methylbenzyl-2-phenyl-3- n -butyl-benzimidazolium chloride utilized the method developed by Diver and coworkers (Scheme 3-2).^{65, 66} Mono-aminated product **III-6** could be effected with catalytic $\text{Pd}_2(\text{dba})_3$ and *rac*-BINAP to couple 1,2-dibromo benzene (**III-4**) to α -methyl benzylamine (**III-5**). A second palladium catalyzed coupling event between **III-6** and α -methyl benzylamine can be performed to give bis-aminated product **III-7**. An attempt to synthesize **III-7** in one step using an excess of **III-5** with **III-4** resulted in less than 20% of bis-aminated product **III-7**. Subjecting **III-7** to acidic conditions with triethyl orthoformate provides the chiral benzimidazolium salt with either a chloride (**III-8**) or an iodide (**III-9**) counterion. The yield of the first amination step is moderate because the bis-aminated product (**III-7**) was also recovered in 8-12% yield. Although the yield for the second step was not impressive, the starting material **III-6** could be recovered and recycled to produce more bis-aminated product **III-7**.

Scheme 3-2. Synthesis of (*S*)- α -methylbenzyl substituted benzimidazolium salts

The synthesis of a non- C_2 -symmetric chiral benzimidazolium salt (**III-14**) requires five steps (Scheme 3-3). The sequence begins with the same mono-amination procedure shown in Scheme 3-2 to provide **III-6**. An ammonia equivalent is required to install the second amine, and benzophenone imine was chosen for this purpose. The use of benzophenone imine as an ammonia equivalent was originally reported by Buchwald.¹⁹⁶ Since this report, other ammonia equivalents that are more atom-economical have been developed for palladium-catalyzed aminations.^{197–202} Benzophenone imine **III-10** was coupled to **III-6** via palladium catalysis. The intermediate **III-11** was purified and subjected to transamination using the nucleophile hydroxylamine hydrochloride to provide the respective unprotected aniline **III-12**. Cyclization to the benzimidazole **III-13** proceeded smoothly with triethyl orthoformate and a catalytic amount of TsOH. Introduction of a simple alkyl chain to the nitrogen with butyl iodide provided the salt **III-14** in 69% yield.

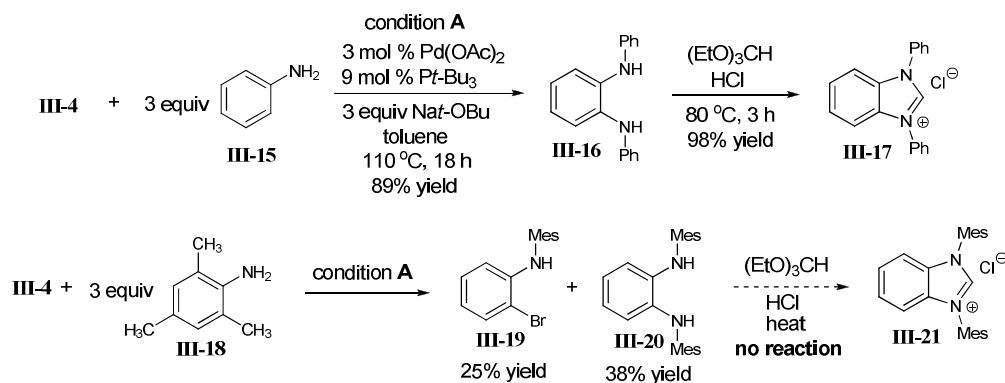
Scheme 3-3. Synthesis of 1-((*S*)-1-phenylethyl)-3-butylbenzimidazolium iodide

3.2.3 Synthesis of 1,3-Diphenylbenzimidazolium iodide and 1-Mesityl-3-Methylbenzimidazolium Iodide Salts

Both 1,3-diphenylbenzimidazolium iodide and 1-mesityl-3-methylbenzimidazolium iodide were synthesized to improve the NHC-catalyzed formal [3+3] cycloaddition reaction between homoenolates and azomethine imines. Synthesis of 1,3-diphenylbenzimidazolium iodide was easily accomplished via a two step synthetic sequence (Scheme 3-4). Using a catalytic amount of palladium acetate and tributyl phosphine as the supporting ligand, the disubstituted product (**III-16**) was isolated as the sole product when adding an excess of aniline **III-15**.²⁰³ Ring closure with triethyl orthoformate, HCl and one drop of formic acid provides **III-17** in excellent yields.²⁰⁴ We applied the same amination strategy towards the synthesis of 1,3-dimesitylbenzimidazole **III-21** and recovered 38% yield of bis-aminated product **III-20** along with 25% of mono-aminated product **III-19**. Switching to *rac*-BINAP as the supporting ligand did not improve the yields (36% yield of **III-19** and 23% yield of **III-20**, not shown). The ring closure to produce salt **III-21** did not yield product even after surveying various conditions. The

reaction was heated in an oil bath and in the microwave with $(\text{EtO})_3\text{CH}$ with different acids and solvents. The observed no reactivity may be attributed to the steric hindrance of the mesityl groups on the nitrogens.

Scheme 3-4. Synthesis of 1,3-diaryl-phenylenediamines

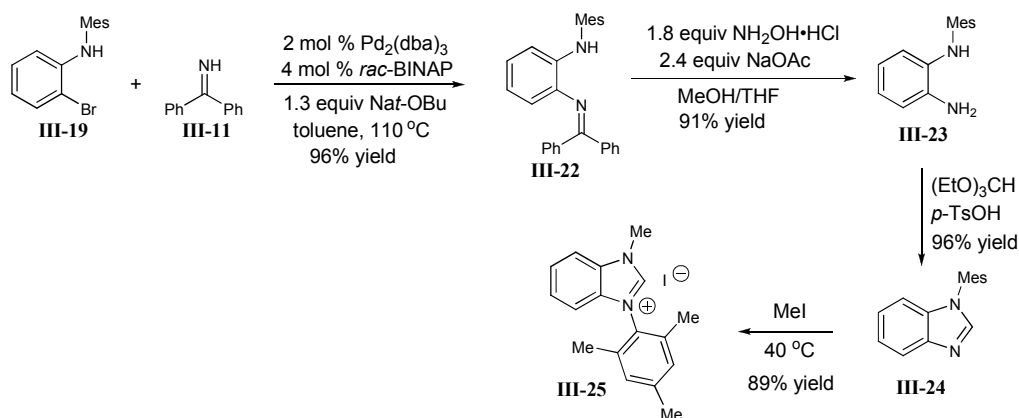


Although we were unsuccessful in making **III-21**, we continued our efforts to synthesize 1-mesityl-3-methylbenzimidazolium iodide **III-25** (Table 3-1). To make this precatalyst, we needed the palladium-catalyzed amination reaction to selectively produce mono-aminated product **III-19** instead of bis-aminated product **III-20**. To achieve this, the amount of amine **III-18** was decreased to 1.2 equivalents, and different ligands were examined. An initial screen with 4 mol % of $\text{Pd}(\text{OAc})_2$ and 12 mol % of Pt-Bu_3 as the ligand resulted in a 1:1 mixture of both products (entry 1). However, by simply switching the ligand to *rac*-BINAP and using double the amount of palladium catalyst, **III-19** was produced in good yields with **III-20** in only trace amounts (entry 2).

Table 3-1. Conditions for selective palladium-catalyzed amination

entry	X	ligand	III-19	III-20
1	4	12 mol % <i>Pt</i> -Bu ₃	36% yield	35% yield
2	8	12 mol % <i>rac</i> -BINAP	88% yield	trace

With a selective method to access **III-19**, we continued to pursue the synthesis of 1-mesityl-3-methylbenzimidazolium iodide **III-25**. Following the same protocol to synthesize **III-14**, amination of **III-19** was performed with benzophenone imine using palladium catalysis; transamination of **III-22** with hydroxylamine hydrochloride provides unprotected aniline **III-23** in good yields. Cyclization to benzimidazole **III-24** proceeded smoothly with triethyl orthoformate and a catalytic amount of TsOH. The final salt (**III-25**) was obtained in an 89% yield upon methylation of **III-24** with iodomethane.

Scheme 3-5. Synthesis of 1-mesityl-3-methylbenzimidazolium iodide

3.3 Synthesis of Triazolium Salts

Another class of heteroazolium salt that is essential to the advancement of NHC catalysis is the triazolium salt. Many triazolium salts are easily accessible from the amino alcohols after four synthetic steps. The amino alcohols used for the synthesis of the triazolium salts are either commercially available or easily accessible. However, certain triazolium salts are derived from amides or lactams. The following section will focus on the successful and failed synthesis of various triazolium salts.

3.3.1 Synthesis of Triazolium Salts Derived from Amino Alcohols

The synthesis of triazolium salts that are derived from amino alcohols requires a method to easily access the amino alcohols. Figure 3-1 shows the amino alcohols that we were interested in, and it was to our favor that compounds **III-26** to **III-28** were commercially available. Amino alcohols **III-29** to **III-31** were derived from the amino acid L-phenylalanine, while amino alcohol **III-32** was derived from camphor.

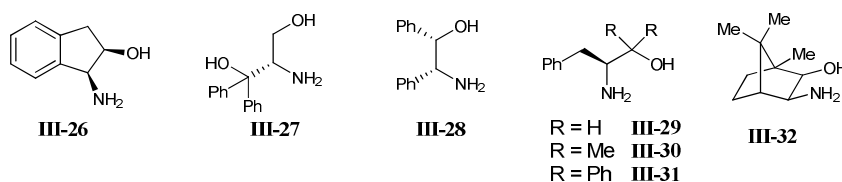
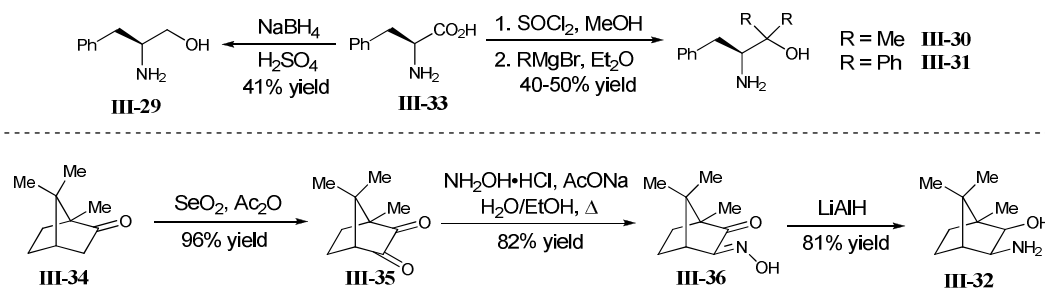


Figure 3-1. Amino alcohols used in the synthesis of triazolium salts

A simple reduction of L-phenylalanine (**III-33**) with NaBH₄ and H₂SO₄ provides the corresponding amino alcohol **III-29** in moderate yields (Scheme 3-6).²⁰⁵ To access **III-30** and **III-31**, the amino acid **III-33** was first esterified by using thionyl chloride and methanol to give the ester·HCl salt in a quantitative yield. Introduction of the geminal dimethyl or geminal

diphenyl substituents to give amino alcohols **III-30** and **III-31**, respectively, was achieved by treatment with excess methyl or phenyl magnesium halide. This method has been shown not to compromise the stereogenic center.²⁰⁶

Scheme 3-6. Synthesis of chiral amino alcohols



The synthesis of the camphor-derived amino alcohol began with treatment of (1*R*)-(+)-camphor (**III-34**) with selenium oxide to give (1*R*)-(+)-camphorquinone (**III-35**) as a yellow solid in high yields.²⁰⁷ The monooximation of **III-35** with a stoichiometric amount of hydroxylamine hydrochloride afforded **III-36** in good yields.²⁰⁸ Reduction of **III-36** was achieved with lithium aluminum hydride to provide the amino alcohol **III-32** in an 81% yield.²⁰⁹

Amino alcohols **III-26**, **III-29** and **III-32** were easily converted to their respective morpholin-3-one after treatment with NaH and ethyl chloroacetate (Table 3-2).²¹⁰ According to the reported procedure by Norman and coworkers, the reaction required 3 hours of heating. Exposure of our amino alcohols to heat resulted in lower yields of the desired product and formation of the side product, morpholin-2-one. However, setting the reaction at 0 °C and slowly increasing the temperature to 23 °C improved the yield of morpholin-3-one while also eliminating side product formation. The method developed by Rovis and coworkers allows easy

access to the triazolium salts from the morpholin-3-one through a one-pot-three-step sequence.²¹¹ Formation of the imidate from the morpholin-3-one and Meerwein's salt in dichloromethane over 12 hours at room temperature followed by addition of the appropriate hydrazine and stirring at room temperature for 2-20 hours gives the hydrazine·HBF₄ salt. Removal of the solvent and heating the red residue in chlorobenzene with triethyl orthoformate for 12 to 20 hours provides NHC precursors **III-38** to **III-43**. The one-pot reaction generally provided moderate yields of the triazoliums salts.

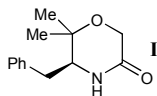
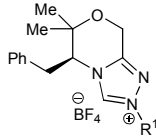
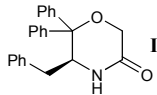
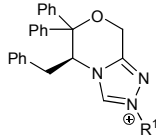
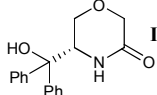
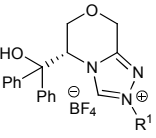
Table 3-2. Synthesis of chiral triazolium salts from amino alcohols

morpholinone	yield (%)	triazolium salt	R ¹	yield (%)
	85		Me III-38 Mes III-39	8 51
	51		Ph III-40 Mes III-41	58 52
	40		Ph III-42 Mes III-43	45 72

Formation of the morpholin-3-one from amino alcohols **III-27**, **III-30** and **III-31** required a modified procedure (Table 3-3). Simply exposing the amino alcohols to ethyl chloroacetate and NaH resulted in no reaction. We decided to synthesize the morpholin-3-one

through a stepwise process in which the amino group was first acylated with chloroacetyl chloride to afford the amide. Under the Finkelstein reaction conditions, halogen exchange with sodium iodide, in acetone provided the alkyl iodide which, readily underwent an intramolecular S_N2 reaction with the tertiary alcohol under basic conditions to give the morpholin-3-one. This three step sequence could be performed in one day and only the last step required purification by flash chromatography. The one-pot-three-step strategy developed by Rovis and coworkers was employed to provide triazolium salts **III-45** to **III-47** in moderate yields, while the stepwise procedure reported by Leeper and coworkers²¹² was used to synthesize **III-44**. It is important to mention that we hypothesized that the geminal disubstituted triazolium salts would provide higher selectivity compared to **III-40** and **III-41**. The geminal disubstitution restricts the rotation of the blocking group (the benzyl group) and projects it into the vicinity of the reaction site.

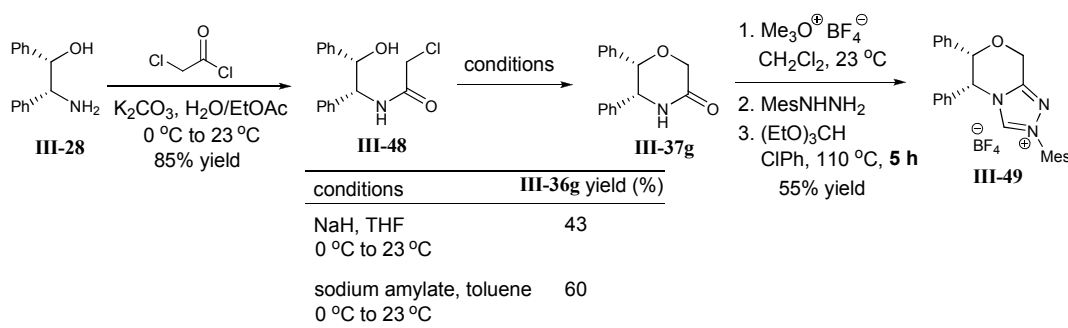
Table 3-3. Synthesis of chiral triazolium salts with modified conditions

$ \begin{array}{c} \text{R} \quad \text{OH} \\ \quad \\ \text{R} \quad \text{CH} \\ \quad \\ \text{R} \quad \text{NH}_2 \end{array} \xrightarrow[\begin{array}{c} \text{2. NaI, acetone} \\ \text{3. NaH, THF} \end{array}]{ \begin{array}{c} \text{1. K}_2\text{CO}_3, \text{H}_2\text{O/EtOAc} \\ \text{Cl}-\text{CH}_2-\text{C}(=\text{O})-\text{Cl} \end{array} } \begin{array}{c} \text{R} \quad \text{O} \\ \quad \\ \text{R} \quad \text{CH} \\ \quad \\ \text{R} \quad \text{NH} \quad \text{C}(=\text{O}) \end{array} \xrightarrow[\begin{array}{c} \text{2. R}^1\text{NHNH}_2 \\ \text{3. (R}^2\text{O)}_3\text{CH} \\ \text{ClPh or MeOH} \\ 110^\circ\text{C} \\ \text{R}^2 = \text{Me or Et} \end{array}]{ \begin{array}{c} \text{1. Me}_3\text{O}^+ \text{BF}_4^- \\ \text{CH}_2\text{Cl}_2, 23^\circ\text{C} \end{array} } \begin{array}{c} \text{R} \quad \text{O} \\ \quad \\ \text{R} \quad \text{CH} \\ \quad \\ \text{R} \quad \text{N} \quad \text{N} \\ \quad \quad \quad \diagup \quad \diagdown \\ \quad \quad \quad \text{N}^+ \quad \text{N}^- \\ \quad \quad \quad \text{BF}_4^- \quad \text{R}^1 \end{array} $				
morpholinone	yield (%)	triazolium salt	R ²	yield (%)
 III-37d	71		Ph III-44	40
			Mes III-45	54
 III-37e	62		Mes III-46	46
 III-37f	65		Mes III-47	32

The synthesis of chiral triazolium salt **III-49** required further modification to develop the synthetic method discussed previously (Scheme 3-7). Acylation of the (1*S*,2*R*)-2-amino-1,2-diphenylethanol (**III-28**) was achieved with chloroacetyl chloride to give the amide product **III-48** in a combined 85% yield after resubjection of the recovered amino alcohol from the first attempt to reaction conditions again. It is important to note that the amino alcohol did not completely dissolve in the reaction but instead formed a cloudy white suspension. Upon formation of the amide product, the reaction became a thick white suspension, and it was isolated by filtration. Resubjection of the filtrate to reactions conditions provided more amide product **III-48**. In the presence of NaH in THF, morpholin-3-one **III-37g** was produced in only a 43% yield along with the formation of an unidentified side product. Halogen exchange of **III-48** with NaI to give the more reactive alkyl iodide did not improve the alkylation reaction to morpholin-3-

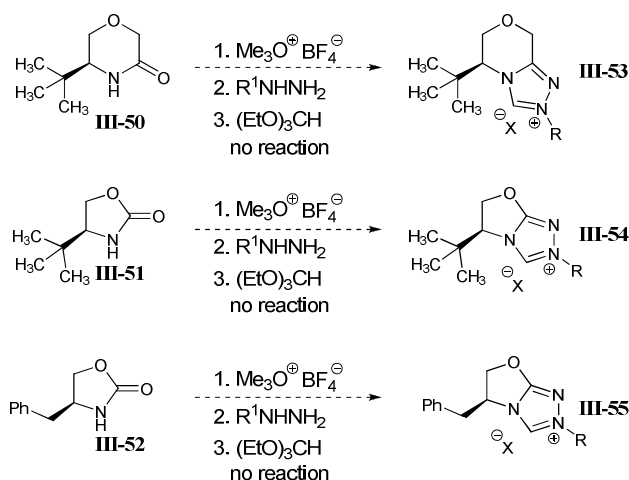
one **III-37g**. By switching to a more sterically hindered base, such as sodium *tert*-pentoxide, resulted in an improved yield (60%) of morpholin-3-one **III-37g**. Finally, the one-pot-three-step sequence to the triazolium salt was examined and was found that as the reaction time of the cyclization step prolonged, the yield of the NHC precursor decreased. Careful monitoring of the reaction by ^1H NMR spectroscopy revealed that the hydrazine·HBF₄ salt decomposed to the morpholin-3-one after allowing the reaction to extend past 5 hours. The optimized conditions begin with the formation of the imidate by stirring morpholin-3-one **III-37g** with Meerwein's salt in dichloromethane for 2-4 hours followed by addition of the mesityl hydrazine to produce the hydrazine·HBF₄ salt in 14-15 hours. After this time, successive treatment of the crude mixture with hexanes and chloroform provides pure hydrazine·HBF₄ salt (see Experimental Section). The red residue was heated in chlorobenzene with triethyl orthoformate. The reaction is complete after 5 hours, and prolonging the reaction only results in decreased yields of **III-49** and increased undesired decomposition. Purification by flash chromatography provides pure chiral triazolium salt **III-49** in a 55% yield.

Scheme 3-7. Synthesis of triazolium salt **III-49**



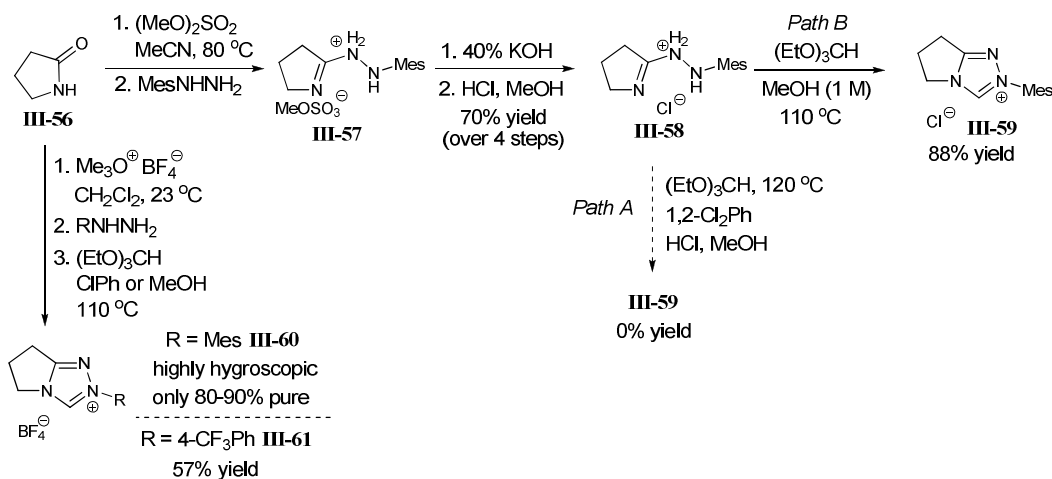
We wanted to apply the developed method towards the synthesis of triazolium salts **III-53** to **III-55** (Scheme 3-8). Morpholin-3-one **III-50** was synthesized by treating *tert*-leucinol with chloroacetyl acetate, and oxazolidin-2-ones **III-51** and **III-52** were synthesized by treating the respective amino alcohols with di-*tert*-butyl dicarbonate.²¹³ Unfortunately, the synthesis of both **III-53** and **III-54** were terminated after the unsuccessful formation of the imidate when morpholin-3-one **III-50** or oxazolidin-2-one **III-51** were exposed to Meerwein's salt. The synthesis of chiral triazolium salt **III-53** failed after attempting to add the hydrazine to the imidate. Further investigations to develop new conditions are necessary. We hypothesized that triazolium salts derived from oxazolidin-2-one instead of morpholin-3-one may provide higher selectivity because the smaller ring size helps project the large side chain closer towards the vicinity of the reaction site.

Scheme 3-8. Attempts to synthesize chiral triazolium salts derived from amino acids

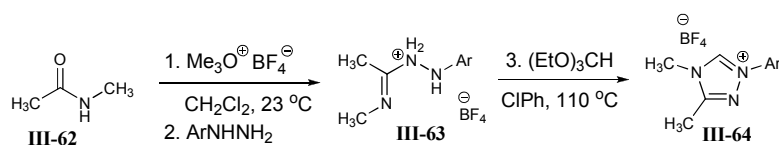


3.3.2 *Synthesis of Triazolium Salts Derived from Lactams or Amides*

We also were interested in synthesizing triazolium salts that are derived from pyrrolidin-2-one **III-56** (Scheme 3-9). Following the procedure reported by Rovis and coworkers,²¹¹ we employed dimethyl sulfate that selectively *O*-alkylated the lactam to the imidate followed by generating the hydrazine salt **III-57** by exposing the imidate to mesityl hydrazine. The salt was neutralized with 40% KOH and then acidified with HCl to give hydrochloric salt **III-58** in a 70% yield. When we continued with the reported procedure (Path A), we found that the cyclization condition with triethyl orthoformate and HCl in 1,2-dichlorobenzene was not applicable towards the synthesis of our triazolium salt **III-59**. Modifications to the reported method were investigated, and we found that simply exposing **III-58** to triethyl orthoformate in MeOH at 110 °C cleanly produces triazolium salt **III-59** in good yields, and no purification was necessary (Path B). We were also interested in making the *N*-mesityl-substituted triazolium salt with the BF₄⁻ counterion **III-60**. Employing the one-pot-three-step sequence²¹¹ previously described above resulted in formation of impure **III-60** as a highly hygroscopic thick brown gel. Purification via flash chromatography only resulted in the decomposition of the NHC precursor. Applying the same procedure to synthesize *N*-(4-trifluoromethyl-phenyl)-substituted triazolium salt **III-61** resulted in a 57% yield of a yellow solid that is air stable. Ring closure was performed in MeOH instead of chlorobenzene.

Scheme 3-9. Synthesis of triazolium salt derived from pyrrolidin-2-one

We also started with *N*-methyl acetamide (**III-62**) to synthesize *N*²-aryl-*N*⁴-methyl-5-methyltriazolium tetrafluoroborates **III-64** (Table 3-4). Application of the one-pot procedure began with *O*-methylation of amide **III-62** with Meerwein's salt to the imidate followed by addition of an aryl hydrazine to produce hydrazine- BF_4 salt **III-63**. Ring closure with triethyl orthoformate in chlorobenzene at 110 °C resulted in the NHC precursor. The one-pot procedure successfully yielded the desired product when the aryl groups were mesityl (**III-64a**), 4-OMePh (**III-64b**) and 4- CF_3Ph (**III-64c**) (entries 1-3). Ring closure was not facilitated with triethyl orthoformate when the aryl substituents were sterically hindered (entries 4-7). Additionally, the unsuccessful ring closure may also be explained by the decreased nucleophilicity of the nitrogens because of the electron-withdrawing substituted aryl group. Additionally, the electron-poor substituents on the aryl groups may contribute to the decreased nucleophilicity of the nitrogens to undergo ring closure with $(\text{EtO})_3\text{CH}$.

Table 3-4. Synthesis of triazolium salts derived from *N*-methyl acetamide

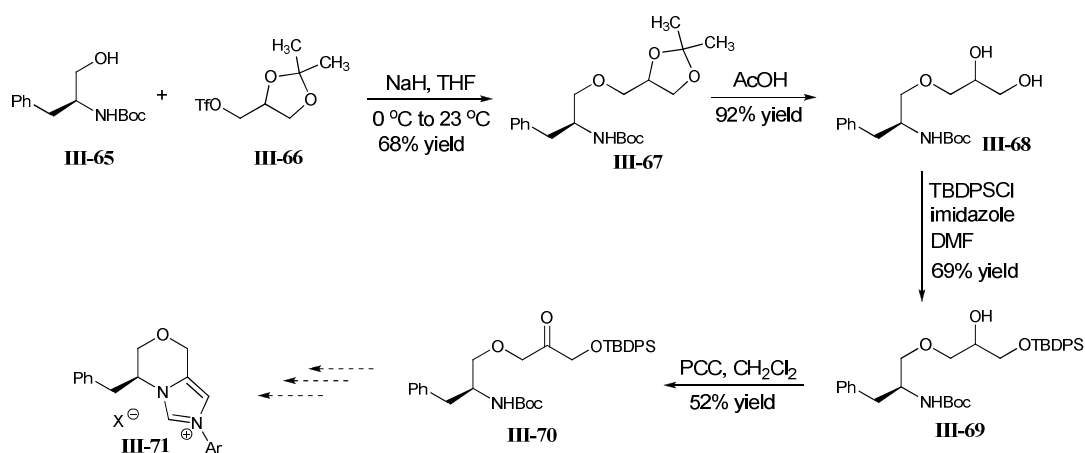
entry	Ar		yield (%)
1	Mes	III-64a	46
2	4-OMePh	III-64b	39
3	4-CF ₃ Ph	III-64c	22
4	2,4,6-Cl ₃ Ph	III-64d	0
5	2-CF ₃ Ph	III-64e	0
6	2,6-Cl ₂ Ph	III-64f	0
7	C ₆ F ₅	III-64g	0

Although the syntheses of triazolium salts **III-64a-c** utilized the same one-pot-three-step conditions as previously reported, the method of purification was modified. The isolation of these new triazolium salts was considerably more challenging than the amino alcohol derived triazolium salts. Upon completion of the last cyclization step, the solvent was removed, and the crude material was purified via flash chromatography (50-100% EtOAc/hexanes then 10% MeOH/ CH_2Cl_2). The initial flush with 50-100% EtOAc/hexanes removes the less polar by-products, while the desired salts were collected as light brown oils or foams upon switching the eluent to 5% MeOH/ CH_2Cl_2 . The triazolium salts **III-63a-c** were isolated as light tan solids upon trituration of the chromatographed light brown oil or foam with a mixture of 3:6.5:0.5 $\text{CH}_2\text{Cl}_2/\text{Et}_2\text{O}/\text{toluene}$.

3.4 Synthesis of Chiral Imidazolium Salts

It is important to produce a library of both chiral imidazolium and triazolium salts since both classes of heterocyclic salts usually behave differently under the same reaction conditions. Synthesis of a chiral imidazolium salt is more challenging compared to the synthesis of a triazolium salt. We attempted to synthesize chiral imidazolium salts derived from amino alcohols (Scheme 3-10). The synthesis commenced with *O*-alkylation of the Boc-protected L-phenylalaninol (**III-65**) with isopropylidenglycerol triflate (**III-66**) followed by deprotection of acetal **III-67** under acetic acid conditions to yield diol **III-68**. Selective protection of the primary alcohol with *tert*-butyldiphenylsilyl chloride provides **III-69**. The secondary alcohol of **III-69** is oxidized to ketone **III-70** with PCC. Deprotection of the amine is necessary to facilitate the imine formation between the free amine and the ketone. Attempts to deprotect and catalyze the imine formation with TFA resulted in decomposition of the starting material. Further investigation is necessary to complete the synthesis of **III-71**.

Scheme 3-10. Synthesis of chiral imidazolium salt



3.5 *Summary*

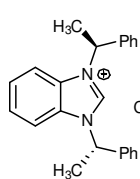
The syntheses of a number of novel catalysts were presented in this last chapter. Although the methods used to synthesize the catalysts were similar, each catalyst required certain modifications to the synthesis or the isolation to successfully produce a new heteroazolium salt. A good synthetic chemist needs to be meticulous and observant to realize the alterations that are necessary for each new catalyst. The ability to access a large number of catalysts has a great impact on the success of the NHC catalysis program in the Scheidt group.

3.6 *Experimental*

General Information. All reactions were carried out under a nitrogen atmosphere in flame-dried glassware with magnetic stirring. THF, Et₂O, CH₂Cl₂, DMF and toluene were purified by passage through a bed of activated alumina.¹³² Reagents were purified prior to use unless otherwise stated following the guidelines of Perrin and Armarego.¹³³ Purification of reaction products was carried out by flask chromatography using EM Reagent silica gel 60 (230-400 mesh). Analytical thin layer chromatography was performed on EM Reagent 0.25 mm silica gel 60-F plates. Visualization was accomplished with UV light and anisaldehyde, ceric ammonium nitrate stain, potassium permanganate, or phosphomolybic acid followed by heating. Melting points were obtained on a Thomas Hoover capillary melting point apparatus and are uncorrected. Infrared spectra (**IR**) were obtained on a Bio-Rad FTS-40 FTIR spectrophotometer. ¹H-NMR spectra were recorded on a Varian Inova 500 (500 MHz) or Mercury 400 (400 MHz) spectrometer and are reported in ppm using solvent as an internal standard (CDCl₃ at 7.26). Data are reported as (ap = apparent, s = singlet, d = doublet, t = triplet, q = quartet, m = multiplet, b = broad; coupling constant(s) in Hz, integration. Proton-decoupled ¹³C-NMR spectra were recorded on a Varian Inova 500 (125 MHz) or Mercury 400 (100 MHz) spectrometer and are reported in ppm using solvent as an internal standard (CDCl₃ at 77.0 ppm). Electrospray mass spectra (ESI-MS) were obtained using a Micromass Quattro II Triple Quadrupole HPLC/MS/MS Mass Spectrometer.

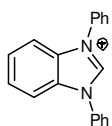
3.6.1 Synthesis of Benzimidazolium Salts **III-8**, **III-9**, **III-14**, **III-17**

The method used to synthesize *N*1,*N*3-Bis (*S*)- α -methylbenzyl-benzimidazolium chloride **III-8**, *N*1,*N*3-Bis (*S*)- α -methylbenzyl-benzimidazolium chloride **III-9**, and 1-[(*S*)-1-phenylethyl]-3-butyl-1*H*-benzimidazolium iodide **III-14** was reported by Diver and coworkers.^{65, 66} The procedure employed to synthesize *N*1,*N*3-diphenylbenzimidazolium chloride **III-17** was reported by Harlan and coworkers²⁰³ and Zou and coworkers.²⁰⁴



***N*1,*N*3-Bis(*S*)- α -methylbenzyl-benzimidazolium chloride (**III-8**):** Isolated a white solid. ¹H NMR (500 MHz, CDCl₃) δ 12.41 (s, 1H); 7.52 (d, *J* = 7.3 Hz, 4H); 7.47-7.28 (m, 10H); 6.28 (q, *J* = 6.8 Hz, 2H); 2.30 (d, *J* = 7.3 Hz, 6H); ¹³C

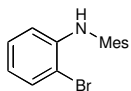
NMR (125 MHz, CDCl₃) δ 142.4, 137.9, 131.3, 129.7, 129.3, 126.9, 126.6, 114.7, 59.4, 21.2.



***N*1,*N*3-diphenylbenzimidazolium chloride (**III-17**):** Isolated a white solid. ¹H

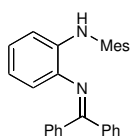
NMR (500 MHz, CDCl₃) δ 11.26 (s, 1H); 8.10 (d, *J* = 6.8 Hz, 4H); 7.81-7.79 (m, 2H); 7.72-7.62 (m, 6H); 7.35-7.29 (m, 2H); ¹³C NMR (125 MHz, CDCl₃) δ 141.9, 132.9, 131.7, 131.1, 130.8, 128.4, 125.6, 114.1.

3.6.1.1 Synthesis of *N*1-Mesityl-*N*3-Methylbenzimidazolium Iodide Salt (**III-25**)



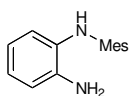
***N*-(2-bromophenyl)-2,4,6-trimethylbenzenamine (**III-19**):** To a flame-dried 50 ml Schlenk flask equipped with a stirbar was added Pd(OAc)₂ (149 mg, 0.714 mmol), *rac*-BINAP (620 mg, 0.995 mmol) and toluene (16.5 mL). It was heated to 60 °C and an orange suspension resulted. Into it was then added 1,2-dibromobenzene (1.96 g, 8.29 mmol), 2,4,6-trimethylaniline (1.35 g, 9.95 mmol) and NaOtBu (620 mg, 10.78 mmol). The reaction

was allowed to reflux at 110 °C with a condenser attached and stirred vigorously until reaction was complete as judged by TLC (10% CH₂Cl₂/hexanes). The reaction was filtered through a pad of celite and rinsed with ethyl acetate (50 mL). Solvent was removed and purified via flash chromatography 0-5% CH₂Cl₂/hexanes. Isolated a white solid (1.99 g, 83% yield). R_f =0.83 (10% CH₂Cl₂/hexanes); ¹H NMR (500 MHz, CDCl₃) δ 7.47 (d, J = 7.9 Hz, 1H); 7.01 (t, J = 7.6 Hz, 1H); 6.58 (t, J = 7.6 Hz, 1H); 6.14 (d, J = 7.9 Hz, 1H); 5.61 (s, 1H); 2.31 (s, 6H); 2.15 (s, 6H).



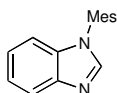
***N*¹-mesityl-*N*²-(diphenylmethylene)benzene-1,2-diamine (III-22):** To a flame-dried 50 ml Schlenk flask equipped with a stirbar was added Pd₂(dba)₃ (68 mg, 0.0737 mmol), *rac*-BINAP (92 mg, 0.147 mmol) and toluene (15 mL). It was

heated to 110 °C with condenser attached for 30 minutes and cooled to room temperature. Into it was then added **III-19** (1.07 g, 3.69 mmol), benzophenone imine (869 mg, 4.79 mmol) and NaO*t*Bu (461 mg, 4.79 mmol). The reaction was allowed to reflux at 110 °C until reaction was complete as judged by TLC (10% CH₂Cl₂/hexanes). The reaction was filtered through a pad of celite and rinsed with ethyl acetate (50 mL). Solvent was removed and purified via flash chromatography 15-30% CH₂Cl₂/hexanes. Isolated a yellow solid (1.38 g, 96% yield). R_f =0.31 (10% CH₂Cl₂/hexanes); ¹H NMR (500 MHz, CDCl₃) δ 7.84 (d, J = 7.5 Hz, 2H); 7.49-7.40 (m, 3H); 7.34 (m, 3H); 7.26 (m, 2H); 6.94 (s, 2H); 6.73 (t, J = 7.5 Hz, 1H); 6.35 (t, J = 7.5 Hz, 1H); 6.23 (d, J = 7.5 Hz, 1H); 6.13 (d, J = 7.9 Hz, 1H); 5.88 (s, 2H); 2.30 (s, 3H); 2.24 (s, 6H).



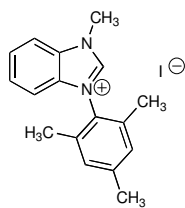
***N*¹-mesitylbenzene-1,2-diamine (III-23):** To a flame-dried 100 ml round bottom

flask equipped with a stirbar was added **III-22** (1.35 g, 3.46 mmol) and dissolved in THF (22 mL) and MeOH (22 mL). Into it was then added NaOAc (681 mg, 8.30 mmol) and NH₂OH·HCl (433 mg, 6.22 mmol). The cloudy orange solution was stirred at room temperature until the reaction was complete as judged by TLC. After 13 h, the light yellow solution was diluted by ethyl acetate and washed with 0.1 N NaOH (2 x 40 mL). Aqueous layer was extracted with ethyl acetate (2 x 30 mL). All organics were dried with Na₂SO₄, filtered and solvent removed. Reaction was purified via flash chromatography 15-30% Et₂O/hexanes. Isolated a tan solid (708 mg, 91% yield). *R_f*=0.29 (25% Et₂O/hexanes); ¹H NMR (500 MHz, CDCl₃) δ 6.92 (s, 2H); 6.79-6.72 (m, 2H); 6.64 (t, *J* = 7.6 Hz, 1H); 6.23 (d, *J* = 7.9 Hz, 1H); 4.76 (s, b, 1H); 3.61 (s, b, 1H); 2.30 (s, 3H); 2.12 (s, 6H).



1-mesityl-1H-benzo[d]imidazole (III-24): To a flame-dried 200 ml round bottom

flask equipped with a stirbar was added **III-23** (1.27g, 5.61 mmol) and dissolved in (EtO)₃CH (61 mL). Into it was added *p*TsOH (107 mg, 0.561 mmol) and the orange solution was stirred at room temperature until the reaction was complete as judged by TLC. After 14 h, the orange solution was diluted with EtOAc and washed with saturated NaHCO₃ (2 x 50 mL). The aqueous layer was extracted with ethyl acetate (2 x 30 mL). The organics were dried with Na₂SO₄, filtered and removed solvent. The reaction was purified via flash chromatography 5% MeOH/CH₂Cl₂. Isolated an orange oil (1.32 g, 99% yield). *R_f*=0.45 (5% MeOH/CH₂Cl₂); ¹H NMR (500 MHz, CDCl₃) δ 7.89 (d, *J* = 7.9 Hz, 1H); 7.86 (s, 1H); 7.34-7.25 (m, 2H); 7.05-7.02 (m, 3H); 2.39 (s, 3H); 1.92 (s, 6H).



***N*¹-mesityl-*N*³-methylbenzimidazolium Iodide (III-25):** Into a flame-dried 50

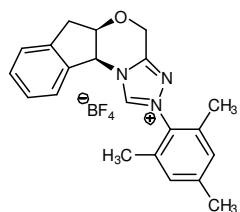
mL round bottom flask equipped with a stirbar was added **III-24** (1.31 g, 5.54 mmol) and MeI (22 mL, 0.25 M). Heat to 40 °C with a condenser attached.

After 16 h, reaction was complete as judged by TLC. Excess MeI was removed

via vacuo and solid was washed with ether and filtered to give pure product; yielding 1.91 g (91%) of **III-25** as a tan solid. Mp: 266-269 °C; IR (film) 3018.1, 2947.8, 1610.2, 1560.3, 1260.7, 753.8, 731.9 cm⁻¹; ¹H NMR (400 MHz, CDCl₃) δ 10.75 (s, 1H); 7.90 (d, *J* = 8.2 Hz, 1H); 7.72 (t, *J* = 7.6 Hz, 1H); 7.62 (t, *J* = 7.6, 1H); 7.23 (t, *J* = 8.2 Hz, 1H); 7.06 (s, 2H); 4.54 (s, 3H); 2.37 (s, 3H); 2.02 (s, 6H); ¹³C NMR (100 MHz, CDCl₃) δ 142.6, 141.9, 135.5, 132.0, 131.4, 130.3, 128.2, 127.9, 127.8, 113.5, 113.3, 35.2, 21.3, 18.2; LRMS (electrospray): Mass calculated for C₁₇H₁₉IN₂ [2M – 126.9]⁺, 629.6. Found 629.1.

3.6.2 Synthesis of Chiral Triazolium Salts Derived from Amino Alcohols

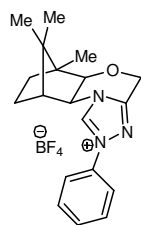
The methods used to synthesize chiral triazolium salts derived from amino alcohols have been reported in literature. The L-phenylalanine was converted to the amino alcohols (**III-29** to **III-31**) following the procedure reported by Masamune and coworkers²⁰⁵ and Davies and coworkers.²⁰⁶ The camphor-derived amino alcohol (**III-32**) was synthesized according to method reported by the laboratories of Lu,²⁰⁷ Hénin,²⁰⁸ and Gawley.²⁰⁹ The procedure followed to convert the amino alcohols to the morpholin-3-ones was reported by Norman and coworkers.²¹⁰ The morpholin-3-ones were subjected to the three-step-one-pot procedure developed by Rovis and coworkers²¹¹ or the stepwise procedure reported by Leeper and coworkers²¹² to produce the triazolium salts. Any modifications to the reported procedures are mentioned below.



***N*²-Mesityl-4*H*,6*H*-indeno[2,1-*b*][1,2,4]triazole[4,3-*d*][1,4]oxazinium**

tetrafluoroborate (III-39): Procedure began with the morpholin-3-one **III-37a** (1.0 g, 5.29 mmol) and is analogous to the method reported by Rovis and

coworkers.²¹¹ Isolated 1.13 mg (52% yield) of **III-39** as an off-white powder. ¹H NMR (500 MHz, CDCl₃) δ 10.22 (s, 1H); 7.45-7.29 (m, 4H); 6.99 (s, 2H); 6.08 (m, 1H); 5.08-5.03 (m, 3H); 3.18-3.14 (m, 2H); 2.38 (s, 3H); 2.05 (s, 6H); ¹H NMR (500 MHz, DMSO-*d*₆) δ 11.14 (s, 1H); 7.62 (d, *J* = 7.8 Hz, 1H); 7.46-7.31 (m, 3H); 7.22 (s, 2H); 6.10 (s, 1H); 5.27 (d, *J* = 16.1 Hz, 1H); 5.08 (d, *J* = 16.1 Hz, 1H); 4.99 (t, *J* = 4.4 Hz, 1H); 3.50 (dd, *J* = 17.1, 4.9 Hz, 1H); 3.18 (d, *J* = 17.1 Hz, 1H); 2.38 (s, 3H); 2.12 (s, 6H).

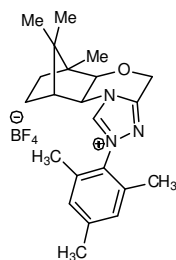


***N*²-Phenyl-(1,7,7-trimethylbicyclo[2.2.1])- [1,2,4]-triazolo[3,4-*c*][1,4] oxazinium**

tetrafluoroborate (III-42): Procedure began with the morpholin-3-one **III-37c**

(215 mg, 1.03 mmol) and is analogous to the method reported by Rovis and

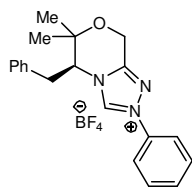
coworkers.²¹¹ Isolated 183 mg (45% yield) of **III-42** as a white solid. ¹H NMR (500 MHz, CDCl₃) δ 10.26 (s, 1H); 7.88-7.86 (m, 2H); 7.51-7.46 (m, 3H); 5.03 (d, *J* = 15.1 Hz, 1H); 4.70 (d, *J* = 15.1 Hz, 1H); 4.46 (d, *J* = 6.8 Hz, 1H); 4.07 (d, *J* = 6.8 Hz, 1H); 2.66 (d, *J* = 4.4 Hz, 1H); 1.86-1.81 (m, 1H); 1.61-1.56 (m, 1H); 1.26-1.19 (m, 2H); 1.00 (s, 3H); 0.98-0.90 (m, 1H); 0.86 (s, 3H); 0.66 (s, 3H); ¹³C NMR (125 MHz, CDCl₃) δ 151.5, 135.2, 130.9, 130.4, 120.9, 84.1, 61.1, 58.9, 50.3, 49.9, 48.5, 32.7, 31.2, 25.7, 21.4, 20.5, 11.3.



***N*²-Mesityl-(1,7,7-trimethylbicyclo[2.2.1]-[1,2,4]-triazolo[3,4-*c*][1,4]**

oxazin-5-ium tetrafluoroborate (III-43): Procedure began with the morpholin-3-one **III-37c** (200 mg, 0.956 mmol) and is analogous to the method reported by Rovis and coworkers.²¹¹ Isolated 302 mg (72% yield) of **III-43** as a white solid.

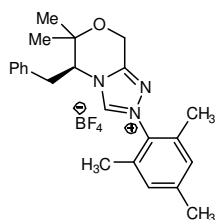
¹H NMR (500 MHz, CDCl₃) δ 9.78 (s, 1H); 6.99 (s, 2H); 5.02 (d, *J* = 14.6 Hz, 1H); 4.72 (d, *J* = 15.1 Hz, 1H); 4.56 (d, *J* = 6.8 Hz, 1H); 4.12 (d, *J* = 7.3 Hz, 1H); 2.64 (d, *J* = 3.9 Hz, 1H); 2.36 (s, 3H); 2.01 (s, 6H); 1.97-1.83 (m, 1H); 1.64-1.59 (m, 1H); 1.29-1.21 (m, 2H); 1.02 (s, 3H); 1.00-0.98 (m, 1H); 0.88 (s, 3H); 0.67 (s, 3H); ¹³C NMR (125 MHz, CDCl₃) δ 151.4, 142.1, 131.3, 129.9, 99.9, 84.3, 61.0, 58.9, 50.4, 49.9, 48.5, 32.9, 25.6, 21.5, 21.4, 20.8, 20.4, 17.2, 11.3.



***N*²-Phenyl-(*S*)-5-benzyl-6,8-dihydro-6,6-dimethyl-5H-[1,2,4]-triazolo [3,4-*c*][1,4]oxazin-5-ium tetrafluoroborate (III-44):** Procedure began with the

morpholin-3-one **III-37d** (445 mg, 2.03 mmol) and is analogous to the method

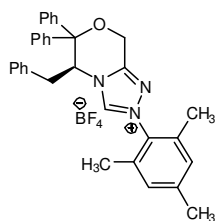
reported by Leeper and coworker²¹² with minor modifications. The reported procedure was modified to provide the tetrafluoroborate counterion by using triethylamine to neutralize the hydrazine·HCl intermediate followed by cyclization to the triazolium salt **III-44** with HBF₄ (54 wt% in Et₂O, 1 equiv) and (MeO)₃CH in methanol. The cyclization reaction was performed in a 25 mL round bottom flask instead of a sealed tube. Isolated 305 mg (40% yield) of **III-44** as a yellow solid. ¹H NMR (500 MHz, CDCl₃) δ 8.50 (s, 1H); 7.50-7.45 (m, 5H); 7.35-7.27 (m, 2H); 7.10 (d, *J* = 7.33 Hz, 2H); 5.20 (d, *J* = 17.1 Hz, 1H); 5.03-4.99 (m, 2H); 3.47-3.43 (m, 1H); 2.96-2.91 (m, 1H); 1.57 (s, 3H); 1.46 (s, 3H); ¹³C NMR (125 MHz, CDCl₃) δ 148.8, 139.7, 135.1, 134.6, 131.3, 130.5, 130.0, 129.9, 128.5, 120.9, 74.1, 64.1, 56.9, 37.2, 25.0, 22.5.



***N*²-Mesityl-(*S*)-5-benzyl-6,8-dihydro-6,6-dimethyl-5*H*-[1,2,4]-triazolo**

[3,4-*c*][1,4]oxazin-4-ium tetrafluoroborate (III-45): Procedure began with the morpholin-3-one **III-37d** (200 mg, 0.912 mmol) and is analogous to the

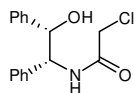
method reported by Rovis and coworkers²¹¹ with minor modifications. The reported procedure was modified by heating the first two steps at 40 °C and each of the three steps were allowed to react for 14-18 h. Isolated 221 mg (54% yield) of **III-45** as a light tan solid. ¹H NMR (500 MHz, CDCl₃) δ 8.43 (s, 1H); 7.35-7.31 (m, 2H); 7.26-7.21 (m, 3H); 6.91 (s, 2H); 5.31-5.28 (m, 1H); 5.22 (d, *J* = 17.6 Hz, 2H); 5.06 (d, *J* = 17.1 Hz, 1H); 3.54-3.51 (m, 1H); 2.98-2.92 (m, 1H); 2.30 (s, 3H); 1.81 (s, 6H); 1.60 (s, 3H); 1.48 (s, 3H); ¹³C NMR (125 MHz, CDCl₃) δ 148.9, 144.0, 142.5, 135.0, 134.7, 130.8, 129.8, 129.5, 129.4, 128.4, 74.3, 63.4, 57.1, 37.1, 25.2, 22.3, 21.4, 17.2.



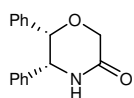
***N*²-Mesityl-(*S*)-5-benzyl-6,8-dihydro-6,6-diphenyl-5*H*-[1,2,4]-triazolo [3,4-*c*][1,4]oxazin-4-ium tetrafluoroborate (III-46):** Procedure began with the

morpholin-3-one **III-37e** (1.25 g, 3.6 mmol) and is analogous to the method reported by Rovis and coworkers.²¹¹ Isolated 1.58 g (77% yield) of **III-46** as a white solid. ¹H NMR (500 MHz, CDCl₃) δ 8.98 (s, 1H); 7.59 (d, *J* = 7.3 Hz, 3H); 7.44-7.19 (m, 12H); 6.89 (s, 2H); 6.49-6.46 (m, 1H); 5.39 (d, *J* = 17.6 Hz, 1H); 4.88 (d, *J* = 17.1 Hz, 1H); 2.99-2.92 (m, 2H); 2.29 (s, 3H); 1.73 (s, 6H); ¹³C NMR (125 MHz, CDCl₃) δ 149.1, 143.6, 142.6, 140.4, 137.2, 134.5, 130.7, 130.1, 129.8, 129.3, 129.2, 128.4, 128.3, 127.6, 127.4, 125.3, 82.1, 69.6, 60.7, 57.9, 37.6, 21.4, 17.0.

3.6.2.1 Synthesis of *N*²-Mesityl-(5*R*, 6*S*)-6,8-dihydro-5,6-diphenyl-5*H*-[1,2,4]triazole-[3,4-*c*][1,4] oxazine tetrafluoroborate (III-48**):**



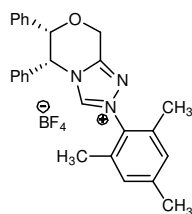
2-Chloro-*N*-((1*R*,2*S*)-2-hydroxy-1,2-diphenylethyl)acetamide (III-48**):** To a flame-dried 200 ml round bottom flask equipped with a stirbar was added K₂CO₃ (5.0 g, 36 mmol) and dissolved in H₂O (51 mL, 0.33 M) and EtOAc (51 mL, 0.33 M). Into the solution was added (1*S*,2*R*)-2-amino-1,2-diphenylethanol **III-28** (3.5 g, 16.4 mmol) and the cloudy white suspension was cooled to 0 °C and the chloroacetyl chloride (3.6 mL, 45.6 mmol) was added dropwise over 10 minutes. After 15 minutes, the white suspension was warmed to room temperature. After 4.5 h, the white solid was filtered, washed with EtOAc and dried under high vacuum to give pure **III-48**. The filtrate was extracted with EtOAc and the organic layer was washed with H₂O (1 x 20 mL) and NaHCO₃ (1 x 20 mL). All organics were dried with Na₂SO₄, filtered and solvent removed. Resubject the filtrate to reaction conditions and additional product was isolated. Isolated **III-48** as a white solid (4.0 g, 85% yield). ¹H NMR (500 MHz, CDCl₃) δ 7.30-7.24 (m, 6H); 7.06-7.03 (m, 4H); 5.28 (dd, *J* = 8.3, 3.9 Hz, 1H); 5.12 (d, *J* = 3.9 Hz, 1H); 4.07 (q, *J* = 15.6 Hz, 1H).



(5*R*,6*S*)-5,6-diphenylmorpholin-3-one (III-37g**):** To a flame-dried 250 ml round bottom flask equipped with a stirbar was added **III-48** (3.95 g, 13.7 mmol) and toluene (137 mL, 0.1 M). The white suspension was cooled to 0 °C and sodium pentoxide (1.8 g, 16.4 mmol) was added. After 15 min, the reaction was allowed to warm to room temperature. After 14 hr, reaction was complete as judged by TLC. Dilute reaction with EtOAc, wash with water (2 x 50 mL) and brine (1 x 50 mL). All organics were dried with Na₂SO₄, filtered and solvent removed. The reaction was purified via flash chromatography, 50-70% EtOAc/hexanes.

$R_f = 0.20$ (50% ethyl acetate/hexanes). Isolated **III-37g** as a white solid (2.1 g, 60% yield).

^1H NMR (500 MHz, CDCl_3) δ 7.20-7.12 (m, 6H); 6.91-6.86 (m, 4H); 6.35 (s, b, 1H); 5.17 (d, $J = 3.4$ Hz, 1H); 4.69-4.64 (m, 2H); 4.51 (d, $J = 17.1$ Hz, 1H).



N^2 -Mesityl-(5*R*, 6*S*)-6,8-dihydro-5,6-diphenyl-5H-[1,2,4]triazolo[3,4-*c*][1,4]

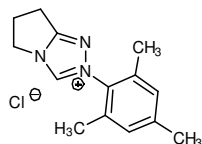
oxazin-2-ium tetrafluoroborate (III-49): Procedure began with the morpholin-3-one **III-37g** (325 mg, 1.28 mmol) and is analogous to the method reported by

Rovis and coworkers²¹¹ with minor modifications. Treatment of **III-37g** with

Meerwein's salt (209 mg, 1.41 mmol) to produce the imidate was complete after 4 h and the mesityl hydrazine (213 mg, 1.41 mmol) was added. The reaction was stirred at room temperature until reaction was complete as judged by ^1H NMR spectroscopy. After 14 h, the reaction was complete and hexanes (75 mL) and precipitate formed. The red/orange solid was isolated via filtration and dissolved in CHCl_3 (50 mL). The cloudy suspension was re-filtered to remove a white solid impurity. The filtrate was concentrated and placed under high vacuum for 1h. The red residue was dissolved in chlorobenzene (6.4 mL, 0.2 M) and $(\text{EtO})_3\text{CH}$ (1.1 mL, 6.4 mmol) was added. The reaction was heated to 110 °C and monitored via ^1H NMR spectroscopy. After 5 h, reaction was complete. Cool reaction to room temperature and remove solvent. The reaction was purified via flash chromatography, 50%, 75% and 100% EtOAc/hexanes. $R_f = 0.60$ (100% ethyl acetate). Isolated 339 mg (55% yield) of **III-49** as a fluffy yellow solid. ^1H NMR (500 MHz, CDCl_3) δ 9.35 (s, 1H); 7.24-7.11 (m, 8H); 6.99 (d, $J = 7.3$ Hz, 2H); 6.88 (d, $J = 7.33$ Hz, 2H); 6.36 (d, $J = 3.4$ Hz, 1H); 5.80 (d, $J = 3.4$, 1H); 5.69 (d, $J = 16.1$ Hz, 1H); 5.39 (d, $J = 16.6$ Hz, 1H); 2.36 (s, 3H); 2.04 (s, 6H); ^{13}C NMR (125 MHz, CDCl_3) δ 150.4, 143.9, 142.6, 134.8, 133.9, 131.2, 130.0, 129.6, 128.8, 128.6, 128.4, 128.1, 126.2, 78.7, 63.3, 62.9, 21.5, 17.4.

3.6.3 Synthesis of Triazolium Salts Derived from Lactams and Amides

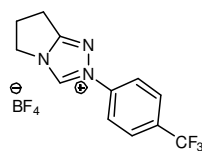
***N*²-Mesityl-6,7-dihydro-5*H*-pyrrolotriazolium chloride (III-59):** Procedure



began with pyrrolidin-2-one and synthesis of the hydrazine·HCl salt (**III-58**) is analogous to the method reported by Rovis and coworkers.²¹¹ Upon isolation of

the hydrazine·HCl salt **III-58**, the salt (400 mg, 1.58 mmol) was dissolved in 800 μ L of MeOH (2 M) (facilitated by heat using a heat gun) and (EtO)₃CH (3.9 mL, 23.7 mmol) was added to result in the formation of a yellow solid. Heat the suspension at 110 °C under N₂ to give an orange solution. The reaction was monitored by ¹H NMR spectroscopy and after 14-18 h reaction was complete. Remove the solvent and wash the orange solid with Et₂O and decant the solvent with a pipet (filtration decomposes **III-59** because it is hygroscopic) and dry the pure solid under high vacuum. Isolated 366 mg (88% yield) of **III-59** as a light tan solid. ¹H NMR (500 MHz, CDCl₃) δ 11.41 (s, 1H); 6.94 (s, 2H); 4.86 (t, *J* = 7.3 Hz, 2H); 3.21 (t, *J* = 7.8 Hz, 2H); 2.89-2.85 (m, 2H); 2.31 (s, 3H); 2.06 (s, 6H); ¹³C NMR (125 MHz, CDCl₃) δ 162.3, 142.0, 135.1, 132.1, 129.8, 48.6, 27.1, 22.3, 21.4, 17.9.

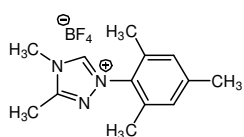
***N*²-((4-trifluoromethyl)phenyl)-6,7-dihydro-5*H*-pyrrolotriazolium**



tetrafluoroborate (III-61): Procedure began with pyrrolidin-2-one and synthesis of the hydrazine·HBF₄ salt is analogous to the method reported by

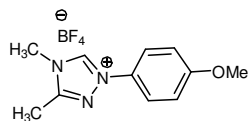
Rovis and coworkers.²¹¹ After isolation of the hydrazine·HBF₄ salt, the salt (861 mg, 3.53 mmol) was dissolved in 1 mL of MeOH (3.4 M) and (EtO)₃CH (7.0 mL, 42.4 mmol) was added and the solution was heated at 110 °C under N₂ to give an orange solution. The reaction was monitored by ¹H NMR spectroscopy and after 46 h reaction was complete. Remove the solvent and titrate with EtOAc and dry the pure solid under high vacuum. Isolated 684 mg (57% yield) of **III-61** as

a light yellow solid. ^1H NMR (500 MHz, CDCl_3) δ 10.71 (s, 1H); 7.98 (d, $J = 8.3$ Hz, 2H); 7.79 (d, $J = 8.8$ Hz, 2H); 4.61 (t, $J = 7.8$ Hz, 2H); 3.26 (t, $J = 7.8$ Hz, 2H); 2.90-2.84 (m, 2H); ^1H NMR (500 MHz, $\text{DMSO}-d_6$) δ 10.85 (s, 1H); 8.16-8.09 (m, 4H); 4.45 (t, $J = 6.8$ Hz, 2H); 3.24 (t, $J = 7.8$ Hz, 2H); 2.80-2.74 (m, 2H); ^1H NMR (500 MHz, CD_3OD) δ 8.10 (d, $J = 8.8$ Hz, 2H); 7.98 (d, $J = 8.8$ Hz, 2H); 4.52 (t, $J = 7.3$ Hz, 2H); 3.27 (t, $J = 7.8$ Hz, 2H); 2.91-2.85 (m, 2H); ^{13}C NMR (125 MHz, CDCl_3) δ 162.5, 137.3, 130.7, 130.4, 125.8, 123.3, 120.1, 45.8, 25.1, 19.7.



N^2 -Mesityl- N^4 -methyl-5-methyltriazolium tetrafluoroborate (III-64a):

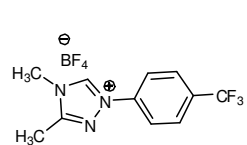
Procedure began with *N*-methyl acetamide and is analogous to the method reported by Rovis and coworkers.²¹¹ The reaction was purified with 50-100% ethyl acetate/hexane followed by 10% MeOH/ CH_2Cl_2 to give an orange oil that is titrated with 3:6.5:0.5 $\text{CH}_2\text{Cl}_2/\text{Et}_2\text{O}$ /toluene yielding 950 mg (46 %) of **III-64a** as a light yellow solid. $R_f = 0.25$ (100% ethyl acetate); Mp: 130-132 °C; IR (film) 3107, 2972, 1597, 1456, 1062 cm^{-1} ; ^1H NMR (500 MHz, CDCl_3) δ 9.51 (s, 1H); 6.97 (s, 2H); 4.03 (s, 3H); 2.67 (s, 3H); 2.64 (s, 3H); 2.02 (s, 6H); ^{13}C NMR (125 MHz, CDCl_3) δ 154.5, 144.9, 141.9, 135.3, 131.2, 129.8, 33.7, 21.4, 17.3, 10.3; LRMS (electrospray): Mass calculated for $\text{C}_{13}\text{H}_{18}\text{BF}_4\text{N}_3$ [$\tilde{\text{M}} \text{BF}_4$] $^+$, 216. Found 216.



N^2 -(4-methoxyphenyl)- N^4 -methyl-5-methyltriazolium tetrafluoroborate

(III-64b): Procedure began with *N*-methyl acetamide and is analogous to the method reported by Rovis and coworkers.²¹¹ The reaction was purified with 50-100% ethyl acetate/hexane followed by 10% MeOH/ CH_2Cl_2 to give brown solid that is dissolved in CH_2Cl_2 and titrated with Et_2O /toluene (3:6.5:0.5 $\text{CH}_2\text{Cl}_2/\text{Et}_2\text{O}$ /toluene) yielding 780 mg (39 %) of **III-**

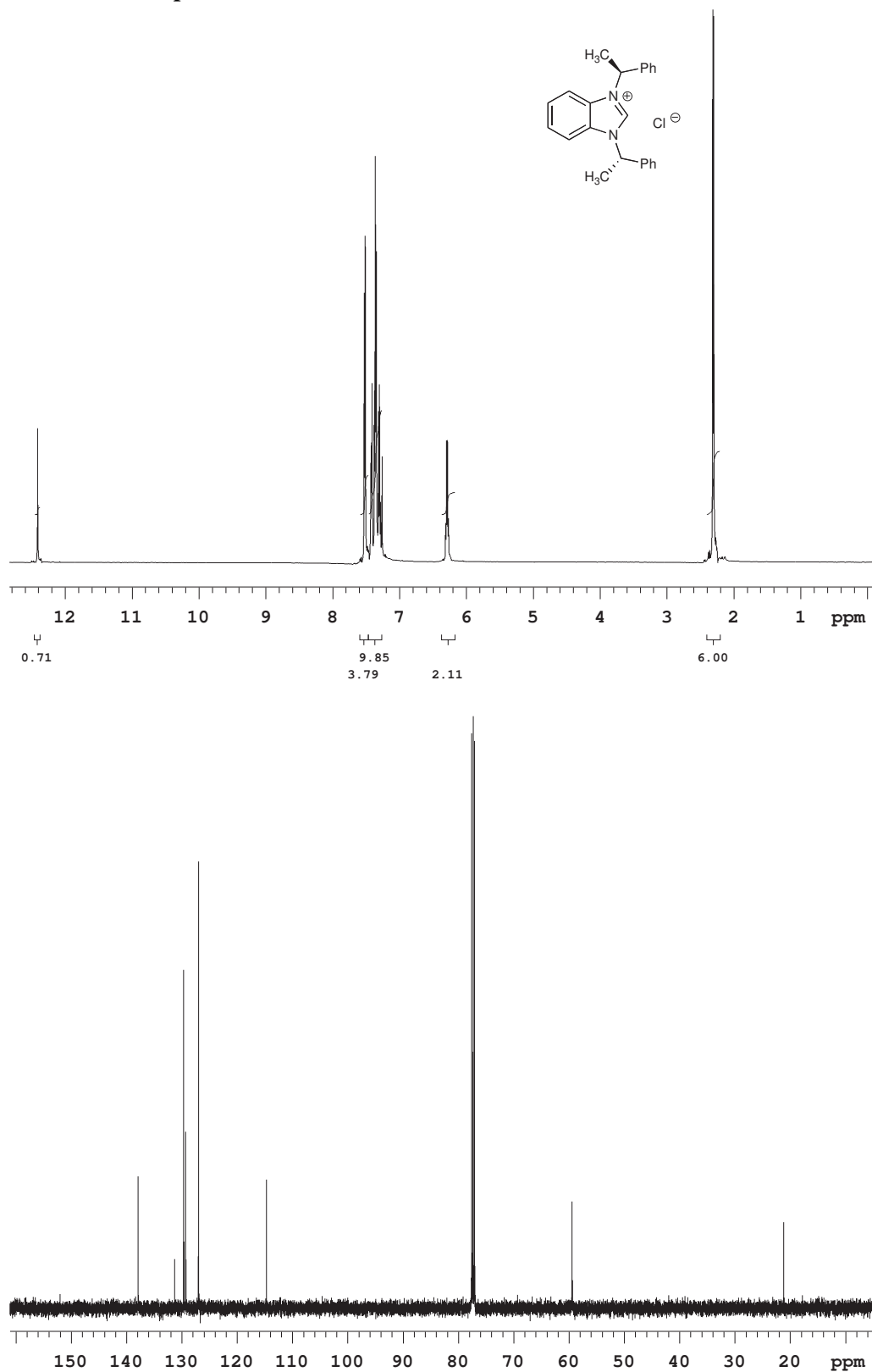
64b as a light yellow solid. $R_f = 0.35$ (10% MeOH/CH₂Cl₂); ¹H NMR (500 MHz, DMSO-d₆) δ 10.55 (s, 1H); 7.87 (d, $J = 8.8$ Hz, 2H); 7.22 (d, $J = 8.8$ Hz, 2H); 3.87 (s, 3H); 3.85 (s, 3H); 2.62 (s, 3H); ¹³C NMR (125 MHz, DMSO-d₆) δ 161.1, 154.8, 128.7, 122.9, 115.9, 56.4, 33.7, 10.4.

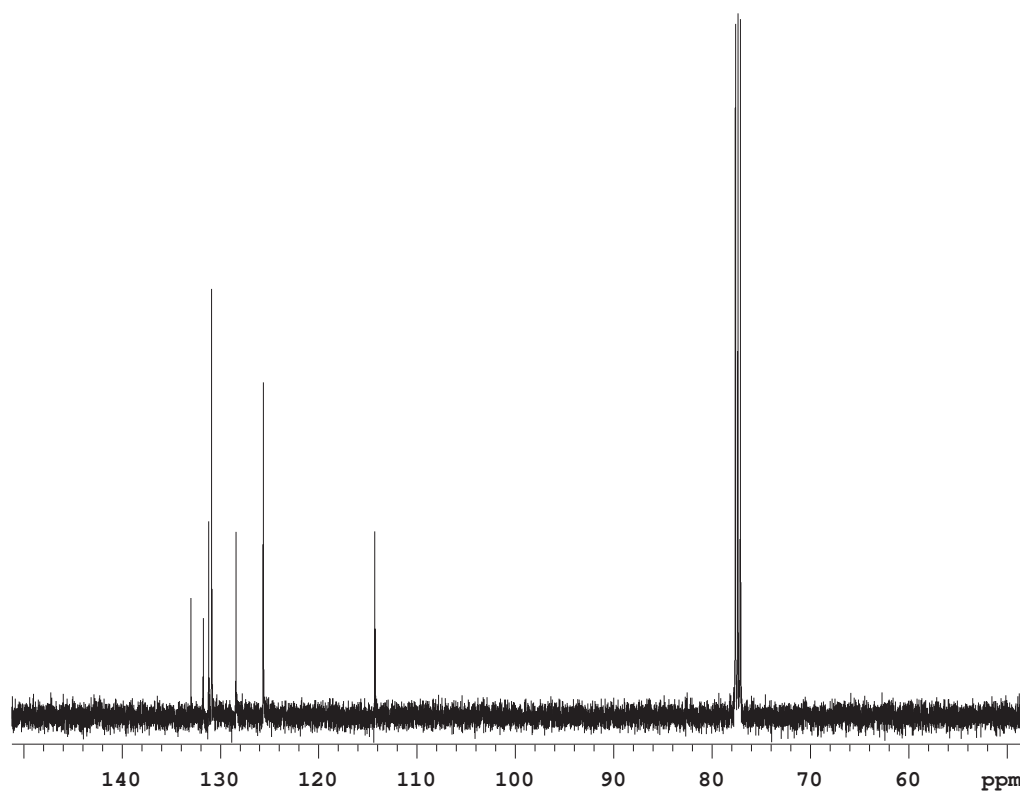
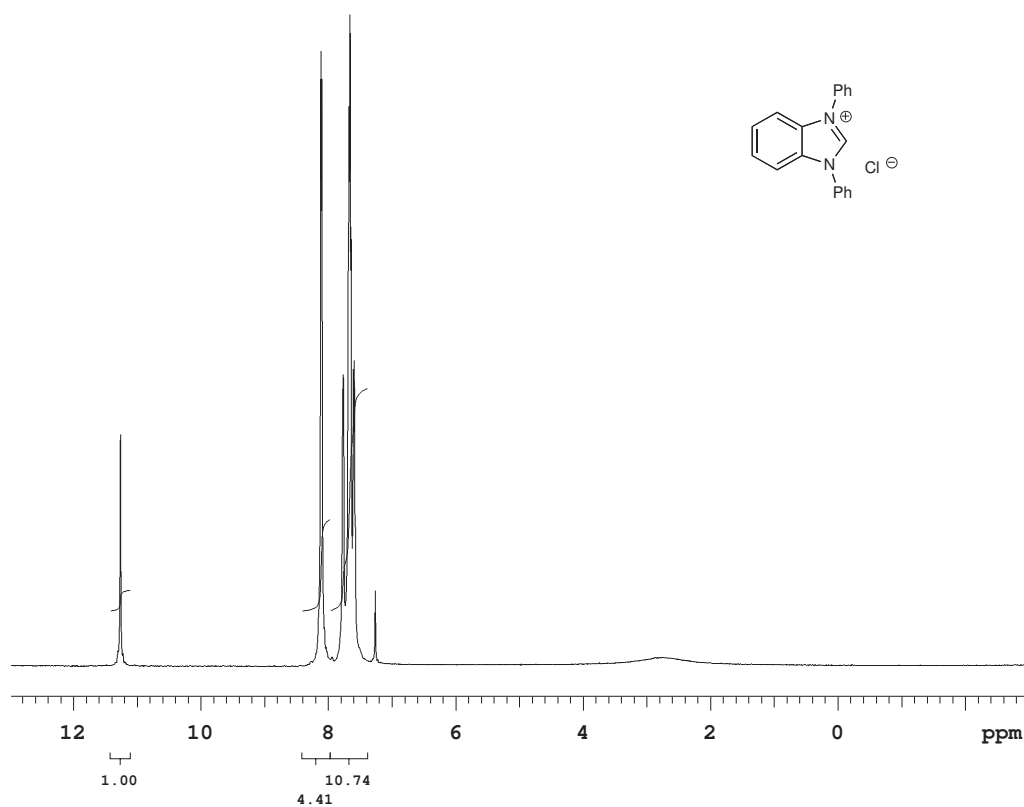


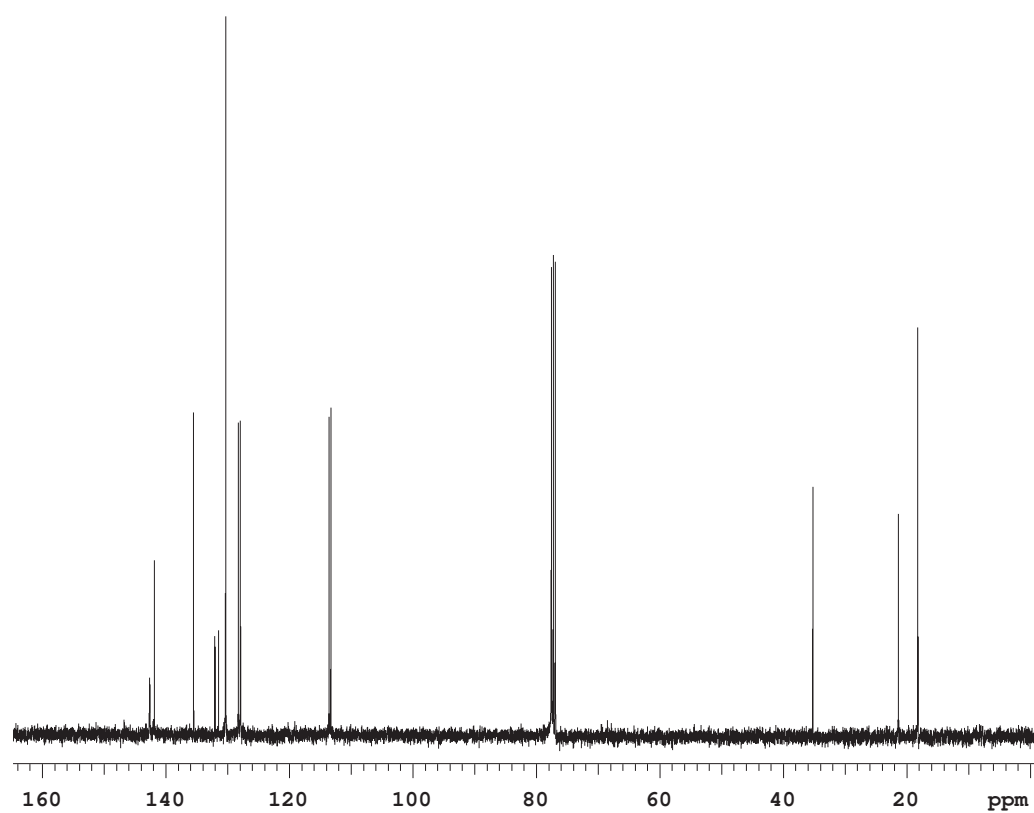
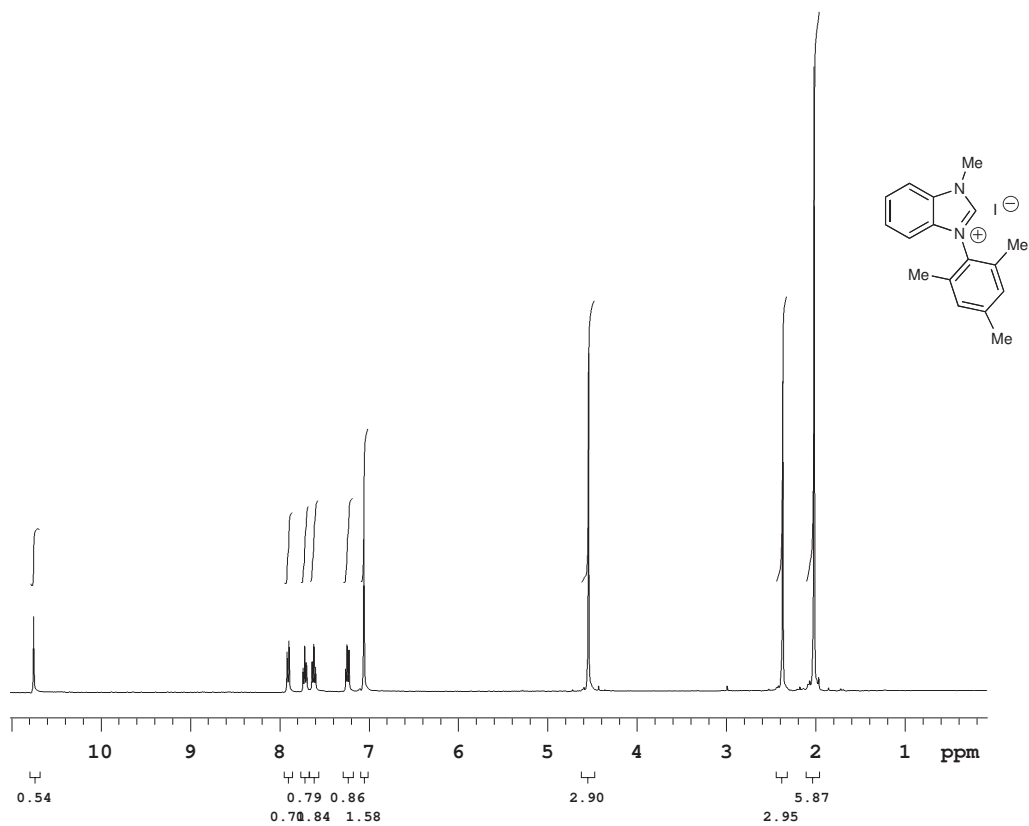
***N*²-((4-trifluoromethyl)-phenyl)-*N*⁴-methyl-5-methyltriazolium**

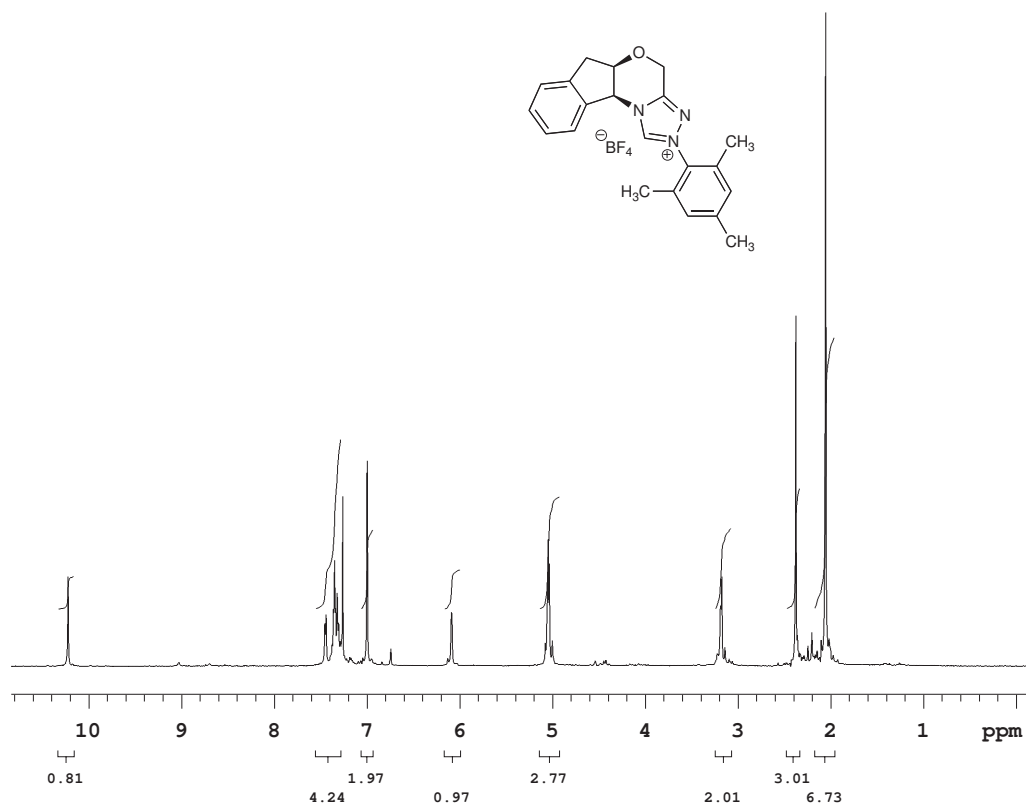
tetrafluoroborate (III-64c): Procedure began with *N*-methyl acetamide and is analogous to the method reported by Rovis and coworkers.²¹¹ The reaction was purified with 50-100% ethyl acetate/hexane followed by 10% MeOH/CH₂Cl₂ to give an orange oil that is titrated with 3:6.5:0.5 CH₂Cl₂/Et₂O/toluene yielding 487 mg (22 %) of **III-64c** as a light yellow solid. $R_f = 0.40$ (10% MeOH/CH₂Cl₂); ¹H NMR (500 MHz, CDCl₃) δ 10.21 (s, 1H); 7.99 (d, $J = 8.3$ Hz, 2H); 7.77 (d, $J = 8.3$ Hz, 2H); 4.02 (s, 3H); 2.67 (s, 3H); ¹H NMR (500 MHz, DMSO-d₆) δ 10.86 (s, 1H); 8.12 (s, 4H); 3.92 (s, 3H); 2.67 (s, 3H); ¹H NMR (500 MHz, CD₃OD) δ 8.10 (d, $J = 8.8$ Hz, 2H); 8.06 (d, $J = 8.3$ Hz, 2H); 3.99 (s, 3H); 2.69 (s, 3H); ¹³C NMR (125 MHz, DMSO-d₆) δ 155.4, 138.5, 130.9, 128.3, 125.3, 123.2, 121.7, 34.0, 10.4.

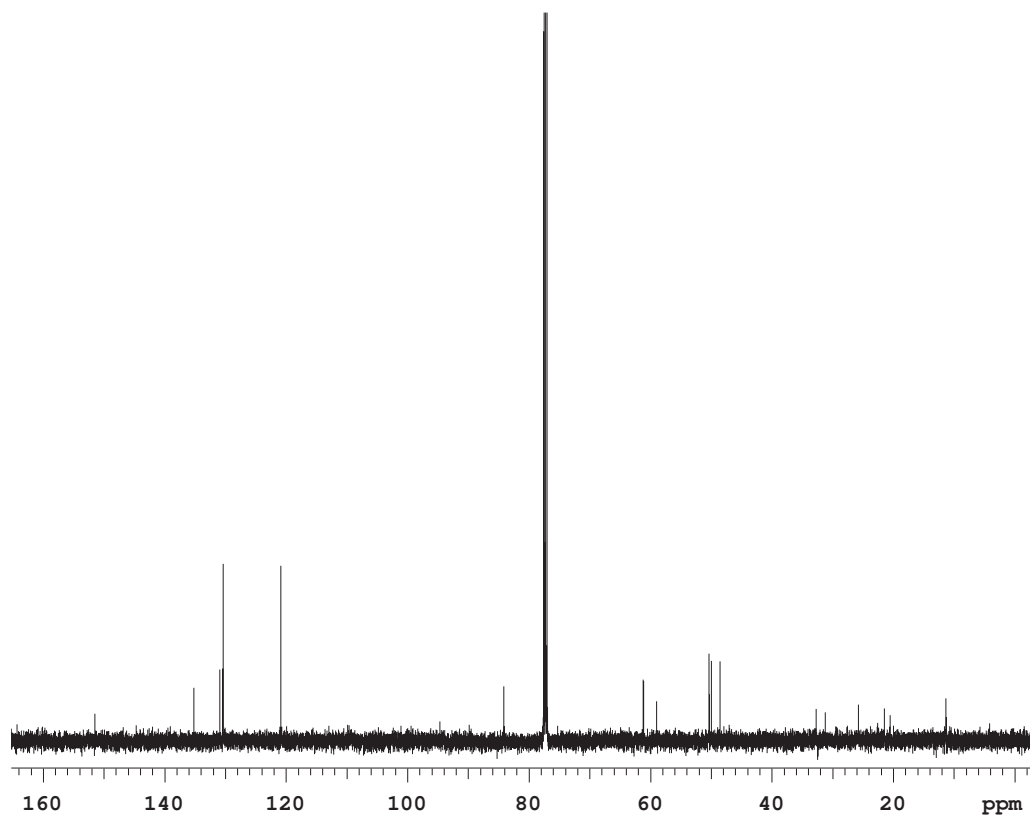
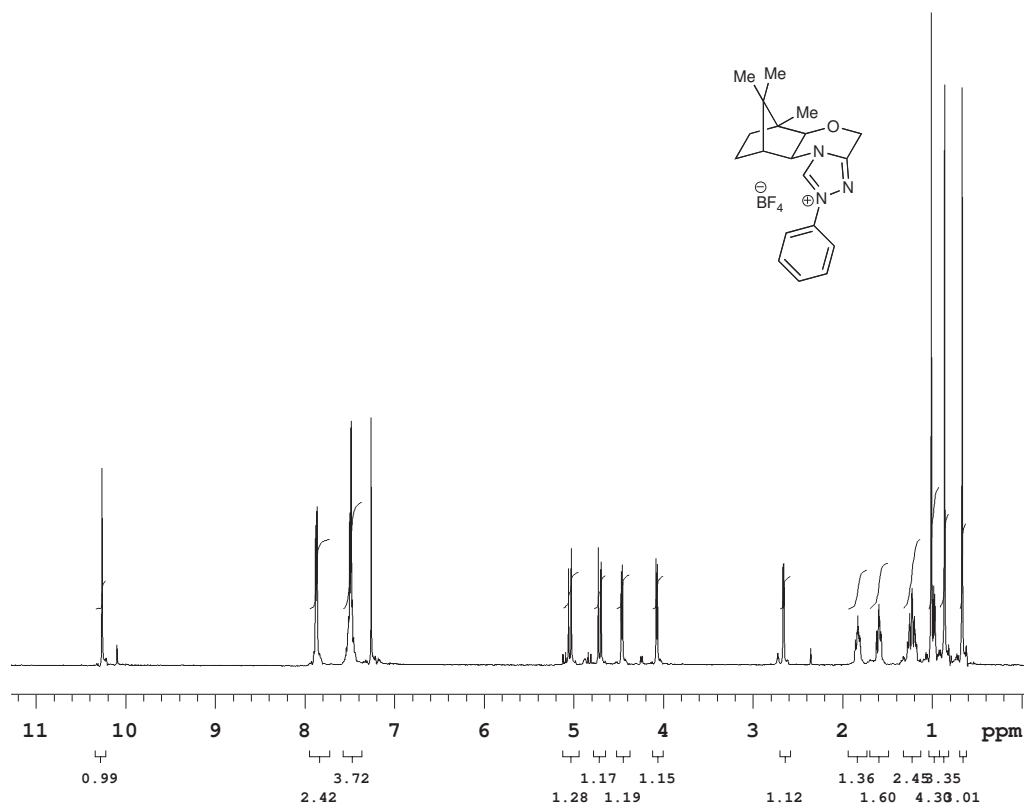
3.6.4 Selected NMR Spectra

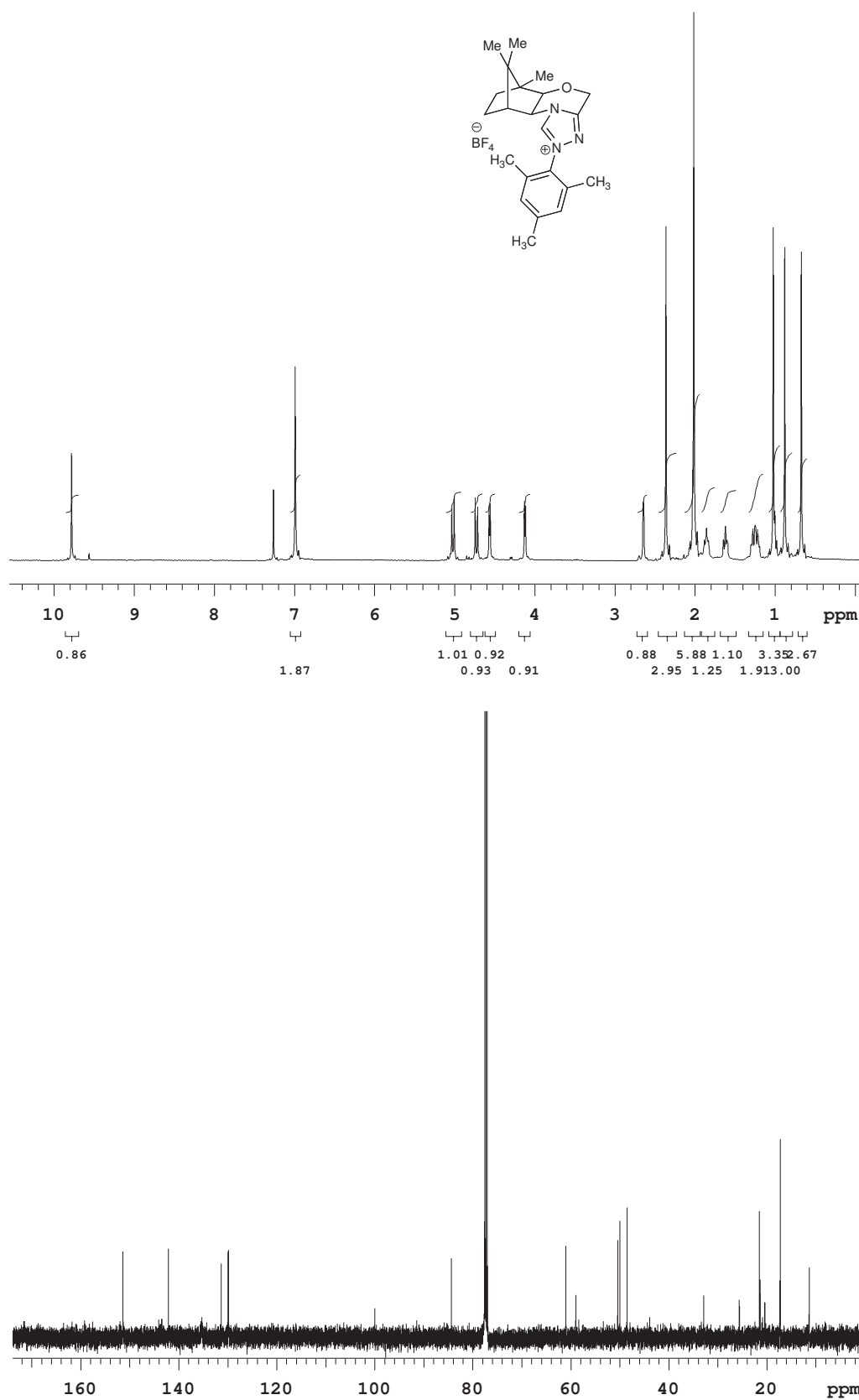


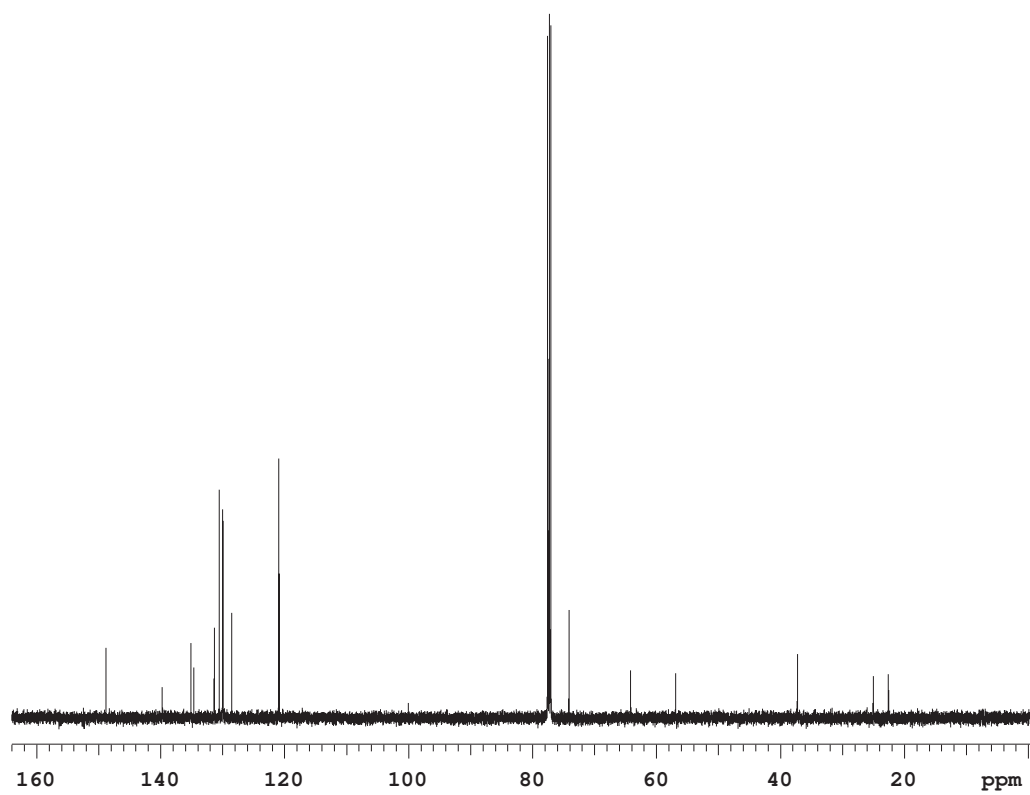
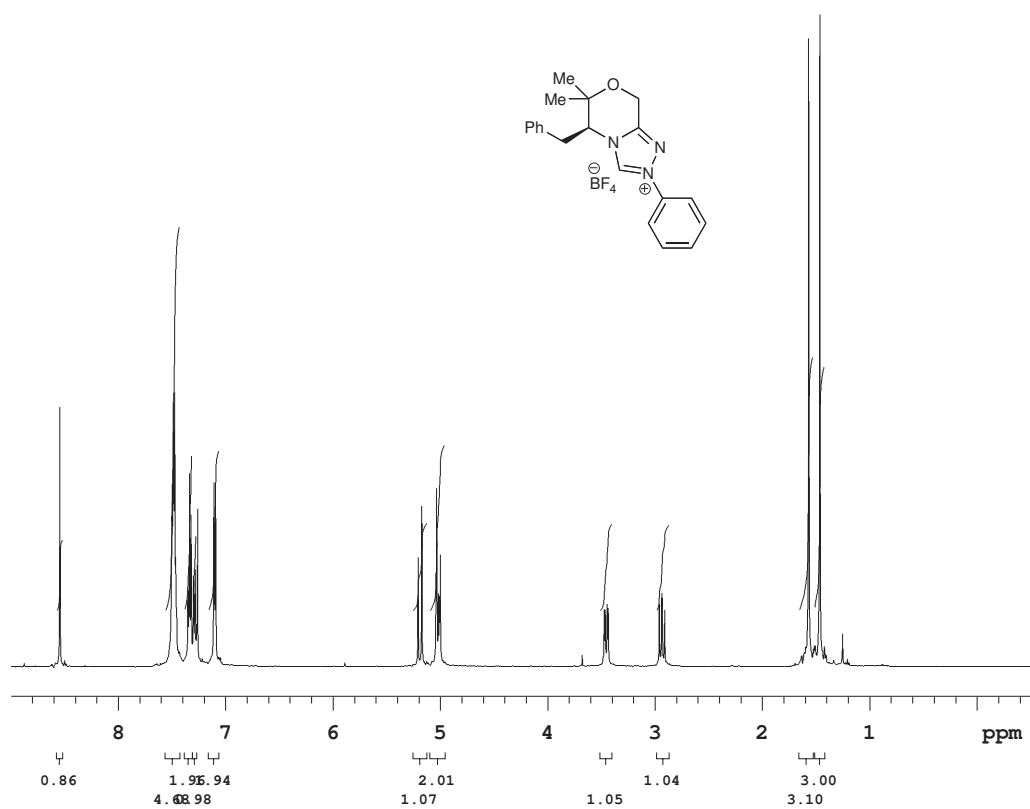


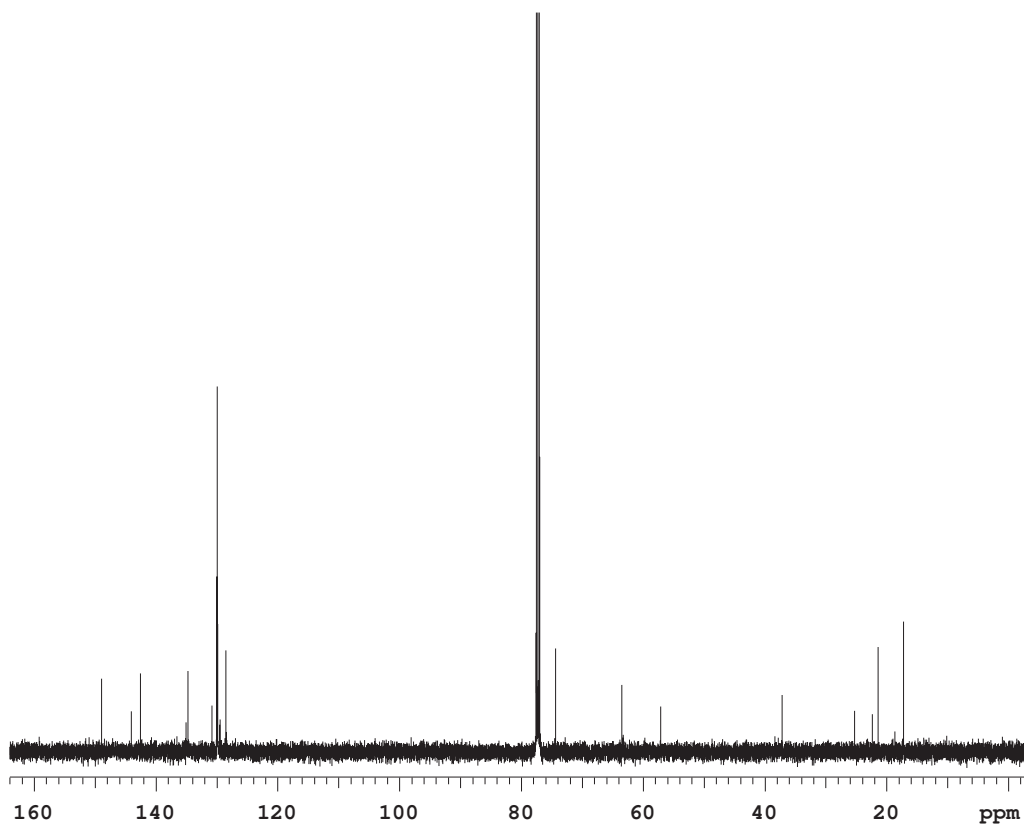
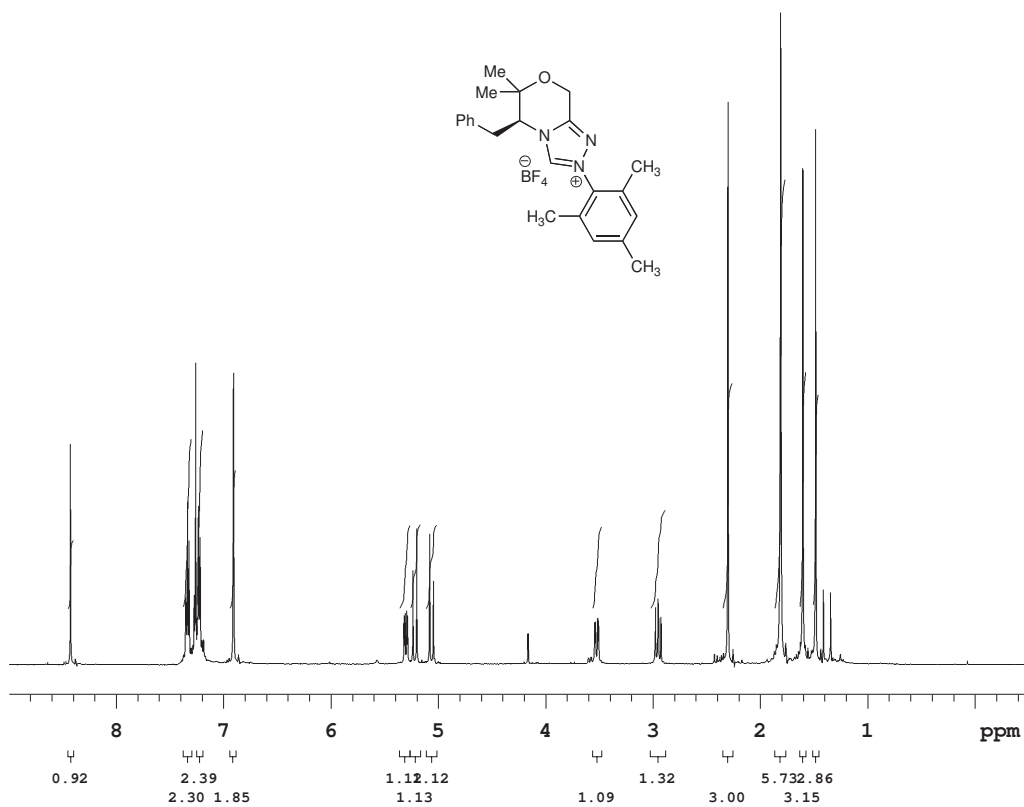


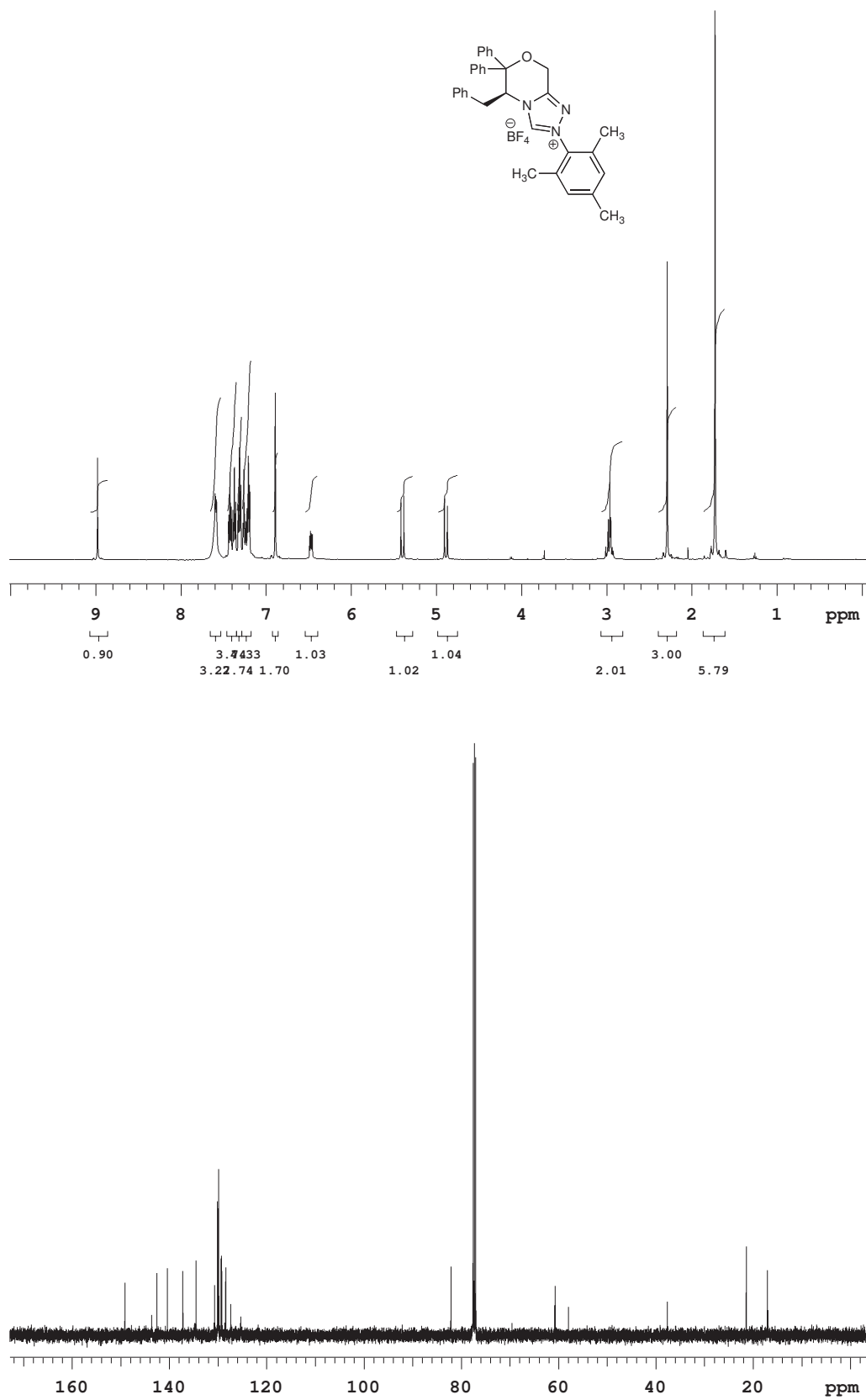


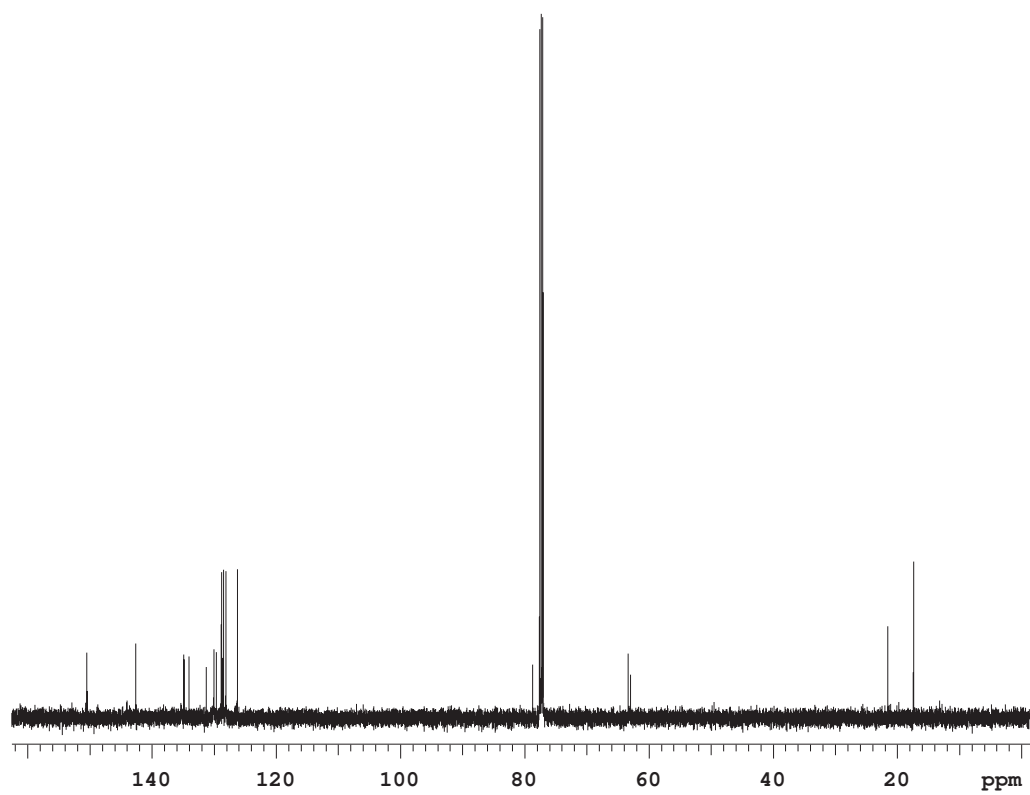
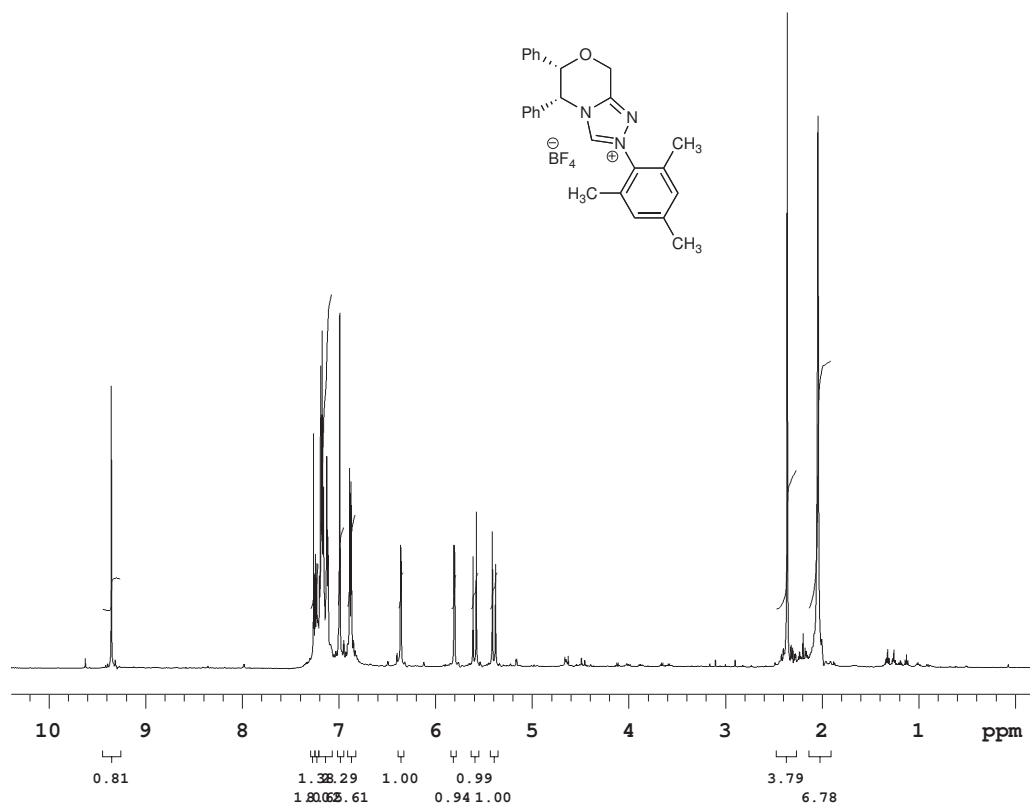


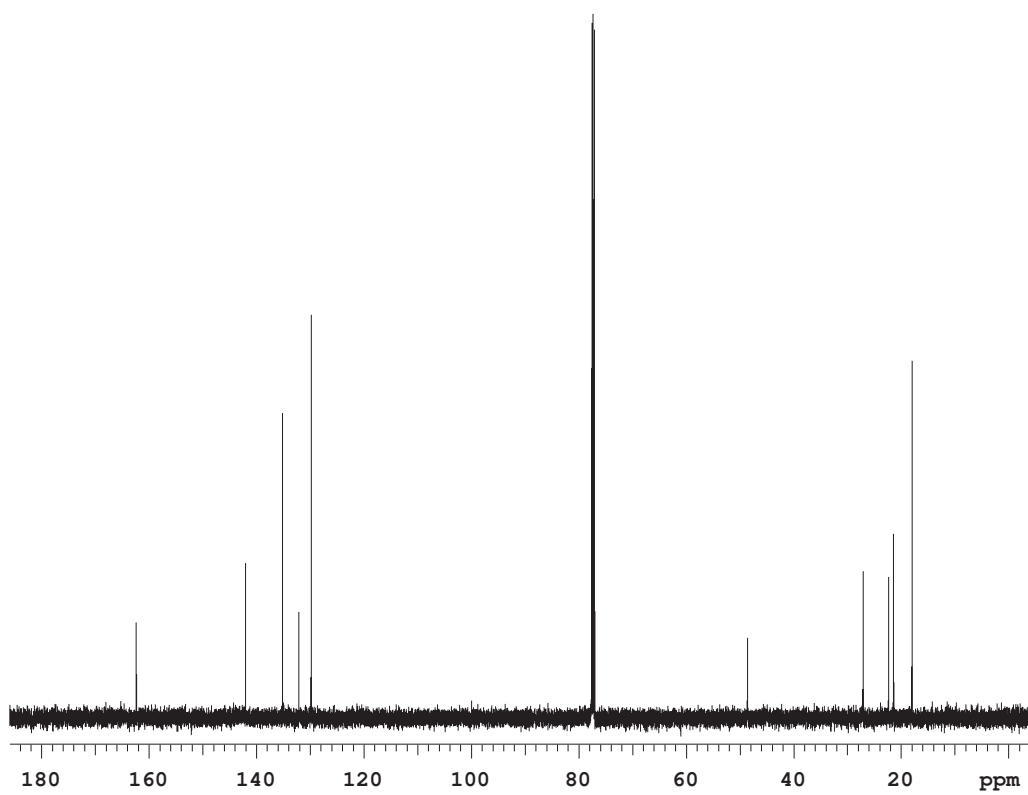
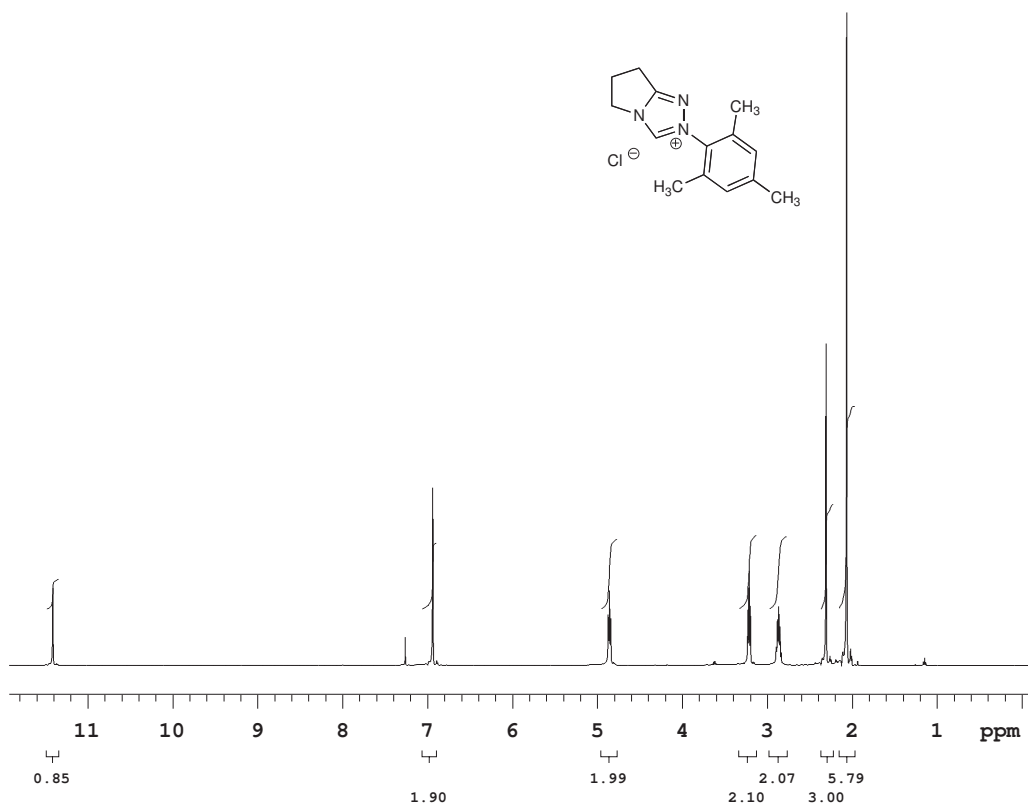


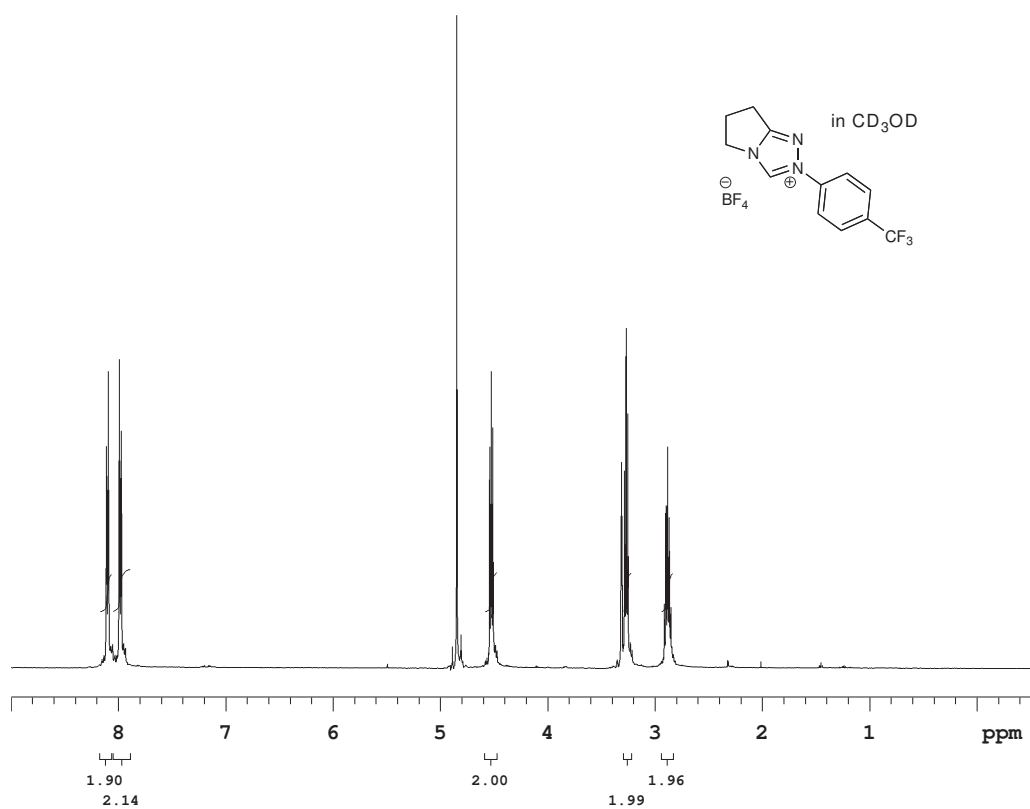
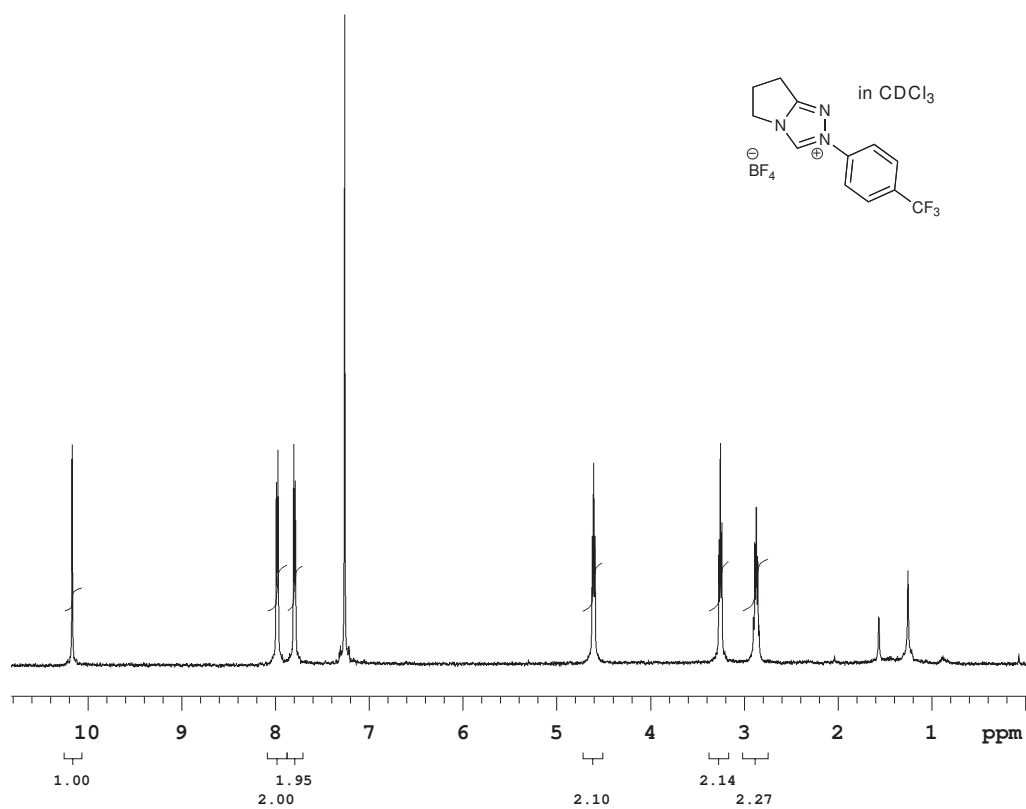


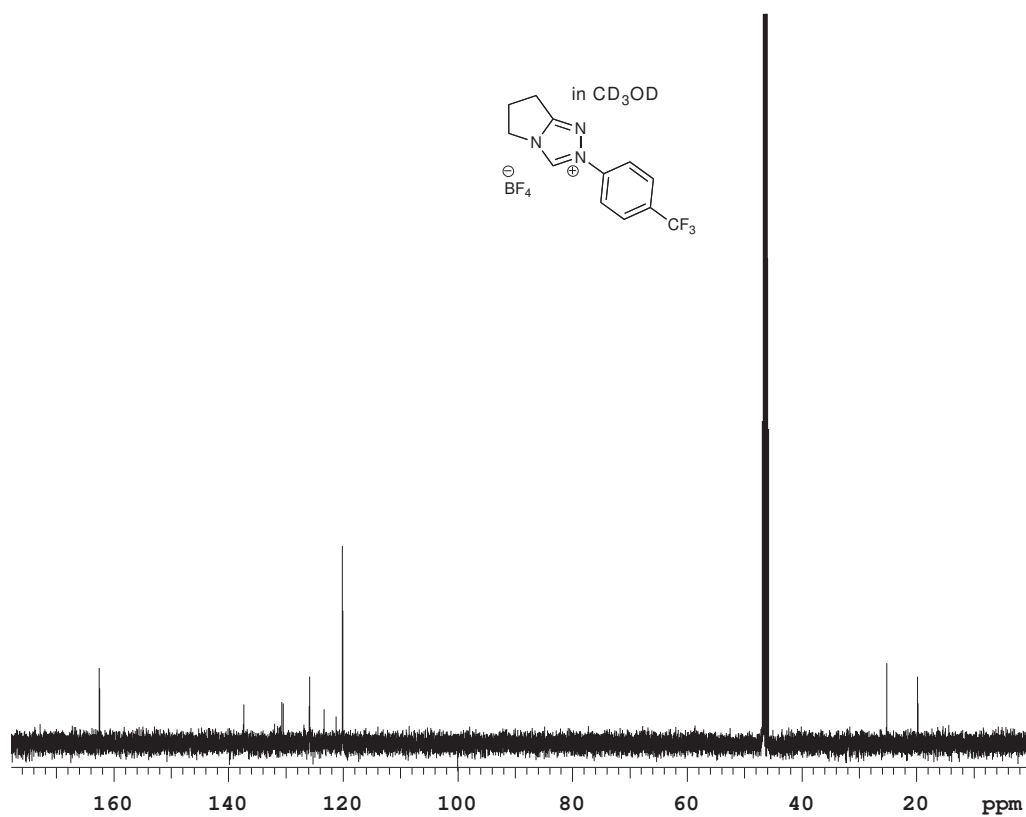


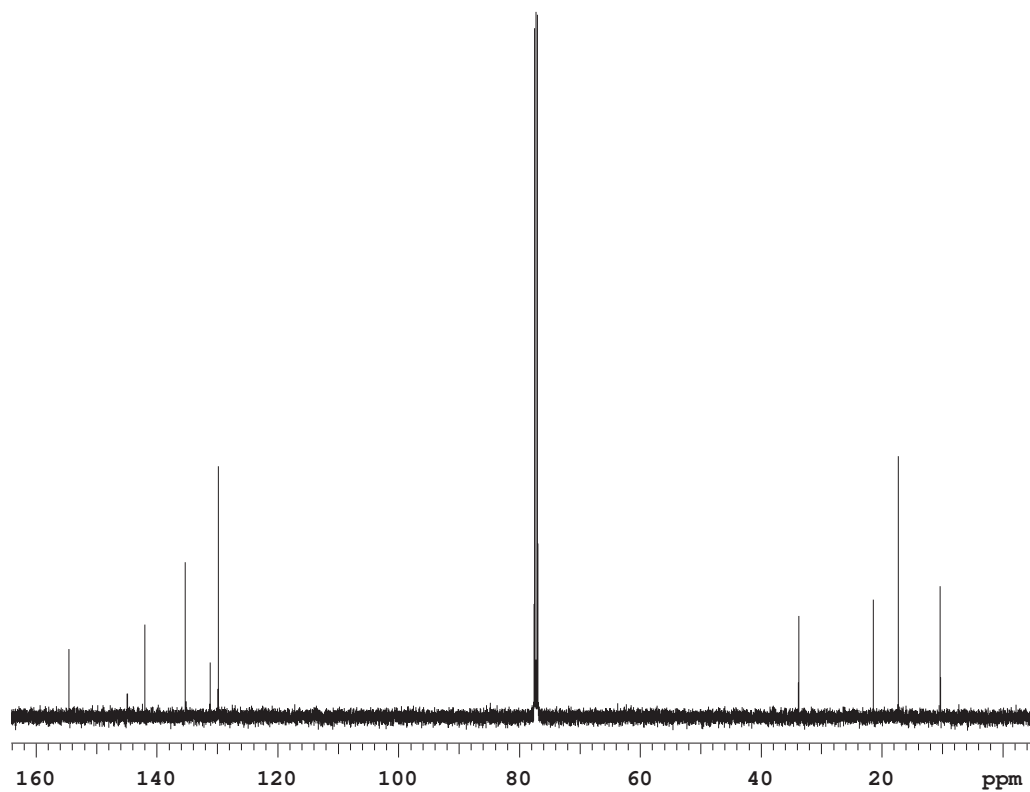
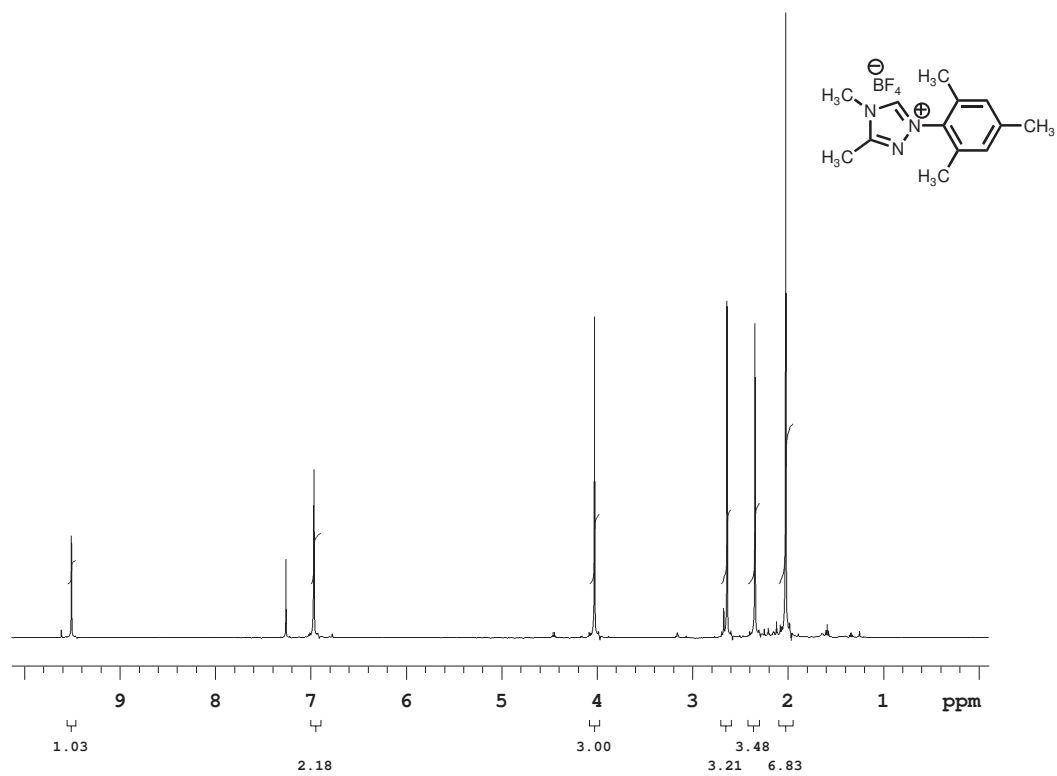


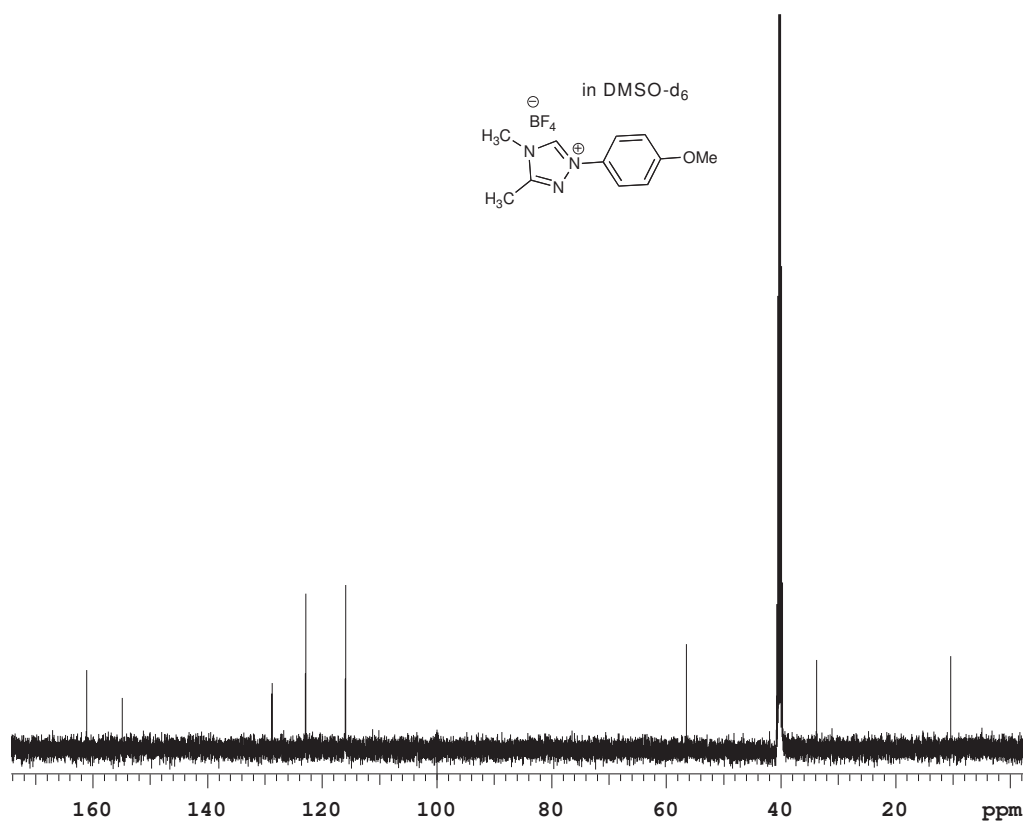
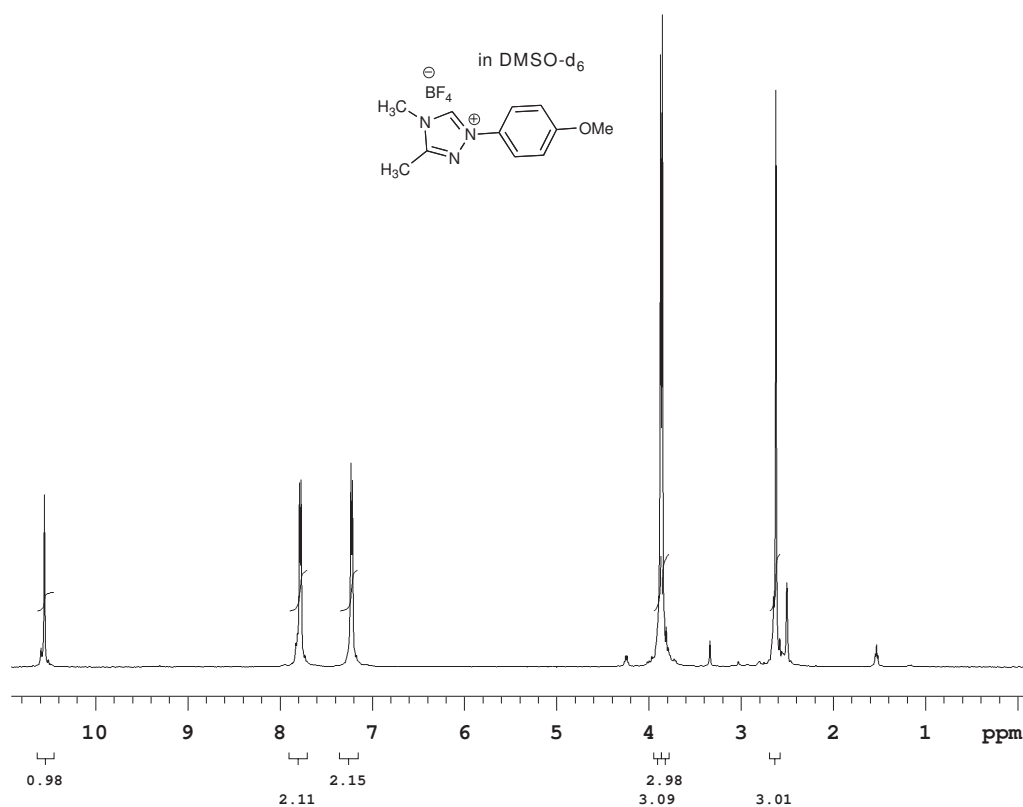


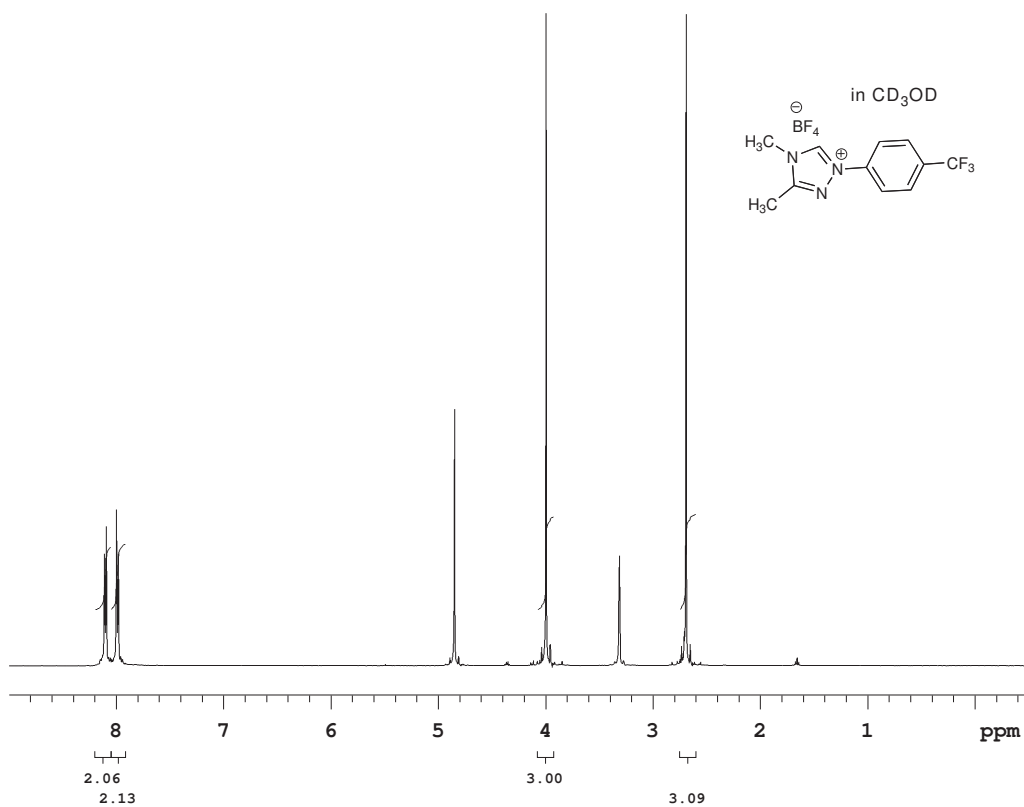
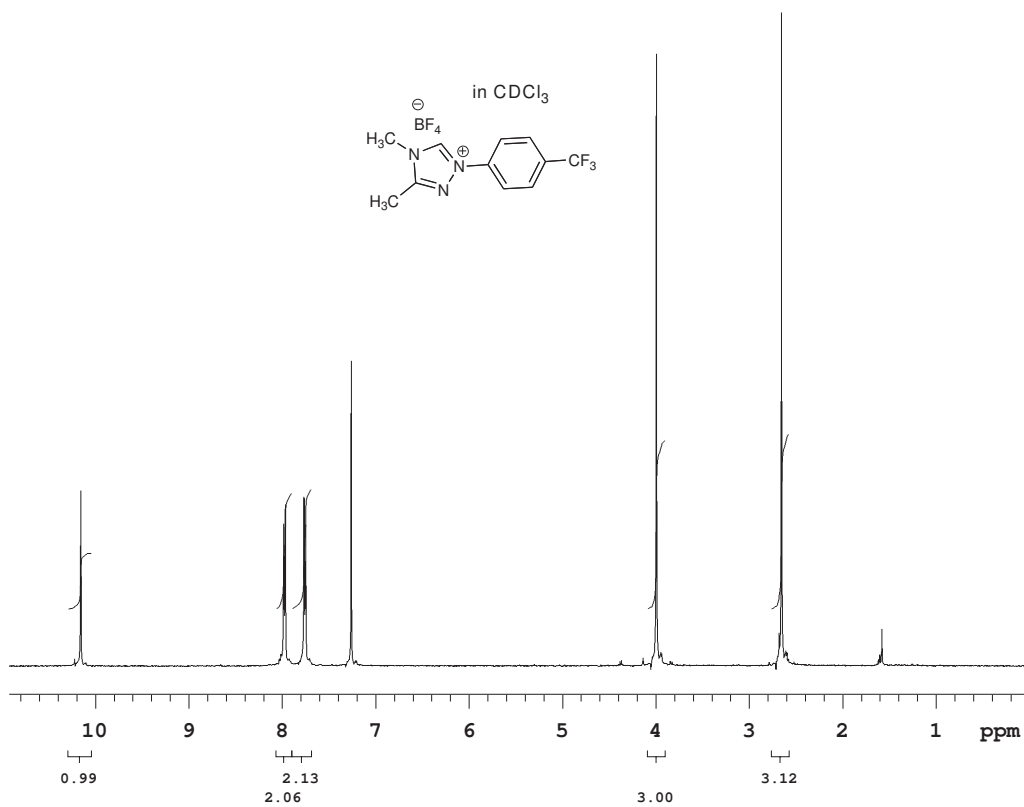


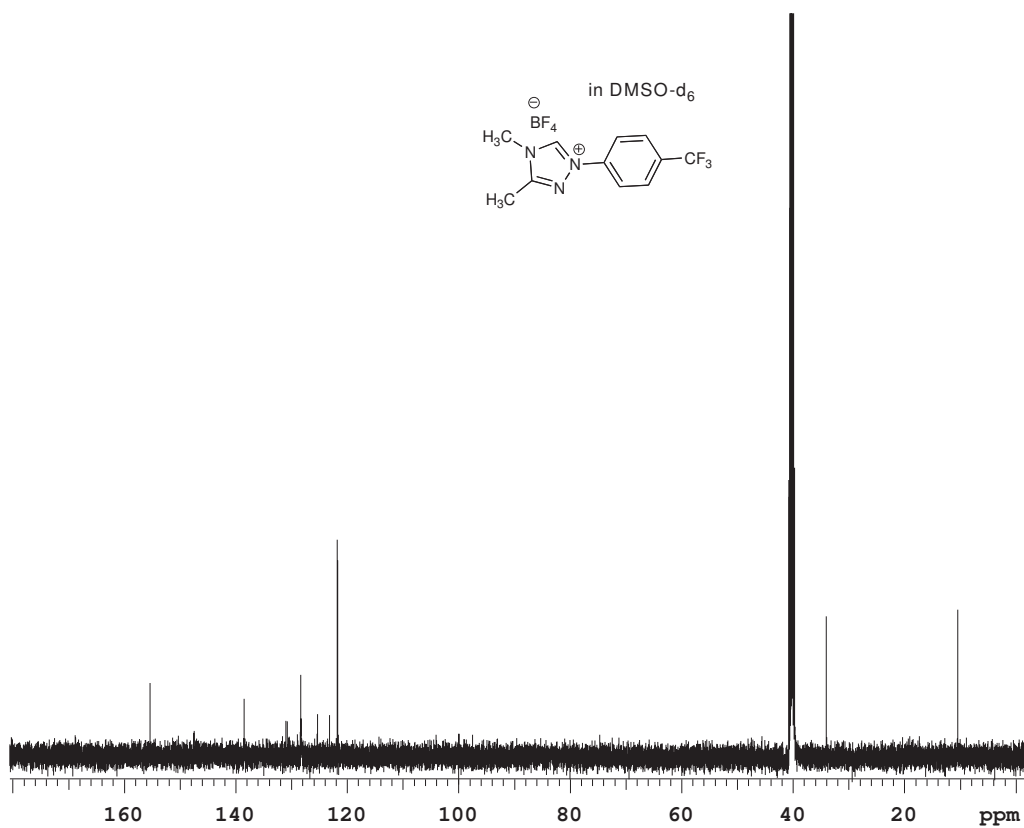
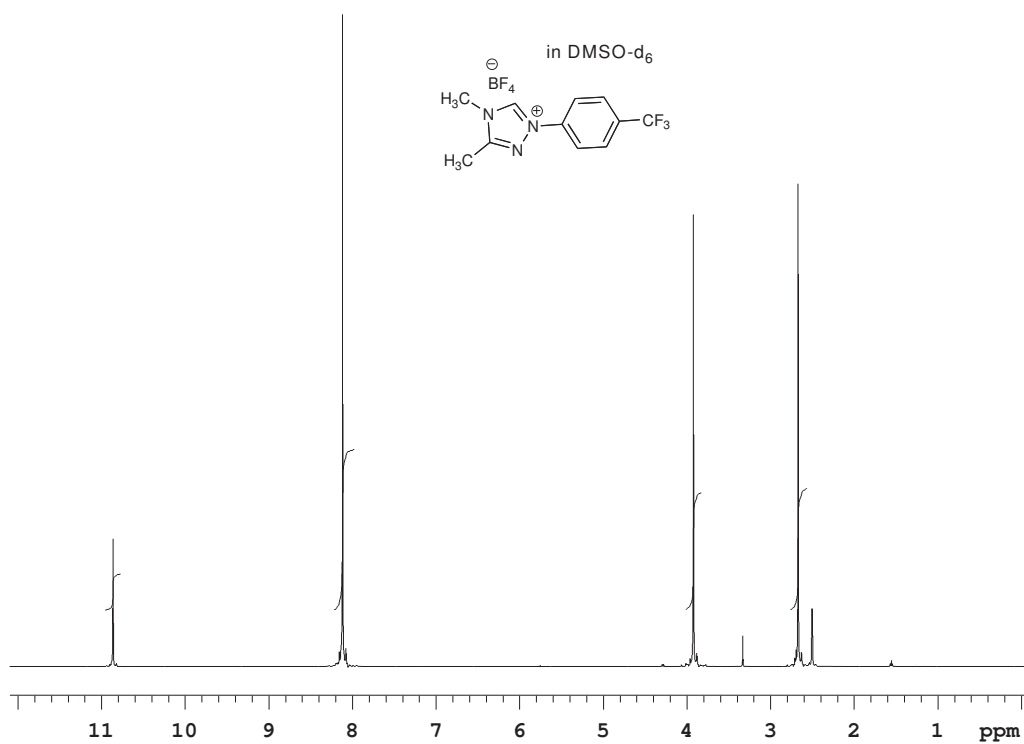












References

- (1) Mizuhara, S.; Tamura, R.; Arata, H. *Proc. Jpn. Acad.* **1951**, 87, 302.
- (2) Sundstrom, M.; Lindqvist, Y.; Schneider, G.; Hellman, U.; Ronne, H. *J. Biol. Chem.* **1993**, 268, (32), 24346-24352.
- (3) Bordwell, F. G.; Satish, A. V. *J. Am. Chem. Soc.* **1991**, 113, (3), 985-990.
- (4) Alder, R. W.; Allen, P. R.; Williams, S. J. *J. Chem. Soc., Chem. Comm.* **1995**, (12), 1267-1268.
- (5) Kim, Y. J.; Streitwieser, A. *J. Am. Chem. Soc.* **2002**, 124, (20), 5757-5761.
- (6) Amyes, T. L.; Diver, S. T.; Richard, J. P.; Rivas, F. M.; Toth, K. *J. Am. Chem. Soc.* **2004**, 126, (13), 4366-4374.
- (7) Wanzlick, H. W. *Angew. Chem., Int. Ed.* **1962**, 74, (4), 129-134.
- (8) Wanzlick, H. W.; Kleiner, H. J. *Angew. Chem., Int. Ed.* **1963**, 75, (24), 1204-1212.
- (9) Schonher.Hj; Wanzlick, H. W. *Liebigs Ann. Chem.* **1970**, 731, 176.
- (10) Schonher.Hj; Wanzlick, H. W. *Chem. Ber.* **1970**, 103, (4), 1037.
- (11) Walentow.R; Wanzlick, H. W. *Naturforsch.* **1970**, B 25, (12), 1421.
- (12) Arduengo, A. J.; Harlow, R. L.; Kline, M. *J. Am. Chem. Soc.* **1991**, 113, (1), 361-363.
- (13) Arduengo, A. J.; Dias, H. V. R.; Harlow, R. L.; Kline, M. *J. Am. Chem. Soc.* **1992**, 114, (14), 5530-5534.
- (14) Dixon, D. A.; Arduengo, A. J. *J. Phys. Chem.* **1991**, 95, (11), 4180-4182.
- (15) Enders, D.; Breuer, K.; Raabe, G.; Runsink, J.; Teles, J. H.; Melder, J. P.; Ebel, K.; Brode, S. *Angew. Chem., Int. Ed.* **1995**, 34, (9), 1021-1023.
- (16) Ugai, T.; Tanaka, S.; Dokawa, S. *J. Pharm. Soc. Jpn.* **1943**, 63, 296.

- (17) Breslow, R. *Journal of the American Chemical Society* **1958**, 80, (14), 3719-3726.
- (18) Enders, D.; Kallfass, U. *Angew. Chem., Int. Ed.* **2002**, 41, (10), 1743-1745.
- (19) Stetter, H.; Dambkes, G. *Synthesis* **1977**, (6), 403-404.
- (20) Stetter, H.; Dambkes, G. *Synthesis* **1980**, (4), 309-310.
- (21) Linghu, X. ; Johnson, J. S. *Angew. Chem., Int. Ed.* **2003**, 42, 2534-2536.
- (22) Linghu, X.; Bausch, C. C.; Johnson, J. S. *J. Am. Chem. Soc.* **2005**, 127, (6), 1833-1840.
- (23) Mattson, A. E.; Scheidt, K. A. *Org. Lett.* **2004**, 6, (23), 4363-4366.
- (24) Mennen, S. M.; Gipson, J. D.; Kim, Y. R.; Miller, S. J. *J. Am. Chem. Soc.* **2005**, 127, (6), 1654-1655.
- (25) Li, G. Q.; Dai, L. X.; You, S. L. *Chem. Commun.* **2007**, (8), 852-854.
- (26) Hachisu, Y.; Bode, J. W.; Suzuki, K. *J. Am. Chem. Soc.* **2003**, 125, (28), 8432-8433.
- (27) Takikawa, H.; Hachisu, Y.; Bode, J. W.; Suzuki, K. *Angew. Chem., Int. Ed.* **2006**, 45, (21), 3492-3494.
- (28) Enders, D.; Niemeier, O. *Synlett* **2004**, (12), 2111-2114.
- (29) Hachisu, Y.; Bode, J. W.; Suzuki, K. *Adv. Synth. Catal.* **2004**, 346, (9-10), 1097-1100.
- (30) Enders, D.; Niemeier, O.; Balensiefer, T. *Angew. Chem., Int. Ed.* **2006**, 45, (9), 1463-1467.
- (31) Stetter, H.; Schrecke, M. *Angew. Chem., Int. Ed.* **1973**, 12, (1), 81-81.
- (32) Christmann, M. *Angew. Chem., Int. Ed.* **2005**, 44, (18), 2632-2634.
- (33) Stetter, H. *Angew. Chem., Int. Ed.* **1976**, 15, (11), 639-647.
- (34) Harrington, P. E.; Tius, M. A. *Org. Lett.* **1999**, 1, (4), 649-651.
- (35) Anjaiah, S.; Chandrasekhar, S.; Gree, R. *Adv. Syn. Cat.* **2004**, 346, (11), 1329-1334.
- (36) Ciganek, E. *Synthesis* **1995**, (10), 1311-1314.
- (37) Enders, D.; Breuer, K.; Runsink, J.; Teles, J. H. *Helv. Chim. Acta.* **1996**, 79, (7), 1899-1902.

- (38) Kerr, M. S.; de Alaniz, J. R.; Rovis, T. *J. Am. Chem. Soc.* **2002**, *124*, (35), 10298-10299.
- (39) Kerr, M. S.; Rovis, T. *Synlett* **2003**, (12), 1934-1936.
- (40) Kerr, M. S.; Rovis, T. *J. Am. Chem. Soc.* **2004**, *126*, (29), 8876-8877.
- (41) Nakamura, T.; Hara, O.; Tamura, T.; Makino, K.; Hamada, Y. *Synlett* **2005**, (1), 155-157.
- (42) Moore, J. L.; Kerr, M. S.; Rovis, T. *Tetrahedron* **2006**, *62*, (49), 11477-11482.
- (43) de Alaniz, J. R.; Rovis, T. *J. Am. Chem. Soc.* **2005**, *127*, (17), 6284-6289.
- (44) Reynolds, N. T.; Rovis, T. *Tetrahedron* **2005**, *61*, (26), 6368-6378.
- (45) Nemoto, T.; Fukuda, T.; Hamada, Y. *Tetrahedron Lett.* **2006**, *47*, (26), 4365-4368.
- (46) Mattson, A. E.; Bharadwaj, A. R.; Scheidt, K. A. *J. Am. Chem. Soc.* **2004**, *126*, (8), 2314-2315.
- (47) Mattson, A. E.; Bharadwaj, A. R.; Zuhl, A. M.; Scheidt, K. A. *J. Org. Chem.* **2006**, *71*, (15), 5715-5724.
- (48) Mattson, A. E.; Zuhl, A. M.; Reynolds, T. E.; Scheidt, K. A. *J. Am. Chem. Soc.* **2006**, *128*, (15), 4932-4933.
- (49) Myers, M. C.; Bharadwaj, A. R.; Milgram, B. C.; Scheidt, K. A. *J. Am. Chem. Soc.* **2005**, *127*, (42), 14675-14680.
- (50) Chow, K. Y. K.; Bode, J. W. *J. Am. Chem. Soc.* **2004**, *126*, (26), 8126-8127.
- (51) Sohn, S. S.; Bode, J. W. *Angew. Chem., Int. Ed.* **2006**, *45*, (36), 6021-6024.
- (52) Bode, J. W.; Sohn, S. S. *J. Am. Chem. Soc.* **2007**, *129*, (45), 13798-13799.
- (53) Reynolds, N. T.; de Alaniz, J. R.; Rovis, T. *J. Am. Chem. Soc.* **2004**, *126*, (31), 9518-9519.
- (54) Reynolds, N. T.; Rovis, T. *J. Am. Chem. Soc.* **2005**, *127*, (47), 16406-16407.
- (55) Vora, H. U.; Rovis, T. *J. Am. Chem. Soc.* **2007**, *129*, (45), 13796-13797.
- (56) He, M.; Uc, G. J.; Bode, J. W. *J. Am. Chem. Soc.* **2006**, *128*, (47), 15088-15089.

- (57) Burstein, C.; Glorius, F. *Angew. Chem., Int. Ed.* **2004**, *43*, 6205-6208.
- (58) Sohn, S. S.; Rosen, E. L.; Bode, J. W. *J. Am. Chem. Soc.* **2004**, *126*, (44), 14370-14371.
- (59) He, M.; Bode, J. W. *Org. Lett.* **2005**, *7*, (14), 3131-3134.
- (60) Nair, V.; Vellalath, S.; Poonoth, M.; Mohan, R.; Suresh, E. *Org. Lett.* **2006**, *8*, (3), 507-509.
- (61) Sohn, S. S.; Bode, J. W. *Org. Lett.* **2005**, *7*, (18), 3873-3876.
- (62) Zeitler, K. *Org. Lett.* **2006**, *8*, (4), 637-640.
- (63) He, M.; Struble, J. R.; Bode, J. W. *J. Am. Chem. Soc.* **2006**, *128*, (26), 8418-8420.
- (64) Nair, V.; Poonoth, M.; Vellalath, S.; Suresh, E.; Thirumalai, R. *J. Org. Chem.* **2006**, *71*, (23), 8964-8965.
- (65) Rivas, F. M.; Riaz, U.; Giessert, A.; Smulik, J. A.; Diver, S. T. *Org. Lett.* **2001**, *3*, (17), 2673-2676.
- (66) Rivas, F. M.; Giessert, A. J.; Diver, S. T. *J. Org. Chem.* **2002**, *67*, (5), 1708-1711.
- (67) Sunitha, K.; Balasubramanian, K. K. *Tetrahedron* **1987**, *43*, (14), 3269-3278.
- (68) Baba, A. I.; Wang, W.; Kim, W. Y.; Strong, L.; Schmehl, R. H. *Syn. Comm.* **1994**, *24*, (7), 1029-1036.
- (69) Clark, C. T.; Milgram, B. C.; Scheidt, K. A. *Org. Lett.* **2004**, *6*, (22), 3977-3980.
- (70) Nicolaou, K. C.; Zhong, Y. L.; Baran, P. S. *J. Am. Chem. Soc.* **2000**, *122*, (31), 7596-7597.
- (71) Nowick, J. S.; Danheiser, R. L. *J. Org. Chem.* **1989**, *54*, (12), 2798-2802.
- (72) Deglinnocenti, A.; Stucchi, E.; Capperucci, A.; Mordini, A.; Reginato, G.; Ricci, A. *Synlett* **1992**, (4), 329-331.
- (73) Capperucci, A.; Degl'Innocenti, A.; Dondoli, P.; Nocentini, T.; Reginato, G.; Ricci, A. *Tetrahedron* **2001**, *57*, (29), 6267-6276.
- (74) Gothelf, K. V.; Jorgensen, K. A. *Chem. Rev.* **1998**, *98*, (2), 863-909.

- (75) Pearson, W. H.; Stoy, P. *Synlett* **2003**, (7), 903-921.
- (76) Gothelf, A. S.; Gothelf, K. V.; Hazell, R. G.; Jorgensen, K. A. *Angew. Chem., Int. Ed. Engl.* **2002**, *41*, (22), 4236-4238.
- (77) Cabrera, S.; Arrayas, R. G.; Carretero, J. C. *J. Am. Chem. Soc.* **2005**, *127*, (47), 16394-16395.
- (78) Kano, T.; Hashimoto, T.; Maruoka, K. *J. Am. Chem. Soc.* **2005**, *127*, (34), 11926-11927.
- (79) Shirakawa, S.; Lombardi, P. J.; Leighton, J. L. *J. Am. Chem. Soc.* **2005**, *127*, (28), 9974-9975.
- (80) Sibi, M. P.; Stanley, L. M.; Jasperse, C. P. *J. Am. Chem. Soc.* **2005**, *127*, (23), 8276-8277.
- (81) Kano, T.; Hashimoto, T.; Maruoka, K. *J. Am. Chem. Soc.* **2006**, *128*, (7), 2174-2175.
- (82) Jen, W. S.; Wiener, J. J. M.; MacMillan, D. W. C. *J. Am. Chem. Soc.* **2000**, *122*, (40), 9874-9875.
- (83) Karlsson, S.; Hogberg, H. E. *Tetrahedron: Asymmetry* **2002**, *13*, (9), 923-926.
- (84) Northrup, A. B.; MacMillan, D. W. C. *J. Am. Chem. Soc.* **2002**, *124*, (11), 2458-2460.
- (85) Dalko, P. I.; Moisan, L. *Angew. Chem., Int. Ed.* **2004**, *43*, (39), 5138-5175.
- (86) Chen, W.; Yuan, X.-H.; Li, R.; Du, W.; Wu, Y.; Ding, L.-S.; Chen, Y.-C. *Adv. Synth. Catal.* **2006**, *348*, 1818-1822.
- (87) Dorn, H.; Otto, A. *Chem. Ber.* **1968**, *101*, (9), 3287-3289.
- (88) Dorn, H.; Otto, A. *Angew. Chem., Int. Ed. Engl.* **1968**, *7*, (3), 214-215.
- (89) Schantl, J.G. *Sci. Synth.* **2004**, *27*, 731.
- (90) Shintani, R.; Fu, G. C. *J. Am. Chem. Soc.* **2003**, *125*, (36), 10778-10779.
- (91) Suarez, A.; Downey, C. W.; Fu, G. C. *J. Am. Chem. Soc.* **2005**, *127*, (32), 11244-11245.
- (92) Shintani, R.; Hayashi, T. *J. Am. Chem. Soc.* **2006**, *128*, (19), 6330-6331.

- (93) Suga, H.; Funyu, A.; Kakehi, A. *Org. Lett.* **2007**, *9*, (1), 97-100.
- (94) Taylor, E. C.; Haley, N. F.; Clemens, R. J. *J. Am. Chem. Soc.* **1981**, *103*, (26), 7743-7752.
- (95) Zeng, X.; Chung, A.; Haran, M.; Jordan, F. *J. Am. Chem. Soc.* **1991**, *113*, (15), 5842-5849.
- (96) Evans, D. A.; Fandrick, K. R.; Song, H. J. *J. Am. Chem. Soc.* **2005**, *127*, (25), 8942-8943.
- (97) Appella, D. H.; Christianson, L. A.; Karle, I. L.; Powell, D. R.; Gellman, S. H. *J. Am. Chem. Soc.* **1996**, *118*, (51), 13071-13072.
- (98) Seebach, D.; Overhand, M.; Kuhnle, F. N. M.; Martinoni, B.; Oberer, L.; Hommel, U.; Widmer, H. *Helv. Chim. Acta* **1996**, *79*, (4), 913-941.
- (99) Seebach, D.; Matthews, J. L. *Chem. Commun.* **1997**, (21), 2015-2022.
- (100) Cheng, R. P.; Gellman, S. H.; DeGrado, W. F. *Chem. Rev.* **2001**, *101*, (10), 3219-3232.
- (101) Liu, M.; Sibi, M. P. *Tetrahedron* **2002**, *58*, (40), 7991-8035.
- (102) Ma, J. A. *Angew. Chem., Int. Ed.* **2003**, *42*, (36), 4290-4299.
- (103) Juaristi, E.; Soloshonok, V. A. *Enantioselective Synthesis of beta-Amino Acids* **2005**, Wiley-VCH: New York, 2005.
- (104) Daniels, D. S.; Petersson, E. J.; Qiu, J. X.; Schepartz, A. *J. Am. Chem. Soc.* **2007**, *129*, (6), 1532-1533.
- (105) Zhuang, W.; Hazell, R. G.; Jorgensen, K. A. *Chem. Comm.* **2001**, (14), 1240-1241.
- (106) Doi, H.; Sakai, T.; Iguchi, M.; Yamada, K.; Tomioka, K. *J. Am. Chem. Soc.* **2003**, *125*, (10), 2886-2887.
- (107) Fadini, L.; Togni, A. *Chem. Commun.* **2003**, (1), 30-31.
- (108) Xu, L. W.; Li, J. W.; Xia, C. G.; Zhou, S. L.; Hu, X. X. *Synlett* **2003**, (15), 2425-2427.
- (109) Xu, L. W.; Xia, C. G.; Li, J. W.; Zhou, S. L. *Synlett* **2003**, (14), 2246-2248.

- (110) Palomo, C.; Oiarbide, M.; Halder, R.; Kelso, M.; Gomez-Bengoa, E.; Garcia, J. M. *J. Am. Chem. Soc.* **2004**, *126*, (30), 9188-9189.
- (111) Shimizu, M.; Nishi, T. *Synlett* **2004**, (5), 889-891.
- (112) Xu, L. W.; Li, L.; Xia, C. G.; Zhou, S. L.; Li, J. W. *Tetrahedron Lett.* **2004**, *45*, (6), 1219-1221.
- (113) Reboule, I.; Gil, R.; Collin, J. *Tetrahedron-Asymmetry* **2005**, *16*, (23), 3881-3886.
- (114) Chen, Y. K.; Yoshida, M.; MacMillan, D. W. C. *J. Am. Chem. Soc.* **2006**, *128*, (29), 9328-9329.
- (115) Sakai, T.; Doi, H.; Tomioka, K. *Tetrahedron* **2006**, *62*, (35), 8351-8359.
- (116) Niu, D. Q.; Zhao, K. *J. Am. Chem. Soc.* **1999**, *121*, (11), 2456-2459.
- (117) Lee, H. S.; Park, J. S.; Kim, B. M.; Gellman, S. H. *J. Org. Chem.* **2002**, *68*, (4), 1575-1578.
- (118) Sibi, M. P.; Prabakaran, N.; Ghorpade, S. G.; Jasperse, C. P. *J. Am. Chem. Soc.* **2003**, *125*, (39), 11796-11797.
- (119) Ibrahim, I.; Rios, R.; Vesely, J.; Zhao, G. L.; Cordova, A. *Chem. Comm.* **2007**, (8), 849-851.
- (120) Anspon, H. D. *Org. Syn.*, Wiley: New York, 1955; Coll. Vol. III, p 711. .
- (121) Ogata, Y.; Takagi, Y. *J. Am. Chem. Soc.* **1958**, *80*, (14), 3591-3595.
- (122) Krageloh, K.; Anderson, G. H.; Stang, P. J. *J. Am. Chem. Soc.* **1984**, *106*, (20), 6015-6021.
- (123) Alonso, F.; Radivoy, G.; Yus, M. *Tetrahedron* **2000**, *56*, (44), 8673-8678.
- (124) Gilbert, A. M.; Failli, A.; Shumsky, J.; Yang, Y.; Severin, A.; Singh, G.; Hu, W.; Keeney, D.; Petersen, P. J.; Katz, A. H. *J. Med. Chem.* **2006**, *49*, (20), 6027-6036.

- (125) Ahern, M. F.; Leopold, A.; Beadle, J. R.; Gokel, G. W. *J. Am. Chem. Soc.* **1982**, *104*, (2), 548-554.
- (126) Bassam, F.; Jones, R. G. *J. Chem. Soc. Perkin Trans. II* **1985**, (11), 1759-1765.
- (127) Xun, S. D.; LeClair, G.; Zhang, J. D.; Chen, X.; Gao, J. P.; Wang, Z. Y. *Org. Lett.* **2006**, *8*, (8), 1697-1700.
- (128) Srinivasan, V.; Jebaratnam, D. J.; Budil, D. E. *J. Org. Chem.* **1999**, *64*, (15), 5644-5649.
- (129) Klapars, A.; Antilla, J. C.; Huang, X. H.; Buchwald, S. L. *J. Am. Chem. Soc.* **2001**, *123*, (31), 7727-7729.
- (130) Chan, A.; Scheidt, K. A. *J. Am. Chem. Soc.* **2006**, *128*, (14), 4558-4559.
- (131) Evans, D. A.; Scheidt, K. A.; Downey, C. W. *Org. Lett.* **2001**, *3*, (19), 3009-3012.
- (132) Pangborn, A. B.; Giardello, M. A.; Grubbs, R. H.; Rosen, R. K.; Timmers, F. J. *Organometallics* **1996**, *15*, (5), 1518-1520.
- (133) Perrin, D. D.; Armarego, W. L. *Purification of Laboratory Chemicals 3rd ed.*, Pergamon Press: Oxford, 1988.
- (134) Kirsch, G.; Prim, D.; Leising, F.; Mignani, G. *J. Heterocyclic Chem.* **1994**, *31*, (4), 1005-1009.
- (135) Hesse, S.; Kirsch, G. *Synthesis* **2001**, (5), 755-758.
- (136) Baldwin, J. E.; Mackenzieturner, S. C.; Moloney, M. G. *Tetrahedron* **1994**, *50*, (31), 9411-9424.
- (137) Battistuzzi, G.; Cacchi, S.; Fabrizi, G. *Org. Lett.* **2003**, *5*, (5), 777-780.
- (138) Barton, P.; Laws, A. P.; Page, M. I. **1994**, *J. Chem. Soc., Perkin Trans. 2*, (9), 2021-2029.
- (139) Kurono, N.; Sugita, K.; Takasugi, S.; Tokuda, M. *Tetrahedron* **1999**, *55*, (19), 6097-6108.

- (140) Kita, Y.; Akai, S.; Yamamoto, M.; Taniguchi, M.; Tamura, Y. *Synthesis* **1989**, (4), 334-337.
- (141) Peterson, P. E.; Stepanian, M. *J. Org. Chem.* **1988**, 53, (9), 1903-1907.
- (142) Arndtsen, B. A.; Bergman, R. G.; Mobley, T. A.; Peterson, T. H. *Acc.Chem. Res.* **1995**, 28, (3), 154-162.
- (143) Shilov, A. E.; Shul'pin, G. B. *Chem. Rev.* **1997**, 97, 2879-2932.
- (144) Labinger, J. A.; Bercaw, J. E. *Nature* **2002**, 417, (6888), 507-514.
- (145) Ritleng, V.; Sirlin, C.; Pfeffer, M. *Chem. Rev.* **2002**, 102, (5), 1731-1769.
- (146) Lersch, M.; Tilset, M. *Chem. Rev.* **2005**, 105, (6), 2471-2526.
- (147) Sakai, K.; Oda, O.; Nakamura, N.; Ide, J. *Tetrahedron Lett.* **1972**, (13), 1287-1290.
- (148) Lochow, C. F.; Miller, R. G. *J. Am. Chem. Soc.* **1976**, 98, (5), 1281-1283.
- (149) Suggs, J. W. *J. Am. Chem. Soc.* **1978**, 100, (2), 640-641.
- (150) Campbell, R. E.; Lochow, C. F.; Vora, K. P.; Miller, R. G. *J. Am. Chem. Soc.* **1980**, 102, (18), 5824-5830.
- (151) Milstein, D. *J. Chem. Soc., Chem. Comm.* **1982**, (23), 1357-1358.
- (152) Kampmeier, J. A.; Harris, S. H.; Mergelsberg, I. *J. Org. Chem.* **1984**, 49, (4), 621-625.
- (153) Larock, R. C.; Oertle, K.; Potter, G. F. *J. Am. Chem. Soc.* **1980**, 102, (1), 190-197.
- (154) James, B. R.; Young, C. G. *J. Chem. Soc., Chem. Comm.* **1983**, (21), 1215-1216.
- (155) James, B. R.; Young, C. G. *J. Organomet. Chem.* **1985**, 285, (1-3), 321-332.
- (156) Fairlie, D. P.; Bosnich, B. *Organometallics* **1988**, 7, (4), 936-945.
- (157) Fairlie, D. P.; Bosnich, B. *Organometallics* **1988**, 7, (4), 946-954.
- (158) Barnhart, R. W.; Wang, X. Q.; Noheda, P.; Bergens, S. H.; Whelan, J.; Bosnich, B. *J. Am. Chem. Soc.* **1994**, 116, (5), 1821-1830.

- (159) Barnhart, R. W.; Wang, X. Q.; Noheda, P.; Bergens, S. H.; Whelan, J.; Bosnich, B. *Tetrahedron* **1994**, *50*, (15), 4335-4346.
- (160) Barnhart, R. W.; Bosnich, B. *Organometallics* **1995**, *14*, (9), 4343-4348.
- (161) Barnhart, R. W.; McMorran, D. A.; Bosnich, B. *Inorg. Chim. Acta* **1997**, *263*, (1-2), 1-7.
- (162) Barnhart, R. W.; McMorran, D. A.; Bosnich, B. *Chem. Commun.* **1997**, (6), 589-590.
- (163) Bosnich, B. *Acc.Chem. Res.* **1998**, *31*, (10), 667-674.
- (164) Wu, X. M.; Funakoshi, K.; Sakai, K. *Tetrahedron Lett.* **1992**, *33*, (42), 6331-6334.
- (165) Sakai, K. *J. Synth. Org. Chem. (Jpn.)* **1993**, *51*, 733-743.
- (166) Fujio, M.; Tanaka, M.; Wu, X. M.; Funakoshi, K.; Sakai, K.; Suemune, H. *Chem. Lett.* **1998**, (9), 881-882.
- (167) Lenges, C. P.; Brookhart, M. *J. Am. Chem. Soc.* **1997**, *119*, (13), 3165-3166.
- (168) Aloise, A. D.; Layton, M. E.; Shair, M. D. *J. Am. Chem. Soc.* **2000**, *122*, (50), 12610-12611.
- (169) Tanaka, K.; Fu, G. C. *J. Am. Chem. Soc.* **2001**, *123*, (46), 11492-11493.
- (170) Kundu, K.; McCullagh, J. V.; Morehead, A. T. *J. Am. Chem. Soc.* **2005**, *127*, (46), 16042-16043.
- (171) Marder, T. B.; Roe, D. C.; Milstein, D. *Organometallics* **1988**, *7*, (6), 1451-1453.
- (172) Jun, C. H.; Hong, J. B.; Lee, D. Y. *Synlett* **1999**, (1), 1-12.
- (173) Jun, C. H.; Moon, C. W.; Lee, D. Y. *Chem. Eur. J.* **2002**, *8*, (11), 2423-2428.
- (174) Claisen, L. *Ber.* **1887**, *20*, 646.
- (175) Tishchenko, W. *J. Russ. Phys. Chem. Soc.* **1906**, *38*, 355.
- (176) Tishchenko, W. *Chem. Zentr.* **1906**, *II*, 1309-1311.
- (177) Tishchenko, W. *Chem. Zentr.* **1906**, *II*, 1552-1556.

- (178) Tishchenko, W. *J. Russ. Phys. Chem. Soc.* **1906**, 38, 482.
- (179) Kurti, L.; Czako *Strategic Applications of Named Reactions in Organic Synthesis*, Elsevier Academic Press: Oxford, 2005; pp 456.
- (180) Morita, K.; Nishiyama, Y.; Ishii, Y. *Organometallics* **1993**, 12, (9), 3748-3752.
- (181) Inoue, H.; Higashiura, K. *J. Chem. Soc., Chem. Comm.* **1980**, (12), 549-550.
- (182) Miyashita, A.; Suzuki, Y.; Nagasaki, I.; Ishiguro, C.; Iwamoto, K.; Higashino, T. *Chem. Pharm. Bull.* **1997**, 45, (8), 1254-1258.
- (183) Katritzky, A. R.; Harris, P. A. *J. Org. Chem.* **1991**, 56, (17), 5049-5051.
- (184) Moriarty, R. M.; Berglund, B. A.; Rao, M. S. C. *Synthesis* **1993**, (3), 318-321.
- (185) Kotali, A.; Papapetrou, M.; Dimos, V.; Harris, P. A. *Org. Prep. Proc., Int.* **1998**, 30, (2), 177-181.
- (186) Hill, R. A.; Sutherland, A. *Nat. Prod. Rep.* **2005**, 22, 436-438.
- (187) Nishizono, N.; Baba, R.; Nakamura, C.; Oda, K.; Machida, M. *Org. Biomol. Chem.* **2003**, 1, (21), 3692-3697.
- (188) Choi, Y. M.; Emblidge, R. W. *J. Org. Chem.* **1989**, 54, (5), 1198-1200.
- (189) Laumen, K.; Seemayer, R.; Schneider, M. P. *J. Chem. Soc., Chem. Comm.* **1990**, (1), 49-51.
- (190) Vedejs, E.; Daugulis, O.; Diver, S. T. *J. Org. Chem.* **1996**, 61, (2), 430-431.
- (191) Imoto, H.; Imamiya, E.; Momose, Y.; Sugiyama, Y.; Kimura, H.; Sohda, T. *Chem. Pharm. Bull.* **2002**, 50, (10), 1349-1357.
- (192) Levy, A.; Rakowitz, A.; Mills, N. S. *J. Org. Chem.* **2003**, 68, (10), 3990-3998.
- (193) Seebach, D.; Beck, A. K.; Gysi, P.; Vecchia, L. L. *Org. Synth.* **2004**, Coll. Vol. X, 349.
- (194) Kikugawa, Y. *Synthesis* **1981**, (2), 124-125.

- (195) Miyashita, A.; Matsuda, H.; Iijima, C.; Higashino, T. *Chem. Pharm. Bull.* **1990**, *38*, (5), 1147-1152.
- (196) Wolfe, J. P.; Ahman, J.; Sadighi, J. P.; Singer, R. A.; Buchwald, S. L. *Tetrahedron Lett.* **1997**, *38*, (36), 6367-6370.
- (197) Bolm, C.; Hildebrand, J. P. *Tetrahedron Lett.* **1998**, *39*, (32), 5731-5734.
- (198) Hori, K.; Mori, M. *J. Am. Chem. Soc.* **1998**, *120*, (30), 7651-7652.
- (199) Jaime-Figueroa, S.; Liu, Y. Z.; Muchowski, J. M.; Putman, D. G. *Tetrahedron Lett.* **1998**, *39*, (11), 1313-1316.
- (200) Mann, G.; Hartwig, J. F.; Driver, M. S.; Fernandez-Rivas, C. *J. Am. Chem. Soc.* **1998**, *120*, (4), 827-828.
- (201) Huang, X. H.; Buchwald, S. L. *Org. Lett.* **2001**, *3*, (21), 3417-3419.
- (202) Lee, S.; Jorgensen, M.; Hartwig, J. F. *Org. Lett.* **2001**, *3*, (17), 2729-2732.
- (203) Wenderski, T.; Light, K. M.; Ogrin, D.; Bott, S. G.; Harlan, C. J. *Tetrahedron Lett.* **2004**, *45*, (37), 6851-6853.
- (204) Huang, W.; Guo, E. P.; Xiao, Y. J.; Zhu, M. F.; Zou, G.; Tang, J. *Tetrahedron* **2005**, *61*, (41), 9783-9790.
- (205) Abiko, A.; Masamune, S. *Tetrahedron Lett.* **1992**, *33*, (38), 5517-5518.
- (206) Davies, S. G.; Sanganee, H. J.; Szolcsanyi, P. *Tetrahedron* **1999**, *55*, (11), 3337-3354.
- (207) Xu, P. F.; Chen, Y. S.; Lin, S. I.; Lu, T. J. *J. Org. Chem.* **2002**, *67*, (7), 2309-2314.
- (208) Mboungoumpassi, A.; Henin, F.; Muzart, J.; Pete, J. P. *Bull. Soc. Chim. Fr.* **1993**, *130*, (2), 214-217.
- (209) Gawley, R. E.; Zhang, P. S. *J. Org. Chem.* **1996**, *61*, (23), 8103-8112.
- (210) Norman, B. H.; Kroin, J. S. *J. Org. Chem.* **1996**, *61*, (15), 4990-4998.

- (211) Kerr, M. S.; de Alaniz, J. R.; Rovis, T. *J. Org. Chem.* **2005**, *70*, (14), 5725-5728.
- (212) Knight, R. L.; Leeper, F. J. *J. Chem. Soc., Perkin Trans. I* **1998**, (12), 1891-1893.
- (213) Knolker, H. J.; Braxmeier, T. *Tetrahedron Lett.* **1998**, *39*, (51), 9407-9410.

Appendix 1

Structure Refinement Data, Atomic Coordinates, Bond Lengths and Bond Angle Data for the Crystal Structure I-115m

Crystal structure data provided by Dr. Charlotte Stern (Northwestern University, c-stern@northwestern.edu) and solved by Troy Reynolds (Northwestern University, t-reynolds2@northwestern.edu)

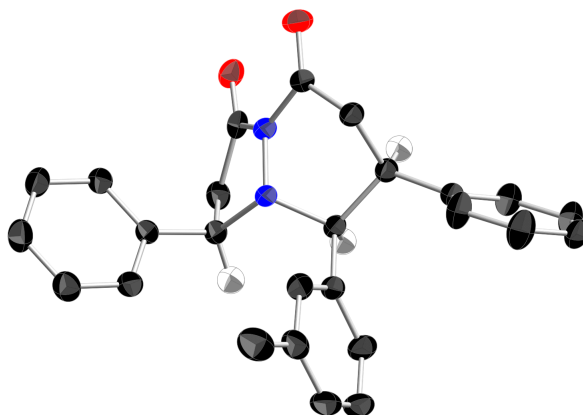
X-Ray Crystal Structure Analysis for I-115m

Figure A.1.1. The diastereoselectivity of **I-115m** was determined by X-ray crystallography. Pyridazinone **I-115m** was crystallized from slow-diffusion of hexanes into methylene chloride.

Table A.1.1. Crystal data and structure refinement for **I-115m**.

Identification Code	s26um
Empirical formula	C ₂₆ H ₂₄ N ₂ O ₂
Formula weight	396.47
Temperature	153 (2) K
Wavelength	0.71073 Å
Crystal System	Monoclinic
Space group	P-1
Unit cell dimensions	a = 9.4020 (7) Å α = 93.6650(10)°. b = 10.0753 (7) Å β = 95.4380 (10)°. c = 10.8800 (8) Å γ = 91.5370 (10)°.
Volume	1023.34 (13) Å ³
Z	2
Absorption coefficient	0.082 mm ⁻¹
F(000)	420
Theta range for data collection	1.88 to 28.82°
Index ranges	-12 ≤ h ≤ 12, -13 ≤ k ≤ 13, -14 ≤ l ≤ 14
Reflections collected	4750
Independent reflections	4137
Completeness of theta = 28.82°	98.7%
Absorption correction	None
Refinement method	Full-matrix least-squares on F ²
Data/ restraints/ parameters	4750/0/281
Goodness-of-fit on F ²	1.061

Final R indices [$I > 2\sigma(I)$] $R1 = 0.0678$, $wR2 = 0.1805$
 R indices (all data) $R1 = 0.0612$, $wR2 = 0.1746$

Table A.1.2. Atomic coordinates and equivalent isotropic displacement parameters ($\text{\AA}^2 \times 10^3$) for **I-115m**. $U(\text{eq})$ is defined as one third of the traces of the orthogonalized U^{ij} tensor.

	x	y	z	U(eq)
C1	0.89261(19)	0.40262(17)	0.40866(15)	0.0261(4)
C2	0.76481(19)	0.48806(18)	0.42032(17)	0.0290(4)
C3	0.65163(18)	0.39174(17)	0.46004(15)	0.0256(4)
C4	0.55712(18)	0.32172(17)	0.35358(15)	0.0251(3)
C5	0.60381(19)	0.29806(18)	0.23619(16)	0.0292(4)
C6	0.5142(2)	0.2346(2)	0.14022(17)	0.0342(4)
C7	0.3755(2)	0.1962(2)	0.15991(19)	0.0379(4)
C8	0.3283(2)	0.2175(2)	0.27644(19)	0.0362(4)
C9	0.41930(19)	0.27897(19)	0.37289(17)	0.0304(4)
C10	0.96511(19)	0.19543(17)	0.51457(16)	0.0269(4)
C11	0.92647(19)	0.14191(17)	0.63379(16)	0.0269(4)
C12	0.89631(18)	0.26403(17)	0.71980(15)	0.0243(3)
C13	0.75874(18)	0.33226(17)	0.66682(15)	0.0246(3)
C14	0.61976(19)	0.29545(19)	0.71858(16)	0.0294(4)
C15	0.5444(2)	0.1783(2)	0.67904(17)	0.0341(4)
C16	0.4124(2)	0.1481(2)	0.72244(19) 0	.0399(5)
C17	0.3596(2)	0.2378(3)	0.8082(2)	0.0470(6)
C18	0.4327(2)	0.3536(3)	0.8486(2)	0.0448(5)
C19	0.5632(2)	0.3841(2)	0.80346(18)	0.0382(5)
C20	0.90166(18)	0.23525(17)	0.85482(15)	0.0258(3)
C21	0.9809(2)	0.3210(2)	0.94208(18)	0.0357(4)
C22	0.9943(2)	0.2964(2)	1.06702(19)	0.0408(5)
C23	0.9277(2)	0.1854(2)	1.10637(17)	0.0368(4)
C24	0.8481(3)	0.1004(2)	1.0208(2)	0.0461(5)
C25	0.8345(2)	0.1248(2)	0.89591(18)	0.0400(5)
C26	0.3280(3)	0.0294(3)	0.6728(3)	0.0519(6)
N1	0.86872(15)	0.29142(14)	0.47540(13)	0.0242(3)
N2	0.73646(15)	0.29301(14)	0.53109(12)	0.0236(3)
O1	0.99650(14)	0.42288(13)	0.35390(11)	0.0317(3)
O2	0.07027(15)	0.17087(15)	0.46236(13)	0.0376(3)

Table A.1.3. Anisotropic displacement parameters ($\text{\AA}^2 \times 10^3$) for **I-115m**.

	U^{11}	U^{22}	U^{33}	U^{23}	U^{13}	U^{12}
C1	0.0312(8)	0.0274(8)	0.0185(7)	0.0002(6)	0.0011(6)	-0.0035(6)

C2	0.0333(9)	0.0264(8)	0.0265(8)	0.0033(6)	-0.0022(7)	0.0013(7)
C3	0.0275(8)	0.0273(8)	0.0222(8)	0.0024(6)	0.0012(6)	0.0062(6)
C4	0.0260(8)	0.0253(8)	0.0239(8)	0.0031(6)	0.0006(6)	0.0054(6)
C5	0.0278(8)	0.0343(9)	0.0258(8)	0.0044(7)	0.0024(7)	0.0021(7)
C6	0.0395(10)	0.0399(10)	0.0231(8)	0.0025(7)	0.0021(7)	0.0012(8)
C7	0.0402(10)	0.0417(11)	0.0298(9)	0.0016(8)	-0.0045(8)	-0.0066(8)
C8	0.0298(9)	0.0417(11)	0.0368(10)	0.0050(8)	0.0012(8)	-0.0043(8)
C9	0.0294(9)	0.0344(9)	0.0282(9)	0.0046(7)	0.0043(7)	0.0050(7)
C10	0.0279(8)	0.0285(8)	0.0245(8)	-0.0008(6)	0.0036(6)	0.0056(6)
C11	0.0308(8)	0.0266(8)	0.0239(8)	0.0030(6)	0.0041(6)	0.0069(6)
C12	0.0259(8)	0.0248(8)	0.0222(8)	0.0020(6)	0.0025(6)	0.0016(6)
C13	0.0270(8)	0.0277(8)	0.0194(7)	0.0011(6)	0.0034(6)	0.0048(6)
C14	0.0279(8)	0.0404(10)	0.0218(8)	0.0081(7)	0.0052(6)	0.0094(7)
C15	0.0293(9)	0.0466(11)	0.0275(9)	0.0063(8)	0.0052(7)	0.0020(8)
C16	0.0297(9)	0.0582(13)	0.0337(10)	0.0168(9)	0.0034(8)	0.0010(9)
C17	0.0325(10)	0.0796(17)	0.0347(11)	0.0267(11)	0.0144(8)	0.0176(10)
C18	0.0479(12)	0.0601(14)	0.0320(10)	0.0165(9)	0.0178(9)	0.0236(11)
C19	0.0446(11)	0.0465(11)	0.0273(9)	0.0113(8)	0.0114(8)	0.0195(9)
C20	0.0259(8)	0.0302(8)	0.0218(8)	0.0025(6)	0.0027(6)	0.0051(6)
C21	0.0446(11)	0.0327(10)	0.0288(9)	0.0002(7)	0.0001(8)	-0.0019(8)
C22	0.0518(12)	0.0424(11)	0.0259(9)	-0.0036(8)	-0.0041(8)	0.0019(9)
C23	0.0445(11)	0.0453(11)	0.0214(8)	0.0045(7)	0.0037(7)	0.0088(9)
C24	0.0630(14)	0.0460(12)	0.0295(10)	0.0115(9)	0.0031(9)	-0.0107(10)
C25	0.0525(12)	0.0408(11)	0.0254(9)	0.0045(8)	-0.0009(8)	-0.0114(9)
C26	0.0439(12)	0.0538(14)	0.0598(15)	0.0146(11)	0.0078(11)	0.0000(10)
N1	0.0248(7)	0.0278(7)	0.0209(7)	0.0029(5)	0.0055(5)	0.0032(5)
N2	0.0232(7)	0.0296(7)	0.0189(6)	0.0031(5)	0.0038(5)	0.0051(5)
O1	0.0335(7)	0.0374(7)	0.0244(6)	0.0021(5)	0.0057(5)	-0.0072(5)
O2	0.0354(7)	0.0460(8)	0.0342(7)	0.0049(6)	0.0124(6)	0.0141(6)

Table A.1.4. Hydrogen coordinates and isotropic displacement parameters ($\text{\AA}^2 \times 10^3$) for **I-115m**.

	x	y	z	U(eq)
H2A	0.7326	0.5243	0.3403	0.035
H2B	0.7869	0.5628	0.4835	0.035
H3	0.590(2)	0.441(2)	0.517(2)	0.031
H5	0.6979	0.3257	0.2219	0.035
H6	0.5476	0.2176	0.0612	0.041
H7	0.3131	0.1554	0.0937	0.046
H8	0.2340	0.1902	0.2903	0.043
H9	0.3871	0.2919	0.4528	0.036
H11A	1.0063	0.0916	0.6718	0.032
H11B	0.8407	0.0818	0.6183	0.032
H12	0.977(2)	0.330(2)	0.714(2)	0.029

H13	0.775(2)	0.431(2)	0.678(2)	0.029
H15	0.5826	0.1174	0.6216	0.041
H17	0.2709	0.2179	0.8392	0.056
H18	0.3949	0.4135	0.9072	0.054
H19	0.6135	0.4654	0.8307	0.046
H21	1.0269	0.3979	0.9160	0.043
H22	1.0492	0.3562	1.1252	0.049
H23	0.9368	0.1677	1.1914	0.044
H24	0.8016	0.0240	1.0474	0.055
H25	0.7787	0.0651	0.8383	0.048
H26A	0.2685	0.0499	0.5979	0.078
H26B	0.2666	0.0007	0.7348	0.078
H26C	0.3922	-0.0421	0.6525	0.078

Table A.1.5. Bond lengths (\AA) for **I-115m**.

C1-O1	1.211
C1-N1	1.398(2)
C1-C2	1.507(3)
C2-C3	1.532(2)
C3-N2	1.499(2)
C3-C4	1.515(2)
C4-C9	1.394(2)
C4-C5	1.398(2)
C5-C6	1.388(3)
C6-C7	1.390(3)
C7-C8	1.388(3)
C8-C9	1.391(3)
C10-O2	1.210(2)
C10-N1	1.402(2)
C10-C11	1.508(2)
C11-C12	1.547(2)
C12-C20	1.512(2)
C12-C13	1.560(2)
C13-N2	1.498(2)
C13-C14	1.517(2)
C14-C15	1.383(3)
C14-C19	1.395(3)
C15-C16	1.402(3)
C16-C17	1.392(3)
C16-C26	1.461(3)
C17-C18	1.365(4)
C18-C19	1.398(3)
C20-C25	1.384(3)
C20-C21	1.389(3)
C21-C22	1.392(3)

C22-C23	1.379(3)
C23-C24	1.375(3)
C24-C25	1.391(3)
N1-N2	1.4339(19)

Table A.1.6. Bond angles (degrees) for **I-115m**.

O1-C1-N1	125.47(16)
O1-C1-C2	105.95(14)
C1-C2-C3	103.46(14)
N2-C3-C4	110.55(13)
N2-C3-C2	104.22(13)
C4-C3-C2	114.26(14)
C9-C4-C5	118.69(16)
C9-C4-C3	119.21(15)
C5-C4-C3	122.10(16)
C6-C5-C4	120.72(17)
C5 C6 C7	119.92(18)
C8-C7-C6	119.97(18)
C7-C8-C9	119.91(18)
C8-C9-C4	120.75(17)
O2-C10-N1	122.27(16)
O2-C10-C11	126.74(16)
N1-C10-C11	110.70(14)
C10-C11-C12	106.41(14)
C20-C12-C11	113.62(14)
C20-C12-C13	115.47(14)
C11-C12-C13	109.98(13)
N2-C13- C14	105.82(13)
N2-C13-C12	107.38(13)
C14-C13-C12	117.16(14)
C15-C14-C19	119.15(18)
C15-C14-C13	121.30(16)
C19-C14-C13	119.48(18)
C14-C15-C16	121.03(19)
C17-C16-C15	118.5(2)
C17-C16-C26	120.7(2)
C15-C16-C26	120.7(2)
C18-C17-C16	121.35(19)
C17-C18-C19	119.9(2)
C14-C19-C18	120.1(2)
C25-C20-C21	117.99(17)
C25-C20-C12	123.09(16)
C21-C20-C12	118.89(16)
C20-C21-C22	121.32(19)
C23-C22-C21	120.00(19)
C24-C23-C22	119.12(18)

C23-C24-C25	121.0(2)
C20-C25-C24	120.58(19)
C1-N1-C10	128.99(15)
C1-N1-N2	113.68(13)
C10-N1-N2	116.01(13)
N1-N2-C13	111.84(12)
N1-N2-C3	103.17(12)
C13-N2-C3	112.51(13)

Appendix 2

Structure Refinement Data, Atomic Coordinates, Bond Lengths and Bond Angle Data for the Crystal Structure II-19n

Crystal structure data provided by Dr. Charlotte Stern (Northwestern University, c-stern@northwestern.edu) and solved by Troy Reynolds (Northwestern University, t-reynolds2@northwestern.edu)

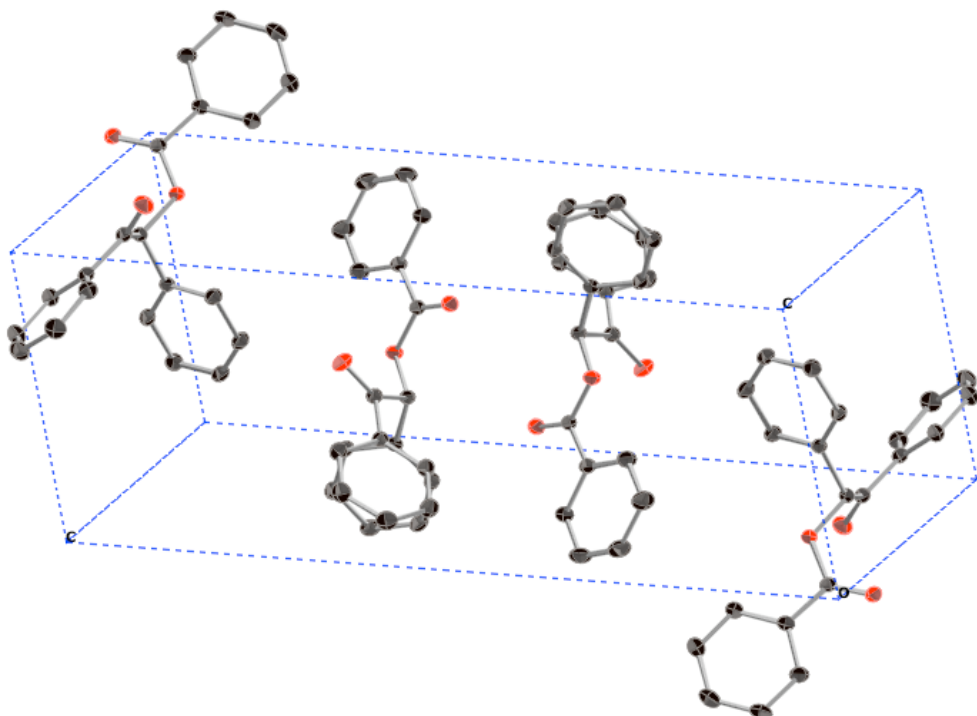
X-Ray Crystal Structure Analysis for II-19n

Figure A.2.1. The diastereoselectivity of **II-19n** was determined by X-ray crystallography. Pyridazinone **II-19n** was crystallized from slow-diffusion of hexanes into methylene chloride.

Table A.2.1. Crystal data and structure refinement for **II-19n**.

Identification Code	s08tm	
Empirical formula	C ₂₁ H ₁₆ O ₃	
Formula weight	316.34	
Temperature	153 (2) K	
Wavelength	0.71073 Å	
Crystal System	Monoclinic	
Space group	P2(1)/c	
Unit cell dimensions	a = 8.6694 (7) Å	$\alpha = 90.00^\circ$.
	b = 22.1068(17) Å	$\beta = 100.1520 (10)^\circ$.
	c = 8.7642(7) Å	$\chi = 90.00^\circ$.
Volume	1653.4 (2) Å ³	
Z	4	
Absorption coefficient	0.084 mm ⁻¹	
F(000)	664	
Crystal size	4.3 x 3.5 x 2.3 mm ³	

Theta range for data collection	2.52 to 28.40°
Index ranges	-11≤h≤11, -29≤k≤28, -11≤l≤11
Reflections collected	4808
Independent reflections	4032
Completeness of theta = 28.40°	98.7%
Absorption correction	None
Refinement method	Full-matrix least-squares on F ²
Data/ restraints/ parameters	4032/0/281
Goodness-of-fit on F ²	1.039
Final R indices [I>2sigma(I)]	R1 = 0.0412, wR2 = 0.1141
R indices (all data)	R1 = 0.0488, wR2 = 0.1212

Table A.2.2. Atomic coordinates and equivalent isotropic displacement parameters ($\text{\AA}^2 \times 10^3$) for **II-19n**. U(eq) is defined as one third of the traces of the orthogonalized U^{ij} tensor.

	x	y	z	U(eq)
O3	0.49728(9)	0.37280(3)	0.48279(9)	0.02805(19)
O1	0.46023(10)	0.45033(4)	0.31423(9)	0.0324(2)
O2	0.77319(11)	0.36059(4)	0.40442(10)	0.0394(2)
C10	0.63502(12)	0.37935(5)	0.73999(12)	0.0246(2)
C7	0.42781(12)	0.39972(5)	0.35068(12)	0.0254(2)
C17	0.92108(13)	0.42253(5)	0.59669(12)	0.0268(2)
C1	0.30613(13)	0.36040(5)	0.25949(12)	0.0276(2)
C9	0.62288(12)	0.40537(5)	0.57829(12)	0.0250(2)
C15	0.62324(13)	0.41608(5)	0.86601(13)	0.0288(2)
C16	0.77395(13)	0.39415(5)	0.51380(12)	0.0274(2)
C14	0.63138(16)	0.39061(6)	1.01198(13)	0.0356(3)
C2	0.28014(16)	0.30161(6)	0.30521(15)	0.0372(3)
C6	0.21617(16)	0.38401(6)	0.12491(14)	0.0362(3)
C18	0.92192(13)	0.47510(5)	0.68457(14)	0.0310(2)
C13	0.64911(17)	0.32900(6)	1.03285(14)	0.0385(3)
C12	0.66038(18)	0.29219(5)	0.90725(14)	0.0403(3)
C11	0.65469(16)	0.31746(5)	0.76164(13)	0.0352(3)
C5	0.10043(17)	0.34884(7)	0.03784(16)	0.0447(3)
C20	1.20253(15)	0.46970(6)	0.75162(16)	0.0407(3)
C22	1.06255(14)	0.39417(6)	0.58571(14)	0.0344(3)
C19	1.06337(15)	0.49912(6)	0.76054(15)	0.0378(3)
C21	1.20210(15)	0.41722(6)	0.66529(16)	0.0410(3)
C3	0.16546(18)	0.26647(7)	0.21666(17)	0.0468(3)
C4	0.07510(18)	0.29042(7)	0.08347(17)	0.0475(3)

Table A.2.3. Anisotropic displacement parameters ($\text{\AA}^2 \times 10^3$) for **II-19n**.

	U^{11}	U^{22}	U^{33}	U^{23}	U^{13}	U^{12}
O3	0.0314(4)	0.0274(4)	0.0229(4)	0.0022(3)	-0.0022(3)	-0.0039(3)
O1	0.0417(5)	0.0269(4)	0.0267(4)	0.0027(3)	0.0008(3)	-0.0009(3)
O2	0.0441(5)	0.0445(5)	0.0303(4)	-0.0118(4)	0.0084(4)	0.0040(4)
C10	0.0250(5)	0.0262(5)	0.0218(5)	0.0012(4)	0.0017(4)	0.011(4)
C7	0.0281(5)	0.0269(5)	0.0210(5)	-0.0003(4)	0.0039(4)	0.0033(4)
C17	0.0299(5)	0.0284(5)	0.0226(5)	0.0029(4)	0.0056(4)	-0.0008(4)
C1	0.0280(5)	0.0312(5)	0.0230(5)	-0.0027(4)	0.0025(4)	0.0012(4)
C9	0.0282(5)	0.0234(5)	0.0219(5)	0.0001(4)	0.0002(4)	-0.0019(4)
C15	0.0346(6)	0.0245(5)	0.0279(5)	-0.0004(4)	0.0072(4)	0.0005(4)
C16	0.0341(6)	0.0263(5)	0.0215(5)	0.0015(4)	0.0044(4)	-0.0008(4)
C14	0.0502(7)	0.0334(6)	0.0250(5)	-0.0047(4)	0.0113(5)	-0.0038(5)
C2	0.0423(7)	0.0347(6)	0.0314(6)	0.0010(5)	-0.0020(5)	-0.0050(5)
C6	0.0415(7)	0.0358(6)	0.0279(6)	-0.0007(5)	-0.0028(5)	0.0028(5)
C18	0.0294(6)	0.0301(5)	0.0335(6)	-0.0013(4)	0.0052(4)	-0.0011(4)
C13	0.0571(8)	0.0350(6)	0.0227(5)	0.0042(4)	0.0054(5)	-0.0058(5)
C12	0.0664(9)	0.0245(6)	0.0288(6)	0.0026(4)	0.0051(6)	0.0004(5)
C11	0.0553(7)	0.0261(5)	0.0234(5)	-0.0020(4)	0.0050(5)	0.0014(5)
C5	0.0451(7)	0.0495(8)	0.0334(6)	-0.0051(5)	-0.0098(5)	0.0028(6)
C20	0.0292(6)	0.0475(7)	0.0439(7)	-0.0021(6)	0.0022(5)	-0.0067(5)
C22	0.0363(6)	0.0358(6)	0.0321(6)	-0.0018(5)	0.0091(5)	0.0027(5)
C19	0.0353(6)	0.0346(6)	0.0428(7)	-0.0058(5)	0.0045(5)	-0.0056(5)
C21	0.0293(6)	0.0487(7)	0.0458(7)	-0.0009(6)	0.0085(5)	0.0040(5)
C3	0.0547(8)	0.0391(7)	0.0430(7)	-0.0017(6)	-0.0012(6)	-0.0144(6)
C4	0.0439(8)	0.0528(8)	0.0413(7)	-0.0118(6)	-0.0049(6)	-0.0103(6)

Table A.2.4. Hydrogen coordinates and isotropic displacement parameters ($\text{\AA}^2 \times 10^3$) for **II-19n**.

	x	y	z	U(eq)
H3	0.150(2)	0.2255(8)	0.2479(19)	0.052(5)
H11	0.6660(19)	0.2928(7)	0.6754(19)	0.045(4)
H13	0.6504(19)	0.3119(7)	1.1341(19)	0.046(4)
H20	1.301(2)	0.4856(8)	0.806(2)	0.063(5)
H5	0.035(2)	0.3653(8)	-0.055(2)	0.054(5)
H6	0.231(2)	0.4258(8)	0.0939(19)	0.049(4)
H21	1.302(2)	0.3955(8)	0.664(2)	0.056(5)
H4	-0.007(2)	0.2653(8)	0.0211(19)	0.051(4)
H19	1.0666(18)	0.5362(7)	0.8212(18)	0.042(4)
H22	1.0601(18)	0.3579(7)	0.5258(18)	0.039(4)
H12	0.6712(19)	0.2485(8)	0.9186(19)	0.049(4)
H14	0.6189(19)	0.4169(7)	1.0986(18)	0.044(4)

H18	0.8192(18)	0.4967(6)	0.6905(17)	0.035(3)
H2	0.340(2)	0.2853(7)	0.3984(19)	0.046(4)
H15	0.6081(16)	0.4590(7)	0.8519(15)	0.032(3)
H9	0.6010(15)	0.4486(6)	0.5782(14)	0.025(3)

Table A.2.5. Bond lengths (Å) for **II-19n**.

O3-C7	1.3460(12)
O3-C9	1.4434(12)
O1-C7	1.2103(13)
O2-C16	1.2113(13)
C10-C11	1.3877(15)
C10-C15	1.3889(15)
C10-C9	1.5159(14)
C7-C1	1.4865(15)
C17-C18	1.3935(16)
C17-C22	1.3958(16)
C17-C16	1.4905(15)
C1-C2	1.3902(17)
C1-C6	1.3956(16)
C9-C16	1.5353(16)
C15-C14	1.3881(16)
C14-C13	1.3793(18)
C2-C3	1.3865(18)
C6-C5	1.3870(18)
C18-C19	1.3932(17)
C13-C12	1.3861(17)
C12-C11	1.3860(16)
C5-C4	1.381(2)
C20-C21	1.385(2)
C20-C19	1.3849(19)
C22-C21	1.3829(18)
C3-C4	1.391(2)

Table A.2.6. Bond angles (degrees) for **II-19n**.

C7-O3-C9	117.11(8)
C11-C10-C15	119.48(10)
C11-C10-C9	119.24(9)
C15-C10-C9	121.26(9)
O1-C7-O3	123.11(10)
O1-C7-C1	125.06(10)
O3-C7-C1	111.81(9)
C18-C17-C22	119.59(10)

C18-C17-C16	122.76(10)
C22-C17-C16	117.65(10)
C2-C1-C6	119.90(11)
C2-C1-C7	121.83(10)
C6-C1-C7	118.27(10)
O3-C9-C10	105.89(8)
O3-C9-C16	108.13(8)
C10-C9-C16	111.08(9)
C14-C15-C10	119.80(10)
O2-C16-C17	121.89(10)
O2-C16-C9	120.28(10)
C17-C16-C9	117.70(9)
C13-C14-C15	120.60(11)
C3-C2-C1	119.95(12)
C5-C6-C1	119.85(12)
C17-C18-C19	120.02(11)
C14-C13-C12	119.75(11)
C11-C12-C13	119.90(11)
C12-C11-C10	120.46(11)
C4-C5-C6	120.10(12)
C21-C20-C19	120.39(12)
C21-C22-C17	120.06(12)
C20-C19-C18	119.75(12)
C22-C21-C20	120.15(12)
C2-C3-C4	119.91(13)
C5-C4-C3	120.29(12)

Appendix 3

Structure Refinement Data, Atomic Coordinates, Bond Lengths and Bond Angle Data for the Crystal Structure II-54

Crystal structure data provided by Dr. Charlotte Stern (Northwestern University, c-stern@northwestern.edu) and solved by Troy Reynolds (Northwestern University, t-reynolds2@northwestern.edu)

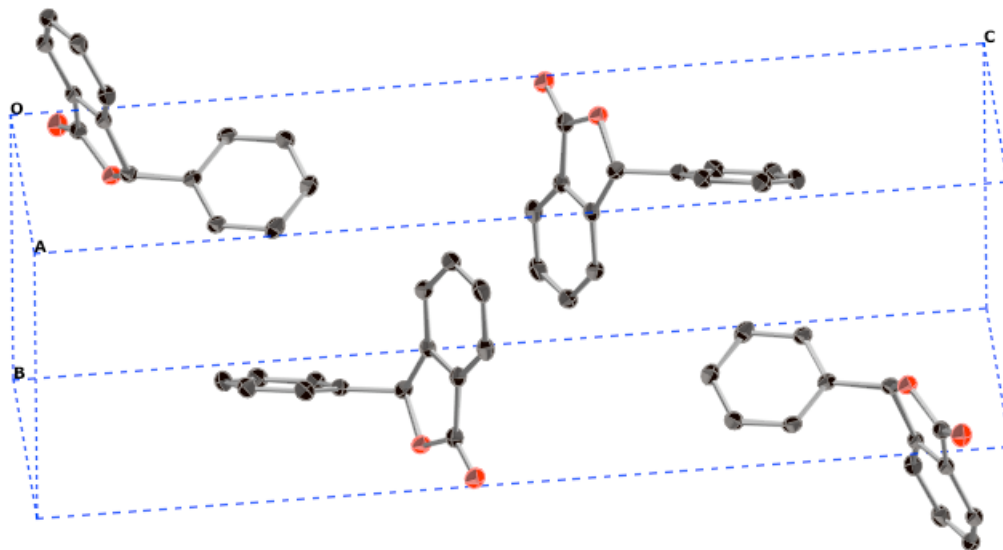
X-Ray Crystal Structure Analysis for II-54

Figure A.3.1. The diastereoselectivity of **II-54** was determined by X-ray crystallography. Pyridazinone **II-54** was crystallized from slow-diffusion of hexanes into methylene chloride.

Table A.3.1. Crystal data and structure refinement for **II-54**.

Identification Code	s12tm	
Empirical formula	C ₁₄ H ₉ O ₂	
Formula weight	209.21	
Temperature	153 (2) K	
Wavelength	0.71073 Å	
Crystal System	Monoclinic	
Space group	P2(1)/c	
Unit cell dimensions	a = 6.0122 (8) Å	$\alpha = 90.00^\circ$.
	b = 7.4709 (10) Å	$\beta = 91.549 (2)^\circ$.
	c = 23.148 (3) Å	$\chi = 90.00^\circ$.
Volume	1039.4 (2) Å ³	
Z	4	
Absorption coefficient	0.089	
F(000)	664	
Crystal size	4.1 x 1.9 x 1.4 mm ³	
Theta range for data collection	2.73 to 28.53°	
Index ranges	-8 ≤ h ≤ 7, -9 ≤ k ≤ 9, -29 ≤ l ≤ 30	

Reflections collected	4320
Independent reflections	2479
Completeness of theta = 28.53°	99.5%
Absorption correction	None
Refinement method	Full-matrix least-squares on F ²
Data/ restraints/ parameters	2479/0/185
Goodness-of-fit on F ²	1.095
Final R indices [I>2sigma(I)]	R1 = 0.1557, wR2 = 0.0572
R indices (all data)	R1 = 0.1648, wR2 = 0.0731

Table A.3.2. Atomic coordinates and equivalent isotropic displacement parameters ($\text{\AA}^2 \times 10^3$) for **II-54**. U(eq) is defined as one third of the traces of the orthogonalized U^{ij} tensor.

	x	y	z	U(eq)
O1	1.0687(2)	0.79527(18)	0.39428(6)	0.0302(3)
O2	1.3960(2)	0.7632(2)	0.44171(7)	0.0368(4)
C9	0.8118(3)	0.6933(2)	0.31753(8)	0.0261(4)
C4	0.8682(3)	0.6889(3)	0.38136(8)	0.0261(4)
C1	1.2222(3)	0.6967(3)	0.42504(8)	0.0288(4)
C10	0.6130(3)	0.7687(3)	0.29772(9)	0.0291(4)
C14	0.9561(3)	0.6183(3)	0.27803(9)	0.0314(5)
C2	1.1359(3)	0.5144(3)	0.43131(8)	0.0271(4)
C12	0.7010(4)	0.6948(3)	0.20033(9)	0.0353(5)
C13	0.9012(4)	0.6200(3)	0.21965(9)	0.0340(5)
C5	0.8042(4)	0.3514(3)	0.40499(9)	0.0323(5)
C3	0.9262(3)	0.5080(3)	0.40546(8)	0.0264(4)
C6	0.8998(4)	0.2019(3)	0.43104(10)	0.0378(5)
C7	1.1128(4)	0.2084(3)	0.45673(9)	0.0385(5)
C8	1.2327(4)	0.3655(3)	0.45772(9)	0.0329(5)
C11	0.5574(4)	0.7685(3)	0.23904(10)	0.0356(5)

Table A.3.3. Anisotropic displacement parameters ($\text{\AA}^2 \times 10^3$) for **II-54**.

	U ¹¹	U ²²	U ³³	U ²³	U ¹³	U ¹²
O1	0.0264(7)	0.0303(7)	0.0337(8)	0.0007(6)	-0.0037(6)	-0.0004(5)
O2	0.0239(7)	0.0499(9)	0.0363(9)	-0.0006(7)	-0.0033(6)	-0.0049(6)
C9	0.0237(9)	0.0239(9)	0.0306(10)	0.0022(7)	-0.0010(7)	0.0001(7)
C4	0.0199(8)	0.0283(9)	0.0299(10)	-0.0017(8)	-0.0007(7)	0.0019(7)
C1	0.0243(9)	0.0357(10)	0.0267(10)	-0.0007(8)	0.0028(7)	0.0037(8)
C10	0.0244(9)	0.0309(10)	0.0320(10)	0.0030(8)	0.0004(8)	0.0037(7)
C14	0.0292(10)	0.0296(10)	0.0356(11)	0.0039(8)	0.0014(8)	0.0073(8)
C2	0.0257(9)	0.0316(10)	0.0241(9)	-0.0018(7)	0.0029(7)	0.0029(7)
C12	0.0399(11)	0.0369(11)	0.0290(11)	0.0058(9)	-0.0036(9)	-0.0023(9)
C13	0.0401(11)	0.0299(10)	0.0322(11)	-0.0001(8)	0.0063(9)	0.0035(9)

C5	0.0346(10)	0.0348(11)	0.0276(10)	-0.0018(8)	0.0015(8)	-0.0036(8)
C3	0.0263(9)	0.0303(9)	0.0228(9)	-0.0001(7)	0.0040(7)	0.0030(7)
C6	0.0509(13)	0.0321(11)	0.0307(11)	-0.0001(9)	0.0062(9)	-0.0049(10)
C7	0.0548(14)	0.0335(11)	0.0275(11)	0.0041(9)	0.0054(9)	0.0114(10)
C8	0.0341(11)	0.0386(11)	0.0259(10)	0.0002(8)	0.0023(8)	0.0095(9)
C11	0.0283(10)	0.0410(12)	0.0371(12)	0.0099(9)	-0.0043(8)	0.0021(9)

Table A.3.4. Hydrogen coordinates and isotropic displacement parameters ($\text{\AA}^2 \times 10^3$) for **II-54**.

	x	y	z	U(eq)
H4	0.754(4)	0.745(3)	0.4028(10)	0.027(5)
H7	1.172(4)	0.102(3)	0.4724(10)	0.037(6)
H10	0.521(4)	0.826(3)	0.3252(10)	0.027(5)
H12	0.667(4)	0.684(4)	0.1597(12)	0.047(7)
H14	1.088(4)	0.571(3)	0.2913(10)	0.036(6)
H6	0.812(4)	0.094(4)	0.4269(11)	0.045(7)
H8	1.384(4)	0.374(3)	0.4758(11)	0.045(7)
H13	1.006(5)	0.572(4)	0.1922(12)	0.062(8)
H5	0.652(5)	0.355(4)	0.3856(12)	0.051(7)
H11	0.414(4)	0.819(3)	0.2261(11)	0.039(6)

Table A.3.5. Bond lengths (\AA) for **II-54**.

O1-C1	1.366(2)
O1-C4	1.468(2)
O2-C1	1.211(2)
C9-C10	1.387(3)
C9-C14	1.395(3)
C9-C4	1.508(3)
C4-C3	1.500(3)
C1-C2	1.465(3)
C10-C11	1.390(3)
C14-C13	1.382(3)
C2-C3	1.382(3)
C2-C8	1.390(3)
C12-C11	1.376(3)
C12-C13	1.390(3)
C5-C3	1.381(3)
C5-C6	1.386(3)
C6-C7	1.399(3)
C7-C8	1.377(3)

Table A.3.6. Bond angles (degrees) for **II-54**.

C1-O1-C4	110.73(15)
C10-C9-C14	119.46(18)
C10-C9-C4	120.11(17)
C14-C9-C4	120.41(17)
O1-C4-C3	103.33(14)
O1-C4-C9	110.48(15)
C3-C4-C9	115.35(16)
O2-C1- O1	120.63(19)
O2-C1-C2	130.90(19)
O1-C1-C2	108.47(16)
C9-C10-C11	120.32(19)
C13-C14-C9	120.06(19)
C3-C2-C8	121.95(19)
C3-C2 C1	108.10(17)
C8-C2-C1	129.96(18)
C11-C12-C13	120.3(2)
C14-C13-C12	119.98(19)
C3-C5-C6	117.7(2)
C5-C3-C2	120.73(18)
C5-C3-C4	129.99(18)
C2-C3-C4	109.28(17)
C5-C6-C7	121.4(2)
C8-C7-C6	120.7(2)
C7-C8-C2	117.5(2)
C12-C11-C10	119.86(19)
C21-C22-C17	120.06(12)
C20-C19-C18	119.75(12)
C22-C21-C20	120.15(12)
C2-C3-C4	119.91(13)
C5-C4-C3	120.29(12)